Gens, A. (2010). *Géotechnique* **60**, No. 1, 3–74 [**doi:** 10.1680/geot.9.P.109]

Soil–environment interactions in geotechnical engineering

A. GENS*

The range of problems that geotechnical engineers must face is increasing in complexity and scope. Often, complexity arises from the interaction between the soil and the environment – the topic of this lecture. To deal with this type of problem, the classical soil mechanics formulation is progressively generalised in order to incorporate the effects of new phenomena and new variables on soil behaviour. Recent advances in unsaturated soil mechanics are presented first: it is shown that they provide a consistent framework for understanding the engineering behaviour of unsaturated soils, and the effects of suction and moisture changes. Building on those developments, soil behaviour is further explored by considering thermal effects for two opposite cases: high temperatures, associated with the problem of storage and disposal of high-level radioactive waste; and low temperatures in problems of freezing ground. Finally, the lecture examines some issues related to chemical effects on soils and rocks, focusing in part on the subject of tunnelling in sulphate-bearing rocks. In each case new environmental variables are identified, enhanced theoretical formulations are established, and new or extended constitutive laws are presented. Particular emphasis is placed on mechanical constitutive equations, as they are especially important in geotechnical engineering. The lecture includes summary accounts of a number of case histories that illustrate the relevance and implications of the developments described for geotechnical engineering practice.

KEYWORDS: constitutive relations; environmental engineering; partial saturation; snow, ice and frost; suction; temperature effects

La complexité et l'envergure des problèmes que doivent affronter et résoudre les ingénieurs géotechniciens augmentent constamment. Souvent, cette complexité tient à l'interaction entre le sol et l'environnement, qui constitue l'objet de la présente communication. Pour affronter ce type de problèmes, on a généralisé progressivement la formulation classique de la mécanique des sols, afin d'incorporer les effets de variables et de phénomènes nouveaux sur le comportement du sol. On se penche, en premier lieu, sur les progrès réalisés récemment dans la mécanique de sols non saturés. On démontre que ces sols constituent un cadre régulier apportant des connaissances sur le comportement technique des sols non saturés, et les effets de l'aspiration et des fluctuations de l'humidité. Sur la base de ces développements, on poursuit l'exploration du comportement du sol en examinant les effets thermiques dans deux cas opposés : les températures élevées dans le cadre du problème du stockage et de l'élimination de déchets radioactifs de haute activité, et les faibles températures dans les problèmes de congélation du sol. Enfin, la communication examine certaines questions relatives aux effets chimiques sur les sols et les roches, en se concentrant en partie sur le sujet du percement dans des roches sulfatées. On identifie, dans chaque cas, de nouvelles variables environnementales ; en outre, on établit des formulations théoriques perfectionnées, et on présente des lois nouvelles ou renforcées sur la constitution. On se penche en particulier sur des équations constitutives mécaniques, qui jouent un rôle particulièrement important en ingénierie géotechnique. La communication comprend des comptes-rendus sur un certain nombre d'études de cas illustrant la pertinence et les implications des développements décrits pour la pratique de l'ingénierie géotechnique.

INTRODUCTION

Geotechnical engineering, in some form, must be a very old human pursuit (Kerisel, 1987), but it is difficult to pinpoint with any degree of precision the start of soil mechanics, the science that nowadays underlies a great deal of the discipline. There were certainly major contributions in the eighteenth and nineteenth centuries, and of course one of those early giants was William J. Macquorn Rankine, after whom this lecture is named. However, it is commonly agreed that modern soil mechanics was initiated by Terzaghi (1925a, 1925b), who was also responsible for many of its early developments. Because of the immediate success and rapid progress of the subject, he could claim, in his address to the Second International Conference on Soil Mechanics and Foundation Engineering, held in Rotterdam in 1948, that 'In 1936 Soil Mechanics had created what may be termed an ideal of soil behaviour and had given the engineer a set of theoretical concepts which covered all important aspects of soil behaviour.' However, the scope of potential applications of soil mechanics is so wide, and the range of natural materials is so extensive and varied, that it has often proved necessary to expand what can be loosely called classical soil mechanics in order to meet some of the challenges that geotechnical engineers face today and, even more, will face in the future. A somewhat arbitrary and certainly not comprehensive list of geotechnical engineering problems that are likely to require new approaches or, at least, extension of the classical ones is as follows: foundations on collapsing unsaturated soils; radioactive waste disposal; tunnelling in sulphate-bearing materials; climate change effects on slope stability or on permafrost evolution; subsidence due to oil and gas extraction; containment of toxic or hazardous waste; dissolution, degradation and weathering of soils and rocks; CO_2 sequestration: and the behaviour of methane hydrates. Some of those problems are considered in this lecture.

Often, soil behaviour related to such problems is referred to as 'problematic behaviour', and the soils associated with them as 'problematic soils'. However, in this context it is worth quoting a former Rankine lecturer (and also my PhD supervisor), P. R. Vaughan, who once wrote:

'Classical soil mechanics has evolved around a few simplified models which do not fit the properties of most real soils sufficiently for useful and safe predictions to be made ... Since we cannot change the soil to fit the soil mechanics,

Discussion on this paper closes on 1 June 2010; for further details see p. ii.

* Technical University of Catalonia, Barcelona, Spain.

perhaps we should change the soil mechanics to fit the soil. The theory which fails to fit their behaviour is problematic, not the soil.' (Vaughan, 1999)

Indeed, many of the soil mechanics developments in the last few decades can be seen as an attempt to modify the classical approaches to fit real soil behaviour. It must be added that, often, it is not only the soil itself that may seem problematic; complexity also arises from the interaction between the soil and the environment—the topic of this lecture. The term 'environment' is used here in a rather all-encompassing way, perhaps somewhat different from the usual one. Taken to the limit, even pore pressure should be viewed as an environmental variable.

Some landmarks of classical soil mechanics

Before going beyond classical soil mechanics, it is worthwhile examining some of its basic tenets, because there are important lessons to learn. Obviously, a starting point must be the principle of effective stress (Terzaghi, 1936). The principle is often illustrated, though not very rigorously (Muir Wood, 2004), by establishing equilibrium across a wavy plane joining interparticle contacts (Fig. 1). This simple illustration highlights several features of the approach that underlies much of classical soil mechanics: the material is multiphase (solid and liquid in this case); the microstructure is implicitly considered (a microstructural picture of the soil is used as support for understanding); a new variable, pore pressure, is incorporated; and there is coupling between mechanical variables (stresses) and hydraulic variables (pore pressures).

Another basic component of classical soil mechanics is the theory of consolidation, which also goes back to Terzaghi himself (Terzaghi & Frölich, 1936). However, the general three-dimensional theory was established by Biot (1941). If the soil is assumed isotropic linear elastic, the consolidation equation can be expressed as

$$\frac{k}{\gamma_w} \nabla^2 p_w = \frac{k}{\gamma_w} \left(\frac{\partial^2 p_w}{\partial x^2} + \frac{\partial^2 p_w}{\partial y^2} + \frac{\partial^2 p_w}{\partial z^2} \right) = \frac{\partial p_w}{\partial t} - \frac{1}{3} \frac{\partial p_t}{\partial t} \quad (1)$$

where k is the permeability of the soil; γ_w is the unit weight of water; m is the inverse of the bulk modulus; p_w is the pore water pressure; p_t is the mean total stress; x, y and z are space coordinates; and t is time.

This is, of course, well known, and part of any undergraduate syllabus. It is interesting, however, to identify the basic components that underlie this very familiar expression.

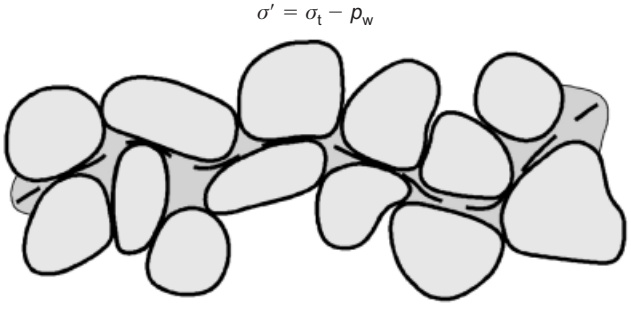

Fig. 1. Illustration of the principle of effective stresses (Lambe & Whitman, 1979). σ' is the effective stress, σ_t the total stress, and p_w the pore water pressure

Equation (1) is in fact derived from a combination of balance equations and constitutive laws. The balance equations express the conservation of the solid mass, the water mass and momentum (equilibrium).

Solid mass balance:

$$\frac{\partial \rho_s (1-n)}{\partial t} + \nabla \cdot \left[(1-n) \rho_s \dot{\boldsymbol{u}} \right] = 0 \quad (2)$$

Water mass balance:

$$\frac{\partial \rho_w n}{\partial t} + \nabla \cdot (\boldsymbol{j}_w) = 0 \quad (3)$$

Equilibrium:

$$\nabla \cdot \boldsymbol{\sigma}_t + \boldsymbol{b} = 0 \quad (4)$$

where ρ_s is the density of the solid phase, ρ_w is the water density, n is the porosity (volume of pores over volume of soil), $\boldsymbol{u}$ are displacements, $\boldsymbol{j}_w$ is the total flux of water, $\boldsymbol{\sigma}_t$ are total stresses, and $\boldsymbol{b}$ are the body forces. ∇ is the gradient operator.

The constitutive equations are very simple in this case.

Darcy's law for water flow:

$$\boldsymbol{q}_w = -k \nabla (p_w + \gamma_w z) \quad (5)$$

Isotropic linear elasticity:

$$\mathrm{d}\varepsilon_v = m \mathrm{d}p' = \frac{1}{K} \mathrm{d}p' \quad (6)$$

where q_w is the water flow, z is the vertical coordinate, ε_v is the volumetric strain, p' is the mean effective stress, and K is the bulk modulus of the soil. Combining equations (2), (3), (4), (5) and (6), equation (1) is readily recovered.

Therefore Biot's consolidation equation results in fact from the combination of a set of balance equations that express some basic physical principles (conservation of mass and momentum) with specific constitutive laws that describe the particular behaviour of the materials under consideration. All of them have to be satisfied simultaneously. Indeed, it is necessary to solve the mechanical (stress–strain) problem and the hydraulic (water flow) problem together in a coupled manner. A coupled hydromechanical analysis thereby results, the unavoidable consequence of tackling coupled problems. The same scheme of combining balance equations and constitutive equations will be maintained when extending the classical formulation to more general cases.

Finally, the picture of classical soil mechanics would not be complete if critical state soil mechanics (CSSM) was not included, a development that came much later (Roscoe *et al.*, 1958; Roscoe & Burland, 1968; Schofield & Wroth, 1968). CSSM provided a unifying framework that brought together many key features of saturated soil behaviour, such as shear behaviour, volume change, strength, dilatancy and yield, in an integrated and consistent manner. Since then, soil behaviour has been usefully described in terms of concepts such as yield surfaces, bounding surfaces or limit state surfaces. The same approach is used in this lecture.

Structure and objectives of the lecture

In this brief review of classical soil mechanics, a number of basic themes have been identified, which include the following.

(*a*) The soil is a multiphase material.
(*b*) Microstructure is implicitly considered as an aid to understanding.

(*c*) New additional variables are required to fully describe soil behaviour—pore pressure in this case.
(*d*) The relevant phenomena are often coupled phenomena, leading to coupled analysis.
(*e*) Finally, it is possible to employ unifying frameworks of the critical state type.

The objective of the lecture is to try to extend and generalise classical soil mechanics to incorporate new types of soil behaviour, and the effects of new environmental variables. Three partially overlapping topics are discussed. Unsaturated soils, a subject closely associated with the effects of suction, are considered first. Then thermal effects are examined, taking into account two extreme cases: high temperatures, associated with the problem of storage and disposal of high-level radioactive waste; and low temperature in problems of freezing ground. Finally, the lecture explores some issues related to chemical effects on soils and rocks, focusing, to some extent, on the subject of tunnelling in sulphate-bearing rocks.

For consistency, the required developments should be congruent with the underlying themes of classical soil mechanics. Accordingly, for each of those topics, it will be necessary to

(*a*) identify additional (environmental) variables
(*b*) establish more general theoretical formulations that may require additional or enhanced balance equations
(*c*) propose new or extended constitutive equations, paying special attention to the mechanical constitutive laws, which are often the most relevant ones for geotechnical engineering.

The aims are both understanding and application to practice. This requires soil behaviour, constitutive modelling, analysis, and field observations to be brought together as required. The lecture includes summaries of case histories that illustrate the transfer of the developments described to engineering practice.

UNSATURATED SOILS: SUCTION AND COUPLED FORMULATION

General

Unsaturated soils are simply soils in which the pore space is occupied by more than a fluid, normally liquid and gas (Fig. 2). A basic variable characterising this type of soil is the liquid degree of saturation (often abbreviated to degree of saturation), S_l, which is the proportion of the pores occupied by the liquid phase. The gas degree of saturation, S_g, can be defined in a similar way; obviously, $S_l = 1 - S_g$.

Unsaturated soils give rise to very characteristic types of geotechnical problem. For instance, it is well known that slopes involving unsaturated soils are prone to failure during rainy periods, owing to the loss of strength associated with the increase of degree of saturation. Fig. 3 shows an example, the Kwun Lung Lau landslide, which occurred in Hong Kong on 23 July 1994 (Wong & Ho, 1997). It resulted in five fatalities, and was closely related to the saturation and weakening of the soil mass arising from heavy rainfall that occurred in the 48 h before the landslide, when a precipitation of 547 mm was recorded nearby. Interestingly, however, rainfall had largely ceased about 10 h before the failure. The ground was made of a rather permeable fill overlying partially weathered volcanic tuff. The forensic investigation concluded that the landslide was most likely to have been caused by the ingress of a large volume of water as a result of leakage from underground services (stormwater pipes and a sewer), bringing about an increase of degree of saturation and a reduction of the shear strength of the ground (Wong & Ho, 1997).

A different but also typical problem involving unsaturated soils is the damage to structures caused by the collapse of the foundation soil due to wetting. In spite of the use of the term *collapse*, this phenomenon does not involve failure, but the compression of the soil due to an increase in degree of saturation. Often, poorly compacted fills are involved (Charles, 2008), but collapse behaviour is also observed in natural materials. An interesting example of foundation collapse occurring in natural soil took place in Via Settembrini, Naples, on 15 September 2001, as illustrated in Fig. 4 (Viggiani, 2007, personal communication). The foundation soil was composed of a layer of pyroclasts overlying a tuff (Fig. 5). In spite of the loose character of the pyroclastic soil, the foundation had remained stable for a long time, until the material was wetted by water coming through disused ancient wells that were connected to a blocked deep-water cistern (Pellegrino, 2005). A heavy rainstorm resulting in 130–160 mm rainfall in 3 h caused the water to overflow the wells and saturate parts of the foundation soils (Fig. 5). Maximum settlements of the order of 200 mm were measured from the start of monitoring, some time after the event. It was estimated that the observed collapse settlement corresponded to a water table rise of about 12 m (Feola *et al.*, 2004).

Clearly, a proper account of the behaviour of unsaturated soils must incorporate, among other features, these basic effects of wetting on strength and deformation.

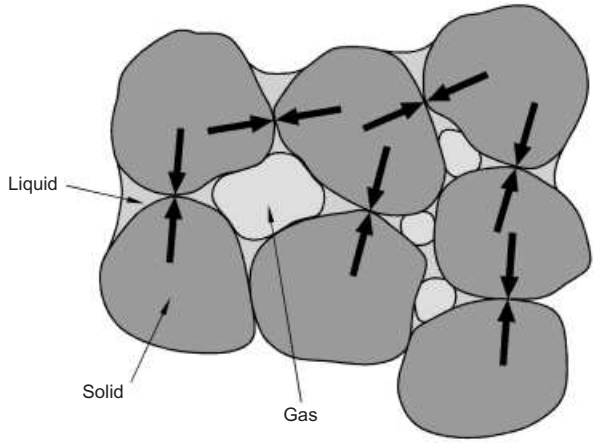

Fig. 2. Scheme of an unsaturated soil

Fig. 3. Kwun Lung Lau landslide, Hong Kong (photograph from http://hkss.cedd.gov.hk/hkss/eng/photo_gallery/)

Fig. 4. Collapse of a foundation on loose pyroclastic soil in Via Settembrini, Naples (Viggiani, 2007, personal communication)

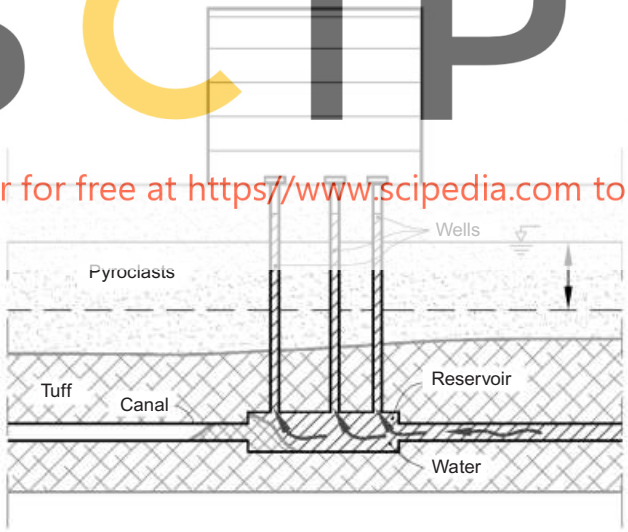

Fig. 5. Wetting of the foundation soil due to overflow of disused wells. The saturation of part of the pyroclastic layer caused collapse settlements in the foundation of a building in Via Settembrini, Naples (Pellegrino, 2005)

An additional variable: suction

It has long been recognised (e.g. Croney, 1952; Burland & Ridley, 1996) that an adequate understanding of the behaviour of unsaturated soils requires the proper consideration of suction. In this context it is useful to recall the definition of the soil–water (total) potential: the amount of work that must be done per unit mass of pure water in order to transport reversibly and isothermally an infinitesimal quantity of water from a reservoir of pure water at a specified elevation and gas pressure to the soil point under consideration. It can be readily verified that the work done corresponds to a variation in free energy per unit mass (e.g. Aitchison *et al.*, 1965). Potential has therefore units of energy per unit mass (L^2T^{-2}; J/kg). Total potential controls the flow of water: water flows from regions of high water potential towards regions of lower water potential. If there is no flow between two masses of water, it necessarily means that the water potentials are the same in the two zones.

In 1965 a review panel in the Symposium on Moisture Equilibrium and Moisture Changes in Soils Beneath Covered Areas (Aitchison *et al.*, 1965) proposed a division of the total potential into four different components: gravitational potential, ψ_g; gas pressure potential, ψ_p; matric potential, ψ_m; and osmotic potential, ψ_o.

$$\psi = \psi_g + \psi_p + \psi_m + \psi_o \tag{7}$$

Although there is a certain degree of arbitrariness in this division, it has proved very useful in the context of geotechnical engineering. The gravity potential is given by the difference in elevations; the gas pressure potential is related to the applied gas pressure; osmotic potential depends on differences in solute concentrations (across a semi-permeable membrane); and the matric potential is related to the interaction between liquid and solid. In soil science, gas pressure potential is generally replaced by overburden potential, a more general concept. Although this division into components is useful for a better understanding, it should be stressed that the only parameter controlling the mass transfer of water is the sum of all four components.

With respect to the mechanical behaviour of unsaturated soils, the situation is more complex, as it is by no means true that all potential components have a similar effect. In fact, it is obvious that gravitational potential does not affect mechanical behaviour in any significant way. In addition, experimental results (Fredlund & Morgenstern, 1977; Tarantino *et al.*, 2000) and some theoretical considerations for soils with incompressible grains (Alcoverro, 2003) indicate that the gas pressure potential should have no influence on mechanical behaviour either. Therefore only osmotic potential and matric potential, the latter two components of potential, affect the mechanical response of unsaturated soils in any significant way. Again, there is no reason for the two potential components to have equivalent effects. In fact, it can be easily checked experimentally that their influences on mechanical behaviour are quite different, and depend on the type of soil (Aitchison, 1965). Osmotic effects require some kind of semi-permeable membrane. Because of the small pore sizes in clays and the electric fields within them, clayey materials may in some cases exhibit membrane properties restricting, to some degree, the passage of certain chemical components through the soil (Mitchell, 1991). In non-active soils, osmotic effects are likely to be negligible. Consequently, attention is focused mainly on matric potential.

As an alternative to potential, the concept of suction is often used. If energy (or work) is considered per unit volume (instead of per unit mass), the resulting variable is called suction, and it is expressed in terms of pressure ($ML^{-1}T^{-2}$; kN/m^2), with a sign change to avoid using negative values. Thus matric suction is denoted by s and osmotic suction by s_o. The sum of matric and osmotic suctions is often called total suction, $s_t = s + s_o$. Total suction is related to relative humidity (RH) via Kelvin's law,

$$\begin{aligned} \mathrm{RH} &= \frac{p_v}{(p_v)^0} = \frac{\theta_g^w}{(\theta_g^w)^0} \\ &= \exp\left(\frac{-s_t M_w}{RT\rho_w}\right) \end{aligned} \tag{8}$$

where p_v is the partial vapour pressure; $(p_v)^0$ is the equilibrium vapour pressure at the same temperature and zero suction; θ_g^w is the vapour concentration; $(\theta_g^w)^0$ is the reference vapour concentration at the same temperature; M_w is the molecular mass of water (18·016 kg/kmol); R is the universal gas constant (8·314 J/(mol K)); and T is the absolute temperature in kelvin.

Matric suction is often associated with capillary phenomena. Indeed, in some circumstances the water in the soil will form menisci between particles (Fig. 6). Surface tension and interface curvature give rise to a difference between water pressure (p_w) and air pressure (p_a) that is generally equated to matric suction, $s = p_a - p_w$. In addition, the presence of menisci in the particle contacts generates interparticle forces (Fig. 2). As those forces are roughly aligned with the normal of the contact, they tend to have a stabilising influence on the soil skeleton.

Fisher (1926) computed the value of the interparticle force generated by a liquid meniscus between two spheres of equal radii in contact. The solution is plotted in Fig. 7(a) in terms of meniscus angle and in Fig. 7(b) in terms of suction. The calculation considers both the effect of the negative pressure over the area of the meniscus and the effects of the surface tension in the gas/liquid interface. The resulting force magnitude depends on the value of the surface tension, and on the diameter of the spheres. The variation of the force with suction is not large: the effect of an increased suction is offset partially by the reduction of the meniscus area. Interparticle forces have also been computed for the cases in which the spheres are either not in contact or overlap (Gili & Alonso, 2002).

However, soils are much more complex than a bundle of capillary tubes, and this is especially so when small-size particles are predominant, as in fine-grained soils. Actually matric suction (or potential) should be considered as a first approximation as the sum of two components, a capillary component and an adsorptive component, the relative importance of which depends on the type of soil and the water content; the adsorptive component will tend to predominate in fine-grained soils (Nitao & Bear, 1996). Accordingly, Fuller *et al.* (1999) proposed that the matric potential (equated to the chemical potential of the liquid/vapour interface) has two terms, a capillary one (C) and an adsorptive one (A),

$$\psi_m = C(\kappa_c) + A(h) \tag{9}$$

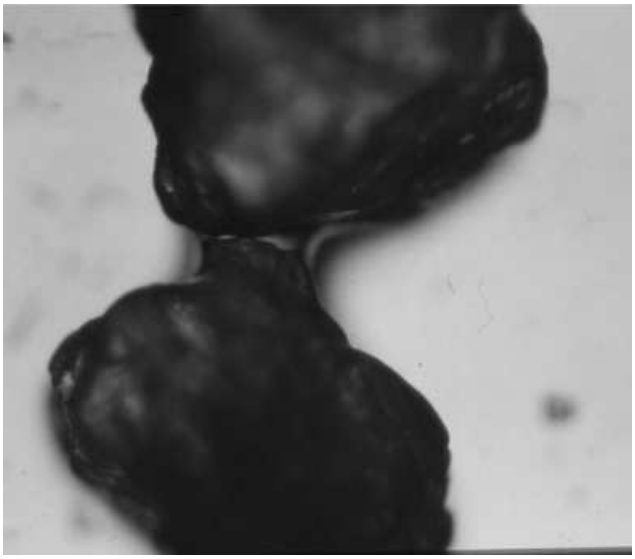

Fig. 6. Meniscus between two sand particles (Gili, 1988)

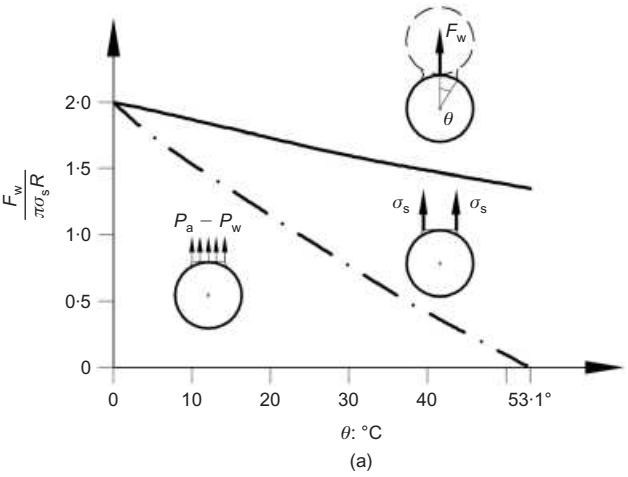

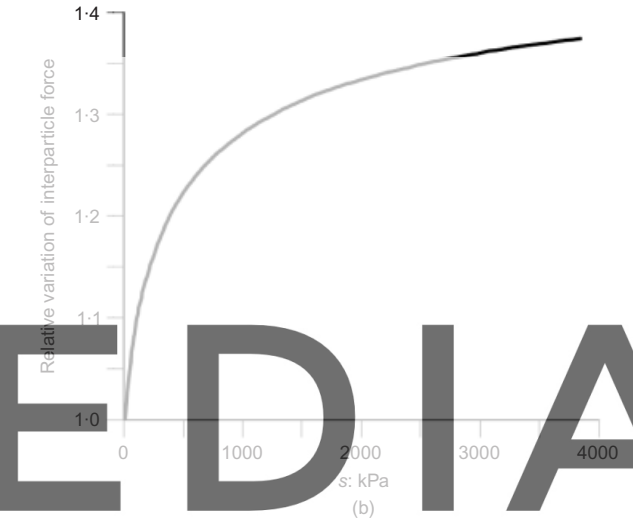

Fig. 7. Capillary-induced interparticle force computed from Fisher (1926) solution: (a) variation with meniscus wetting force with meniscus wetting angle (σ_s is the surface tension and R the radii of the spheres); (b) relative variation of interparticle force with suction

where κ_c is the mean curvature of the interface, and h is the thickness of the film of adsorbed water. The capillary component can be derived from the Laplace equation, and, for the adsorptive component, Philip (1977) proposed an empirical expression. Thus

$$C(\kappa) = \frac{-2\sigma_s \kappa}{\rho_w}; \quad A(h) = \frac{-\lambda' RT}{h} \tag{10}$$

where σ_s is the surface tension and λ' is a positive constant. The adsorptive component is in fact the result of a complex interaction of, among others, long-range (> 500 Å) electrostatic forces (as in diffuse double layer theory) and short-range (< 100 Å) van der Waals and hydration forces that control molecular interactions of water near the solid surfaces (Derjaguin *et al.*, 1987). Other molecular forces that may contribute to the potential are hydrogen bonding, osmosis, and charged surface–dipole attraction. Because of the intricate nature of the geometry of pore space, the matric suction or matric potential has to be evaluated experimentally, and the distinction between the two components is likely to remain, except for especial cases, at a conceptual level. Indeed, a sharp distinction between capillary and adsorptive potential is unlikely; there is probably a gradual

transition as the distance to the solid particle surface reduces. Capillary potential will tend to dominate in granular soils, and in soils with high degrees of saturation, whereas the adsorptive potential will be more significant in clayey soils, especially at low water contents.

Partly for historical reasons it is usual to express matric suction, over the full range of degrees of saturation, in terms of pressure difference ($s = p_a - p_w$) as if the capillary model was valid. However, it is more appropriate to think of matric suction as a variable that expresses quantitatively the degree of attachment of the liquid to the solid phase that results from the general solid/water/interface interaction. This perspective should help to dispel the misgivings that are sometimes expressed about the physical meaning of negative pressures reaching values of hundreds of MPa. Those large suction values refer to the very large potential of the water immediately adjacent to the solid surface, but they should not be viewed as pressures in the conventional bulk thermodynamic sense. Care should be taken, therefore, not to equate automatically all matric suction effects to capillary phenomena: in some instances the capillary model is quite unrealistic.

The fact that the two components of matric suction are lumped together in a single variable, and that, in addition, they are difficult to separate experimentally, should not lead to the conclusion that their effects on mechanical behaviour are equivalent. Actually, such effects should depend on the relative importance of each of the two components, and thereby on the type of soil being examined. Indeed, much of the variability of the soil response to matric suction changes is likely to be related to the different effects of the capillary and adsorptive components, and to their varying proportions. An extensive discussion on the same issues has been presented recently (Baker & Frydman, 2009).

If matric suction is basically related to molecular forces, it should be largely independent of gravitational potential. It is possible to compute a capillary length of water κ_c^{-1} below which gravitational effects should be negligible (De Gennes *et al.*, 2004). At normal temperatures

$$\kappa_c^{-1} = \sqrt{\gamma_{ws}/\rho_w g} \approx 2\,\text{mm} \quad (10)$$

where g is the gravity acceleration. Since the pores of most soils are well below this capillary length, matric suction should be independent of gravitational forces.

The performance of a series of centrifuge tests on unsaturated soils within the framework of the MUSE (Mechanics of Unsaturated Soils for Engineering) Marie Curie framework has provided an opportunity to check this conclusion (Casini *et al.*, 2009). The tests were conducted in the LCPC centrifuge at Nantes (France). The material tested is Jossigny silt (w_L = 32·3%, I_P = 15·3%), statically compacted to a dry unit weight γ_d around 14·5 kN/m^3 and a water content w of about 13%, The sample was placed in a cylindrical container 300 mm in diameter and 300 mm long (Fig. 8). Two sets of tensiometers, provided by ENPC-CERMES (Paris) and by Durham University, were installed at different heights on opposite sides of the sample. Here, only the readings of the tensiometers during acceleration and deceleration are examined. Fig. 9(a) shows the evolution of pore pressures measured in one of the tensiometers sets (CERMES) during the acceleration stage. Initial pore pressures are negative, corresponding to the suctions set up during compaction. There is some response of the tensiometers during the 7 min acceleration from 1g to 50g, but this is probably due to the reaction of the measurement devices: it is noteworthy that, at the end of the acceleration, suction values are very similar to the initial ones. Certainly, the increase of gravitational forces by 50 times has not made

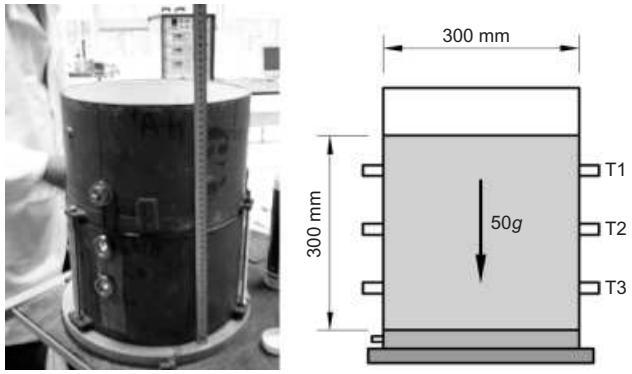

Fig. 8. Specimen of compacted unsaturated Jossigny silt for testing in the LCPC centrifuge

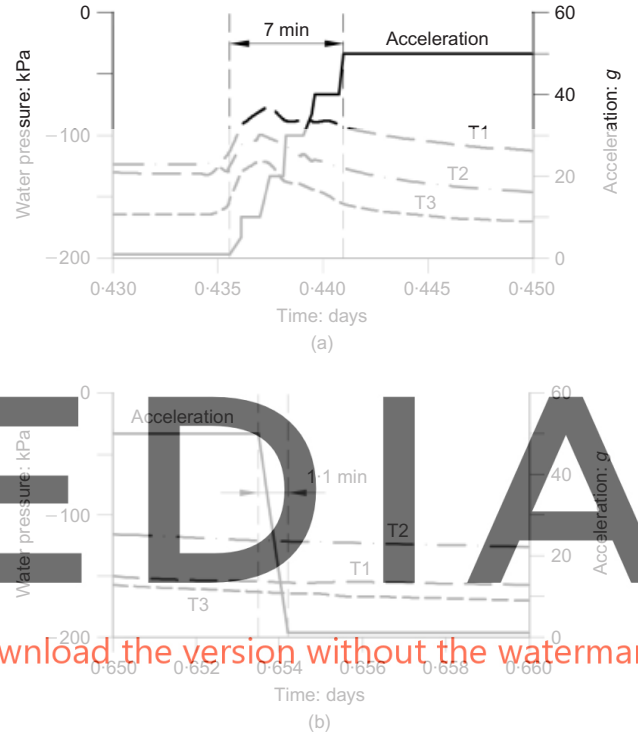

Fig. 9. Evolution of pore pressures in a centrifuge test on Jossigny silt: (a) acceleration stage; (b) deceleration stage

a significant impact on the measured suction. Of course, in the longer term there will be changes in pore pressures, but they correspond to the consolidation process associated with the new stress state in the specimen. The observations are even more clear-cut during the deceleration stage from 50g to 1g, which occurs in just over a minute. As Fig. 9(b) shows, the pore pressure readings do not react at all to the change of centrifuge acceleration, indicating the insensitivity of matric suction to gravitational forces.

Enhanced hydromechanical coupled formulation for unsaturated soils

To develop an appropriate coupled formulation for unsaturated soils, it is convenient to make a distinction between phases and species. It is postulated that the porous medium is composed of three species—mineral (–), water (w) and air (a)—distributed in three phases: solid (s), liquid (l) and gas (g). In this case it is assumed that the mineral species and the solid phase coincide. However, the liquid phase may contain dissolved air, and the gas phase is a mixture of

water vapour and dry air. The water and liquid phase and the air and gas phase no longer coincide. Although air is a mixture of gases, it is considered here as a single species. The distinction of phases and species is reflected in the notation: superscripts refer to species and subscripts refer to phases. For example, volumetric mass (partial density) of a species in a phase (e.g. vapour, water in gas phase θ_g^w) is the product of the mass fraction of that species, ω_g^w, and the bulk density of the phase, ρ_g: that is, $\theta_g^w = \omega_g^w \rho_g$. Thus the total density of the gas phase, ρ_g, is the sum of the partial densities of air, θ_g^a, and vapour, θ_g^w:

$$\rho_g = \theta_g^a + \theta_g^w \tag{12}$$

As indicated in the Introduction, the formulation must be a combination of balance equations and constitutive equations: they are described in the following sections.

Balance equations. There were several early developments of coupled hydro-mechanical (HM) formulations for unsaturated soils using different simplifying assumptions and numerical techniques (e.g. Lloret & Alonso, 1980; Alonso & Lloret, 1982; Richards, 1984; Dakshanamurthy *et al.*, 1984; Justo *et al.*, 1985; Alonso *et al.*, 1988). Subsequently, formulations rooted on more general theories have been put forward (e.g. Ehlers *et al.*, 2005, using the theory of porous media; or Loret & Khalili, 2000, and Khalili *et al.*, 2008, based on the theory of mixtures). The formulation described here is based on the general approach of Olivella *et al.* (1994) applied to the specific case of isothermal problems involving unsaturated soils. To establish the mass balance equations, the compositional approach is adopted. It consists of balancing the species rather than the phases: total species equations are obtained by adding over all phases the equation of balance of each species. In this way phase exchange terms cancel out, which is particularly useful when equilibrium is assumed.

The macroscopic balance of any thermodynamic property π (per unit mass) in a continuum can be expressed by

$$\frac{\partial}{\partial t}(\rho\pi) + \nabla \cdot (\boldsymbol{j}_\pi) - f^\pi = 0 \tag{13}$$

where ρ is the mass of the species per unit volume containing π; $\boldsymbol{j}_\pi$ is the total flux of π with respect to a fixed reference system; and f^π is the rate of production/removal of π per unit volume. It is important to stress here that $\boldsymbol{j}_\pi$ is expressed in relation to a fixed reference system, because corrections may be required if the solid phase moves significantly. Total flux can be decomposed into two components: an advective one (phase motion) and a non-advective one (motion of the species inside the phase). That is,

$$\boldsymbol{j}_\pi = \rho\pi\boldsymbol{v} + \boldsymbol{i}_\pi \tag{14}$$

where $\boldsymbol{v}$ is the mass weighted mean velocity and $\boldsymbol{i}_\pi$ is the non-advective flux. Using this decomposition, equation (13) coincides with the general equation given by Hassanizadeh & Gray (1980).

The mass balance for water can be established following the approach outlined above and illustrated in Fig. 10. Considering a representative elementary volume (REV) of the soil, the water mass balance equation must verify that the change in the amount of water inside the REV must be equal to the net inflow/outflow of water (plus any sink or source term that may exist). The net inflow/outflow is of course equivalent to the divergence of the total flow. Because unsaturated soils are being considered, it is necessary to account for the water in liquid and gas form, both in the storage term and in the flux term. Therefore the mass balance equation for the water is expressed as

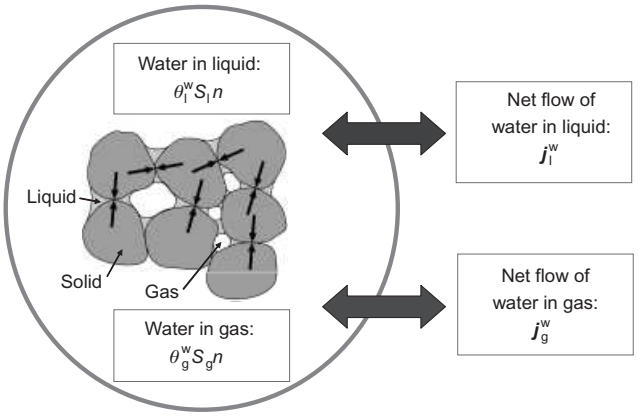

Fig. 10. Scheme to establish the equation for mass balance of water

$$\frac{\partial}{\partial t}\left(\theta_l^w S_l n + \theta_g^w S_g n\right) + \nabla \cdot \left(\boldsymbol{j}_l^w + \boldsymbol{j}_g^w\right) = f^w \tag{15}$$

where $\boldsymbol{j}$ is total flux and f^w is the sink/source term.

Following the same procedure, the equation for the mass balance of air is

$$\frac{\partial}{\partial t}\left(\theta_l^a S_l n + \theta_g^a S_g n\right) + \nabla \cdot \left(\boldsymbol{j}_l^a + \boldsymbol{j}_g^a\right) = f^a \tag{16}$$

The equations for the mass balance of solid (mineral) and equilibrium remain the same as in the saturated case:

$$\frac{\partial}{\partial t}[\theta_s(1-n)] + \nabla \cdot (\boldsymbol{j}_s) = 0 \tag{17}$$

$$\nabla \cdot \boldsymbol{\sigma}_t + \boldsymbol{b} = 0 \tag{18}$$

Equations (15), (16), (17) and (18) are the set of fundamental balance equations that must be satisfied simultaneously at every instant of time and at every point of the domain of interest. As will be shown in a later section, it is in fact possible to eliminate the solid mass balance equation by making use of the concept of material derivative, reducing the number of balance equations from four to three. More details about those transformations and the incorporation into numerical codes are given in Olivella *et al.* (1994), Olivella *et al.* (1996b) and Gens & Olivella (2001a).

Constitutive equations. Constitutive equations are key components of the formulation, because they describe the specific way in which a particular material or material component behaves. They are also important for an additional reason. Many of the phenomena incorporated in the formulation are coupled with each other; the coupling is often reflected in the definition of the constitutive law. Table 1 lists the main constitutive laws required to complete the coupled formulation for unsaturated soils. Those relevant to this section are indicated as HM (hydromechanical). Because of its special significance, the mechanical constitutive law is discussed in the next section.

Advective flow of liquid and gas is assumed to be governed by Darcy's law. Although Darcy's law can be derived from the equation of the linear momentum balance for the liquid phase (neglecting inertial and viscous effects), here it is treated as a constitutive law. It is expressed as:

$$\boldsymbol{q}_l = -\boldsymbol{K}_l(\nabla p_l - \rho_l \boldsymbol{g}) \tag{19a}$$

$$\boldsymbol{q}_g = -\boldsymbol{K}_g(\nabla p_g - \rho_g \boldsymbol{g}) \tag{19b}$$

$\boldsymbol{K}$, the permeability tensor, is often also called the hydraulic

Table 1. Constitutive equations and equilibrium restrictions

Phenomena	Equation	Variable	Formulation
Constitutive equations			
Advective flow of liquid and gas	Darcy's law	$\boldsymbol{q}_l$, $\boldsymbol{q}_g$	HM, THM, THMC
Water absorption/desorption	Retention curve	S_l, S_g	HM, THM, THMC
Diffusive flow of vapour and dissolved air	Fick's law	$\boldsymbol{i}_g^w$, $\boldsymbol{i}_l^a$	HM, THM, THMC
Stress–strain behaviour	Mechanical constitutive model	σ	HM, THM, THMC
Solid density variation	Phase density relationship	ρ_s	HM, THM, THMC
Liquid density variation	Phase density relationship	ρ_l	HM, THM, THMC
Gas density variation	Ideal gas law	ρ_g	HM, THM, THMC
Heat conduction	Fourier's law	$\boldsymbol{i}_c$	THM, THMC
Kinetic-controlled chemical reactions	Chemical kinetics	R_i	THMC
Equilibrium restrictions			
Evaporation/condensation of water	Kelvin's law	ω_g^w	HM, THM, THMC
Dissolution of air in water	Henry's law	ω_l^a	HM, THM, THMC
Equilibrium chemical reaction	Chemical equilibrium	X_i	THMC

HM, hydromechanical; THM, thermo-hydromechanical; THMC, thermo-hydromechanical-chemical.

conductivity, for consistency with other conductivity parameters. The permeability (or hydraulic conductivity) tensor has a certain structure, given by

$$\boldsymbol{K} = \left(\frac{\boldsymbol{k}}{\mu_\alpha}\right) k_r \tag{20}$$

where $\boldsymbol{k}$ is the intrinsic permeability, μ is the fluid viscosity, and k_r is the relative permeability. Intrinsic permeability is not a constant; it depends on porosity, pore size and pore structure. Relative permeability depends on suction (or degree of saturation), and may vary enormously, depending on the saturation state of the soil. As an example, Fig. 11 shows the variation of relative permeability for two rather coarse Hong Kong soils: a colluvium, and a residual soil of decomposed granite (Fredlund & Rahardjo, 1993). The relative permeability (and therefore the hydraulic conductivity) reduces by several orders of magnitude over rather modest increases of suction. This variation of permeability with suction controls, for instance, the infiltration of water into hill slopes, with the obvious subsequent influence on stability. Indeed, in flow through unsaturated soils, the variation of relative permeability is often a dominant feature of the problem.

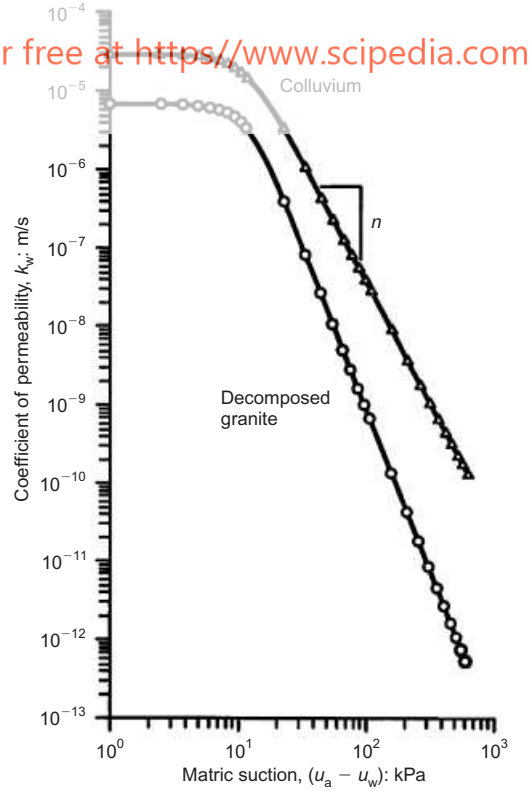

Fig. 11. Variation of relative permeability with suction for two Hong Kong soils (Fredlund & Rahardjo, 1993)

The relationship between suction and degree of saturation (or water content) is defined by the retention curve (or soil-water characteristic curve, SWCC). It exhibits hysteretic behaviour, and is strongly dependent on the pore size distribution of the soil. It is also a very important relationship for flow in unsaturated soils, because it largely controls the storage capacity of the soil. Many different analytical expressions have been proposed for this constitutive law (Fredlund, 2006).

The diffusive flows of species inside a phase (vapour in the gas phase, dissolved air in the liquid phase) are governed by Fick's law: gradients of concentration are the driving thermodynamic force for this type of flow. For instance, in the case of vapour diffusion, the constitutive law can be written as

$$\begin{aligned} \boldsymbol{i}_g^w &= -\boldsymbol{D}_g^w \nabla \omega_g^w \\ &= -\left(\rho_g n S_g \tau D_m^w \boldsymbol{I} + \rho_g \boldsymbol{D}_g'\right) \nabla \omega_g^w \end{aligned} \tag{21}$$

where $\boldsymbol{i}_g^w$ is the diffusive (non advective) flow of vapour, $\boldsymbol{D}_g^w$ is the vapour dispersion tensor, τ is tortuosity, D_m^w is the diffusion coefficient of vapour in air, and $\boldsymbol{D}_g'$ is the mechanical dispersion tensor. Tortuosity is an empirical parameter that is intended to account for the fact that vapour diffusion takes place inside a porous medium.

Finally, liquid density depends on liquid pressure in a quasi-linear manner, defined by the corresponding bulk modulus K_l. The bulk modulus of water, usually the dominant species in the liquid phase is about $2{\cdot}2 \times 10^6$ MPa, although it increases at very high pressures. In contrast, the gas density variation is non-linear with respect to pressure, in accordance with the ideal gas law $p_g V = n_m RT$, where V is volume and n_m is the number of moles.

In this particular formulation it is also assumed that

evaporation/condensation of water and the dissolution of air in the liquid phase are always in equilibrium. The corresponding equilibrium restrictions are given by Kelvin's law (equation (8)) for the vapour concentration in the gas phase and Henry's law for the amount of water dissolved in the liquid phase. Additional information on the adopted constitutive laws and on the parameters that define them is given in Olivella *et al.* (1996a) and Gens & Olivella (2000).

CONSTITUTIVE MODELS FOR THE MECHANICAL BEHAVIOUR OF UNSATURATED SOILS

The Barcelona Basic Model (BBM)

Early attempts to represent the behaviour of unsaturated soils focused on the prediction of shear strength using a single stress variable that would play a role similar to that of Terzaghi's effective stress for saturated soils (e.g. Bishop *et al.*, 1960). This approach had severe limitations when trying to describe the full behaviour of unsaturated soils, and especially the volumetric collapse (compression) behaviour upon wetting (Jennings & Burland, 1962). As a consequence, two separate stress variables, typically net stresses and suction, were often used to characterise unsaturated soil behaviour (Coleman, 1962; Bishop & Blight, 1963; Fredlund & Morgenstern, 1977). Net stress is defined as the excess of total stress over gas pressure, given by

$$\boldsymbol{\sigma} = \boldsymbol{\sigma}_{\mathrm{t}} - p_{\mathrm{g}}\boldsymbol{I} \tag{22}$$

where $\boldsymbol{\sigma}$ is the net stress, $\boldsymbol{\sigma}_{\mathrm{t}}$ is the total stress, and $\boldsymbol{I}$ is the identity tensor.

Relationships, in the form of state or constitutive surfaces, were established between those two stress variables and volume change. Sometimes state surfaces for other variables, such as degree of saturation, were also derived (Matyas & Radhakrishna, 1968; Aitchison & Martin, 1973; Fredlund & Morgenstern, 1976; Lloret & Alonso, 1985). State surfaces, however, were limited when trying to model the general behaviour of unsaturated soils. Issues of irreversibility, yield and stress path dependency are not easily accommodated in this type of framework. Also, state surfaces usually addressed partial aspects of behaviour without establishing consistent links between different features of behaviour.

In this context there were advantages in trying to develop a constitutive model within the general framework of elasto-plasticity. One of the objectives of this development was to try to place unsaturated soil mechanics closer to the mainstream of saturated soil mechanics, which for constitutive descriptions of soil behaviour was dominated largely by the concepts underlying critical state soil mechanics. The aim was to construct a complete and consistent framework capable of providing qualitative predictions by simple hand manipulation of the components of the model, in much the same way that the critical state framework had been used. This implied the necessity of using net stresses and suction as constitutive variables. If other stress variables are used, it is quite difficult—and often impossible—to draw the stress paths of conventional laboratory tests in an effective manner. This main goal guided many of the choices adopted in the definition of the model, and explains the extreme simplicity of a number of its features.[†] The development of such a framework should offer some significant benefits. It would

(*a*) provide a consistent framework for an integrated understanding of the various features of unsaturated soil behaviour
(*b*) assist in the identification of basic parameters and reference states governing soil behaviour
(*c*) furnish bases for the further development of more complex constitutive laws, and enable the performance of numerical analysis for application to engineering problems.

The model was fully described in Alonso *et al.* (1990), and in a more summary form in Gens *et al.* (1989). Indeed, the use of the concepts of the model to represent unsaturated soil behaviour was first introduced qualitatively in Alonso *et al.* (1987), before the mathematical formulation was formally presented. Only a brief account of the main elements of the model is included here. In the following, it is assumed, for simplicity, that suction equal to zero is equivalent to saturation. In practice, a soil may remain saturated as long as the suction does not go beyond the air entry value of the material.

A starting point for the development of the model is depicted schematically in Fig. 12(a), where the idealised results of consolidation tests under constant suction are shown. The yield point is located beyond the saturated consolidation line (corresponding to the line $s = 0$), and moves further to the right as suction increases. The stabilising forces due to suction allow the material to sustain a higher applied stress at a given void ratio: the higher the suction, the higher is the stress that can be sustained before yield. The various yield points are plotted in isotropic p–s (mean net stress–suction) space in Fig. 12(b). By joining them together, a yield curve, denoted as LC (loading–collapse), results.

Let us assume that a specimen of unsaturated soil is located on the yield curve LC_1 (Fig. 13) and that the applied stress p is increased at constant suction. The state of the soil will follow the path indicated by L (loading), and the yield curve will move from position LC_1 to LC_2. According to plasticity theory, the movement of the yield curve is associated with irreversible plastic volumetric strains, which would be equal to the plastic volumetric strains that would be obtained from a consolidation test on a saturated sample ($s = 0$) going from $(p_0^*)_1$ to $(p_0^*)_2$. Assuming a hardening law of the Cam-clay type, the plastic volumetric strain, $\mathrm{d}\varepsilon_{\mathrm{v}}^{\mathrm{p}}$ is expressed as

$$\mathrm{d}\varepsilon_{\mathrm{v}}^{\mathrm{p}} = \frac{\lambda(0) - \kappa}{1 + e}\frac{\mathrm{d}p_0^*}{p_0^*} \tag{23}$$

where $\lambda(0)$ is the slope of the saturated virgin consolidation line, κ is the slope of the unloading–reloading line (assumed independent of suction), and e is the void ratio.

Let us now consider a specimen at the same starting point on yield curve LC_1, but now the sample is wetted (i.e. suction is reduced) under constant stress. The movement of the LC yield curve is the same as before, and the same irreversible plastic volumetric stains will ensue. These strains correspond to collapse deformation upon wetting, and arise naturally from the basic formulation of the model. Therefore the LC yield curve links together, in some way, the compressive strains due to loading with the collapse strains due to wetting. In the BBM, the expression for the shape of the LC yield surface is derived from the variation of the post-yield slope (in semi-logarithmic space) of the consolidation lines at different suctions:

$$\left(\frac{p_0}{p^{\mathrm{c}}}\right) = \left(\frac{p_0^*}{p^{\mathrm{c}}}\right)^{\frac{\lambda(0)-\kappa}{\lambda(s)-\kappa}} \tag{24}$$

[†] Unknowingly, the developers of the model were following the advice 'sometimes the best way to answer questions is to leap boldly into the void with the risky tactic of deliberate over-simplification' of the philosopher Daniel C. Dennett (1995): *Darwin Dangerous Idea: Evolution and the Meanings of Life*. New York: Touchstone

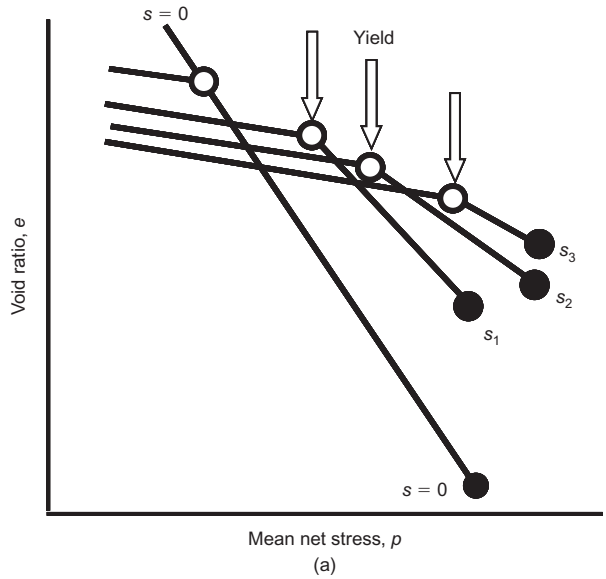

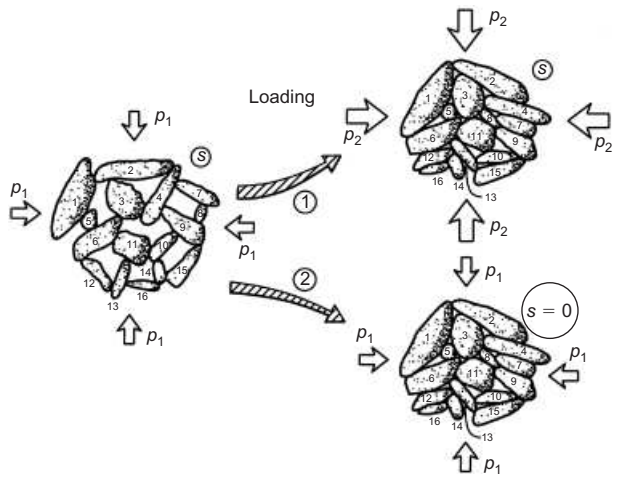

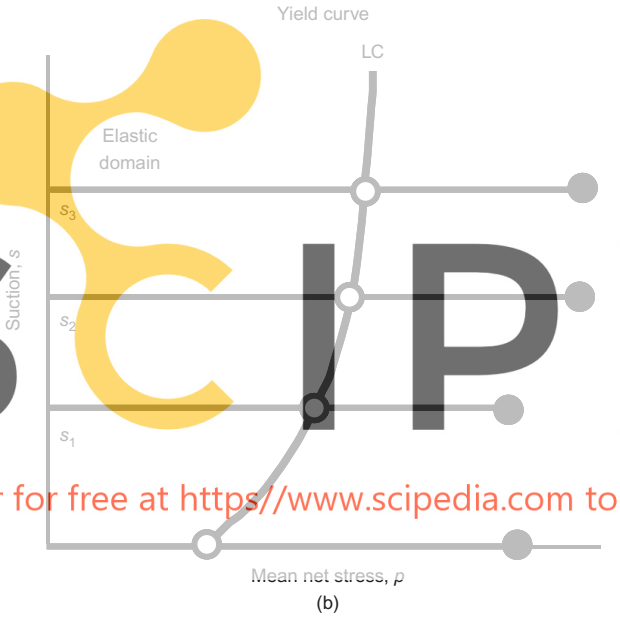

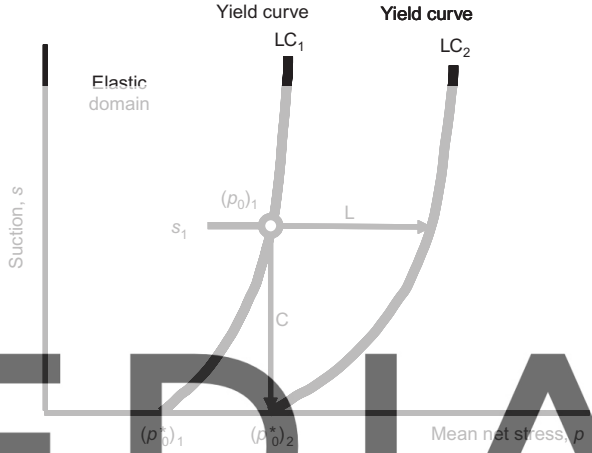

Fig. 13. Displacement of the LC yield curve on loading at constant suction (path L) and wetting at constant applied stress (path C)

Fig. 12. (a) Idealised scheme of consolidation lines at different suction values: (b) definition of the LC (loading–collapse) yield curve in the isotropic plane

$$\lambda(s) = \lambda(0)\left[(1 - r)\exp(-\beta s) + r\right] \tag{25}$$

where p_0 is the yield mean stress, $\lambda(s)$ is the slope of the virgin consolidation line for a specific value of suction, p^c is a reference stress, and r and β are model parameters.

The extension of the model to include deviatoric stresses and strains is illustrated in Fig. 14. In the q–p space (q is the triaxial deviatoric stress), the curve indicated by the label $s = 0$ represents the yield surface for saturated conditions. To emphasise the compatibility with saturated models, the ellipse of the Modified Cam-clay (MCC) model was chosen, but other yield surface shapes could equally have been used. As suction increases, the ellipse size also increases. On the right-hand side, p_0 increases in accordance with the shape of the LC yield curve. On the left-hand side, p_s increases linearly with suction. The implicit assumption here is that the friction angle (or the slope of the critical state line) is not affected by suction, but the apparent cohesion increases in proportion to suction. The formulation is completed with a flow rule that may be chosen to be associated or non-associated.

The model is summarised in Fig. 15, which shows a three-dimensional view of the yield surface in p-q-s space. It is a graphic way to illustrate the generalisation of the saturated framework via the inclusion of an additional variable, suction. The BBM model defined in this way collapses into the MCC model when suction becomes zero and saturated conditions are reached. The original BBM model also included a suction increase (SI) yield surface that accounts for the irreversible strains that occur when suction increases beyond maximum past values, but it is not discussed here. In order not to clutter the paper with unnecessary details, the full model equations have not been presented: they can be seen in Alonso *et al.* (1990). The conversion of the model from triaxial space to a fully three-dimensional one is straightforward (Gens, 1995).

The choice of net stresses and suction as stress variables implies that there may be lack of continuity in the transition between saturated and unsaturated states, a point that is discussed more fully later. Another feature of the BBM is the assumption that there is a link between the shape of the LC yield surface and the post-yield slopes of the virgin consolidation lines at different suctions. Depending on the values of parameters p^c and r (equations (24) and (25)), computed collapse strains will either continuously increase or decrease with applied stress (Wheeler *et al.*, 2002). However, it is not possible to predict collapse strains that

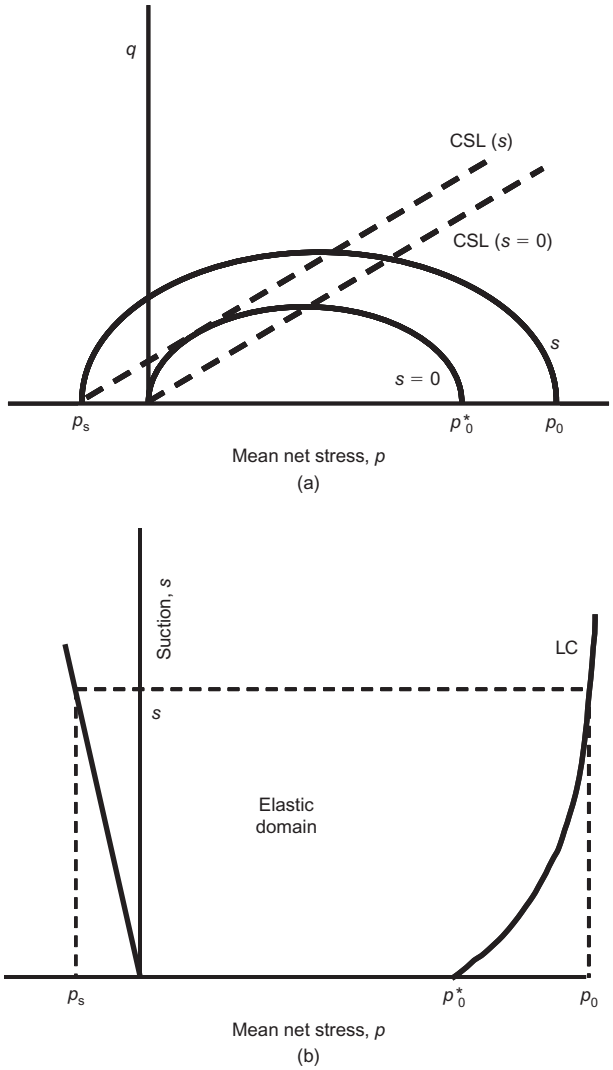

Fig. 14. (a) Yield surfaces in the q–p plane for saturated ($s = 0$) and unsaturated conditions (s); (b) trace of the yield surface in the p–s isotropic plane

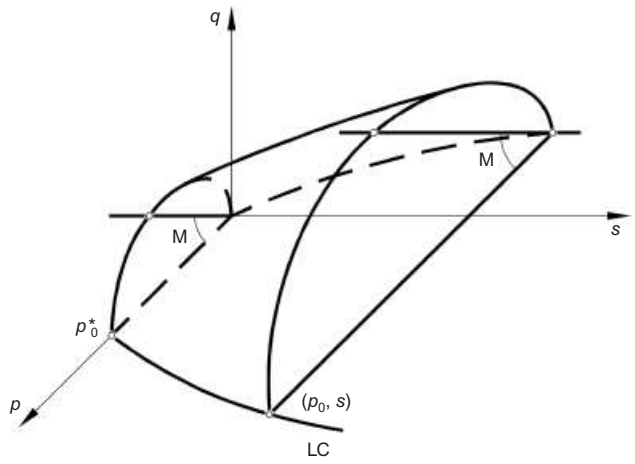

Fig. 15. Three-dimensional view of the yield surface in (p, q, s) stress space

increase with stresses, go through a maximum value and reduce down to zero at very high stresses. In fact, the monotonic variation of volumetric stiffness with suction is not an essential feature of the model; a good representation of unsaturated soil behaviour requires only that yield increase with suction, but makes no demands on the evolution of post-yield stiffness. Equally, the link between consolidation line slopes and the shape of the LC curve can be dropped without affecting the type of predictions obtained. What is necessary, however, is that the size of the yield surface increases with suction.

A constitutive model was developed early on (Josa *et al.*, 1992), based on BBM principles but without associating the LC shape with post-yield stiffness. The new model adopted the succession of LC yield surfaces shown in Fig. 16. As the magnitude of collapse strains is related to the distance between p_0^* and p_0^∞, the collapse strains do not increase indefinitely, but go through a maximum value corresponding to the LC surface, labelled M. Collapse strains become zero at high stresses, as expected in real soils. In addition, the relationship between the variation of void ratio and $\ln p$ becomes non-linear. In spite of the changes, the model maintained a predictive capability similar to that of the BBM.

Other modifications were proposed by Wheeler & Sivakumar (1995) using model functions more closely based on experimental results, and by Cui *et al.* (1995) and Cui & Delage (1996), adopting a saturated yield function typical of anisotropically consolidated soils. As discussed later, double structure models incorporating the BBM were also developed to account for the special characteristics of expansive clay behaviour (Gens & Alonso, 1992; Alonso *et al.*, 1999; Sánchez *et al.*, 2005).

Returning to the original BBM, it can be stated that, in spite of its simplicity, the model provides a consistent and complete tool to predict unsaturated soil behaviour while being compatible with conventional models for saturated soils. The model is consistent because it was based on classical hardening plasticity theory, and it is complete in the sense that it gives a prediction for any prescribed change of stresses, strains and/or suction. As shown in the next section, the model reproduces satisfactorily quite a number of typical features of unsaturated soil behaviour. Naturally, if a close quantitative reproduction of soil behaviour is sought, it will be necessary to resort to constitutive laws of a higher degree of complexity.

Some features of unsaturated soil behaviour

To focus the discussion, most attention is paid here to the modelling of collapse and strength behaviour, two fundamental aspects of unsaturated soil behaviour relevant to engineering applications. It is well recognised that the behaviour of an unsaturated collapsing soil upon wetting is dependent on the magnitude of applied stress. Collapse (compression) strains are observed only when the applied

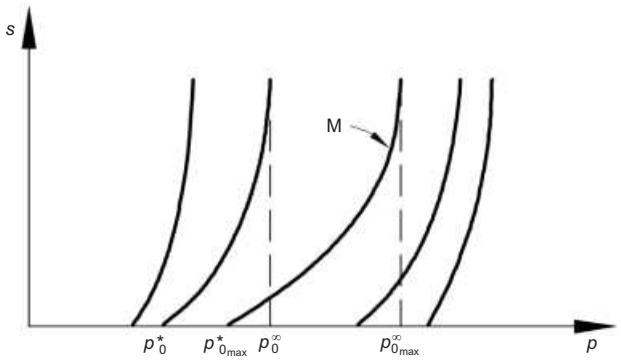

Fig. 16. Succession of LC yield surfaces in the model of Josa *et al.* (1992). It predicts a maximum of collapse at yield surface M

stresses are larger than a certain threshold value: below this, only small volume increases are observed, except, of course, when dealing with expansive clays. Fig. 17 shows a typical example of this behaviour, obtained from wetting triaxial tests on K_0-consolidated samples of compacted Lower Cromer Till (Maswoswe, 1985). In this case, the threshold value is under 100 kPa. This type of behaviour arises directly from the formulation of the BBM model, as illustrated in Fig. 18. If the state of the material is at a point such as C, wetting results in collapse strains, the magnitude of which can be derived from the movement of the LC yield curve from its initial position LC_i to its final location LC_C. However, if the applied stress is low (such as that corresponding to point A), the stress path during wetting lies completely in the elastic domain, and only a small elastic swelling will ensue. It can also be seen in Fig. 18 that, when the soil collapses on wetting, the final state of the soils lies on, or very close to, the virgin consolidation line of the saturated soil. This is again a commonly observed behaviour in many unsaturated soils, and it is predicted by the model. Since the movement of the LC yield surface is the same whether wetting from C to N or consolidating under saturated conditions to MN (Fig. 18(a)), the plastic volumetric strains will be the same. Elastic strains will also be equal, as they are stress path independent. Therefore the total volumetric strains predicted by the model are equal for the two cases, and hence the final state of the soil after collapse will be the same as that obtained in virgin consolidation in saturated conditions.

An additional prediction arises from inspection of Fig. 18. There must be a range of intermediate stress magnitudes (such as that corresponding to point B) for which the volumetric behaviour upon wetting is more complex. According to the model formulation, if a specimen is wetted from point B, it should exhibit small swelling strains initially, followed by larger irreversible compression strains as the LC yield curve is crossed. This behaviour should therefore be observed in some wetting tests, but only if they are performed with suction control; otherwise only the net collapse strains due to flooding of the sample are measured.

A comprehensive experimental study on the collapse behaviour of compacted Pearl clay ($w_L = 49$, $I_P = 27$) using a suction-controlled triaxial apparatus has been reported by Sun *et al.* (2004, 2007c). Internal measurements by local transducers provided the necessary information to track volume changes during the test, always a major issue in triaxial testing of unsaturated soils (Fig. 19). The samples were formed at various initial densities, and wetting was performed under different applied stresses. The behaviour

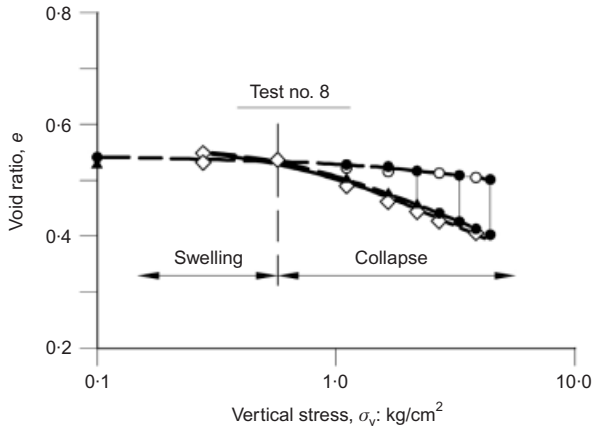

Fig. 17. Wetting tests on K_0-consolidated samples of compacted Lower Cromer Till under different applied stresses (Maswoswe, 1985)

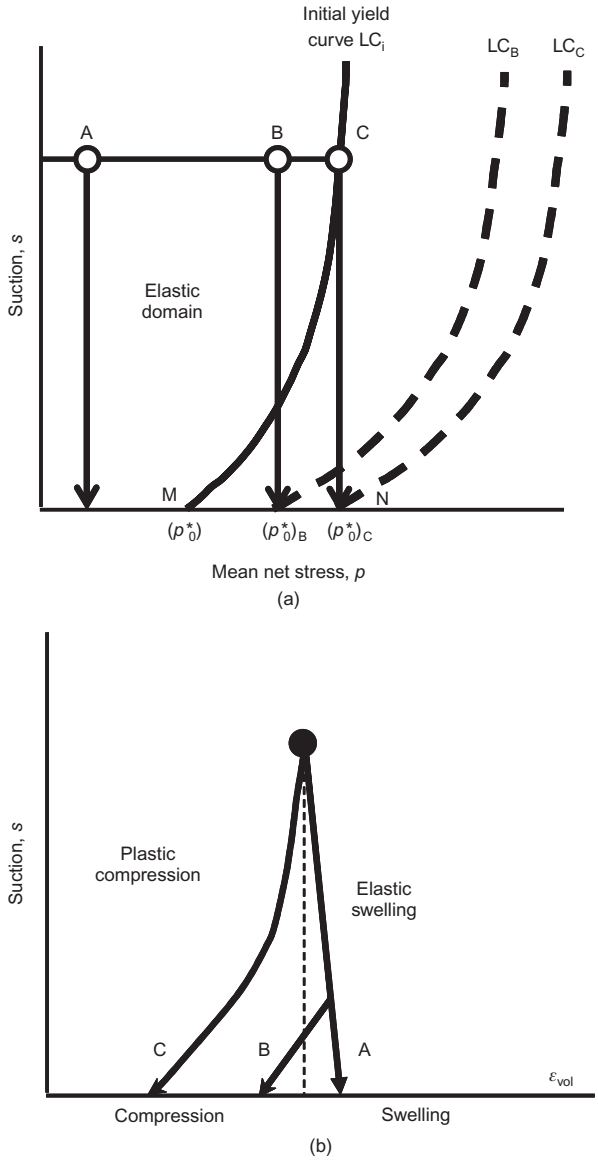

Fig. 18. (a) Stress paths for wetting tests performed under three different applied stresses; (b) predicted volumetric strains for wetting tests performed under three different applied stresses

observed has confirmed well-established features of unsaturated soil behaviour: collapse strains are larger for the looser samples and, after wetting, the soil state lies very close to the saturated consolidation line (Fig. 20). In this case, collapse strains do not increase monotonically with increasing wetting stress, but they exhibit a maximum at an intermediate value. Focusing on a particular set of tests, Fig. 21(a) shows the evolution of volumetric strains in three wetting tests as suction is reduced. It is interesting to note that, for the test under the lowest applied stress (49 kPa), the specimen initially swells on wetting until reaching a suction value where the strain direction reverses and collapse compressive strains start accumulating. This is the strain reversal predicted by the BBM, and corresponds to an initial location of the LC yield curve as that depicted in Fig. 21(b). In fact, similar observations of strain reversal have been made in suction-controlled tests carried out by, among others, Escario & Sáez (1973) and Sivakumar (1993). The fact that such a very specific feature of behaviour arises naturally from the BBM formulation is interpreted as an encouraging sign of the basic soundness of the model.

An intriguing observation on path dependence behaviour of unsaturated soils was reported by Barden *et al.* (1969). They

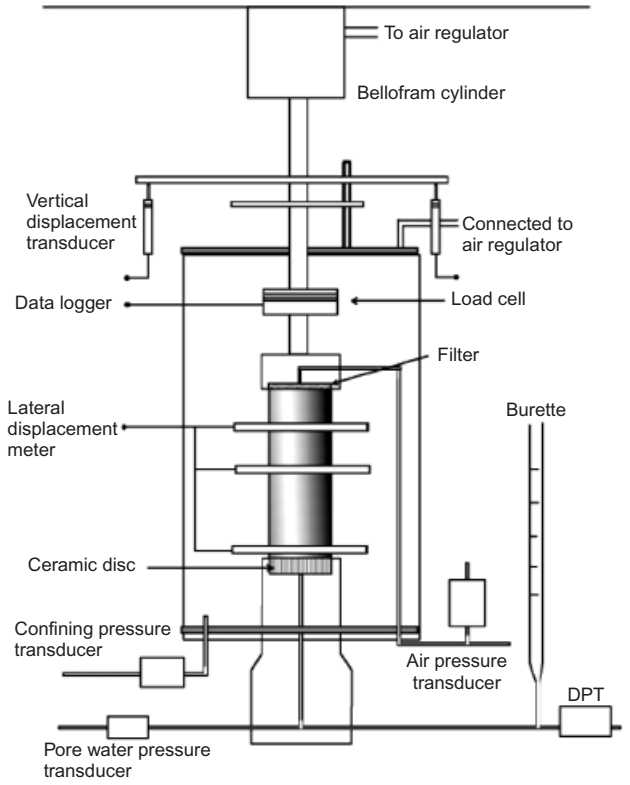

Fig. 19. Triaxial apparatus for unsaturated soils (Sun *et al.*, 2004)

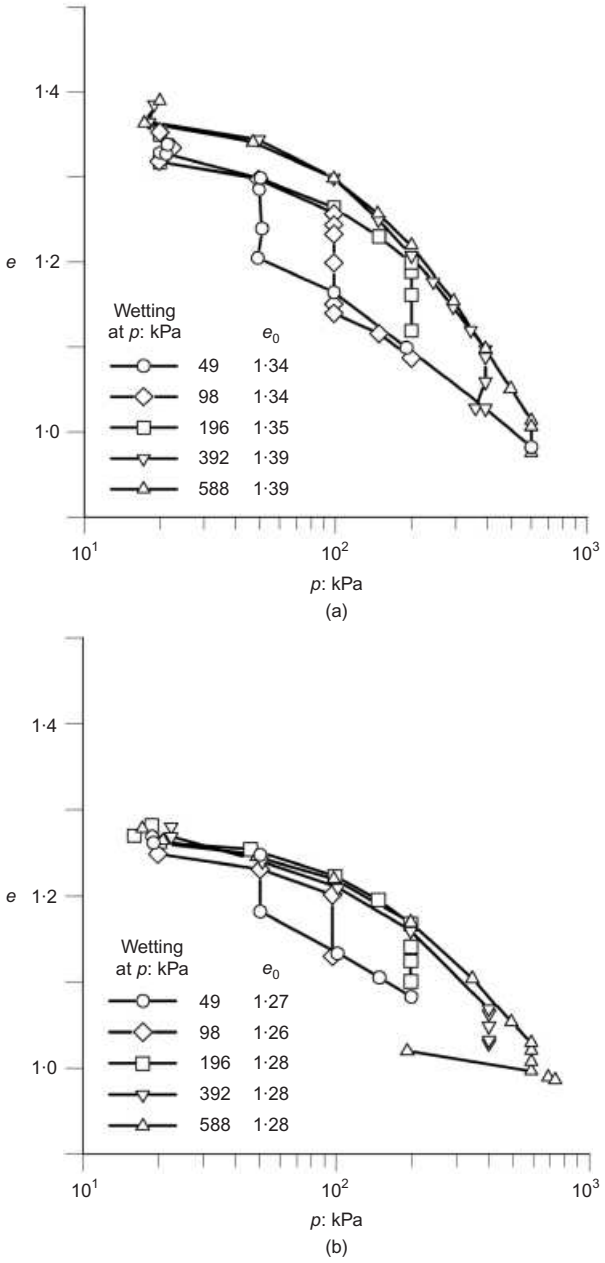

Fig. 20. Volume change behaviour of compacted Pearl clay involving wetting under different isotropic stresses (Sun *et al.*, 2004)

performed suction-controlled oedometer tests on a low-plasticity clay ($w_L = 20\%$, $w_P = 10\%$) compacted to half normal Proctor energy at a water content slightly dry of optimum. They observed that if the soil state moved between two points along different stress paths, there was no stress-path dependence of volumetric strains if the stress paths followed involved only loading or wetting stages (Fig. 22). The corresponding interpretation according to the BBM model is depicted in Fig. 23. The final location of the LC is the same for all stress paths, and therefore a stress-path-independent total volumetric strain is predicted for all tests. In contrast, when the stress path involved loading and drying stages, the final volumetric strain turned out to be stress path dependent (Fig. 24). This different behaviour is also expected from the application of the BBM. As Fig. 25 shows, in this case the final locations of the LC yield curves differ, and different volumetric strains are therefore predicted for the two stress paths. The specimen that underwent drying at the higher stress moved the LC yield curve more to the right, and therefore larger volumetric strains are predicted. The experimental results (Fig. 24) agree with this qualitative prediction.

As indicated above, in the BBM the higher strength of unsaturated soils is accounted for by the increase of the magnitude of the left intercept of the yield surface, p_s, with suction. The relationship was assumed to be linear in the original model, for simplicity. Although there have been several conflicting reports on the potential effects of suction on the value of the friction angle ϕ' (e.g. Fredlund *et al.*, 1978, 1987; Gulhati & Satija, 1981; Ho & Fredlund, 1982; Karube, 1983; Delage *et al.*, 1987; Gan & Fredlund, 1988; Toll, 1990; Khalili & Khabbaz, 1998; Toll & Ong, 2003), the assumption of a constant ϕ' value appears to be acceptable in many cases. Escario & Sáez (1986) performed a series of suction-controlled shear box tests on several unsaturated soils. A typical result is shown in Fig. 26(a). Although some variation of friction angle can be discerned, the effect of suction is apparently not large. Escario & Jucá (1989) presented data for the increase of strength over a very wide suction range (Fig. 26(b)). It is apparent that the relationship is very far from linear; indeed, the effect seems to taper off at high suction values. Modification of the BBM to incorporate a non-linear increase of strength with suction is of course straightforward, at the cost of some slight additional complexity and at least one extra parameter.

A basic component of CSSM for saturated soils is the existence of critical state surfaces unifying strength and volume change behaviour. Similarly, the BBM predicts the existence of a critical state surface for each suction value. Wheeler & Sivakumar (1995) presented an extensive series of carefully conducted suction-controlled triaxial tests on compacted kaolin. They were able to identify critical state lines for all the values of suction that they applied, in agreement with the BBM. As an example, Fig. 27 shows the critical state lines obtained for a suction of 200 kPa. The precise location and slope of the critical state lines, however, differed from the model predictions.

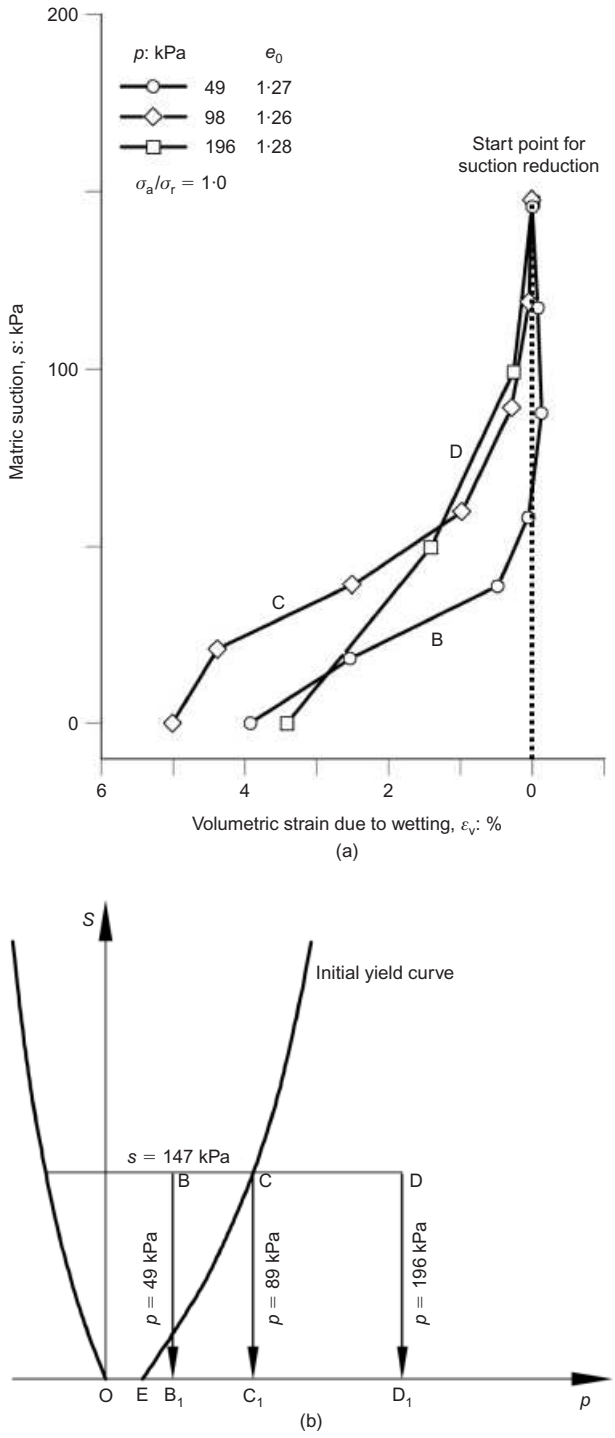

Fig. 21. (a) Volume change behaviour of compacted Pearl during wetting at three different isotropic stresses; (b) interpretation in terms of initial LC yield curve position (Sun *et al.*, 2004)

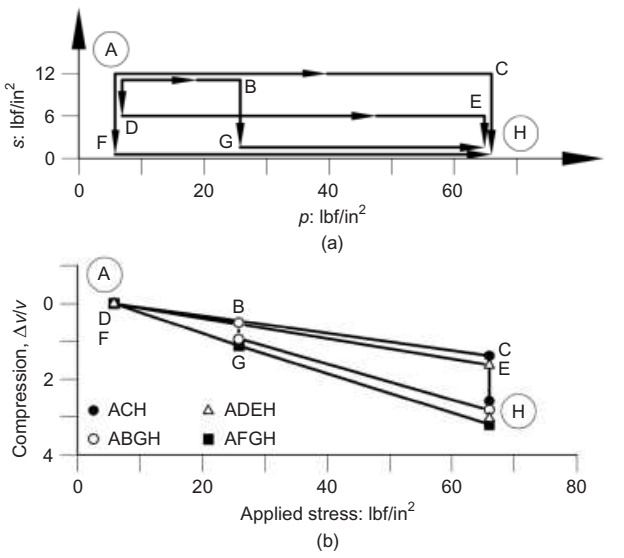

Fig. 22. Tests on a low-plasticity clay with different stages of loading and wetting (Barden *et al.*, 1969): (a) stress paths followed from common point A to common point H; (b) observed volumetric deformation for four different stress paths

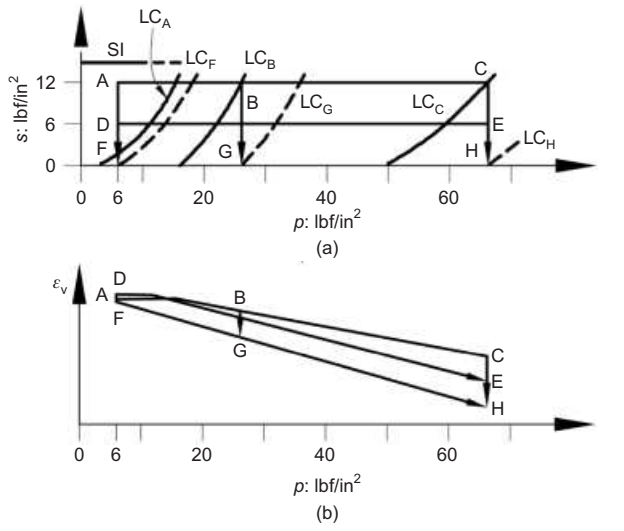

Fig. 23. Tests involving loading and wetting stages: (a) locations of the LC curves during the tests; (b) predictions of the volumetric strains from the BBM model

Although the BBM has undoubtedly been quite successful in representing the fundamental features of unsaturated soil behaviour using a very basic formulation, more complex models are required to achieve a closer reproduction of experimentally observed behaviour, and to incorporate new features of behaviour. Some instances are presented in the following sections.

A microstructure-based constitutive model

As an example of a later generation of models, the constitutive law presented in Gallipoli *et al.* (2003) is briefly discussed here. The model tries to incorporate in a more direct manner the effect of suction on behaviour, using a greatly idealised picture of the microstructure of a granular soil. Suction can affect the behaviour of an unsaturated soil by

(*a*) changing the average skeleton stress through changes in the average fluid pressure acting in the soil pores, or by
(*b*) providing an additional bonding force at particle contacts, often ascribed to capillary phenomena in the water menisci.

For a given suction, two regions can be envisaged in an unsaturated soil: the first, corresponding to the smaller pores, may be totally saturated, whereas the second, corresponding to the larger pores, contains gas and liquid in the form of interparticle menisci (Fig. 28). The relative proportions of each region vary as suction changes. An important insight (Karube & Kato, 1994; Wheeler & Karube, 1996; Wheeler *et al.*, 2003) is to realise that a variation in suction affects

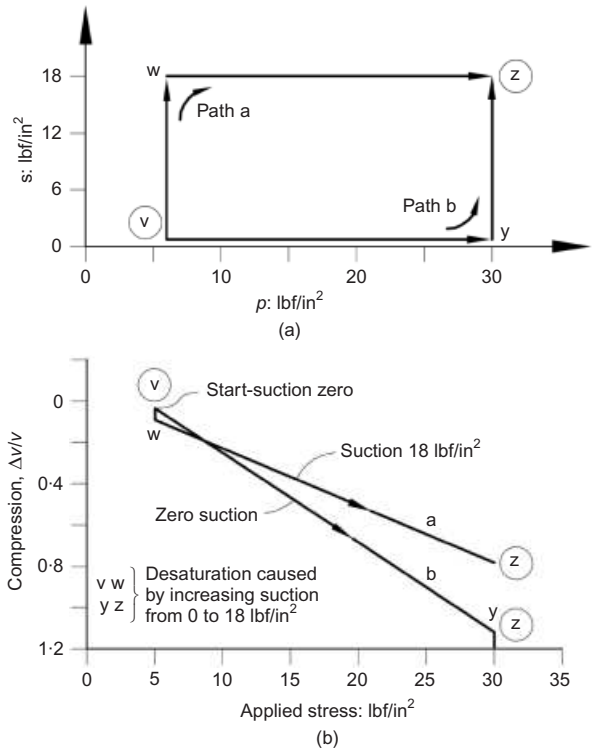

Fig. 24. Tests on a low-plasticity clay with different stages of loading and drying (Barden *et al.*, 1969): (a) stress paths followed from common point V to common point Z; (b) observed volumetric deformation for two different stress paths

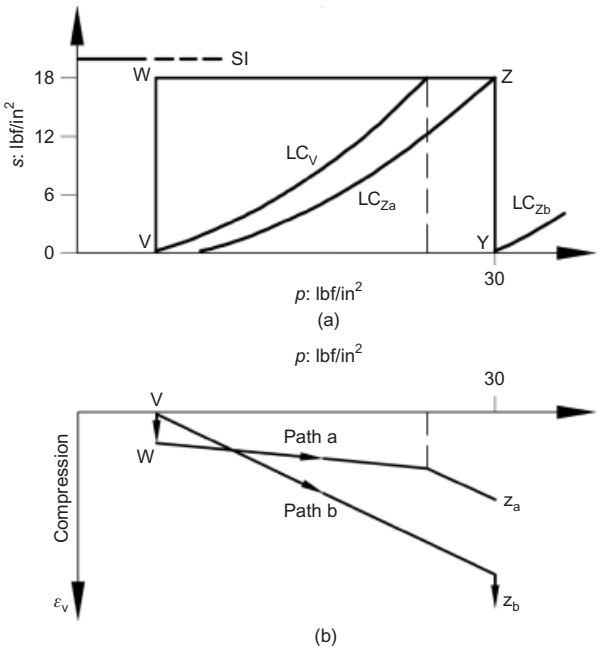

Fig. 25. Tests involving loading and drying stages: (a) locations of the LC curves during the tests; (b) predictions of the volumetric strains from the BBM model

the average skeleton stress owing to pore pressure changes in the saturated regions, whereas the modifications of the capillary-induced bonding occur in the menisci/gas region. The selection of constitutive variables for the model attempts to introduce those physical insights explicitly, although in a very approximate manner.

A first constitutive variable represents the average skeleton stress that has the same form as Bishop's (1959) expression for effective stresses,

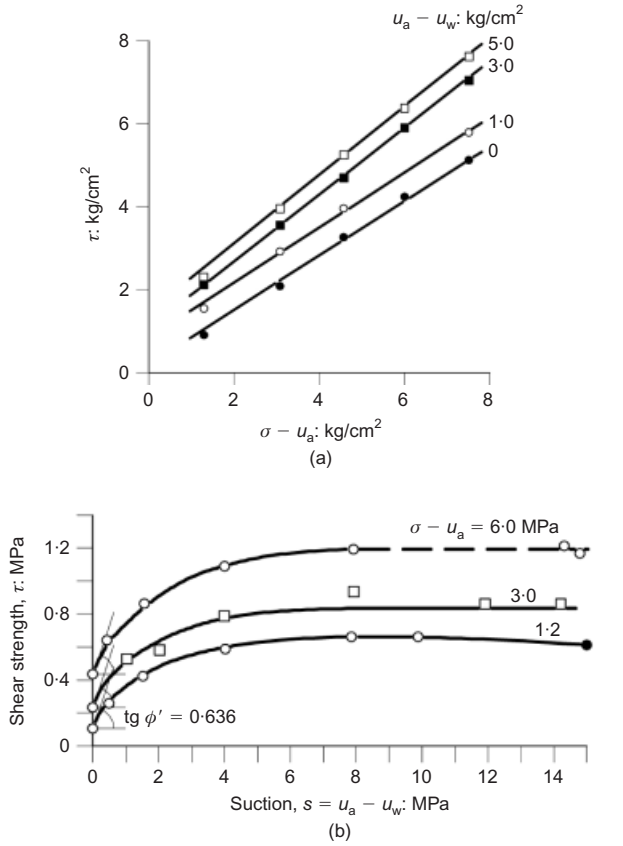

Fig. 26. Results of suction-controlled shear box tests on Guadalix red clay: (a) strength envelopes for different suctions (Escario & Sáez, 1986); (b) increase of shear strength over a large range of suctions (Escario & Jucá, 1989)

$$\boldsymbol{\sigma}' = \boldsymbol{\sigma}_t - p_g \boldsymbol{I} + \chi(p_g - p_l)\boldsymbol{I} \tag{26}$$

or, equivalently, in index form,

$$\sigma'_{ij} = (\sigma_t)_{ij} - p_g \delta_{ij} + \chi(p_g - p_l)\delta_{ij} \tag{27}$$

where δ_{ij} is Kronecker's delta. From this perspective, χ is a scaling parameter averaging the effect of the matric suction over a representative volume of soil. Although there have been some proposals that χ should be related to area fractions (e.g. Vanapalli *et al.*, 1996; Loret & Khalili, 2002; Laloui *et al.*, 2003), those fractions are difficult to estimate in practice. Here, the common approach of adopting volume averaging is used by making χ equal to the degree of saturation S_l. The average skeleton stress is also frequently called Bishop's stress.

The second constitutive variable must be related to the bonding effect of the capillary forces at interparticle contacts. Indeed, there are several analogies that can be identified between the behaviour of bonded/cemented soils and the behaviour of unsaturated soils (Kavvadas, 2000), although they are not exactly equivalent (Laloui & Nuth, 2009). Similarly to bonded soil, interparticle forces provide a stabilising effect with respect to relative movement and slippage between particles. Features of unsaturated soil behaviour must be the result of the bonding and debonding phenomena associated with the formation and disappearance of water menisci of interparticle contacts. A difference between unsaturated and cemented soils is that, in the latter, if the bonds are damaged they very rarely will heal: degradation is largely irreversible. In unsaturated soils, menisci may disappear and reappear in response to changes in suction and deformation. Those bonding/debonding effects

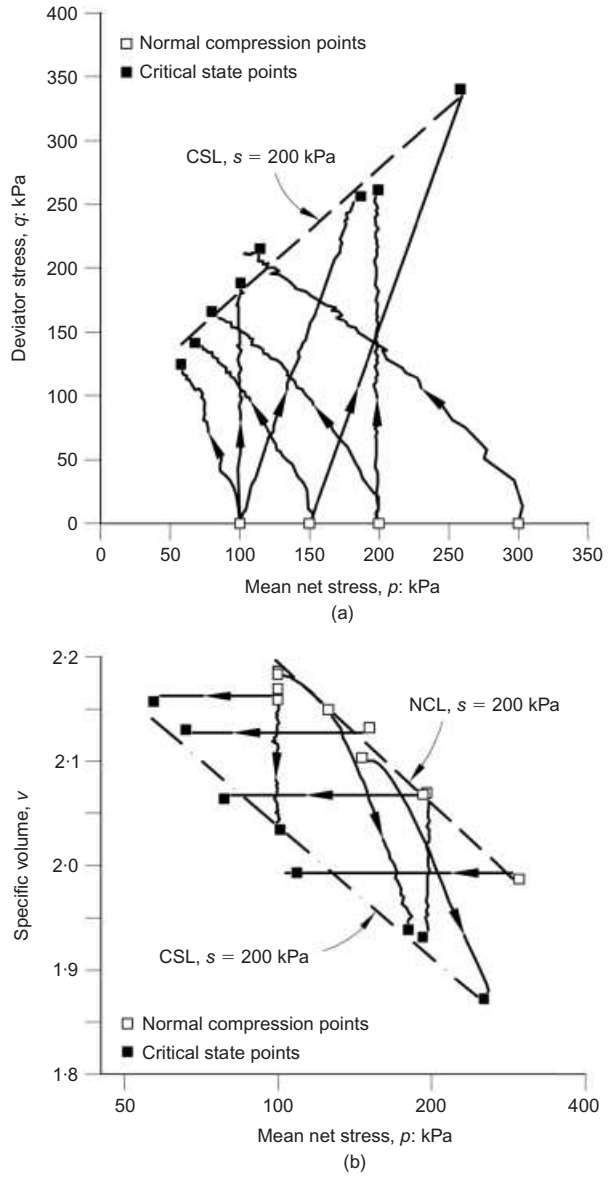

Fig. 27. Critical state lines for compacted kaolin samples tested at a constant suction of 200 kPa in the triaxial apparatus (Wheeler & Sivakumar, 1995): (a) deviator stress against mean net stress; (b) specific volume against mean net stress (log)

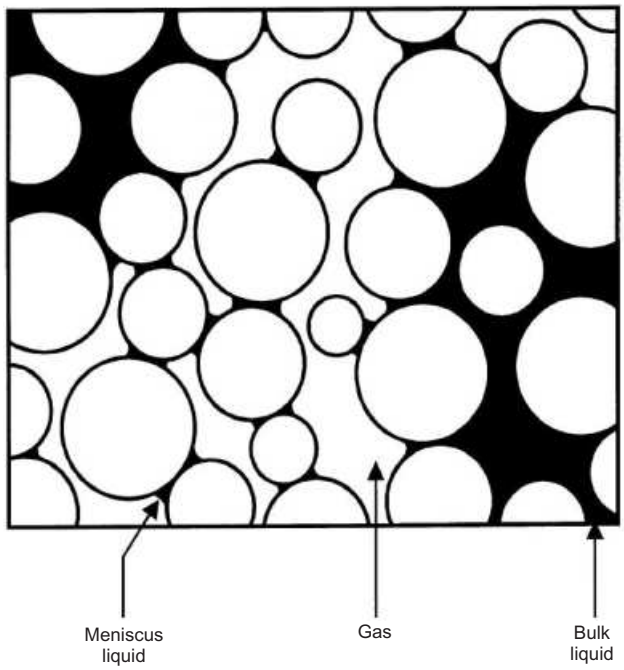

Fig. 28. Schematic view of an unsaturated soil, showing saturated regions and menisci/gas regions (Wheeler *et al.*, 2003)

cannot be easily accounted for by using the average skeleton stress alone, and a suitable constitutive variable related to the bonding phenomena, ξ, must be selected for this purpose.

The overall magnitude of the bonding force will be the product of (a) the number of water menisci per unit volume of the solid fraction and (b) the mean intensity of the interparticle forces created by the menisci. As a first approximation, it is assumed that the number of menisci is proportional to the percentage of volume occupied by the gas/menisci region, roughly $1 - S_l$. Thus the bonding-related stress variable is

$$\xi = (1 - S_l) f(s) \tag{28}$$

where $f(s)$ is the mean interparticle force, which is presumed to be dependent on suction. The function $f(s)$ is evaluated using Fisher's (1926) solution, plotted in Fig. 7.

Interparticle forces provide the bonding effect that underlies the capacity of unsaturated soils to form looser arrangements that would not be stable if the material were saturated. It is reasonable to expect that, if the variable ξ is representative of the interparticle forces, it should be directly related to the additional void ratio that an unsaturated soil is capable of sustaining. To test this hypothesis, results from isotropic compression tests performed under several suctions by Sivakumar (1993) and Sharma (1998) are considered. Sivakumar (1993) tested compacted Speswhite kaolin and Sharma (1998) a compacted mixture of bentonite and kaolin.

Figure 29 shows that the experimental results can be unified by considering that the ratio e/e_s depends on the bonding variable ξ through

$$\frac{e}{e_s} = 1 - a[1 - \exp(b\xi)] \tag{29}$$

where e is the void ratio at a specific applied average skeleton (Bishop's) stress and suction; e_s is the void ratio in the saturated virgin consolidation line at the same applied average skeleton stress; and a and b are fitting parameters. The ratio e/e_s therefore, represents the excess void ratio sustained by the unsaturated soil, and it is a simple function of the bonding variable ξ. In Gallipoli *et al.* (2003) it is further shown that the same function of the bonding variable also applies to the critical state of kaolin (Wheeler & Sivakumar, 2000) and of other soils such as a lateritic gravel (Toll, 1990). It is perhaps somewhat unexpected that a framework based on a capillary model is able to represent so successfully the behaviour of soils containing a significant proportion of clayey particles. However, the approach appears to have a wide range of applicability: recent results presented by Gallipoli *et al.* (2008) demonstrate that the same approach applies successfully to the consolidation and critical state data of Jossigny silt (Cui, 1993) and of Barcelona clayey silt (Barrera, 2002).

Using these two stress variables, a constitutive model can be developed following the same steps as in the construction of the BBM (Gallipoli *et al.*, 2003). The resulting model has a somewhat higher degree of complexity, but it is capable of reproducing fairly involved features of behaviour using a single yield surface. An example is provided in Fig. 30(a), where the results of a test performed by Sharma (1998)

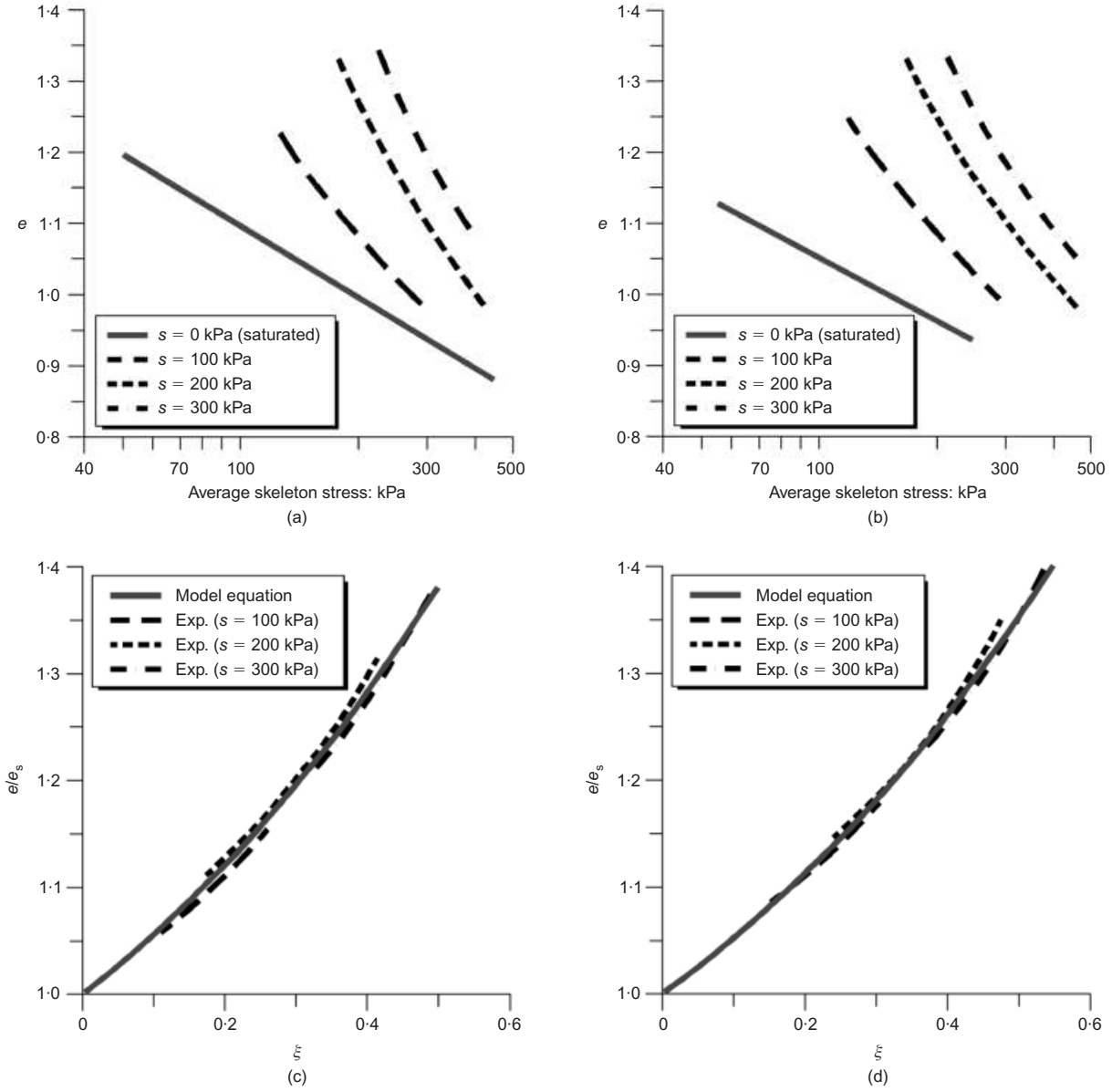

Fig. 29. (a) Normal isotropic compression lines at constant suction in terms of average skeleton stress (Sharma, 1998); (b) excess void ratio over the stable saturated void ratio (e/e_s) as a function of the bonding variable ξ (data by Sharma, 1998); (c) normal isotropic compression lines at constant suction in terms of average skeleton stress (Sivakumar, 1993); (d) excess void ratio over the stable saturated void ratio (e/e_s) as a function of the bonding variable ξ (data by Sivakumar, 1993) (Gallipoli *et al.*, 2003)

involving two cycles of wetting and drying are plotted together with the computed results using the model. Good agreement can be noted, in spite of the rather intricate behaviour observed. Fig. 30(b) shows the stress path followed by the test (in the space defined by the average skeleton stress and the bonding variable ξ) and the successive locations of the LC yield curve of the model. Naturally, to be able to draw the stress paths, it is necessary to know the value of the degree of saturation throughout the test. It is quite apparent that, in the space of the new variables, the stress paths followed by simple drying/wetting tests become quite involved and non-intuitive. It is interesting to note that the additional compression that is observed in both drying stages would not be obtained by the BBM model unless an additional yield surface with a complex hardening behaviour was specified. In the new model, the behaviour is readily reproduced employing a single LC yield surface and no additional assumptions.

Coupling hydraulic and mechanical behaviour

The hydraulic constitutive behaviour linking suction and degree of saturation (or water content) plays an important role in the case of unsaturated soils: retention curve and mechanical behaviour are in fact coupled. Changes in degree of saturation per se produce mechanical effects whereas, in turn, soil deformation modifies the degree of saturation. In the BBM and other models, the hydraulic behaviour was simply represented by an ad hoc state surface. If the model is defined in terms of net stresses, the hydraulic component is separate from the mechanical one, so inaccuracies in the hydraulic formulation do not affect directly mechanical predictions, except when soil parameters are made to depend on water content (Chiu & Ng, 2003; Thu *et al.*, 2007). On the other hand, in models where the degree of saturation or other hydraulic parameters enter the definition of the constitutive variables, the hydraulic-mechanical constitutive coupling must be carefully considered.

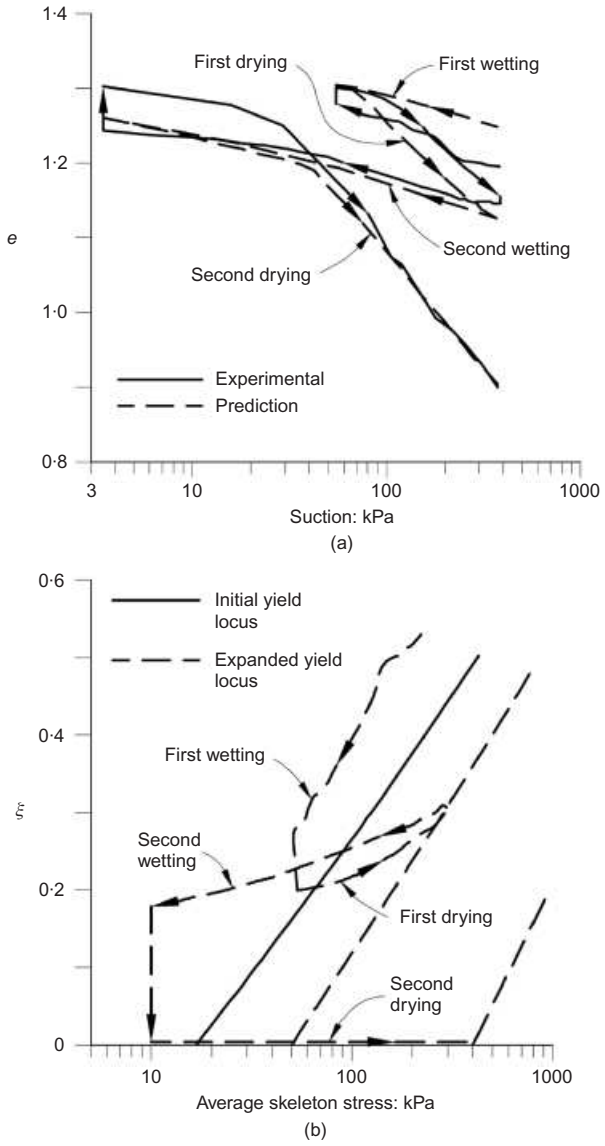

Fig. 30. (a) Experimental results and model predictions for wetting–drying cycles of a specimen of compacted bentonite–kaolin mixture subjected to a constant isotropic net stress of 10 kPa (experimental data from Sharma, 1998); (b) stress path and location of the successive yield curves (Gallipoli *et al.*, 2003)

The hydraulic component of the constitutive model for unsaturated soils was first explicitly taken into account by Wheeler (1996) and Dangla *et al.* (1997). Probably, the first full attempt to couple the hydraulic and mechanical components of the model was presented in Vaunat *et al.* (2000b). Hydraulic hysteresis and irreversible changes of degree of saturation were considered in the context of elasto-plasticity and coupled to the BBM model via the specification of two additional yield surfaces: SI (suction increase) for drying processes and SD (suction decrease) for wetting processes. Subsequently, Wheeler *et al.* (2003), based on concepts put forward in Buisson & Wheeler (2000), proposed an elasto-plastic constitutive modelling coupling hydraulic hysteresis and mechanical behaviour. By an adequate choice of stress variables and hydraulic behaviour, very simple shapes (straight lines) of the LC, SI and SD could be adopted, the complexity of the behaviour arising from the coupling between the three yield curves.

The consistent incorporation of the hydraulic component allows the resulting constitutive law to be considered in a thermodynamic context along the lines proposed by Collins & Houlsby (1997). This has been done by Sheng *et al.* (2004), using a hydraulic model that incorporates hydraulic hysteresis in an elasto-plastic framework. Again, the hydraulic model is coupled to the mechanical component through the formulation of additional SI and SD yield curves. For simplicity, in this particular model the three yield curves are not coupled, but move independently of each other. The constitutive variables selected to develop the formulation are the average skeleton stress (or Bishop's stress) and suction. The constitutive model is depicted graphically in Fig. 31.

For uncoupled materials in which the elastic modulus is independent of plastic strain, it should be possible to separate the plastic work increment into two components (Collins & Hilder, 2002),

$$\mathrm{d}W^{\mathrm{p}} = \mathrm{d}\psi_2 + \mathrm{d}\phi \tag{30}$$

where $\mathrm{d}W^{\mathrm{p}}$ is the plastic work increment, $\mathrm{d}\psi_2$ is the increment of the part of the Helmholtz free energy that depends

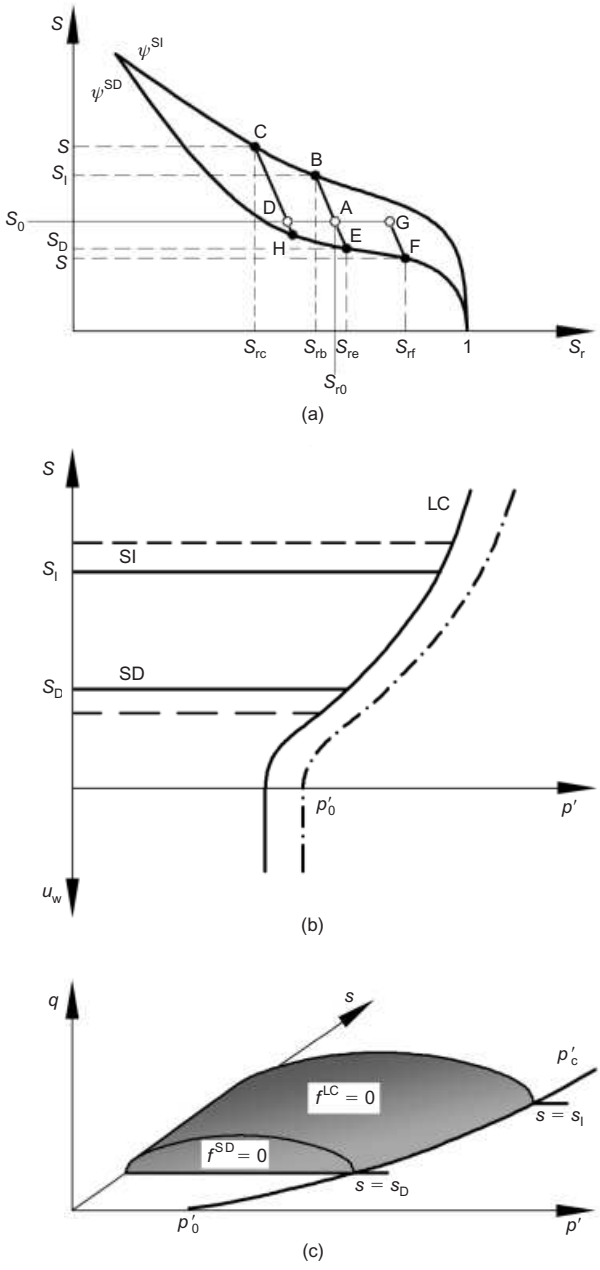

Fig. 31. Coupled hydraulic-mechanical constitutive law (Sheng *et al.*, 2004): (a) hydraulic behaviour under constant void ratio; (b) SI, SD and LC yield curves in the isotropic plane; (c) three-dimensional view of the yield surfaces

on plastic strains only, and $d\phi$ is the dissipation increment. The basic thermodynamical requirements for the constitutive model are that (a) the dissipation is strictly positive for any non-zero plastic strain, and (b) the free energy $d\psi_2$ yields zero when integrated over a closed loop of plastic strain.

In triaxial stress variables, the plastic work increment can be written as

$$dW^p = p' d\varepsilon_v^p + q d\varepsilon_\gamma^p + n s_I dS_l^p + n s_D dS_l^p \quad (31)$$

where p' is the mean Bishop's stress, q is the triaxial deviatoric stress, ε_v is the volumetric strain, ε_γ is the triaxial deviatoric strain, n is the porosity, s is suction and S_l is the degree of saturation. The superscript p denotes plastic. The third and fourth terms will occur when the SI or SD yield curves are engaged respectively. To obtain a suitable formulation from the thermodynamical point of view, it is necessary to postulate that the flow rule of the SI and SD yield surfaces is associated, and that therefore plastic volumetric and plastic deviatoric strains are caused only by the movement of the LC yield curve. In this case it is possible to identify the two thermodynamic functions with the correct set of properties,

$$d\psi_2 = \frac{1}{2} p' d\varepsilon_v^p + n s_I dS_r^p + n s_D dS_r^p \quad (32)$$

$$d\phi = \frac{1}{2} p' \frac{(d\varepsilon_v^p)^2 + (M^2/\zeta)(d\varepsilon_\gamma^p)^2}{\sqrt{(d\varepsilon_v^p)^2 + (M^2/\zeta)(d\varepsilon_\gamma^p)^2}} \geqslant 0 \quad (33)$$

where M is the slope of the critical state line in q–p' space, and ζ is a parameter defining the flow rule of the main yield surface ($\zeta = 1$, for associated plasticity). The dissipation function (equation (33)) is obviously strictly positive whenever the plastic strains are non-zero, as required. Equations (32) and (33) indicate that the plastic yielding at the suction-increase and suction-decrease yield surfaces does not contribute to the plastic dissipation, but only to the plastic work. This means that all plastic work associated with a plastic increment of degree of saturation is stored, and can be recovered during a reversed plastic increment of saturation. This plastic work is very much the same as the 'locked-in elastic energy' due to the shift or back stress described in Collins & Hilder (2002).

In this way, it has been demonstrated that it is possible to construct a hydromechanical constitutive law, accepting some restrictive assumptions, consistent with a thermodynamical framework. Tamagnini & Pastor (2005) have performed a similar exercise for a generalised plasticity model, showing that this thermodynamic consistency is not limited to a single class of models.

Cemented unsaturated soils

Most of the experimentally observed behaviour mentioned above has been obtained from laboratory tests on compacted soils; far less information is available for natural unsaturated soils. The unavoidable variability of natural soils makes them less suited to fundamental investigation, as it is quite difficult to achieve adequate repeatability of test results. An additional complexity arises from the fact that soils in arid regions are likely to be cemented to some degree. Wind-blown deposits such as loess exhibit open structures and a certain amount of rather soft bonding: this is also the case for other natural materials such as volcanic aggregates, as well as gypseous, salty and carbonated silts and sands. Residual soils are also frequently bonded as a relict of the rock structure still present to some degree within the weathered soil.

Building on the contribution by Leroueil & Vaughan (1990), Gens & Nova (1993) proposed a set of conceptual bases for developing constitutive models for saturated bonded or cemented soils. It is based on the introduction of a bonding parameter that allows a bonded soil to sustain a higher void ratio than would be possible for the same soil without any bonding (Fig. 32(a)). The outcome is a series of classical yield surfaces, the sizes of which increase with increasing amount of bonding (Fig. 32(b)). The parallels with the effect of suction in unsaturated soils are evident, suggesting that a model for cemented unsaturated soils could be obtained by simply adding the effects of suction to those of bonding. However, the situation may be more complex, because there may be some interaction between the effects of suction and bonding, as surmised in Alonso & Gens (1994). Lack of experimental evidence at the time prevented this issue from being settled.

Subsequently, Leroueil & Barbosa (2000) carried out a systematic, well-controlled series of constant strain rate (CSR) oedometer tests on artificially cemented and uncemented soils under controlled suction (Figs 33(a) and 33(b)). The samples were made by statically compacting a Brazilian saprolite from gneiss at a water content of 14% and void ratio of 1·4. In one of the test series, 2% cement was added to the

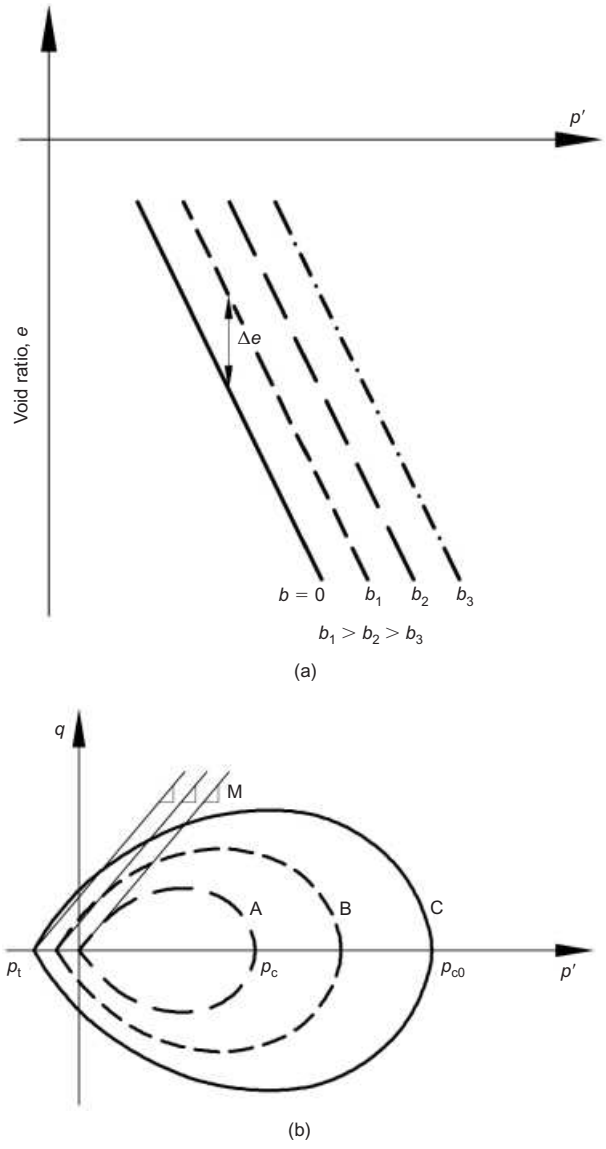

Fig. 32. (a) Consolidation lines for soils with increasing degrees of bonding; (b) successive yield surfaces for soils with increasing degrees of bonding (surface A corresponds to unbonded material) (Gens & Nova, 1993)

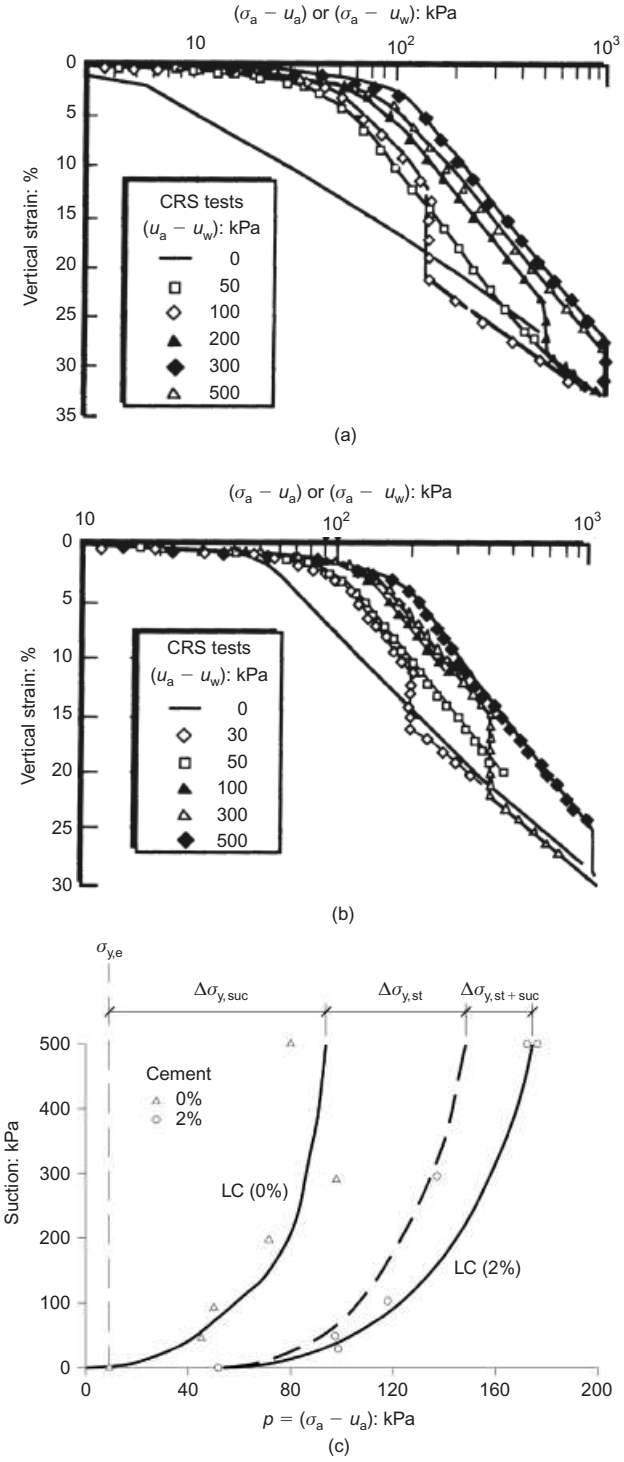

Fig. 33. (a) One-dimensional compression curves for uncemented samples; (b) one-dimensional compression curves for (2%) cemented samples; (c) loading–collapse (LC) curves for cemented and uncemented soil (Leroueil & Barbosa, 2000)

soil before compaction to obtain a bonded soil. The specimens were subsequently cured for 45 days before testing. The results in terms of yield stress points are plotted in Fig. 33(c). Curve LC(0%) is the LC yield curve for the uncemented soil. It was found that cementation increased the yield stress for the saturated sample by $\Delta\sigma_{y,st}$. If the bonding effect could be simply added to that of suction, the dashed LC line of Fig. 33(c) would be obtained. Instead the curve LC(2%) is observed: suction appears to reinforce the effect of bonding. One likely reason may be that the cement strength increases with suction, although there may be also some fabric differences between cemented and uncemented soils (Leroueil & Barbosa, 2000). Further developments in the constitutive description of unsaturated bonded soils have recently been presented (Garitte *et al.*, 2006; Yang *et al.*, 2009).

Porous materials containing oil and water

Sometimes the two fluids occupying the pore space are oil and water, a frequent situation in petroleum or environmental engineering. From a conceptual point of view, however, the condition of the porous material is very similar to that of an unsaturated soil containing air and water: there is a wetting fluid, water, and a non-wetting fluid, oil in this case (Fig. 34). Therefore capillary and suction phenomena should be analogous, although, naturally, the properties of the interface are quite different. Matric suction corresponds to the difference between oil and water pressures, and stabilising forces should appear at the interparticle contacts owing to the presence of water menisci and water/oil interfaces.

This similarity has been exploited by Delage *et al.* (1996), De Gennaro *et al.* (2004) and Priol *et al.* (2005, 2006) in their studies of oil-reservoir chalks. Fig. 35(a) shows the results of constant suction oedometer consolidation tests on Lixhe chalk containing different proportions of oil in the pores: the larger the proportion of oil, the larger is the suction. The consolidation lines plot more to the right for the higher oil contents and higher suctions, the same behaviour as in conventional unsaturated soils. The analogous behaviour also extends to collapse behaviour. Fig. 35(b) shows the effect of wetting of a sample under constant stress. Although it is difficult to achieve full water saturation, even a limited increase in water content (and therefore suction reduction) causes significant compressive strains. This situation would be akin to that occurring in an oilfield when resorting to flooding to increase production or to stabilise reservoir pressures.

To a large extent the authors were able to interpret their experimental results and model them successfully in terms of a standard unsaturated soil model such as the BBM (Fig. 36). It must be borne in mind that, in chalk, wetting-induced compression results from a combination of loss of capillary forces and from weakening of the interparticle bonds—a complex physico-chemical interaction. Although it is likely that the second mechanism is the more significant one, it appears, nevertheless, that the overall phenomenon can be adequately represented by using oil–water suction as a key parameter (De Gennaro *et al.*, 2004).

Constitutive variables and model classification

Some examples of constitutive models for the mechanical behaviour of unsaturated soils have been presented in the

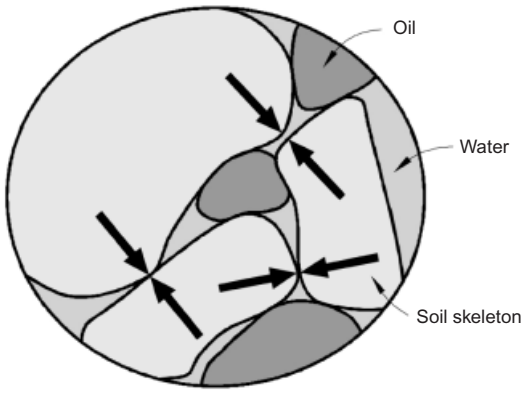

Fig. 34. Schematic representation of an unsaturated material containing oil and water in its pore space

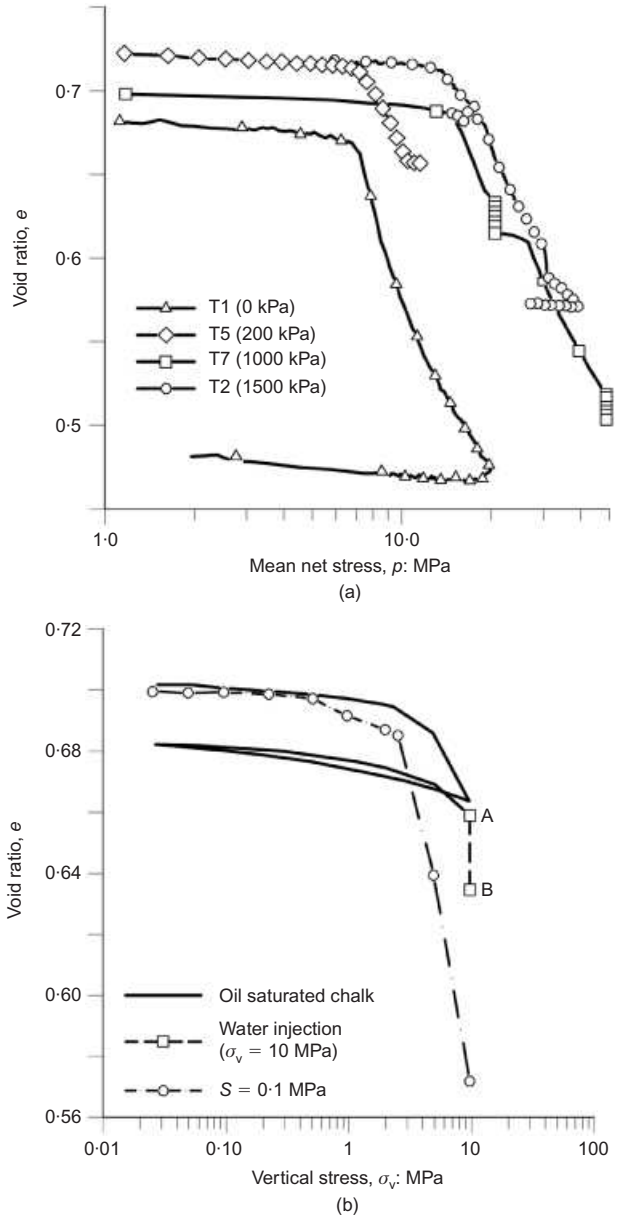

Fig. 35. Suction-controlled oedometer tests on oil-containing Lixhe chalk: (a) consolidation tests with different suctions (modified from Priol *et al.*, 2005); (b) wetting test at constant stress (De Gennaro *et al.*, 2004)

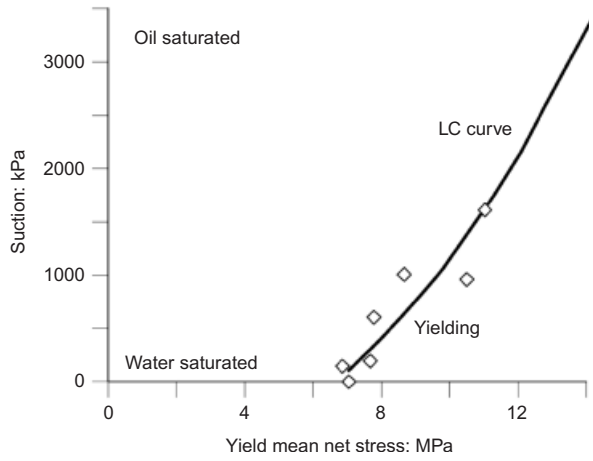

Fig. 36. LC yield curve for oil-containing Lixhe chalk (De Gennaro, personal communication 2007)

previous sections to illustrate the range of possibilities in this respect. Numerous constitutive models for unsaturated soils have been developed in recent years: many of them adopt a classical elasto-plastic framework, but other types of formulation have also been used, such as generalised plasticity (Bolzon *et al.*, 1996; Sánchez *et al.*, 2005; Tamagnini and Pastor, 2005) or hypoplasticity (Masin & Khalili, 2008). To conclude this section on mechanical constitutive models for unsaturated soils, a series of general remarks on these constitutive developments are presented. For more detailed comments, several review articles on the subject are available (Gens, 1996; Wheeler & Karube, 1996; Jommi, 2000; Wheeler, 2005; Gens *et al.*, 2006, 2008b; Sheng & Fredlund, 2008; Sheng *et al.*, 2008b).

A variety of constitutive variables have been used to define the different models, a matter that has sparked a certain amount of controversy. In principle, any relevant variable can be selected as a constitutive variable but, for engineering purposes, constitutive laws are usually (but not always) defined in stress space: that is, using scalar, vector or tensor variables that have units of stresses. However, it would be possible to adopt other types of variable (e.g. degree of saturation, water content) if they had a greater descriptive or predictive power.

There is general agreement that at least two constitutive variables are generally required to represent adequately the full range of unsaturated soil behaviour, that is, including strength and deformation. As stated by Jommi (2000): 'In fact, no single stress variable has ever been found which, substituted for effective stress, allows a description of all the aspects of the mechanical behaviour of a given soil in the unsaturated range.' It is convenient to refer to them as the first and second constitutive variables (FCV and SCV). They are intentionally not called constitutive stress variables, to leave open the possibility that variable types other than stresses might be adopted. Usually, the FCV tries to account for the overall stress state of the soil, whereas the SCV tends to address mainly the effects of suction changes. Thus, if the constitutive variables chosen are net stresses and suction (as in the BBM), the FCV (net stress) responds to loading changes whereas the SCV (suction) deals with environmental actions related to suction variations. The same comment can be made if, as in the model of Gallipoli *et al.* (2003) described above, average skeleton stress and a bonding parameter are used. In any case, in the majority of constitutive models developed, those two constitutive variables normally adopt the general form

FCV:

$$(\sigma_t)_{ij} - p_g \delta_{ij} + \mu_1(s, S_l)\delta_{ij} \tag{34a}$$

SCV:

$$\mu_2(s, S_l) \tag{34b}$$

The FCV is expressed as a modified stress tensor; in contrast, for the SCV, aiming to represent the additional effects of suction, a scalar is usually adopted. However, one of the main effects of suction is the generation of stabilising interparticle forces. It would be reasonable to expect, as pointed out by Li (2003) and Scholtès *et al.* (2009), that the SCV should incorporate some kind of fabric measure of the soil; the variable would then no longer be a scalar, more likely a tensor. Indeed, if suction effects have a tensorial form, it is questionable that an averaged pressure in the fluid phase is an adequate representation of the role of suction, even when defining the FCV (Scholtès *et al.*, 2009). In any case, the use of a tensorial form for the effects of suction is difficult to accomplish, owing to the complexity of determining the soil fabric and its variation as soil deforms. Accord-

ingly, scalar definitions of the SCV have been dominant hitherto. It can be argued that suction has a different physical nature from stress variables (Lu, 2008), and some objections have been put forward concerning the validity of combining stresses and suction into a single expression (Baker & Frydman, 2009). However, there does not seem to be any *a priori* reason against a constitutive variable combining different types of variable if an adequate description of soil behaviour is thereby achieved.

Ideally, the selected constitutive variables should be independent of the constitutive parameters or the state of the material, so that the constitutive space remains invariant throughout (Sheng *et al.*, 2008a). This condition is easily met in the case of saturated soils, but it is not always possible when dealing with unsaturated materials. Indeed, in saturated materials other than soils (e.g. rock or concrete), state and material parameters must be often incorporated in the definition of effective stresses for constitutive purposes (Jardine *et al.*, 2004).

A constitutive variable that has been frequently used, and for which a special status is sometimes claimed, is written as

$$\sigma'_{ij} = (\sigma_t)_{ij} - p_g\delta_{ij} + S_l(p_g - p_l)\delta_{ij} \tag{35}$$

As stated before, this variable has been called Bishop's stress (Bolzon *et al.*, 1996; Tamagnini, 2004) and also average skeleton stress (Jommi, 2000; Gallipoli *et al.*, 2003; Wheeler *et al.*, 2003). Other terms that have also been used are Bishop's effective stress, average stress (Sheng *et al.*, 2004) and generalised effective stress (Laloui & Nuth, 2009). It should be noted, however, that Bishop (1959) used a scaling factor $\chi(S_l)$ and not S_l in his expression for effective stress. In the context of unsaturated soils, equation (35) was probably first used by Schrefler (1984).

Interestingly, equation (35) arises as a relevant stress variable for unsaturated soils from a number of theoretical studies. For instance, it has been obtained by Hassanizadeh & Gray (1980) from the entropy inequality exploited by way of the Colemann–Noll principle; by Lewis & Schrefler (1987), using volume averaging; by Hutter *et al.* (1999) from mixture theory; and by Ehlers *et al.* (2004) from the theory of porous media. However, other studies reach different conclusions: Dangla *et al.* (1997) and Coussy & Dangla (2002), using an energy approach to extend Biot's theory of poroelasticity, end up with a stress variable that contains an additional term related to the work performed by the interfaces. Alternatively, Gray & Schrefler (2001), using a macroscale thermodynamic approach, conclude that the scaling parameter χ should be not the degree of saturation but the fraction of solid surface in contact with the wetting fluid. This approach is further enhanced by transferring microscale thermodynamics to the macroscale in a systematic way: additional terms related to the interfaces appear (Gray & Schrefler, 2007). Borja (2006) formulated a mechanical theory in which porous continua are viewed as a dense distribution of strong discontinuities. From the associated energy formulation, a relevant stress variable for unsaturated soils is obtained that contains the term $(1 - K/K_s)$, familiar from the work of Skempton (1961) and Nur & Byerlee (1971). K is the bulk modulus of the soil skeleton, and K_s is the bulk modulus of the solid constituent. Finally, Coussy (2007) and Coussy *et al.* (2009), using an alternative thermodynamic approach, find that the relationship between the scaling factor $\chi(S_l)$ and the degree of saturation is specific to the material examined, and depends particularly on the assumptions made regarding its microstructure. In summary, it appears that no unique expression for the relevant stress variable is obtained independently of the set of adopted assumptions.

An important contribution to this issue was made by Houlsby (1997), who derived, under reasonably general conditions, the rate of work input per unit volume of unsaturated soil (W),

$$W \equiv \frac{p_g n(1 - S_l)\dot{\rho}_g}{\rho_g} - (p_g - p_l)n\dot{S}_l + \left\{(\sigma_t)_{ij} - \left[S_l p_l + (1 - S_l)p_g\right]\delta_{ij}\right\}\dot{\varepsilon}_{ij} \tag{36}$$

where ρ_g is the gas density and ε_{ij} are the strains. In this expression the work performed by the flow of fluids is not included, and it is also assumed that, on average, the contractile skin moves with the soil skeleton—perhaps the most questionable assumption. If the gas compressibility term is neglected, the work rate input is

$$W \equiv -(p_g - p_l)n\dot{S}_l + \left\{(\sigma_t)_{ij} - \left[S_l p_l + (1 - S_l)p_g\right]\delta_{ij}\right\}\dot{\varepsilon}_{ij} \tag{37}$$

It is now possible to define sets of stress and strain variables that are conjugate to each other. An immediate choice is

$$\begin{pmatrix} (\sigma_t)_{ij} - \left[S_l p_l + (1 - S_l)p_g\right]\delta_{ij} \\ n(p_g - p_l) \end{pmatrix} \Leftrightarrow \begin{pmatrix} \dot{\varepsilon}_{ij} \\ -\dot{S}_l \end{pmatrix} \tag{38}$$

where Bishop's stress is conjugate to strains, and a modified suction is conjugate to degree of saturation. However, equation (37) can be rearranged to give the following conjugates stresses and strains:

$$\begin{pmatrix} (\sigma_t)_{ij} - p_g\delta_{ij} \\ (p_g - p_l) \end{pmatrix} \Leftrightarrow \begin{pmatrix} \dot{\varepsilon}_{ij} \\ \dot{\varepsilon}_w = \left(-n\dot{S}_l + S_l\dot{\varepsilon}_v\right) \end{pmatrix} \tag{39}$$

Now, net stress is conjugate to strains and suction is conjugate to the volumetric water content, $\varepsilon_w = nS_l$. From this perspective, therefore, the work input expression does not provide a criterion to select one set of constitutive variables in preference to the other.

However, the choice of constitutive variables is not neutral; it has a significant influence on the nature of the constitutive law developed. To examine this issue it has proved convenient to classify the constitutive laws according to the choice of FCV (Gens, 1996); a similar classification has been explored in Nuth & Laloui (2008).

Class I models adopt a FCV with $\mu_1 = 0$: that is, net stresses are used. In general, for those models, the following statements apply.

(*a*) The stress paths of conventional tests and typical loading situations are easily represented: these types of model are well suited to illustrating conceptual constitutive developments.
(*b*) The constitutive variable is independent of the material state.
(*c*) If suction is the SCV, the two constitutive variables are independent (except for the gas pressure). However, the conjugate strain variables are not independent (equation (39)).
(*d*) Continuity of constitutive variables and behaviour is not ensured at the saturated/unsaturated transition. Some procedures have been proposed to achieve continuity in numerical analysis (Vaunat *et al.*, 1997).
(*e*) The hydraulic component of the model is independent of the mechanical one; specific mechanical effects of degree of saturation are not included.

(*f*) An independent function is required to model the increase of shear strength with suction.

A recent constitutive model of this class, the SFG model (Sheng *et al.*, 2008a), is able to overcome several of the shortcomings listed above.

In class II models $\mu_1(s)$ is a function of suction, but does not include degree of saturation. In this case, the following apply.

(*a*) Representation of stress paths of conventional tests and typical loading situations is not straightforward.
(*b*) The constitutive variable is still independent of the material state if no additional parameters are included.
(*c*) The two constitutive variables are linked.
(*d*) Continuity of variables and behaviour is not automatically assured at the saturated/unsaturated transition.
(*e*) The hydraulic component of the model is independent of the mechanical one; the specific mechanical effects of degree of saturation are not included.
(*f*) The increase of strength with suction is a result of the constitutive variable definition.
(*g*) Strength and elastic behaviour can be unified with an adequate selection of the FCV (Khalili *et al.*, 2004).

Finally, in class III models, $\mu_1(s, S_l)$ is a function of both suction and degree of saturation. Constitutive models using Bishop's stress as the FCV belong to this class of models.

(*a*) Representation of the stress paths of conventional tests and typical loading situations is complex, and sometimes impossible, if data on the degree of saturation are not available.
(*b*) The constitutive variable depends on degree of saturation and, therefore, on the material state.
(*c*) The two constitutive variables are linked.
(*d*) Continuity is automatically ensured at the saturated/unsaturated transition.
(*e*) The hydraulic component of the model is closely coupled to the mechanical component, and the specific mechanical effects of degree of saturation can be included. Hydraulic and hysteresis effects can be incorporated in a natural way, but the success of the mechanical model is dependent on having an adequate hydraulic relationship. In particular, care should be taken that the product $S_l s$ that enters the definition of Bishop's stress should not take unrealistic large values at low degrees of saturation (Loret & Khalili, 2002). In that range, suctions can have extremely large magnitudes, and the product sS_l may reach absurdly high values that disrupt any model prediction.
(*f*) The increase of strength with suction is a result of the constitutive variable definition.
(*g*) Strength and elastic behaviour can be unified with an adequate selection of the FCV.

In Table 2, the main characteristics of the different model categories are listed, together with various published constitutive laws for unsaturated soils, classified according to their FCV. All three possibilities have been widely used. For the current state of the question, therefore, the selection of constitutive variables to develop constitutive models for unsaturated soils remains a matter of convenience. Sometimes Class I models are called independent stress models and Class II and Class III models effective stress[‡] models, suggesting that there is a fundamental difference between the two types of model when, in fact, they are closely related. Indeed, it is perfectly possible to transform a constitutive relationship developed in terms of the simpler constitutive variables (Class I) to a more complex stress space (Class II and III), as done by Sheng *et al.* (2003a) for the BBM and by Kohler & Hofstetter (2008) for the cap model, proving that the boundaries between the different model classes are fairly porous.

In any case, most constitutive models for unsaturated soils share a common core:

(*a*) the use of two constitutive variables to define the constitutive relationships
(*b*) the formulation of an LC yield curve or some equivalent concept
(*c*) the adoption of a saturated model as reference.

The common form of the unsaturated constitutive models can be expressed as

$$\mathrm{d}\boldsymbol{\sigma}^* = \boldsymbol{D}(\boldsymbol{\varepsilon}, s)(\mathrm{d}\boldsymbol{\varepsilon}) + \boldsymbol{h}(\boldsymbol{\varepsilon}, s)\mathrm{d}s \tag{40}$$

where $\boldsymbol{\sigma}^*$ is the constitutive stress (which depends on the assumptions of the model); $\boldsymbol{D}$ is the stress–strain constitutive matrix; and $\boldsymbol{h}$ is the stress-suction constitutive vector. Both $\boldsymbol{D}$ and $\boldsymbol{h}$ may depend on suction as well as on strains. The most significant addition to the saturated formulation is the second term, which contains the specific effect of suction, the new variable for unsaturated soils. Of course, when the degree of saturation reaches 1, equation (40) should become

$$\mathrm{d}\boldsymbol{\sigma}' = \boldsymbol{D}'(\boldsymbol{\varepsilon})(\mathrm{d}\boldsymbol{\varepsilon}) \tag{41}$$

where $\boldsymbol{\sigma}'$ is Terzaghi's effective stress and $\boldsymbol{D}'$ is the stress–strain matrix of the saturated model.

Numerical implementation of unsaturated constitutive models may require the use of some especial procedures and algorithms (Vaunat *et al.*, 2000a; Sheng *et al.*, 2003a, 2003b, 2008b; Sánchez *et al.*, 2008), but the topic is outside the scope of this lecture.

CASE HISTORIES

Foundation collapse in Pereira Barreto town, Brazil

To demonstrate the application of the developments outlined above to an engineering case, it would ideally be necessary to have a field problem in which the site investigation had included suction-controlled tests, and for which relevant field observations were available. In the case of collapse of foundations those requirements are rarely met, because, in most cases, foundation collapse comes unexpectedly, and only *post mortem* information exists. Fortunately, in the case of the foundation collapses that occurred in the Brazilian town of Pereira Barreto, most of the desired information was obtained both before and after collapse occurred. The interest of the case is enhanced by the fact that the collapse behaviour involved natural rather than compacted soils. Herein only a brief description of the key aspects of the case is presented.

[‡] The frequent use of the term *effective stress* when dealing with unsaturated soils may be misleading in the context of the usual understanding of the term in conventional geotechnical engineering, where it refers to a single combination of total stresses and fluid pressures that controls all aspects of soil behaviour. In unsaturated soils, two constitutive variables are required to fully describe their behaviour, and therefore there is no single stress variable that fulfils the role of effective stress as commonly understood in conventional soil mechanics. Although it is not impossible to envisage the development of a single effective stress model for unsaturated soils by a careful selection of the constitutive variable and of the associated hydraulic component, to the author's knowledge none has been successfully proposed hitherto.

Table 2. Classification of constitutive models for unsaturated soils according to the choice of FCV (first constitutive variable)

Class	FCV	Model features	Examples
I	$(\sigma_t)_{ij} - p_g\delta_{ij}$; $\mu_1 = 0$	Stress paths easily represented. Constitutive variable is independent of the material state. Constitutive variables are independent (except for the gas pressure). Continuity of constitutive variables and behaviour is not ensured at the saturated/unsaturated transition. The hydraulic component of the model is independent of the mechanical component; specific effects of degree of saturation are not included. An independent function is required to model the increase of shear strength with suction.	Alonso *et al.* (1990); Gens & Alonso (1992); Josa *et al.* (1992); Wheeler & Sivakumar (1993, 1995); Cui *et al.* (1995); Cui & Delage (1996); Alonso *et al.* (1999); Vaunat *et al.* (2000b); Rampino *et al.* (2000); Chiu & Ng (2003); Georgiadis *et al.* (2003); Sánchez *et al.* (2005); Thu *et al.* (2007); Sheng *et al.* (2008a)
II	$(\sigma_t)_{ij} - p_g\delta_{ij} + \mu_1(s)\delta_{ij}$	Representation of stress paths not straightforward. Constitutive variable is independent of the material state. The constitutive variables are linked. Continuity of constitutive variables and behaviour is not assured at the saturated/unsaturated transition. The hydraulic component of the model is independent of the mechanical component; specific effects of degree of saturation are not included. The increase of strength with suction is a result of the constitutive variable definition. Strength and elastic behaviour can be unified with an adequate selection of the FCV	Kohgo *et al.* (1993); Modaressi & Abou-Bekr (1994); Pakzad (1995); Modaressi *et al.* (1996); Geiser *et al.* (2000); Loret & Khalili (2000, 2002); Laloui *et al.* (2001); Sun *et al.* (2003); Russell & Khalili (2006); Masin & Khalili (2008)
III	$(\sigma_t)_{ij} - p_g\delta_{ij} + \mu_1(s, S_l)\delta_{ij}$	Representation of stress paths not straightforward and sometimes impossible. Constitutive variable definition incorporates a state parameter (S_l). The two constitutive variables are linked. Continuity is automatically ensured at the saturated/unsaturated transition. The hydraulic component of the model is closely coupled with the mechanical component. The increase of strength with suction is a result of the constitutive variable definition. Strength and elastic behaviour can be unified with an adequate selection of the FCV.	Jommi & di Prisco (1994); Bolzon *et al.* (1996); Jommi (2000); Wheeler *et al.* (2003); Gallipoli *et al.* (2003); Sheng *et al.* (2004); Tamagnini (2004); Laloui & Nuth (2005); Pereira *et al.* (2005); Oka *et al.* (2006); Santagiuliana & Schrefler (2006); Sun *et al.* (2007a, 2007b); Kohler & Hofstetter (2008); Buscarnera & Nova (2009)

Pereira Barreto town is located on the right-hand bank of the Tietê River, near the confluence with the Paraná River in the North West of São Paulo State in Brazil (Fig. 37). A 50 m high dam was constructed just downstream of the town, causing a general rise of the groundwater level in the area; the evolution of the reservoir level is shown in Fig. 38. Because it was known that some of the buildings were founded in potentially collapsible soil, a comprehensive site investigation was performed, including soil borings, in situ tests and laboratory tests. A monitoring system was also installed before the reservoir level rise: this is one of the rare occasions when the development of collapse settlements has been measured in full.

A typical soil profile is presented in Fig. 39. Part of the town is founded on a colluvium layer that overlies a residual soil; the colluvium is a lateritic fine sandy soil without active clay minerals. A thin gravel layer separates colluvium and residual soil. Some typical results from the site investigation are shown in Fig. 40. There are no major differences concerning mineralogy, grading, and Atterberg limits. However, both the SPT and CPT results show that the colluvium is in a much looser state than the residual soil; indeed, collapse behaviour was identified only in the colluvium. It is also noteworthy that the initial degree of saturation of the materials is quite low, in the region of 30–40%, consistent with the climatic conditions at the site. The saturated permeability of the colluvium is rather high: of the order of 10^{-5} m/s.

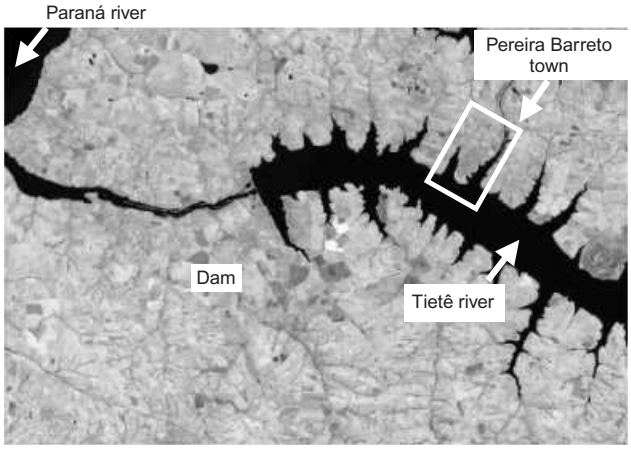

Fig. 37. Location of Pereira Barreto town, São Paulo, Brazil

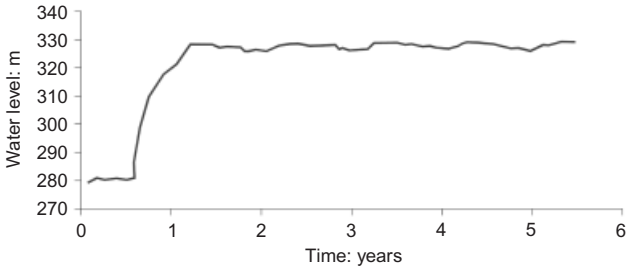

Fig. 38. Evolution of reservoir level elevation with time

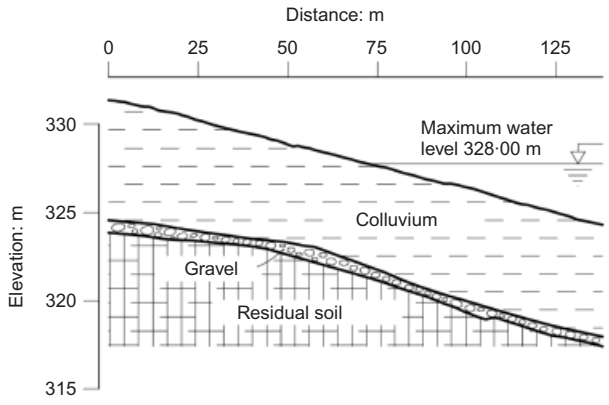

Fig. 39. Soil profile at Pereira Barreto town

As expected, the groundwater table rise brought about collapse settlements that affected some buildings, causing various degrees of damage (Fig. 41). There were about 20 sites monitored. Here only the measurements of two buildings, PB-1 and PB-3, are discussed: they are representative of the range of foundation behaviour encountered. Fig. 42 shows the settlements of two points of the foundation of building PB-1: settlements of more than 100 mm were measured. The foundation was just over 1 m deep in the colluvium. In the same figure, the evolution of the water level as measured in a nearby observation point is also plotted: it can be seen that it reached the lower part of the colluvium layer. The same information for building PB-3 is provided in Fig. 43. The foundation is slightly shallower, and the settlements were significantly smaller, around 20 mm. In this case the water level reached only the gravel layer.

Block samples of the colluvium were obtained from the site and tested in suction-controlled oedometers. Two types of test were run: loading tests under constant suction (Fig. 44(a)), and wetting tests from two suction values (200 kPa and 60 kPa) performed under several applied stresses (Fig. 45(a)). The results obtained correspond to typical behaviour of an unsaturated soil. The consolidation lines (Fig. 44(b)) plot further to the right as suction increases; the saturated consolidation line constitutes the lower behaviour bound. In Fig. 45(b) the results corresponding to the collapse wetting tests performed from a suction of 60 kPa are shown. After collapse, the void ratio–stress state of the soil lies close to the saturated consolidation line. Similar results but higher collapse values were obtained when the samples were flooded at a suction of 200 kPa. The test results have been modelled using the BBM, and the estimated LC yield curve is shown in Fig. 46. The computed collapse strains corresponding to wetting tests from 60 kPa and 200 kPa suction values are compared with the experimental results in Fig. 47. The prediction is good at low stresses, but collapse strains are overestimated at higher stress values. This is a consequence of the inability of the standard BBM to reproduce a maximum of collapse. However, since the agreement was adequate for the relevant stress level range, the BBM, calibrated in this manner, was used to perform the calculations. The challenge is to reproduce the range of observed field behaviour using a single set of parameters obtained from the laboratory testing programme.

The settlements computed in this way have been added to Figs 42(c) and 43(c). The agreement is quite satisfactory. For building PB-1 (Fig. 42(c)) large settlements are predicted, which start only when the water level is already quite high. It is also interesting to note that a rather large reactivation of settlement is computed when a rather modest increase of water level occurs, just as observed. The more muted settlement response of the foundation of building PB-3 (Fig. 43(c)) is also successfully reproduced. The different behaviour is due to the different foundation arrangements and, in particular, to differences in the soil profile. In the latter case the water level does not reach the collapsible colluvium layer, but the variation of suction due to the presence of a higher water table is sufficient to cause some settlements, although of smaller magnitude. The capability of the unsaturated formulation to provide a satisfactory

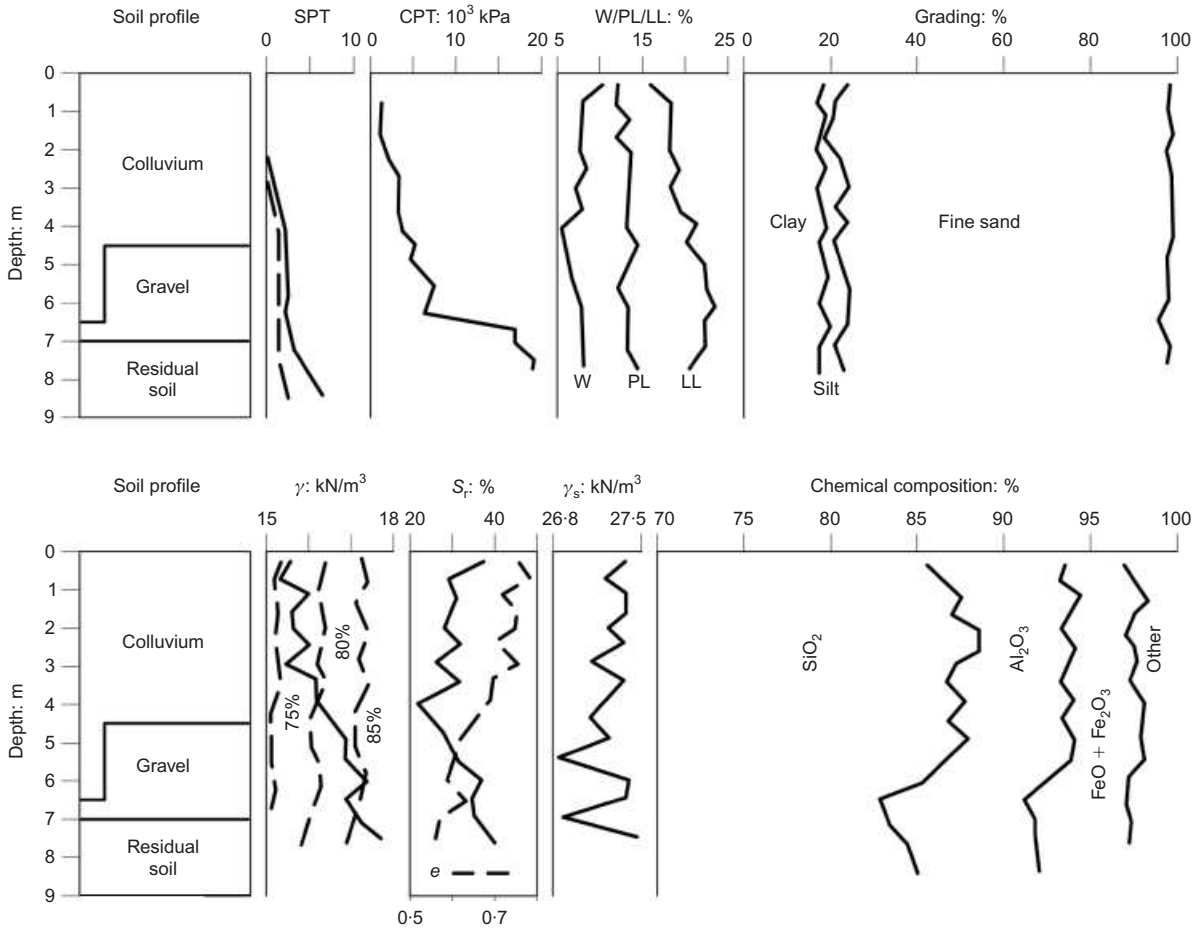

Fig. 40. Soil investigation results at Pereira Barreto town

explanation of the various settlement observations is therefore demonstrated.

Subsidence phenomena in Ravenna, Italy

This case involves ground subsidence on a much larger scale. It is intended to show that the concepts underlying unsaturated soil mechanics can contribute to a better understanding of some of the observations on ground settlement evolution (Menin *et al.*, 2008). Ravenna is located in a low-lying area where surface subsidence is considered a significant threat, and has been subject to continuous observation for over a century (Teatini *et al.*, 2005). The geological setting is illustrated in Fig. 48 (Bertoni *et al.*, 2005). Below about 20 m coastal sandy sediments, there lies a continuous Pleistocene alluvial deposit containing a number of aquifers separated by silty and clayey aquitards. Underneath, a continuous Plio-Pleistocene marine sequence reaches depths of nearly 5000 m. Several gas reservoirs (Fig. 49) have been discovered and exploited in this area, both inland and offshore, at depths ranging from 1000 m to 4500 m. The study of subsidence in the Ravenna area is complex, because settlements are due both to water extraction from the upper alluvial Pleistocene layer and to gas extraction from the deeper marine Plio-Pleistocene deposit. Here only a particular observation related to the Ravenna Terra gas field, the field closest to Ravenna city centre, is examined.

The Ravenna Terra gas field is located between depths of 1650 m and 2000 m. It consists of two main productive levels, pool A and pool B, somewhat offset in plan view. The history of cumulative gas production is plotted in Fig. 50(a). Gas extraction started in 1950, reaching a peak withdrawal in 1966. Most of the gas production was concentrated in the 1960s and early 1970s; no significant gas extraction occurred after 1980. The history of gas production is reflected in the evolution of reservoir pressures (Fig. 50(b)). There is a large drop in pressure during the period of intense gas production, a stabilisation when the gas production rate reduces, and a gradual recovery when gas production has effectively ceased.

It is interesting to consider the history of the gas field using the concepts of unsaturated soil mechanics (Fig. 51). During gas extraction, total stress at depth is basically constant, but gas pressure reduces steadily: net stress therefore increases. At the same time the liquid degree of saturation increases, and therefore suction reduces. The stress path corresponding to this phase is A–B–C–D. If the material enters a collapse range – that is, if it goes beyond the LC yield curve – both the increase in net stress and the suction reduction will contribute to the compression of the material, and therefore to the subsidence. If gas extraction ceases, reservoir pressure will increase at a rate controlled by the inflow of water into the reservoir. During this phase net stresses rise but suction reduces, tending towards a zero value corresponding to full water saturation. However, as illustrated in Fig. 51 (stress path D–E), depending on the slope of the LC curve and of the stress path, further compression and subsidence may result if the effect of suction reduction overcomes the effect of the decrease in net stresses.

Focusing now on the period 1982–1998, it can be verified (Fig. 50) that, during this phase, no gas extraction took place, and that reservoir pressures were clearly increasing. Indeed, the pressures in the aquifers in the upper Pleistocene

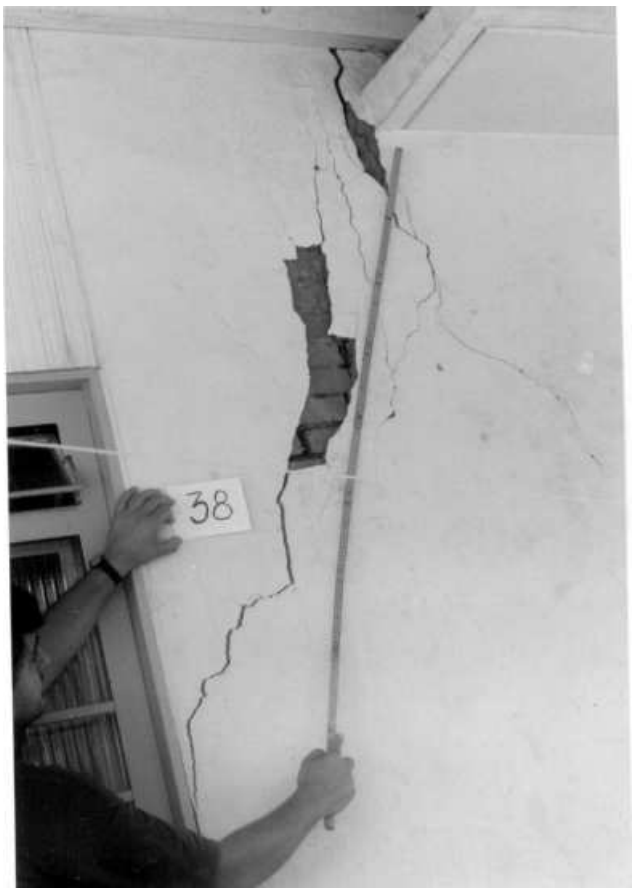

Fig. 41. Collapse settlement due to foundation wetting and building damage (Vilar, 2007, personal communication)

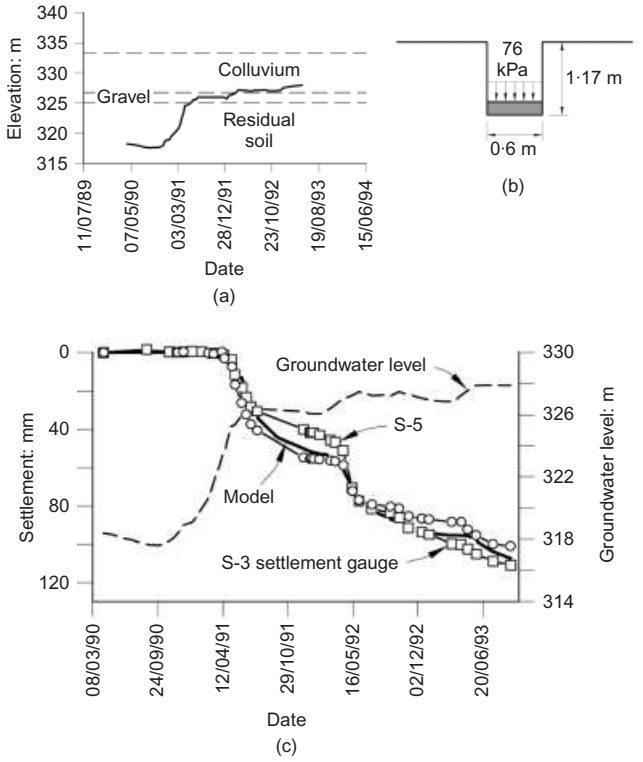

Fig. 42. Building PB-1, Pereira Barreto town: (a) soil profile and water level elevation; (b) foundation; (c) observed and computed foundation settlements

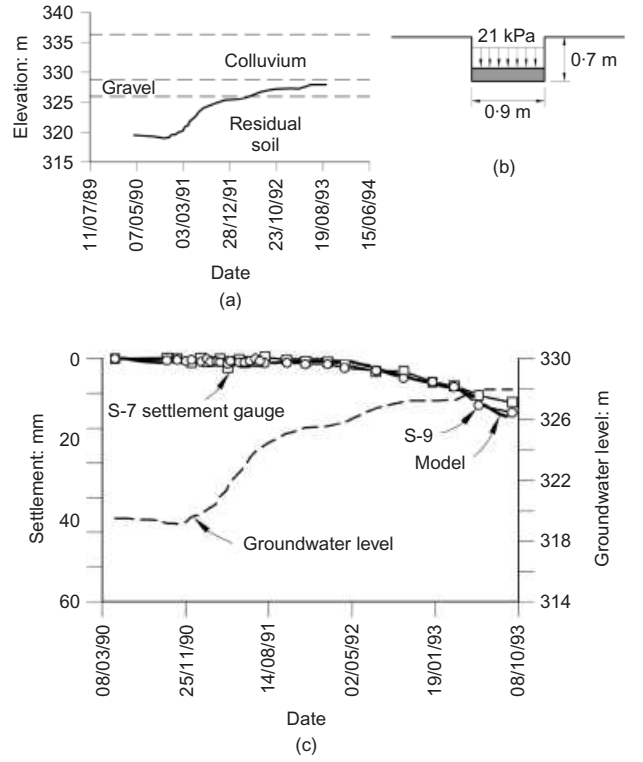

Fig. 43. Building PB-3, Pereira Barreto town: (a) soil profile and water level elevation; (b) foundation; (c) observed and computed foundation settlements

layer appeared to be recovering as well (Brighenti *et al.*, 1994). In spite of this, subsidence continued during this period, albeit at a reduced rate (Fig. 52). A potential cause may be creep phenomena resulting from the previous large subsidence. However, the shape of the subsidence bowl suggests otherwise. The maximum settlements take place in the boundaries of the gas field. The maximum in the centre (point 563) corresponds to the boundary of the upper pool. As the reservoir boundaries are the areas where the water inflow is highest, it can be argued that those settlements are the consequence of reservoir flooding, resulting in a suction reduction. Numerical analyses of the problem yield results consistent with this hypothesis.

Unfortunately, the detailed analysis of the specific situation is too complex to enable firm conclusions to be reached on the specific role that wetting-induced collapse of some of the gas field materials plays in the development of the regional subsidence. However, there are tantalising indications (Menin *et al.*, 2008) that that role could be significant, suggesting that an analysis incorporating unsaturated soil mechanics concepts might be required. The confirmation of

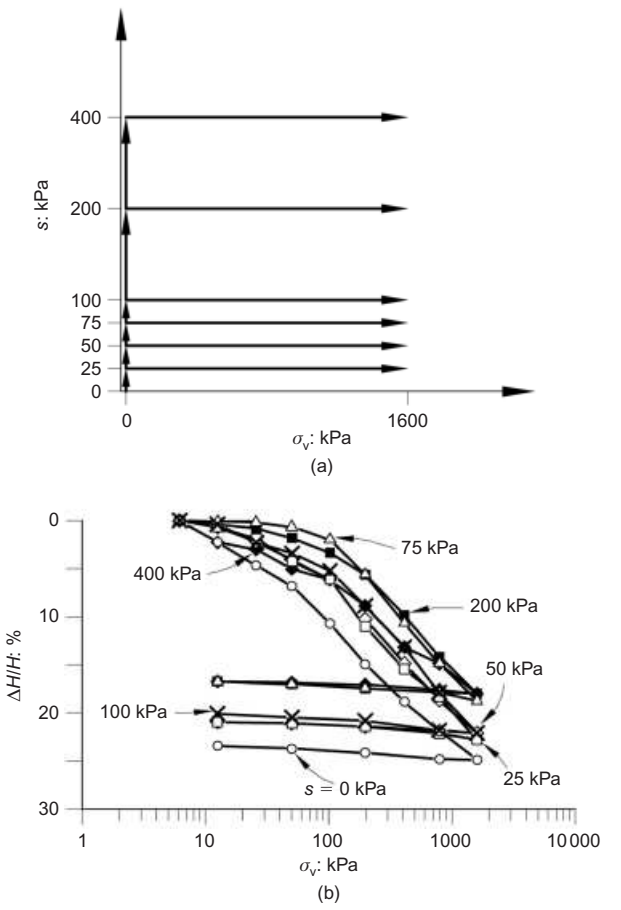

Fig. 44. Loading tests in suction-controlled oedometer: (a) stress paths; (b) test results

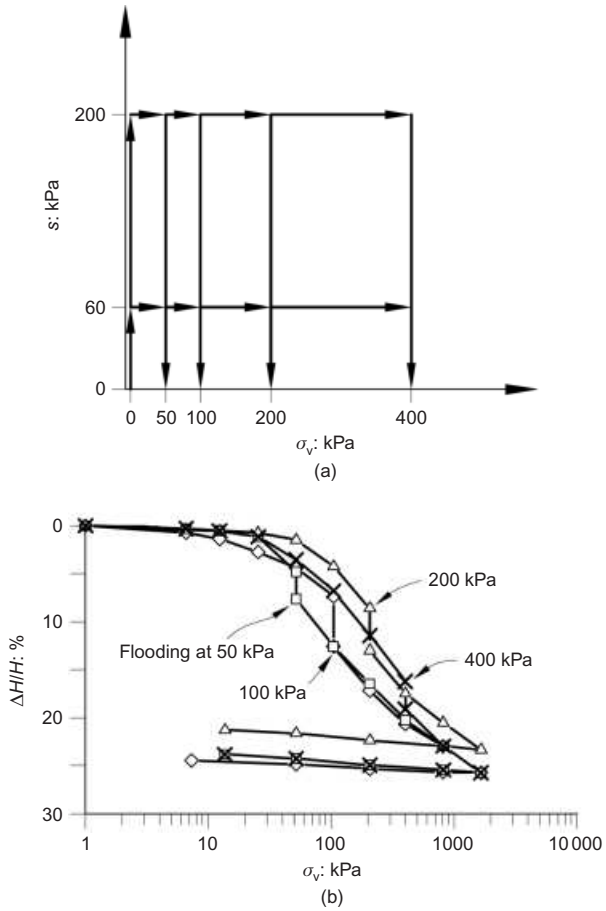

Fig. 45. Wetting collapse tests in suction-controlled oedometers: (a) stress paths; (b) results from collapse wetting tests performed from a suction of 60 kPa

the collapse role would also have strong implications for the use of water flooding and reservoir pressure recovery as a means to control and stop subsidence.

Unsaturated soils: summary

A general formulation for unsaturated soils has included the incorporation of a new variable (suction), the establishment of appropriate balance equations, and the consideration of specific constitutive laws. It has been shown that matric suction plays a key role in understanding the mechanical behaviour of unsaturated soils. A full description of the molecular phenomena underlying matric suction has not been completely developed yet, but the macroscopic concept can be readily used as a major component of unsaturated soil mechanics. The balance equation formulation has incorporated a new equation (air mass balance) and, moreover, the water mass balance equation has been enhanced to consider the possibility of water and air presence in more than one phase. Finally, the vigorous development of elastoplastic constitutive models to describe the mechanical behaviour of unsaturated soils has been reviewed. A variety of constitutive models exist of different degrees of complexity. It has been shown, however, that many of them share a common conceptual core, independently of the specific constitutive variables adopted for their formulation.

Unsaturated soil formulations and constitutive laws have comfortably reached the stage at which they can be applied to the analysis and solution of relevant engineering problems. It is also interesting to remark that the concepts developed in this area appear to have a wider scope of application beyond what would be strictly unsaturated soils. This view will be reinforced in the following sections.

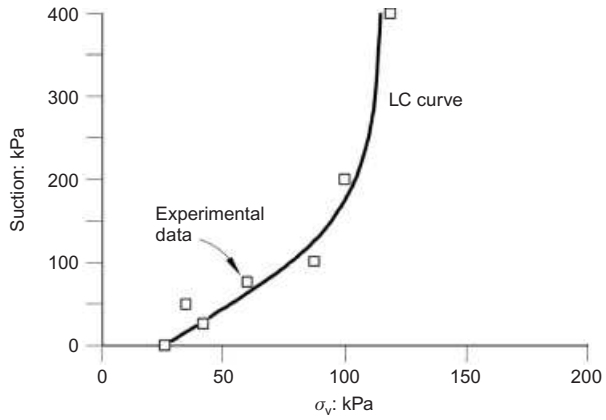

Fig. 46. Experimentally determined LC yield curve for colluvium

THERMAL EFFECTS: HIGH TEMPERATURES

General

There are numerous geotechnical engineering problems in which temperature effects are significant and non-isothermal conditions must be considered, such as landfill engineering, hydrocarbon recovery in oil sands and from oil reservoirs, pipeline engineering, geothermal energy development, drainage enhancement, pavement engineering, and buried power

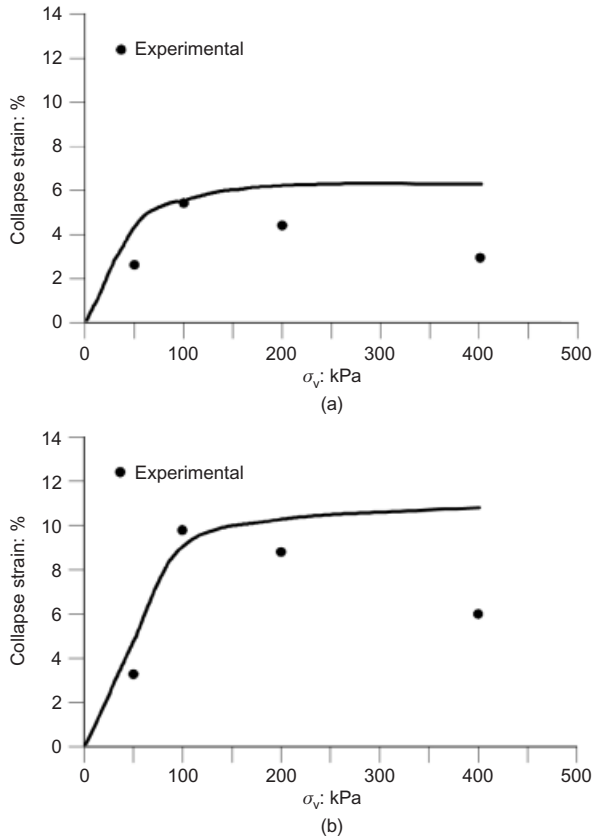

Fig. 47. Computed and observed collapse strains: (a) wetting from 60 kPa suction; (b) wetting from 200 kPa suction

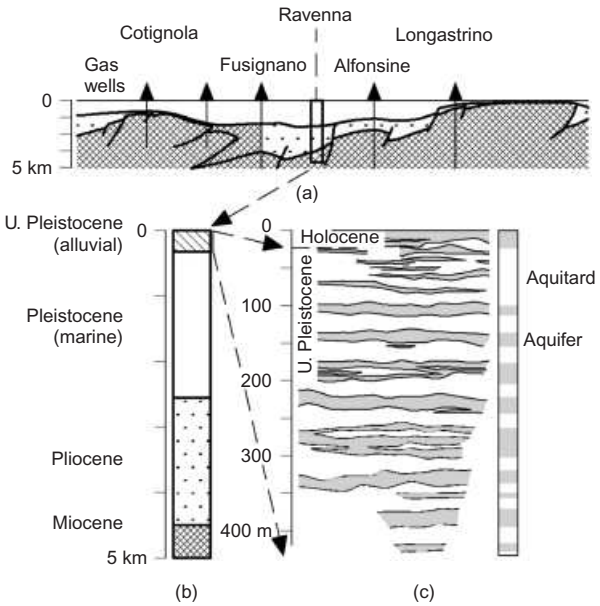

Fig. 48. Geological setting of eastern Po Plain (Bertoni *et al.*, 2005): (a) north–south cross-section; (b) stratigraphic column (Ravenna area); (c) the Ravenna aquifer system

cables. Indeed, any consideration of ground interaction with the atmosphere must contemplate the effects of temperature and energy exchange (Blight, 1997). In recent years various geotechnical problems involving thermal issues have been subjected to particularly intense scrutiny, including energy storage in the ground using geostructures, ground and groundwater as a source of energy, and the storage and disposal of high-level radioactive waste (Clarke, 2009).

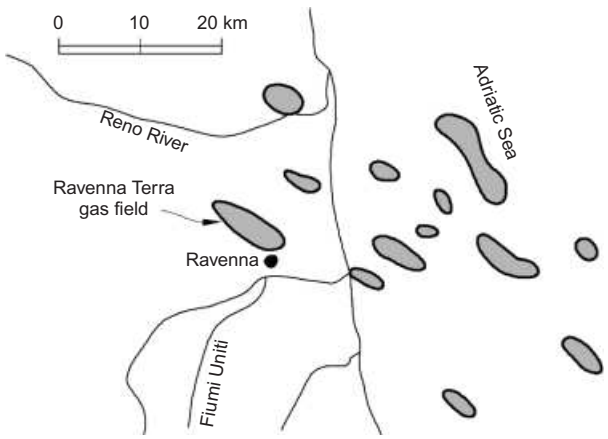

Fig. 49. Gas reservoirs in the Ravenna area (from AGIP, 1996; quoted in Bertoni *et al.*, 2005)

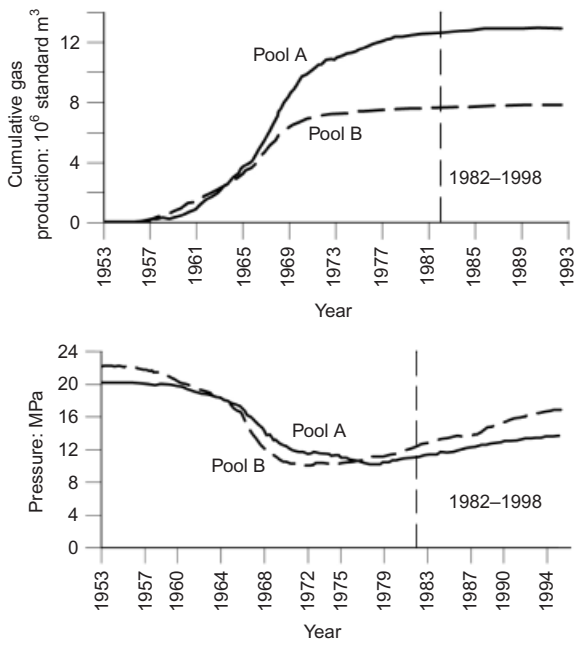

Fig. 50. Ravenna Terra gas field (Menin *et al.*, 2008): (a) cumulative gas production; (b) evolution of reservoir pressure

Problems in the low-temperature range, related to freezing and frozen ground, are examined later.

Coupled thermo-hydromechanical (THM) formulation: balance equations

Several THM formulations have been described in the literature (e.g. Gawin *et al.*, 1995; Thomas & He, 1995, 1997; Khalili & Loret, 2001; Gatmiri & Arson, 2008). In this section the required coupled THM formulation for the high-temperature range is presented, based on the approach put forward in Olivella *et al.* (1994).

In a non-isothermal formulation the new environmental variable is naturally the temperature (Gens, 1997). The formulation also requires an energy balance equation. If thermal equilibrium between the phases is accepted—a reasonable assumption, given the characteristic times of most geotechnical processes—a single equation for the whole medium is sufficient. The energy balance equation is established for the general case of an unsaturated soil with three phases: solid (s), liquid (l) and gas (g). Neglecting any contribution of mechanical work (normally negligible in non-isothermal situations), the balance equation must estab-

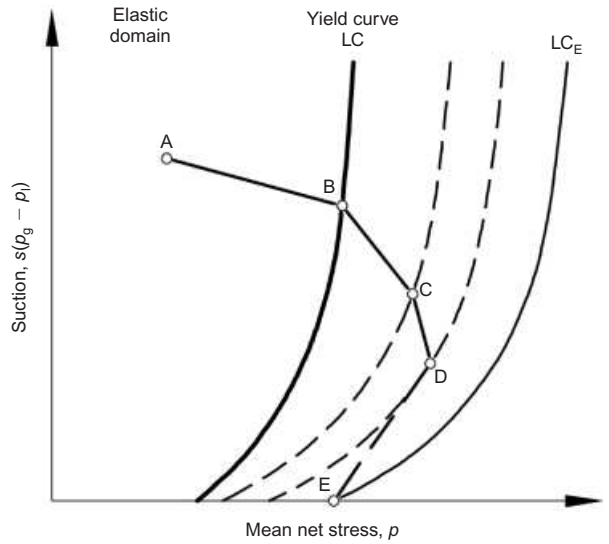

Fig. 51. Possible stress path during gas extraction (A–B–C–D) and pressure recovery (D–E)

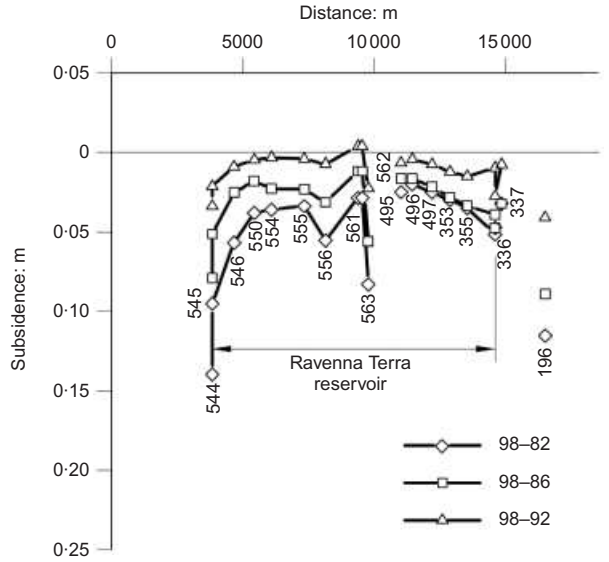

Fig. 52. Subsidence above the Ravenna Terra gas field during the period 1982–1998 (Menin *et al.*, 2008)

lish that the change of internal energy of the three soil phases is equal to the net inflow/outflow of heat energy plus any contribution of a sink/source term (Fig. 53). The resulting expression is

$$\frac{\partial}{\partial t}\left[E_s\rho_s(1-n)+E_l\rho_l S_l n+E_g\rho_g S_g n\right] + \nabla\cdot\left(\boldsymbol{i}_c+\boldsymbol{j}_{Es}+\boldsymbol{j}_{El}+\boldsymbol{j}_{Eg}\right)=f^Q \tag{42}$$

where E is the specific internal energy, $\boldsymbol{i}_c$ is the heat flow by conduction, and $\boldsymbol{j}_E$ is the advective energy fluxes. The first term of the equation is the change of the internal energy of the material, the second one is the net inflow/outflow of heat energy (expressed in terms of a divergence), and f^Q is the sink/source term. Strictly speaking, the addition of a sink/source term contradicts the first law of thermodynamics, and it indicates that the state parameters adopted do not provide a complete description of the system (Houlsby & Puzrin, 2006). It is used in equation (42) as a matter of convenience.

It is accepted that the internal energy for the whole porous medium is the sum of the internal energies of each one of the three phases. They can be expressed as

Solid:

$$E_s = c_s T \tag{43a}$$

Liquid:

$$E_l = \left(c_l^w\omega_l^w + c_l^a\omega_l^a\right)T \tag{43b}$$

Gas:

$$E_g = \left(c_g^w T + l\right)\omega_g^w + c_g^a\omega_g^a T \tag{43c}$$

where c is the specific heat capacity and l is the specific latent heat of evaporation/condensation. The specific heat capacity of liquid water is 4·18 kJ/(kg K) at 25°C, the specific heat of vapour is 1·89 kJ/(kg K) at 100°C, and the specific heat of air at 25°C is 1·01 kJ/(kg K). The variation of these properties over the range of temperatures encountered in most geotechnical problems is small. Because equation (42) has been established in terms of internal energy, the specific heat capacities should be specified at constant volume. However, these values are very difficult to measure in liquids and solids, and so the specific heat capacities at constant pressure are used instead. For liquids and solids the difference can be safely neglected. In the case of gases, the following relationship applies:

$$c_{p,m} - c_{v,m} = R \tag{44}$$

where $c_{p,m}$ and $c_{v,m}$ are the specific heat capacity at constant pressure and constant volume respectively, expressed in molar terms, and R is the gas constant.

The heat flow has several components. The most important heat transport mechanism, in practically all non-

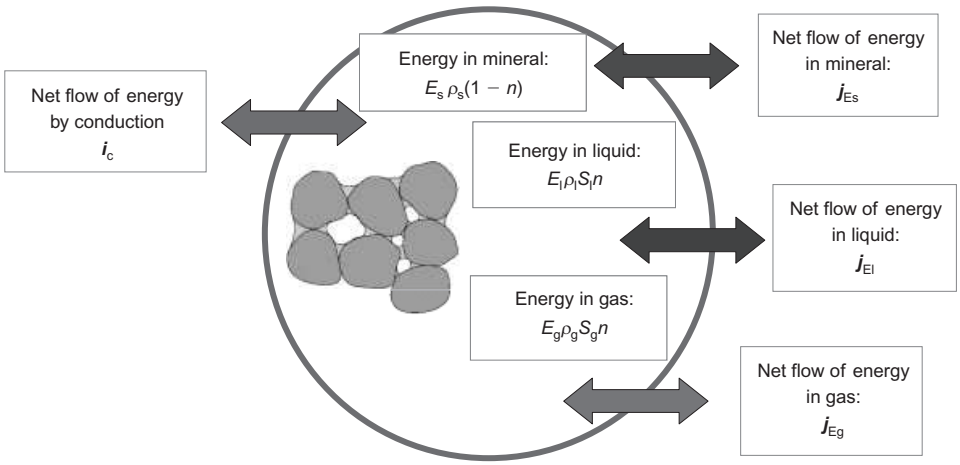

Fig. 53. Scheme to establish the equation for energy balance for an unsaturated soil

isothermal problems, is conduction $\boldsymbol{i}_c$, but for completeness the advective contributions due to the movement of the solid, liquid and gas phases are also included, as follows.

$$\boldsymbol{j}_{Es} = E_s \rho_s (1-n)\dot{\boldsymbol{u}} \tag{45a}$$

$$\boldsymbol{j}_{El} = \boldsymbol{j}_l'^{w} E_l^w + \boldsymbol{j}_l'^{a} E_l^a + E_l \rho_l S_l n \dot{\boldsymbol{u}} \tag{45b}$$

$$\boldsymbol{j}_{Eg} = \boldsymbol{j}_g'^{w} E_g^w + \boldsymbol{j}_g'^{a} E_g^a + E_g \rho_g S_g n \dot{\boldsymbol{u}} \tag{45c}$$

where $\boldsymbol{j}'$ is the flow of the corresponding fluid phase with respect to the solid phase.

Summarising, the coupled THM formulation involves the following balance equations: water mass (equation (15)), air mass (equation (16)), solid mass (equation (17)), energy (equation (42)) and momentum (equilibrium) (equation (18)). As in the HM formulation, it is possible, using the concept of material derivative, to eliminate the equation of solid mass balance (Olivella *et al.*, 1994). The process is summarised here. The material derivative is defined as

$$\frac{D_s(\bullet)}{Dt} = \frac{\partial(\bullet)}{\partial t} + \frac{\mathrm{d}\boldsymbol{u}}{\mathrm{d}t} \cdot \nabla(\bullet) \tag{46}$$

and the solid mass balance equation (equation (17)) becomes

$$\frac{D_s n}{Dt} = \frac{1}{\theta_s}\left[(1-n)\frac{D_s \theta_s}{Dt}\right] + (1-n)\nabla \cdot \frac{\mathrm{d}\boldsymbol{u}}{\mathrm{d}t} \tag{47}$$

and can be incorporated in the other mass and energy balance equations, resulting in the following.

Water mass balance:

$$n\frac{D_s\left(\theta_l^w S_l + \theta_g^w S_g\right)}{Dt} + \left(\theta_l^w S_l + \theta_g^w S_g\right)\frac{D_s n}{Dt} + \left[\left(\theta_l^w S_l + \theta_g^w S_g\right) n\right]\nabla \cdot \frac{\mathrm{d}\boldsymbol{u}}{\mathrm{d}t} + \nabla \cdot \left(\boldsymbol{j}_l'^{w} + \boldsymbol{j}_g'^{w}\right) = f^w \tag{48}$$

Air mass balance:

$$n\frac{D_s\left(\theta_l^a S_l + \theta_g^a S_g\right)}{Dt} + \left(\theta_l^a S_l + \theta_g^a S_g\right)\frac{D_s n}{Dt} + \left[\left(\theta_l^a S_l + \theta_g^a S_g\right) n\right]\nabla \cdot \frac{\mathrm{d}\boldsymbol{u}}{\mathrm{d}t} + \nabla \cdot \left(\boldsymbol{j}_l'^{a} + \boldsymbol{j}_g'^{a}\right) = f^a \tag{49}$$

Energy balance:

$$n\frac{D_s\left(E_l \rho_l S_l + E_g \rho_g S_g\right)}{Dt} + (1-n)\frac{D_s(E_s \rho_s)}{Dt} + \left(E_l \rho_l S_l + E_g \rho_g S_g\right)\nabla \cdot \frac{\mathrm{d}\boldsymbol{u}}{\mathrm{d}t} + \nabla \cdot \left(\boldsymbol{i}_c + \boldsymbol{j}_{Es}' + \boldsymbol{j}_{El}' + \boldsymbol{j}_{Eg}'\right) = f^E \tag{50}$$

Momentum balance (equilibrium):

$$\nabla \cdot \boldsymbol{\sigma}_t + \boldsymbol{b} = 0 \tag{51}$$

The complete set of equations to be solved in the coupled THM formulation described comprises equations (48), (49), (50) and (51). The equilibrium equation is unchanged; it has been included again here for completeness. More information on the transformation of the HM formulation into a THM formulation is given in Gens *et al.* (1997).

Coupled THM formulation: constitutive equations

Thermal and hydraulic behaviour. The effect of temperature is pervasive throughout most physical processes, and consequently temperature enters the definition of constitutive laws when used in a non-isothermal context. New constitutive laws are also required to address specific thermal phenomena (Table 1). For instance, heat conduction is assumed to be governed by Fourier's law,

$$\boldsymbol{i}_c = -\lambda(T)\nabla T \tag{52}$$

where λ is the thermal conductivity. In a multiphase medium, thermal conductivity will be some kind of average of the thermal conductivities of the phases that will depend on the microstructural arrangement of material. If the phase arrangement was in series, the harmonic mean would apply; alternatively, if the phase arrangement was in parallel, the arithmetic mean would be appropriate. For an intermediate situation the geometric mean weighed by volumetric fractions often provides an adequate estimate:

$$\lambda = \lambda_s^{1-n}\lambda_l^{S_l n}\lambda_g^{(1-S_l)n} = \lambda_{sat}^{S_l}\lambda_{dry}^{1-S_l} \tag{53}$$

The thermal conductivities of most of the usual substances making up the solid phase of soils have a limited range of values (with the exception of quartz). Therefore the thermal conductivities of saturated soils are usually in the range 1–3 W/(m K)—a very narrow range compared with that of hydraulic conductivity. The thermal conductivity of liquid water is 0·6 W/(m K) at 25°C. In the gas phase much lower values apply: the thermal conductivity of water vapour is 0·016 W/(m K) at 100°C, and of air is 0·024 W/(m K) at 25°C. Therefore the degree of saturation of the soil has a major impact on the thermal conductivity of an unsaturated porous medium. Although there is some dependence on temperature itself, it is generally minor when compared with the influence of water content or degree of saturation. Fig. 54 shows experimental measurements of thermal conductivity on compacted Febex bentonite (Villar, 2002): the effect of degree of saturation is readily apparent. The geometric mean expression (equation (53)) provides a reasonable agreement with observations.

As noted before, the advective flows of liquid and gas, $\boldsymbol{q}_l$ and $\boldsymbol{q}_g$, are governed by Darcy's law (equations (19) and (20)). Accordingly, temperature-induced viscosity variations should result in corresponding variations of hydraulic conductivity. For reference, the viscosity of water at 20°C is 1 Pa s, but drops gradually to 0·28 Pa s at 100°C, a significant difference.

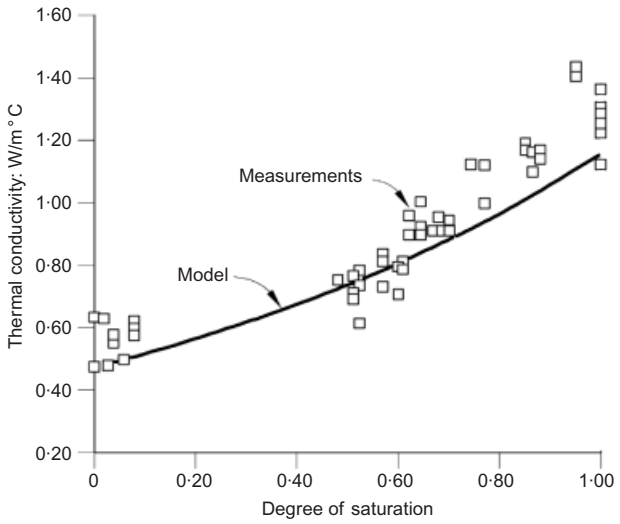

Fig. 54. Variation of the thermal conductivity of Febex bentonite with degree of saturation (Villar, 2002): the prediction of the geometric mean expression (equation (53)) is plotted for comparison

Figure 55 shows the intrinsic permeability (equation (20)) of saturated natural Boom clay obtained in tests on samples of different porosities, conducted at different temperatures in the range 20–90°C. The fact that the relationship found is independent of temperature indicates that the changes of hydraulic permeability are accounted for by the variation of viscosity with temperature (Delage *et al.*, 2000). Similar results have been obtained by Lima (2009), testing the same material. However, results by Romero *et al.* (2001) on compacted Boom clay, Khemissa (1998) on kaolinite, and Volckaert *et al.* (1996) and Cho *et al.* (1999) on montmorillonite suggested that the variation of saturated hydraulic permeability with temperature was less than would be expected from temperature effects on viscosity. Opposite results were obtained by Towhata *et al.* (1993), testing saturated kaolinite. It appears, therefore, that additional factors other than viscosity changes may affect the variation of saturated hydraulic conductivity with temperature, at least for some soils. Information on the effects of temperature on hydraulic conductivity for unsaturated soils is scarcer. Romero *et al.* (1999, 2001) measured the variation of relative permeability with degree of saturation of compacted Boom clay at two temperatures, 22°C and 80°C. As Fig. 56(a) shows, temperature effects appear not to be significant in this case. From the same investigation, Fig. 56(b) shows that the effect of temperature on the retention curve is also slight. Some thermal effects on the retention curve could be expected, at least in the capillary range, as surface tension is affected by temperature, but the effect appears to be small.

Temperature also influences other constitutive laws. For instance, the vapour diffusion coefficient incorporated in Fick's law (equation (21)) is also dependent on temperature. An empirical relationship has been given as

$$D_{\mathrm{m}}^{\mathrm{w}}\left(\mathrm{m}^2/\mathrm{s}\right) = 5{\cdot}9 \times 10^{-12}\frac{T^{2{\cdot}3}}{p_{\mathrm{g}}} \tag{54}$$

where p_{g} is expressed in MPa (Pollock, 1986). A full discussion on vapour transport in non-isothermal conditions is presented in Olivella & Gens (2000).

Liquid water density is also dependent on temperature (Fig. 57(a)), reaching a maximum at 4°C. As a result, the thermal expansion coefficient is also variable with temperature, with increasing values across the liquid water range of temperatures (Fig. 57(b)). The variation of gas density with temperatures can be assumed to be given by the ideal gas law: $p_{\mathrm{g}}V = n_{\mathrm{m}}RT$.

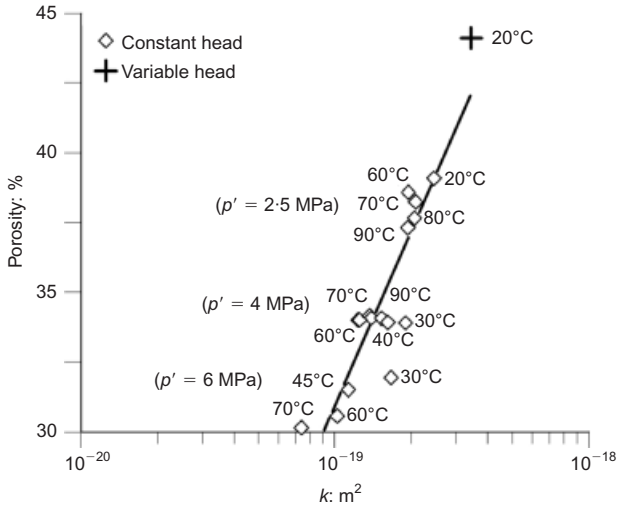

Fig. 55. Variation of intrinsic permeability with porosity at various temperatures: tests on saturated Boom clay (Delage *et al.*, 2000)

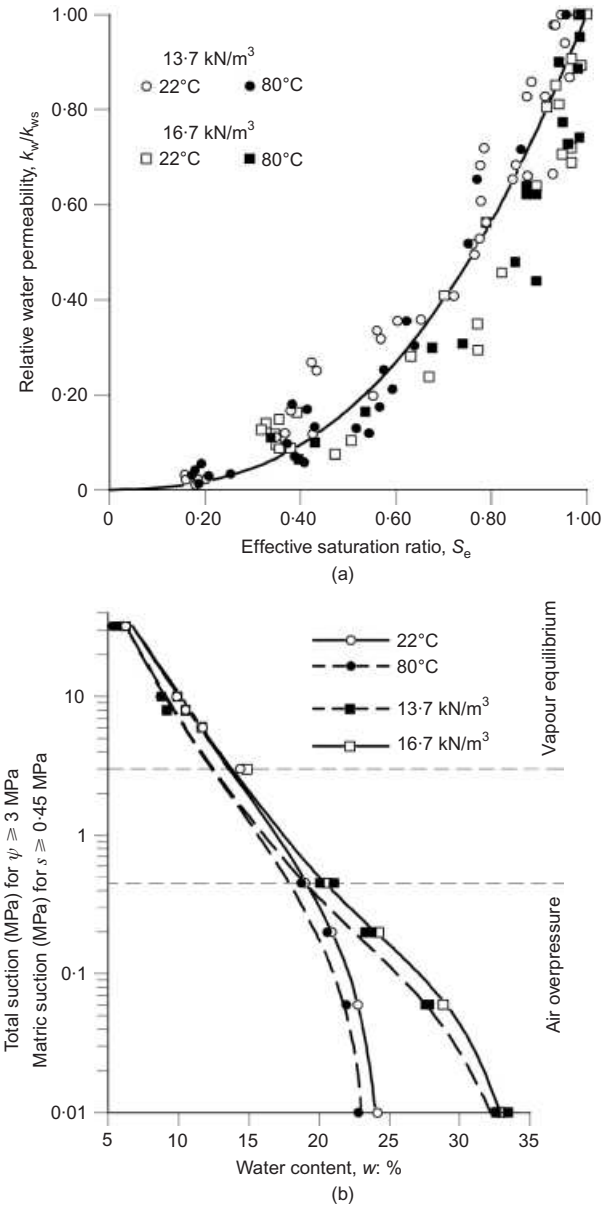

Fig. 56. Tests on compacted unsaturated Boom clay for two porosities and two temperatures (22°C and 80°C) (Romero *et al.*, 2001): (a) variation of relative permeability with effective saturation ratio; (b) retention curves

Finally, the effect of temperature on Kelvin's law, which links suction with vapour concentration (or partial vapour pressure), is twofold. On the one hand, it enters the denominator of the correction term in Kelvin's law (equation (8)). But the equilibrium vapour pressure (and therefore equilibrium vapour concentration) is also dependent on temperature. The following expression gives an adequate estimation of the variation, based on data from Garrels & Christ (1965).

$$p_{\mathrm{v}}^{0}(\mathrm{MPa}) = 136{\cdot}075\exp\left(-\frac{5239{\cdot}7}{T}\right) \tag{55}$$

Thermomechanical behaviour. The effects of temperature on the mechanical behaviour of saturated soils have been the subject of numerous studies (e.g. Campanella & Mitchell, 1968; Hueckel & Baldi, 1990; Baldi *et al.*, 1991; Burghignoli *et al.*, 2000; Delage *et al.*, 2000; Graham *et al.*, 2001; Cekerevac & Laloui, 2004). Temperature has been found to

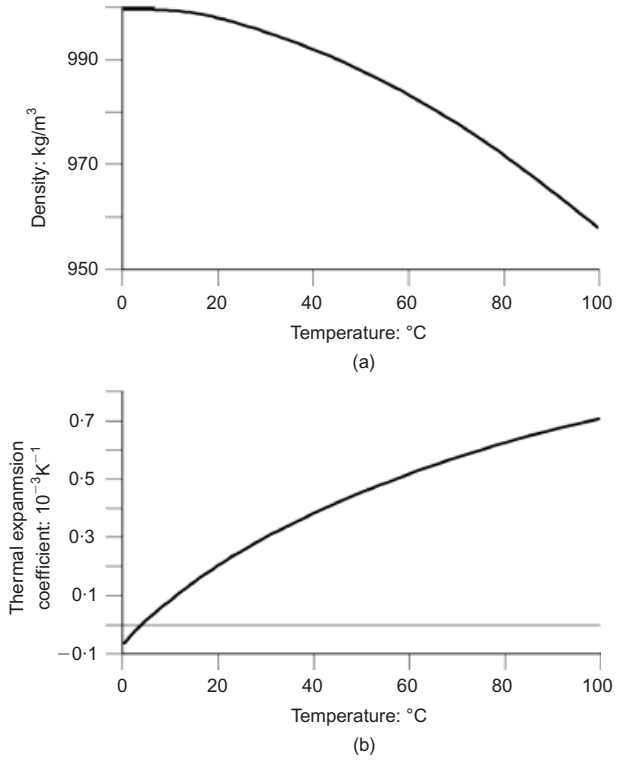

Fig. 57. (a) Variation of liquid water density with temperature; (b) variation of the thermal expansion coefficient of liquid water with temperature

affect, *inter alia*, volume change characteristics, drained and undrained strength, and drained and undrained shear stiffness, although on some occasions there are significant discrepancies between the findings from different studies. Much of the relevant information is collected and discussed in Mitchell & Soga (2005).

One of the most interesting observations concerning temperature effects on mechanical soil behaviour was presented by Baldi *et al.* (1991). They applied a cycle of heating and cooling, between 20°C and 95°C, to saturated Boom clay samples with different overconsolidation ratios (OCRs). The results are shown in Fig. 58. The heavily overconsolidated sample (OCR = 6) dilates upon heating, and contracts during cooling; the thermal strains developed are largely reversible. However, the behaviour of the normally consolidated sample (OCR = 1) is completely different. On heating, the sample undergoes a very large compression; further contraction occurs on cooling, but the volumetric strain magnitude is much smaller. As a result of the heating–cooling cycle, a large irreversible volumetric strain is observed. The lightly overconsolidated sample (OCR = 2) shows a behaviour similar to that of the normally consolidated one, but the irreversible volumetric strains developed are smaller. Subsequent studies have confirmed those observations (e.g. Sultan *et al.*, 2002; Laloui & Cekerevac, 2008).

From the pioneering work of Hueckel & Borsetto (1990), it has been apparent that an effective way to model this type of behaviour is to adopt the assumption that the size of the yield surface reduces with increasing temperature (Graham *et al.*, 2001; Laloui & Cekerevac, 2003; Abuel-Naga *et al.*, 2007, 2009), although in some models an extra volumetric thermal plastic mechanism is added (Cui *et al.*, 2000). It is also satisfactory to record that the reduction of the size of the yield locus with increasing temperature has been independently confirmed experimentally (e.g. Cekerevac & Laloui, 2004; Marques *et al.*, 2004).

Experimental results concerning temperature effects on unsaturated soils are less common (Villar & Lloret, 2004; Tang *et al.*, 2008). Romero (1999) developed a triaxial cell allowing the independent control of suction and temperature (Fig. 59). Axial strains were determined from internal LVDT measurements, and an optical laser system was used to determine lateral strains. Fig. 60(a) shows the variation of volumetric strains measured in heating–cooling tests on

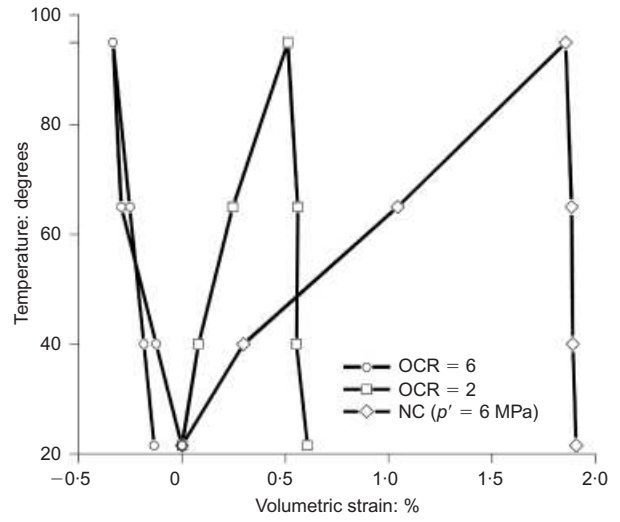

Fig. 58. Variation of volumetric strain with temperature observed in heating–cooling tests on samples of saturated Boom clay with different overconsolidation ratios (OCRs) (Baldi *et al.*, 1991)

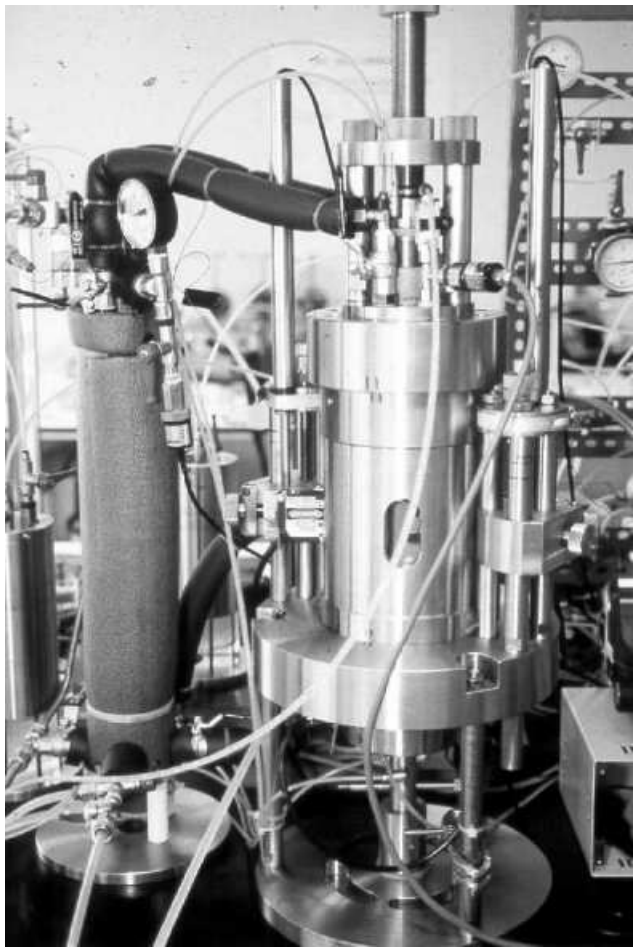

Fig. 59. Triaxial apparatus with independent control of suction and temperature (Romero, 1999)

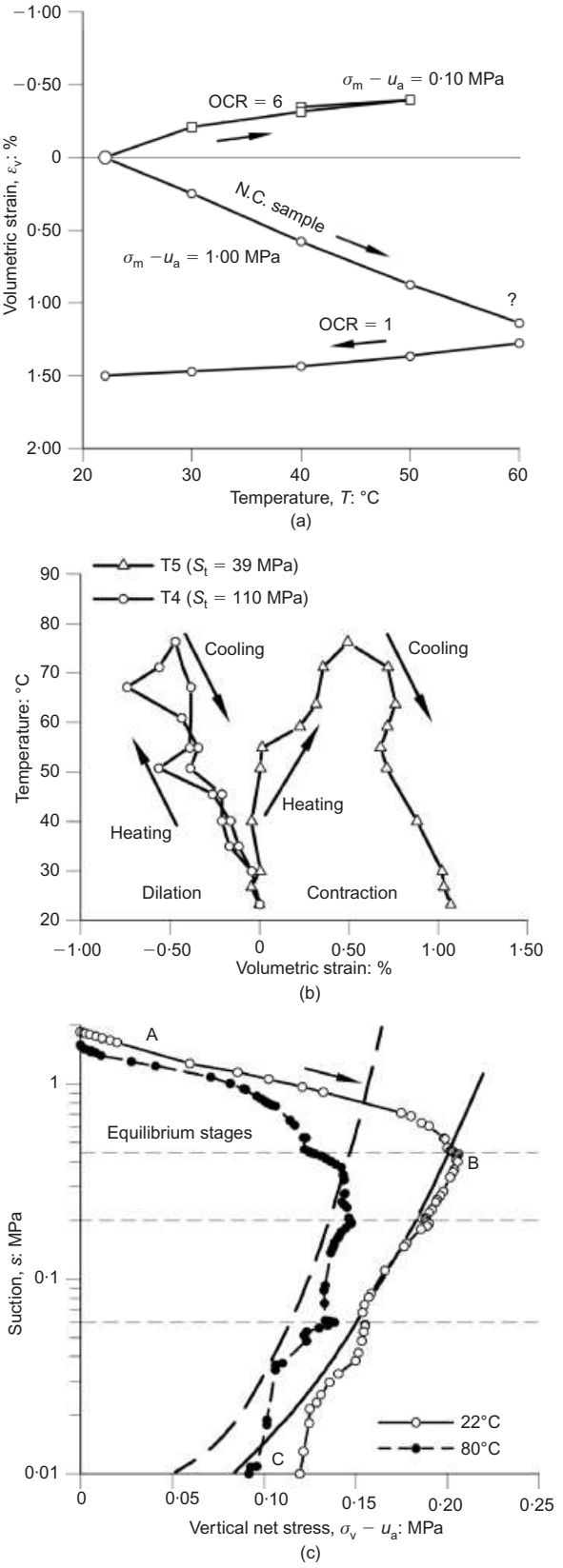

Fig. 60. (a) Variation of volumetric strain with temperature observed in heating–cooling tests on two samples of unsaturated compacted Boom clay with different overconsolidation ratios (Romero, 1999); (b) variation of volumetric strain with temperature observed in heating–cooling tests on two samples of unsaturated compacted MX-80 bentonite at two different suctions (Tang *et al.*, 2008); (c) suction–vertical net stress paths followed by two samples of unsaturated compacted Boom clay in oedometer swelling pressure tests at two temperatures (Romero *et al.*, 2003)

unsaturated samples of compacted Boom clay performed under constant suction. The behaviour is very similar to that of saturated samples for the two overconsolidation ratios OCR = 1 and OCR = 6. In this context the results of heating–cooling tests on two samples of unsaturated compacted MX-80 bentonite reported by Tang *et al.* (2008) are also interesting (Fig. 60(b)). They were performed at the same applied isotropic stress of 5 MPa but with two different total suctions, 39 MPa (Test T5) and 110 MPa (Test T4). Recalling that yield stress increases with suction, the specimen with the higher suction has, effectively, a higher overconsolidation ratio. This is borne out by the result of the experiment: the sample with the higher suction behaves as a highly overconsolidated soil, whereas the behaviour of the sample with the lower suction is what would be expected from a lightly overconsolidated soil. It appears that the stress–suction link characteristic of unsaturated soil mechanics transfers readily to non-isothermal conditions.

Oedometer swelling pressure tests at two temperatures were also performed on unsaturated compacted Boom clay (Romero *et al.*, 2003): the results are shown in Fig. 60(c). The observations strongly suggest that the size of the LC yield curve is smaller at the higher temperature. The dependence of the yield surface size on temperature for unsaturated soils has been comprehensively demonstrated in a recent systematic study performed on Bourke silt ($w_L = 20{\cdot}5\%$, $w_P = 15{\cdot}5\%$) reported by Uchaipichat & Khalili (2009). The specimens were statically compacted to a dry unit weight of 15·3 kN/m^3 at a moisture content of 10·5%. As Fig. 61 shows, the size of the elastic domain reduces for all suction values. Extensive results from Lloret & Villar (2007) on Febex montmorillonite have also confirmed conclusively the reduction of swelling pressure with temperature, consistent with a reduction of the yield surface size.

All these experimental observations appear to lend support to the suggestion (Gens, 1995) that it would be possible to combine a model for unsaturated soils, where the size of the yield surface increases with suction, with a thermoplastic model where the size of the elastic domain reduces with increasing temperature (Fig. 62). The combined equations can then be obtained in a straightforward manner (Gens, 1995). More elaborate models on similar principles have subsequently been presented (e.g. Wu *et al.*, 2004; Bolzon & Schrefler, 2005; François & Laloui, 2008).

The structure of the resulting model has the form

$$\mathrm{d}\boldsymbol{\sigma}^* = \boldsymbol{D}(\boldsymbol{\varepsilon}, s, T)(\mathrm{d}\boldsymbol{\varepsilon}) + \boldsymbol{h}(\boldsymbol{\varepsilon}, s, T)\mathrm{d}s + \boldsymbol{\beta}(\boldsymbol{\varepsilon}, s, T)\mathrm{d}T \quad (56)$$

where a new term appears that represents the independent contribution of temperature to the constitutive behaviour. Now, the constitutive matrix $\boldsymbol{D}$ and the constitutive vectors $\boldsymbol{h}$ and $\boldsymbol{\beta}$ may depend on strains, suction and temperature.

Case history: THM behaviour of an engineered bentonite barrier, the Febex mock-up test

One of the most active fields in which the thermal behaviour of geotechnical materials is especially relevant is that of deep geological storage and disposal of high-level nuclear waste (Gens, 2003; Gens & Olivella, 2001b, 2005; Gens *et al.*, 2009a). High-level nuclear waste (HLW) contains long-lived radionuclides, and it is strongly heat emitting. The aim of geological disposal is to remove it from the human environment, and to ensure that any radionuclide release rates remain below prescribed limits (Chapman & McKinley, 1987). A typical scheme for an underground mined repository involves the sinking of deep shafts or ramps down to a depth of several hundred metres: the actual depth will, of course, be controlled by local geological conditions. Shafts

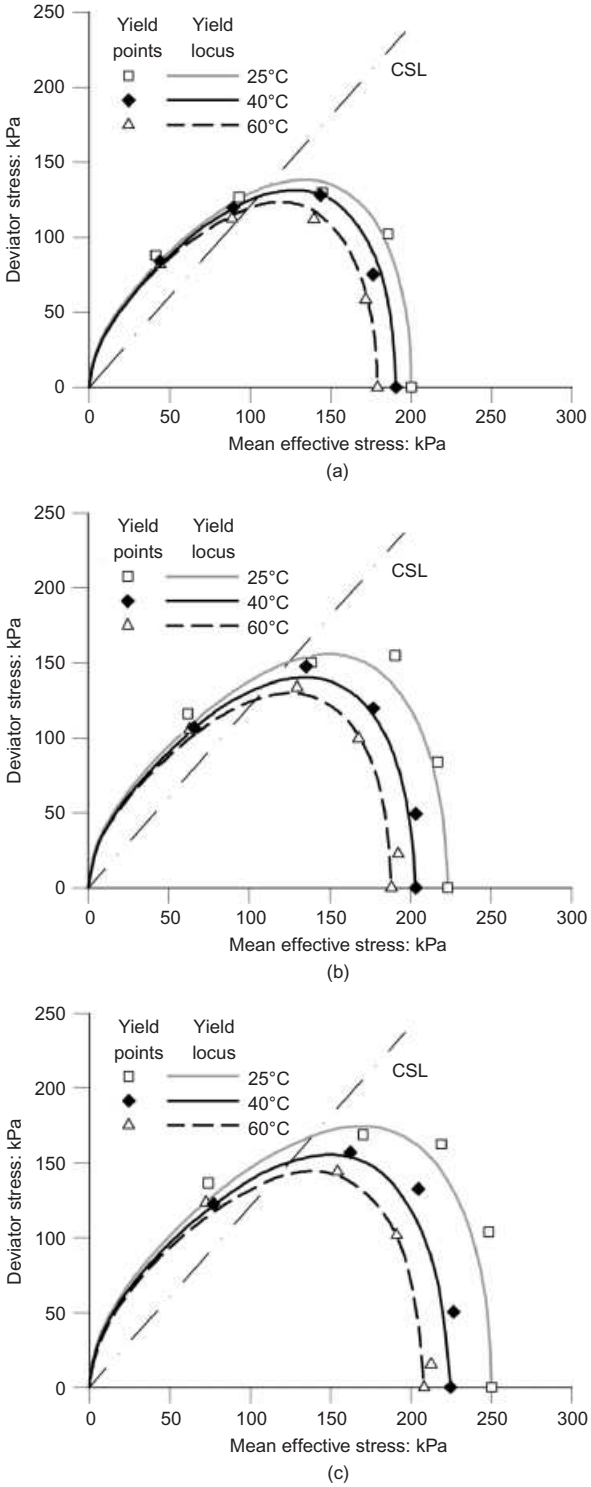

Fig. 61. Evolution of yield locus with temperature at different matric suctions (Uchaipichat & Khalili, 2009): (a) $s = 0$ kPa; (b) $s = 100$ kPa; (c) $s = 300$ kPa. Effective stress is computed from equation (24), using $\chi = 1$ for $s/s_e \leqslant 1$ and $\chi = (s/s_e)^{-\Omega}$ for $s/s_e \geqslant 1$, where s_e is the suction at the transition between saturated and unsaturated states

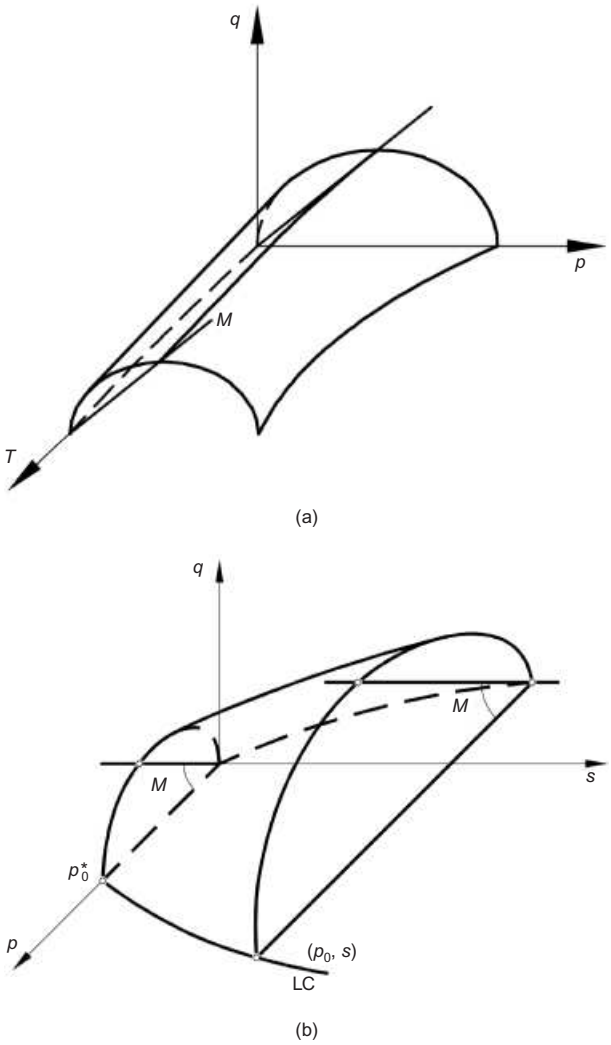

Fig. 62. Combined yield surface for a non-isothermal model for unsaturated soils (Gens, 1995): (a) yield surface section at constant suction; (b) yield surface section at constant temperature

or ramps will provide access to a network of horizontal drifts that constitutes the main repository area (Fig. 63). Canisters containing HLW will be deposited either in horizontal drifts or in vertical boreholes. The space between the canisters and the host rock is generally (but not always) filled by a suitable material to constitute an engineered barrier: normally compacted highly swelling clay (bentonite) is used, but concrete or crushed salt are also considered in some designs.

All disposal designs for HLW resort to the multi-barrier concept to achieve the required degree of waste isolation. If one considers the potential path of a radionuclide from inside the canister to the biosphere, it will need to cross several barriers: the canister itself, the backfill (engineered barrier), and the host rock (geological barrier). Each one of these elements will contribute a degree of safety to the overall disposal system, and their individual and coupled behaviour under real repository conditions must be properly understood to achieve a sufficient degree of confidence in the reliability of the design.

The bentonite barrier fulfils several important functions. In the first instance, a very low hydraulic conductivity restricts water penetration, and the clay barrier also significantly retards solute transport owing to its low diffusion coefficient, and to additional sorption effects. The barrier should also provide a favourable chemical environment and be able to self-heal if subjected to physical perturbations such as cracking and fissuring events. However, the bentonite barrier is subject to very strong thermo-hydromechanical (THM) loading in its initial transient phase. Heating is applied by the canister containing the waste, and at the same time the initially unsaturated bentonite is hydrated by the water supplied by the host rock. Fig. 64 shows some of the coupled thermohydraulic phenomena occurring in the barrier: heat conduction, heat advection, liquid and gas advec-

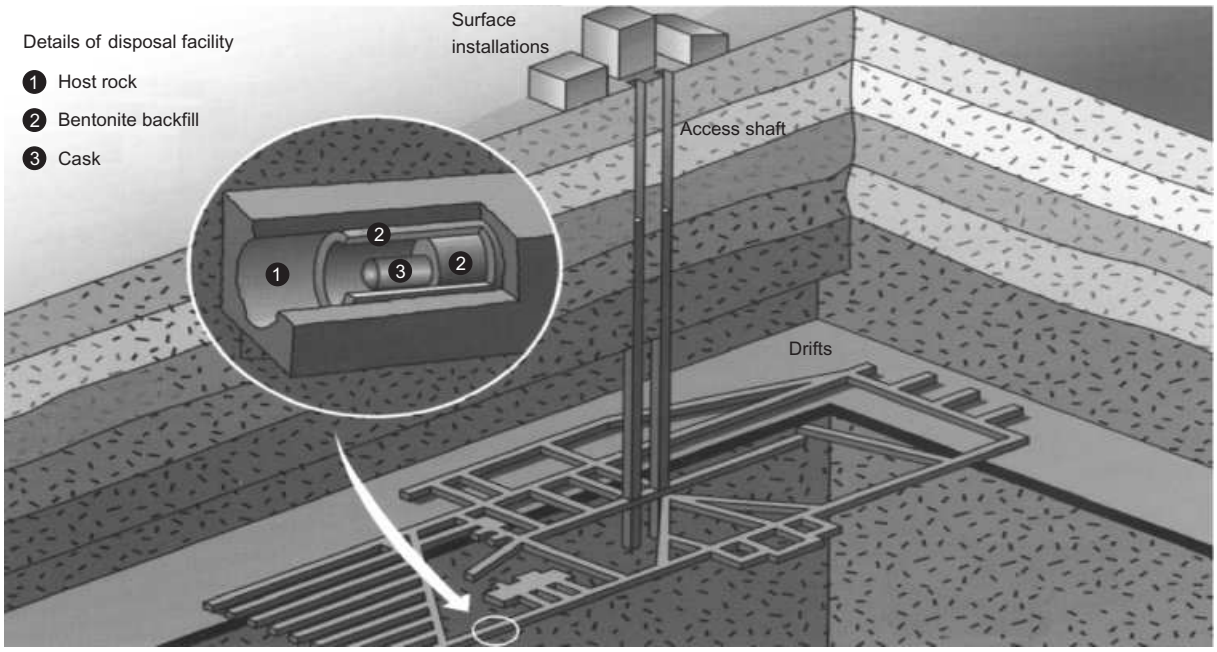

Fig. 63. Scheme of a deep geological repository for high-level nuclear waste

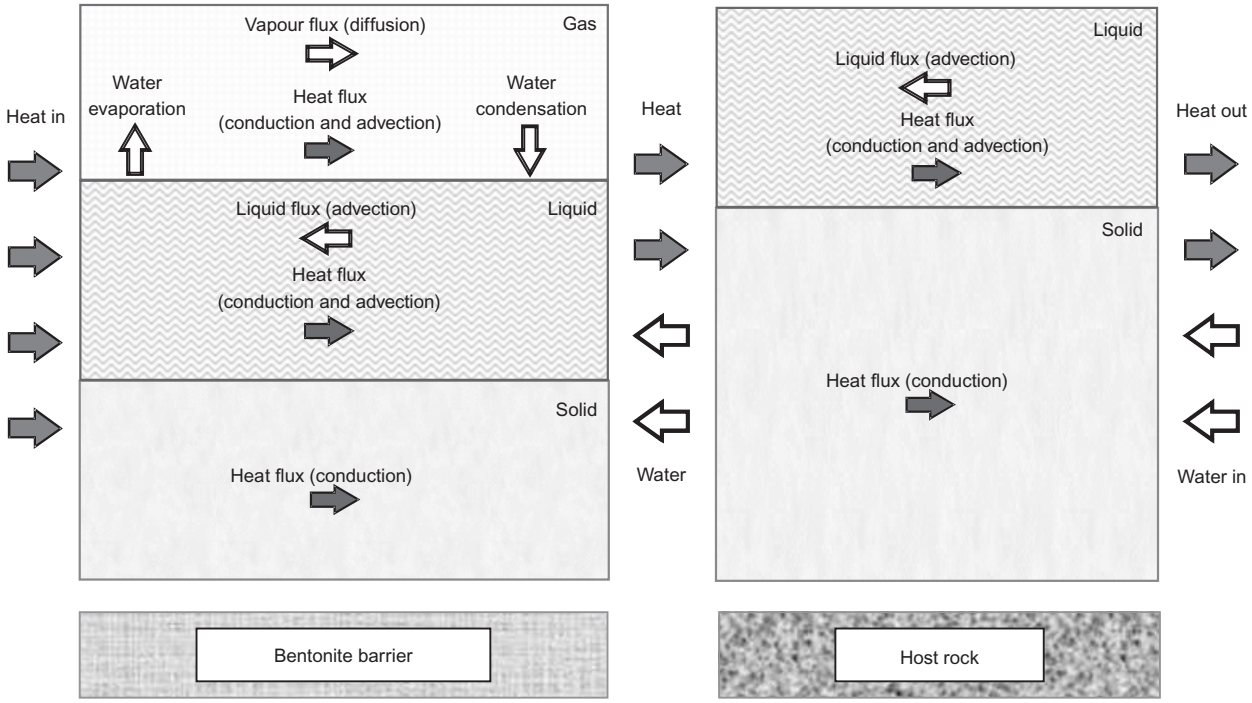

Fig. 64. Scheme of thermo-hydraulic processes occurring in the bentonite barrier and immediately adjacent rock

tive flow, vapour diffusion and phase changes (evaporation/condensation). In addition there are associated mechanical effects linked to the wetting and drying of the unsaturated bentonite. Interaction with the host rock adds additional complexity to the system (Gens *et al.*, 2002a). Although all the phenomena identified are in fact included in the formulation outlined above, the THM behaviour of the engineered bentonite barrier provides a very comprehensive test of its applicability to a real engineering problem.

The issue of HLW disposal is sufficiently important to warrant the performance of full-scale tests simulating repository conditions. These tests are usually conducted in specially built underground laboratories: there are several of them in Europe and elsewhere (Gens, 2003). The Febex test was an experimental programme led by the Spanish agency for radioactive waste (Enresa) to advance understanding of the THM behaviour of the engineered bentonite barrier. It included a full-scale in situ test carried out at the Grimsel test site, an underground laboratory excavated in granite in the Swiss Alps. The test and its associated modelling are described in Gens *et al.* (1998, 2009b). However, attention is instead focused here on the mock-up test, an experiment constructed to a similar scale but performed under more controlled conditions at the Ciemat laboratory in Madrid. A full description of the overall project is given in Huertas *et al.* (2006).

The mock-up test (Fig. 65) simulates an engineered barrier made up of blocks of compacted swelling clay being

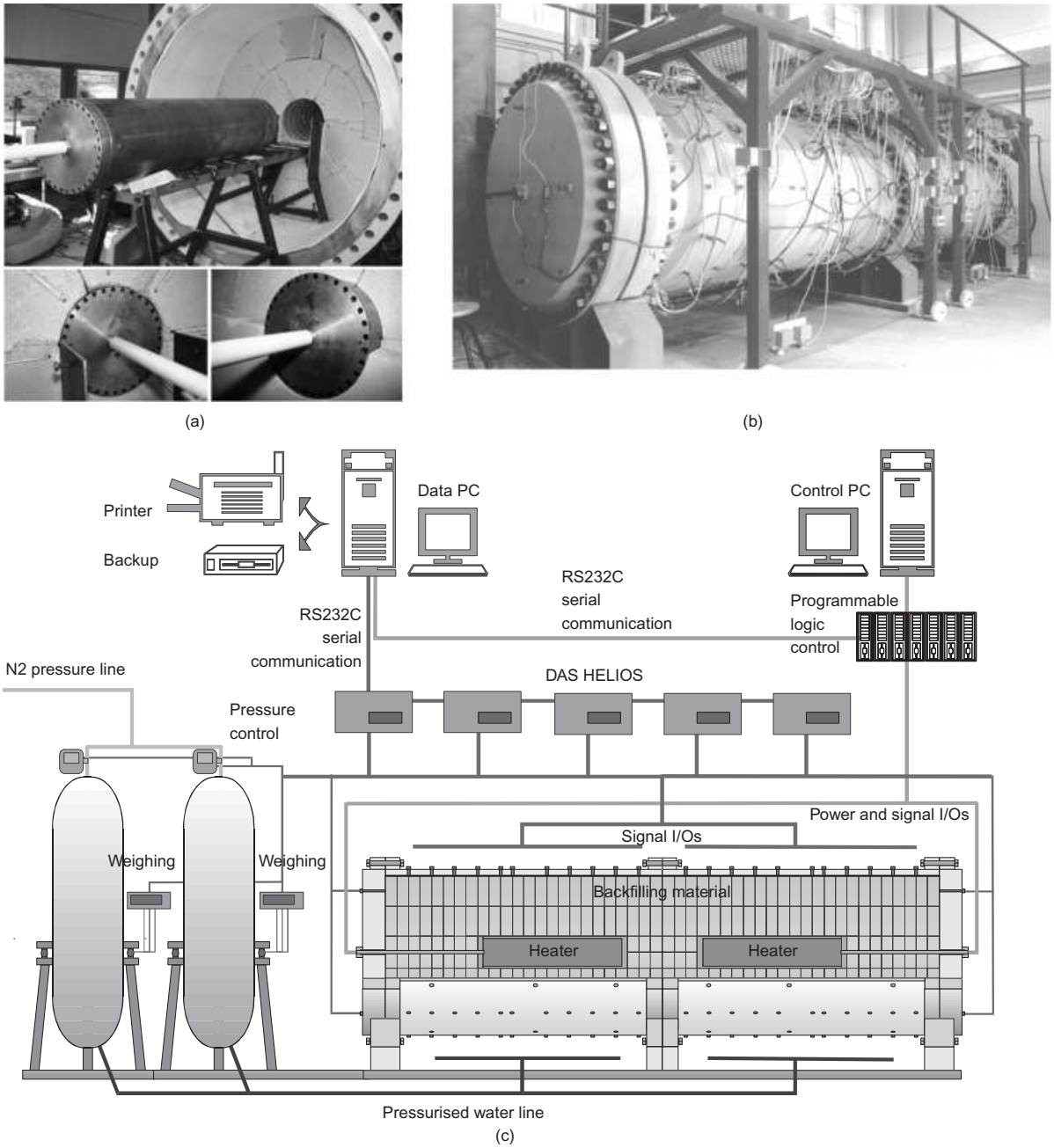

Fig. 65. Febex mock-up test: (a) heater installation; (b) view of the experiment; (c) schematic representation of the main components of the experiment

subject to heating and hydration simultaneously. The clay is a bentonite ($w_L = 98–106$, $w_P = 50–56$), obtained from a quarry in southern Spain. It has high smectite content, in the range 88–96%, and the cation exchange capacity is 100–102 meq/100 g (42% Ca, 33% Mg, 23% Na, 2% K). The bentonite blocks were compacted at a water content of 13·6%, and the average dry density of the barrier (including gaps) is 1·65 Mg/m^3. The initial degree of saturation was 0·715.

The barrier is enclosed in a cylindrical steel body with an inner length of 6·00 m and an inner diameter of 1·62 m, designed to resist the swelling pressures that develop during the test. The dimensions of the experiment are of the same order as in the real system, where the envisaged diameter of the barrier is 2·28 m. More significantly, the thickness of the barrier, 66 cm, is very close to the design one. Two heaters are installed in the axis of the barrier to mimic the heating action of the nuclear HLW. The hydration system supplies water uniformly to the periphery of the barrier through a geotextile placed around the outer boundary of the barrier, and the amount of water entering the barrier is carefully monitored by weight. The test was intensively instrumented for temperature, relative humidity (equivalent to total suction), liquid pressure and total pressure in 24 sections along the barrier. A useful feature of the test is that it is symmetrical with respect to the central section: therefore observations made in sections located at equal distances from the centre should be very similar. This feature provides a very convenient method to assess the reliability of the test results.

The test is temperature controlled: the highest temperature in the contact between heater and clay is kept at 100°C. This is a barrier design requirement designed mainly to avoid mineralogical changes in the bentonite; in fact, the coupled formulation can deal with temperatures higher than 100°C without requiring any modification (Olivella & Gens, 2000). Water was supplied at a constant 0·55 MPa pressure. Be-

cause of the very low permeability of the bentonite, it is necessary to run the test for a very long period of time. Heaters were switched on in February 1997, and the test is still continuing at present. Herein results are given for the first 3421 days of the experiment.

Test observations for the entire duration of the test were predicted at the beginning of the experiment based on the information available at the time: the analysis was labelled OBC (Operational Base Case). To represent the behaviour of the unsaturated compacted clay, the BBM was adopted with a modified elastic component to account for the highly swelling properties of the clay on wetting, as well as the effects of temperature. Full details of all modelling activities are provided in Sánchez & Gens (2006).

Measured and computed temperatures at four different distances from the barrier axis are shown in Fig. 66 for sections in front of the heaters (hot sections) and away from the heaters (cool sections). Temperatures are practically constant throughout the test; predictions are in good agreement with observations for the two types of section. This is not surprising, as heat transport is essentially by conduction; a good estimate of thermal conductivity (Fig. 54) and the use of realistic boundary conditions ensure good correspondence between predictions and measurements, especially in a temperature-controlled test. Heater power requirements are also satisfactorily predicted.

The hydraulic behaviour of the barrier is shown in terms of the evolution of relative humidity with time in Fig. 67. Again the results for hot sections (Fig. 67(a)) and cool sections (Fig. 67(b)) are presented. Four points of the hot sections at different distances from the test axis are considered: 0·22 m (close to the heaters), 0·37 m, 0·55 m (intermediate points) and 0·70 m (close to the outer hydration boundary). They correspond to the locations of the capaci-

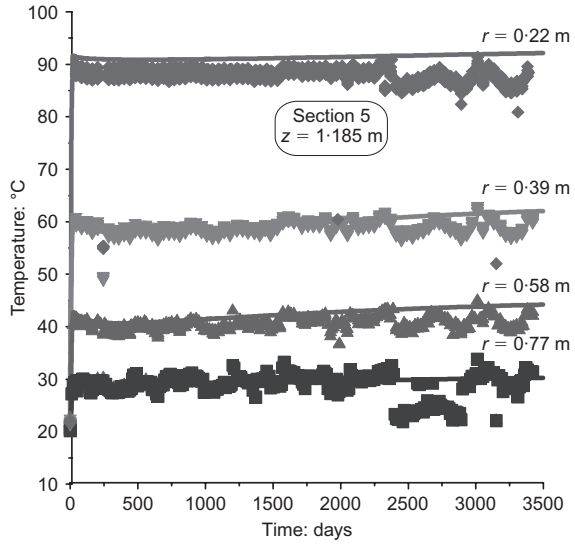

Fig. 66. Temperatures in the Febex mock-up test (observed and computed values): (a) sections A5–B5 in front of the heaters (hot sections); (b) sections A11–B11 away from the heaters (cool sections)

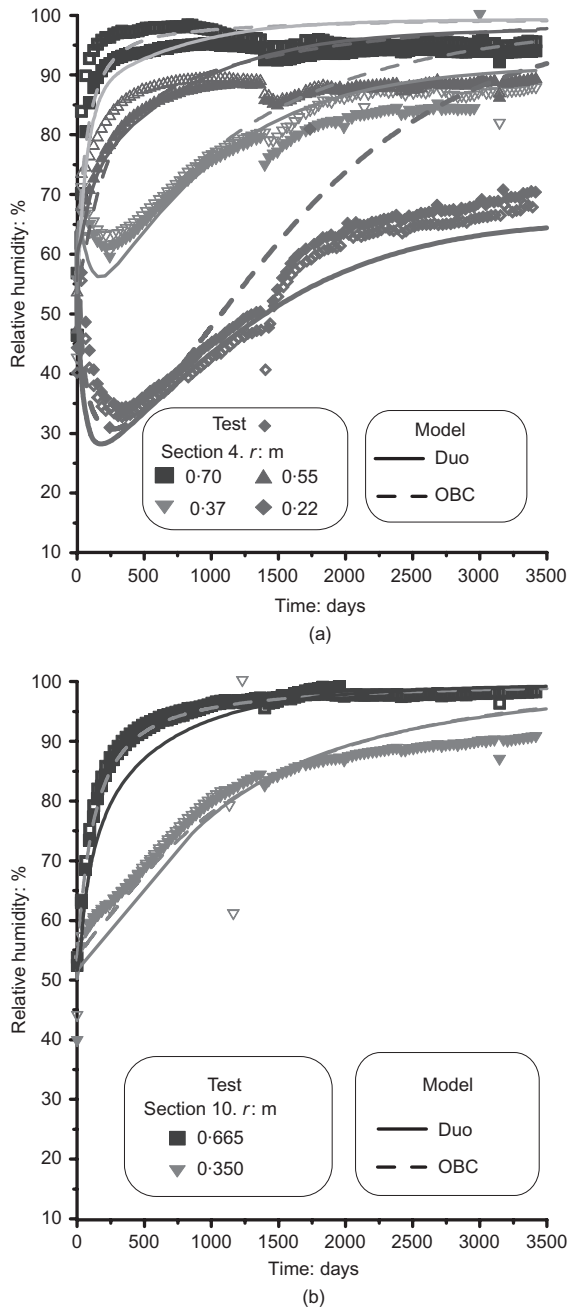

Fig. 67. Relative humidity in the Febex mock-up test (observed and computed values): a) sections A4–B4 in front of the heaters (hot sections); (b) sections A10–B10 away from the heaters (cool sections)

tive relative humidity sensors. The point closest to the heater undergoes an initial severe drying, followed by a more gradual subsequent hydration. Also, before the onset of drying, a temporary increase in relative humidity is detected: this is due to the passage of a vapour front coming from the innermost part of the barrier. Modelling successfully captures the three stages—temporary hydration by vapour, strong drying and final hydration—demonstrating that the phenomena of evaporation, condensation and vapour migration are well reproduced. The same behaviour, albeit in a more muted form, is observed at a distance of 0·37 m from the axis, both in the test and in the modelling. In contrast, at the points closer to the hydration boundary (0·55 m and 0·70 m), only a steady progress of hydration is measured and modelled. A continuous increase of relative humidity is also the behaviour exhibited by the cool sections (Fig. 67(b)). The outlier results obtained on day 1381 and immediately afterwards are the consequence of an unplanned overheating event that occurred on that day.

From Fig. 67(a), it is also apparent that the OBC predictions of relative humidity are very satisfactory up to day 900 or so; subsequently there is an increasing departure of predictions from observations. This lack of agreement for later times is confirmed by the observation of a global hydration variable, the total amount of water entering the bentonite barrier (Fig. 68(a)); differences are also apparent from about day 900 or so. It is evident that the OBC model fails to reproduce correctly the long-term behaviour of the test. Fig. 68(b) shows the development of radial pressures to quite high values of several MPa, owing to the hydration-induced swelling of the bentonite. The OBC analysis overestimates the long-term radial stresses, although inevitably, in the case of stress measurements, observation scatter is larger. Also, stresses were more strongly affected by the overheating episode.

A closer examination of the problem showed that the missing factor in the analysis was consideration of the evolution of the microstructure during the test. With the standard formulation, intrinsic permeability depends only on porosity, but in fact it depends more strongly on pore size and pore structure. In this test the variations of porosity are not large, because of the confinement provided by the heaters and steel container: the experiment is similar to a swelling pressure test. However, compacted bentonite has a very changeable microstructure. This is illustrated in Fig. 69, where micrographs of compacted Febex bentonite, obtained in the environmental scanning electron microscope, are shown for its initial state, for a partially hydrated condition, and for the final saturation state. Initially, the clay particles are clumped together in large aggregates, leaving large inter-aggregate pores between them. Intrinsic permeability is therefore high. However, as hydration advances, aggregates swell and progressively occupy the large pores. The consequence is that a matrix-dominated fabric takes over, with much smaller pores and a much reduced intrinsic permeability.

Fortunately a model for expansive clays was available (Gens & Alonso, 1992; Alonso *et al.*, 1999) that allows the separate, but interdependent, consideration of the two structures identified in the material: a macrostructure made up of a quasi-granular fabric of aggregates and large pores, and a microstructure related to the clay particles and the physicochemical phenomena occurring at that level (Fig. 70). The model attempts to resolve the paradox that the physicochemical phenomena underlying expansive clay behaviour are largely reversible, whereas the overall soil behaviour involves large amounts of irreversible strains. The BBM is used to model the behaviour of the macrostructure, and the relationship between the two levels is provided by appropriate interaction functions. The model has been formulated

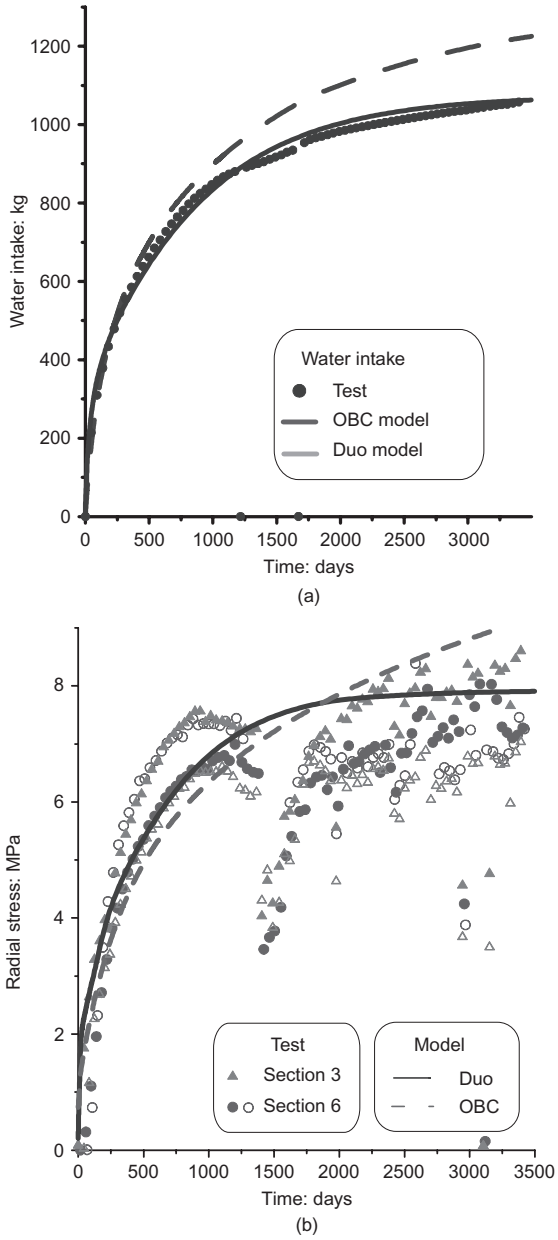

Fig. 68: (a) Water intake in the Febex mock-up test (observed and computed values): (b) radial stresses in sections A3–B3, in front of the heaters (observed and computed values)

mathematically in terms of a generalised plasticity framework (Sánchez *et al.*, 2005).

This constitutive model was adopted as a key component of a new analysis labelled 'Duo'. As it is now possible to track the evolution of macrostructure and microstructure, the intrinsic permeability is made dependent on macrostructure porosity alone. As shown in Figs 67 and 68, the results of the Duo analysis are much closer to observations, especially in the long term. It must be concluded that, in this case, a proper consideration of the fabric of the material and its modification by hydration is essential to achieve a good reproduction of the long-term behaviour of the barrier. It is a powerful reminder of the importance of taking microstructural features into account in the analysis of the problem.

Case history: THM response of an argillaceous host medium, the HE-D test

Beyond the engineered barrier of a HLW disposal scheme, there lies the geological host medium, the behaviour of

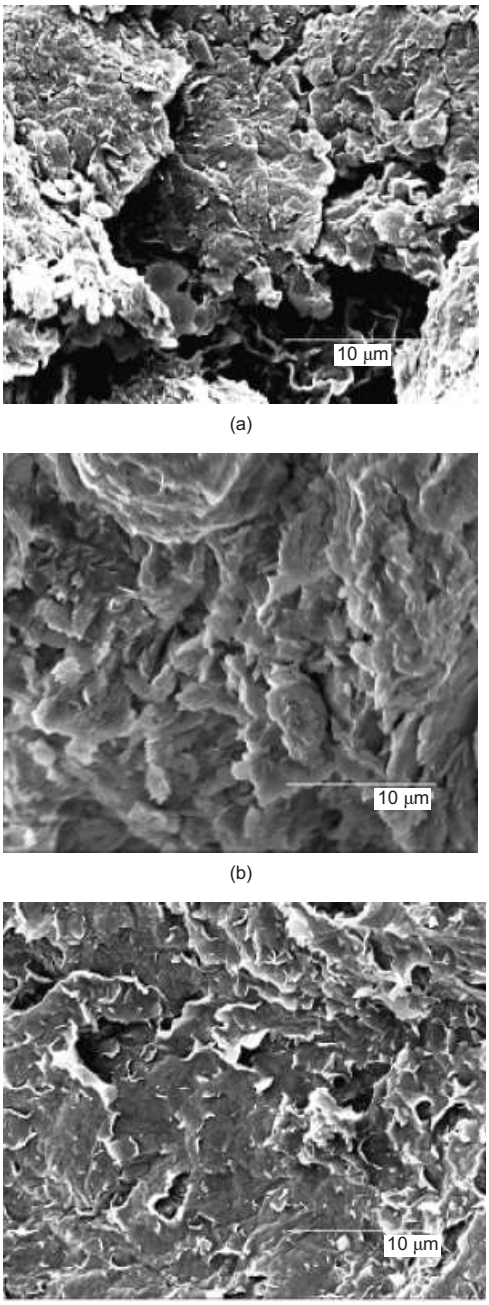

Fig. 69. Micrographs of compacted Febex bentonite (Villar *et al.*, 2004): (a) sample with hygroscopic water content (γ_d = 1·40 Mg/m^3); (b) sample after application of a suction of 10 MPa in isochoric conditions (γ_d final = 1·46 Mg/m^3); (c) sample after saturation in isochoric conditions (γ_d final = 1·43 Mg/m^3)

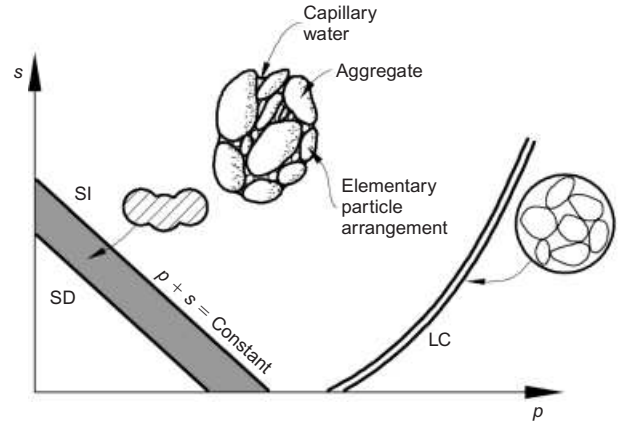

Fig. 70. Schematic representation of the double structure model in the isotropic plane

which must also be examined in detail. In the vicinity of the waste, the geological medium is also subjected to significant THM interactions, especially in the early stages of disposal. Soft argillaceous rocks provide one of the main geological settings considered for hosting HLW repositories. They possess several favourable features: low permeability, significant retardation properties for solute transport, a degree of self-healing capacity, and no foreseeable economic value. An aspect of interest in the assessment of a repository design is the potential generation of an excavation-damaged zone (EDZ) around the cavities excavated for the construction of the repository. The EDZ becomes a zone of higher permeability, and may provide a pathway for preferential radionuclide migration. This issue is especially relevant for soft argillaceous rocks because of their comparatively smaller strength compared with hard crystalline rocks. Thermal effects may enhance the EDZ, because significant pore pressures develop in saturated argillaceous materials owing to the differential thermal expansion of solid and liquid components. These thermally induced pore pressures may cause material damage and, in extreme cases, hydraulic fracture. In either case, an increase of permeability of the damaged or fractured zone ensues.

To examine the response of an argillaceous rock to thermal action in field conditions, an in situ test (HE-D) has been performed in the Mont Terri underground laboratory located in northern Switzerland (Thury & Bossart, 1999). The laboratory is excavated in Opalinus clay, a strongly bedded Mesozoic clay of marine origin. Opalinus clay is an anisotropic indurated clay of low porosity and, for an argillaceous material, significant strength. Some typical parameters are collected in Table 3: several of them depend on the orientation with respect to bedding. The overburden depth at the location of the Mont Terri laboratory varies between 250 m and 320 m.

The HE-D test involved the installation of two heaters in the final section of a 300 mm borehole (D0), drilled horizontally to a total length of 14 m from a niche especially excavated in the main laboratory tunnel. The heaters were 2 m long, with a separation of 0·8 m between them. They were pressurised to a pressure of 1 MPa to ensure good contact with the clay. The response of the clay to the thermal action of the heaters was monitored from boreholes drilled previously in the test area. Temperature, pore pressures and clay displacements were the main parameters measured. Fig. 71 shows a schematic layout of the test including the plan location of the heaters and the instrumentation boreholes. Fig. 72 shows the drilling of the borehole and the installation of one of the heaters. About one month after installation the heaters were switched on, with a total power of 650 W, and were kept at this power for 90 days. Subsequently, the power was increased to 1950 W for an additional period of 248 days. Finally, the heaters were switched off, and the test area was allowed to cool down.

A typical observation of the evolution of temperature and pore pressure is presented in Fig. 73. It was recorded in borehole D3, with the sensors located 1·1 m away from the axis of the experiment in the direction of the bedding planes. Pore pressures react immediately to heating, exhibiting a very strong response. Increments of 2·25 MPa are measured at this particular location: this is a magnitude similar to the estimated minor principal stress in the area. The evolutions of temperature and pore pressures do not

Table 3. Reference parameters for Opalinus clay (Wileveau, 2005)

	Parameter	Orientation to bedding	Reference value	Range
Mineralogy	Clay content: %		62	44–80
	Carbonate content: %		14	6–22
	Quartz content: %		18	10–27
Petrophysical properties	Density, ρ: g/cm^3		2·45	±0·03
	Water content, w: %		6·1	±1·9
	Porosity, n: %		15·7	±2·2
Mechanical properties	Uniaxial compression strength, R_c: MPa	Parallel	10	±6
		Perpendicular	16	±6
	Elastic modulus, E: MPa	Parallel	10 000	±3700
		Perpendicular	4000	±1000
Thermal and thermomechanical properties	Thermal conductivity, λ: W/(m K)	Parallel	2·1	±10%
		Perpendicular	0·995	±10%
	Heat capacity of dry material at 20°C, E_s: J/(kg K)		800	±10%
	Coefficient of linear thermal expansion, α_T: K^{-1}		$2{\cdot}6 \times 10^{-5}$	–
Hydraulic and hydromechanical properties	Hydraulic conductivity of sound clay, K: m/s		10^{-13}	10^{-12} to 10^{-14}
	Biot's coefficient, b		0·6	0·42–0·78

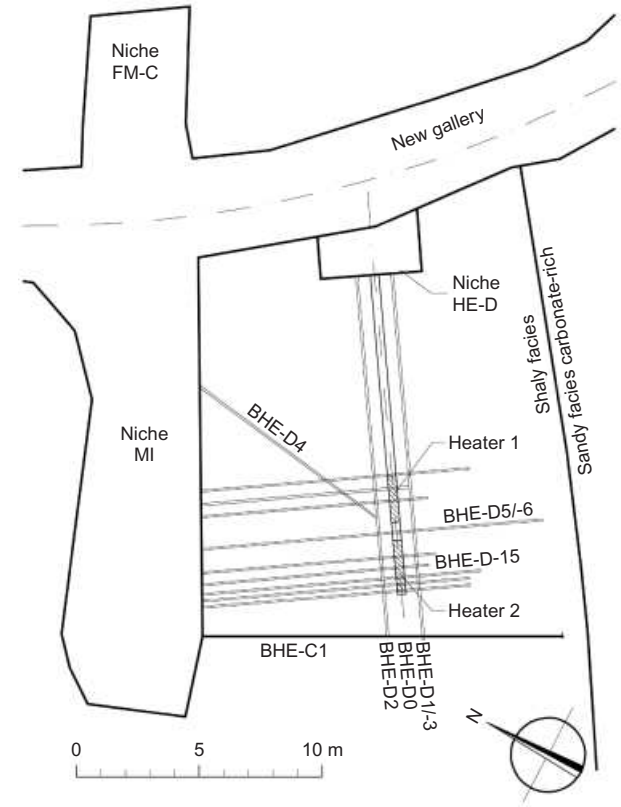

Fig. 71. Schematic layout of the HE-D test performed in the Mont Terri laboratory

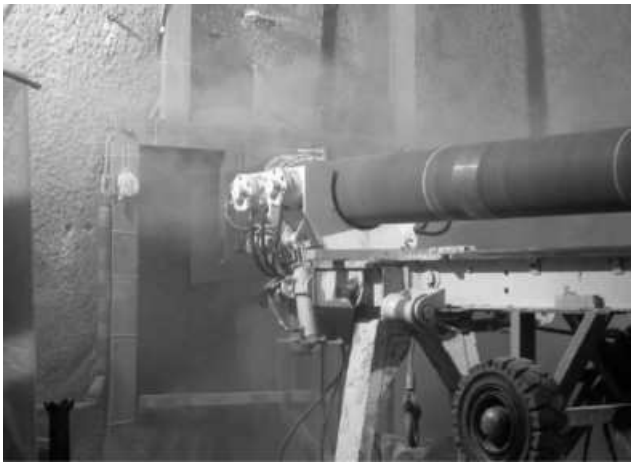

(a)

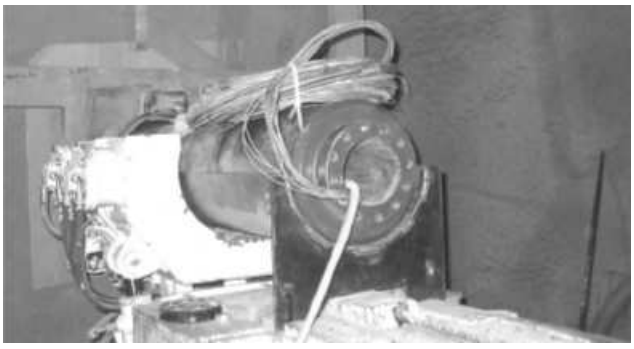

(b)

Fig. 72. Test HE-D: (a) drilling of the main borehole; (b) insertion of one heater

coincide: pore pressure reaches a maximum at a particular time and then decreases, in spite of the fact that temperature continues to rise. The development of pore pressures in the clay is a result of the interplay between the generation of pore pressures due to thermal action and the dissipation of pore pressures due to consolidation. In this case, dissipation by liquid flow overcomes the effects of temperature increase in the later stages of the experiment.

The coupled THM analysis formulation summarised above is required for a proper analysis and interpretation of the test results. However, here the particular case for saturated materials applies, since the Opalinus clay at Mont Terri is saturated, and no desaturation occurred during the test. Consequently, no gas flow description and no air balance equation are required. The resulting water mass balance equation provides an interesting insight into the process of pore water pressure generation. For saturated conditions, the equation for water mass balance (equation (48)) becomes

$$n\frac{D_s\rho_w}{Dt} + \frac{\rho_w}{\rho_s}(1-n)\frac{D_s\rho_s}{Dt} + \rho_w\nabla\frac{\mathrm{d}\boldsymbol{u}}{\mathrm{d}t} + \nabla(\rho_w\boldsymbol{q}_l) = 0 \quad (57)$$

The two first derivatives of this expression can be further developed by taking into account the variation of liquid and

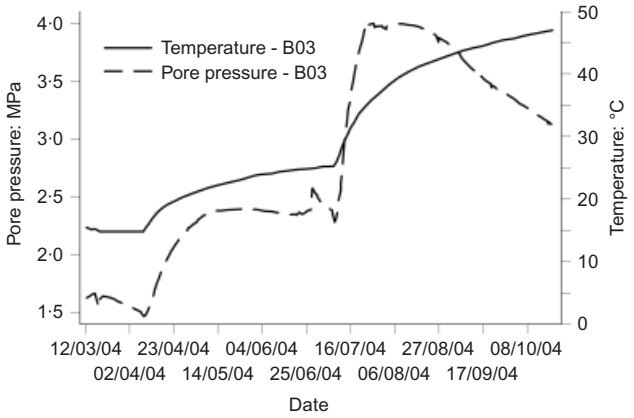

Fig. 73. Test HE-D: evolution of temperature and pore pressures measured in borehole D03

solid densities, which with some simplifications are assumed to be given by

$$\rho_w = \rho_{w0} \exp\left[\beta_w(p_l - p_{l0}) + b_w(T - T_{ref})\right] \quad (58)$$

$$\rho_s = \rho_{s0} \exp\left[\beta_s(p_l - p_{l0}) + 3b_s(T - T_{ref})\right] \quad (59)$$

where β_w and β_s are the water and solid compressibilities respectively, and b_w and b_s are the volumetric and linear thermal expansion coefficients for water and the solid phase respectively. Expanding the first two derivatives of equation (57) results in

$$[nb_w + (1-n)3b_s]\frac{D_s T}{Dt} + n\beta_w \frac{D_s p_l}{Dt} + (1-n)\beta_s \frac{D_s p_l}{Dt} + \nabla \frac{\mathrm{d}\boldsymbol{u}}{\mathrm{d}t} + \frac{\nabla(\rho_w \boldsymbol{q}_l)}{\rho_w} = 0 \quad (60)$$

Equation (60) contains most THM couplings that explain the generation and dissipation of pore pressure when a temperature change is applied to the clay. The first term expresses the differential thermal expansion of solid and liquid phases. The second and third terms are the volume changes of water and solid phase water associated with a pore pressure change; the fourth term is the volume change of the material skeleton (includes contributions from stresses, pore pressures and temperature); and the fifth term is the volume change associated with the flow of water in or out of the element considered. The pore pressure generated and its evolution are the result of the interplay of all these phenomena at each particular point.

A three-dimensional coupled THM analysis was performed so that the anisotropy of the material (thermal conductivity and stiffness) and of the in situ stress system could be accounted for. Because of the special characteristics of the Opalinus clay, a constitutive model has been used that tries to account for the fact that the microstructure of the material is a combination of a clay matrix and cementing bonds. The constitutive law, which is described in Vaunat & Gens (2003a, 2003b), is illustrated in Fig. 74. As in Gens & Nova (1993), bonding results in an increase of the size of the yield surface, but in this case the degradation of the bonds is described by a specific damage model. In this way, matrix and bond behaviour as well as bond damage can be described in an integrated manner. Extension to unsaturated conditions is described in Garitte *et al.* (2006).

A full description of the numerical modelling of the in situ test is presented in Gens *et al.* (2007); only some selected results are discussed here. Fig. 75 shows that the

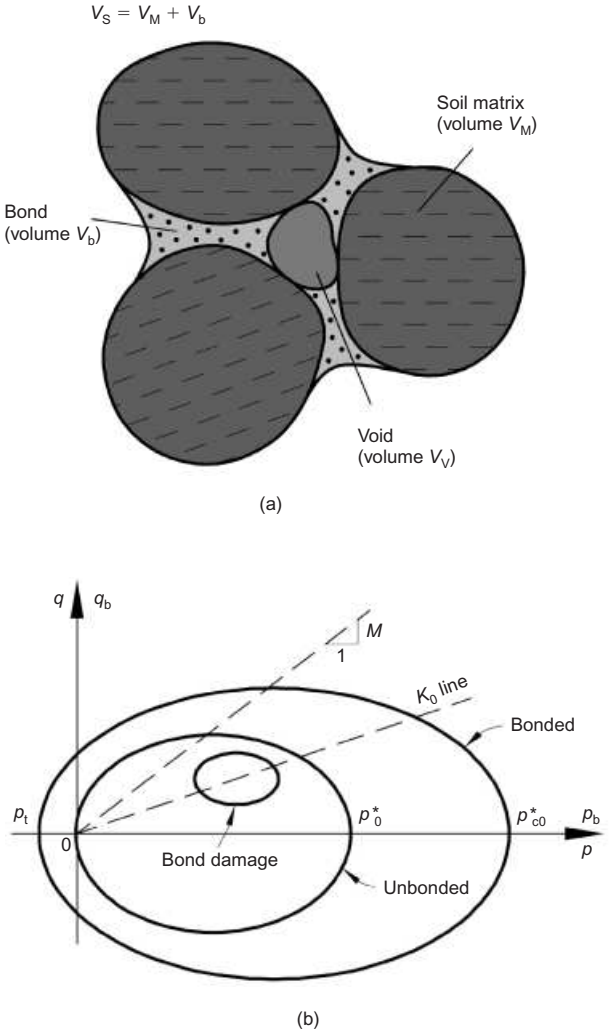

Fig. 74. (a) Conceptual scheme for the constitutive model for Opalinus clay; (b) yield surfaces for bonded and unbonded material and bond damage bubble (q_b and p_b are the stresses on the bonds) (Vaunat & Gens, 2003a, 2003b)

evolution of temperature during the two heating stages is well described by the three-dimensional analysis performed: a modest anisotropy in the temperature contours is discerned, owing to the different values of thermal conductivity parallel to and across the bedding planes. The computations also capture satisfactorily the variation of pore pressure resulting from thermal effects and dissipation (Fig. 76). The analysis revealed that, as the test progressed, the location of the maximum pore pressures gradually moved away from the heater. The measured distribution of dilatant strains close to the heaters and compressive strains away from the heaters was also adequately reproduced by the analysis (Gens *et al.*, 2007).

The mechanical constitutive model adopted provides information on the likely damage experienced by the material as a result of the thermal, hydraulic and mechanical actions. The consequences of damage are a degradation of elastic parameters and an increase in permeability. Fig. 77(a) shows the computed distribution of the unloading elastic modulus at various test times: the predicted size of the damaged zone increases during the heating stage, but does not develop further on cooling. During dismantling of the in situ test a borehole was drilled from the MI niche, perpendicular to the main borehole. The unconfined Young's moduli of a series of samples taken from this borehole at different distances from the heaters were determined by wave velocity measure-

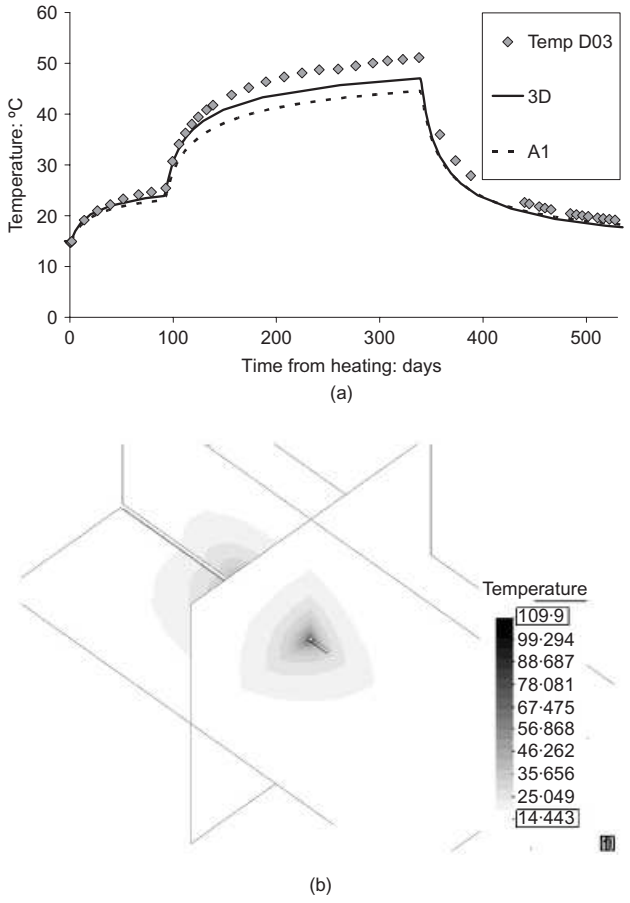

Fig. 75. Test HE-D: (a) observed and computed temperatures in borehole D03; (b) three-dimensional temperature contours at day 338, the end of the second heating stage

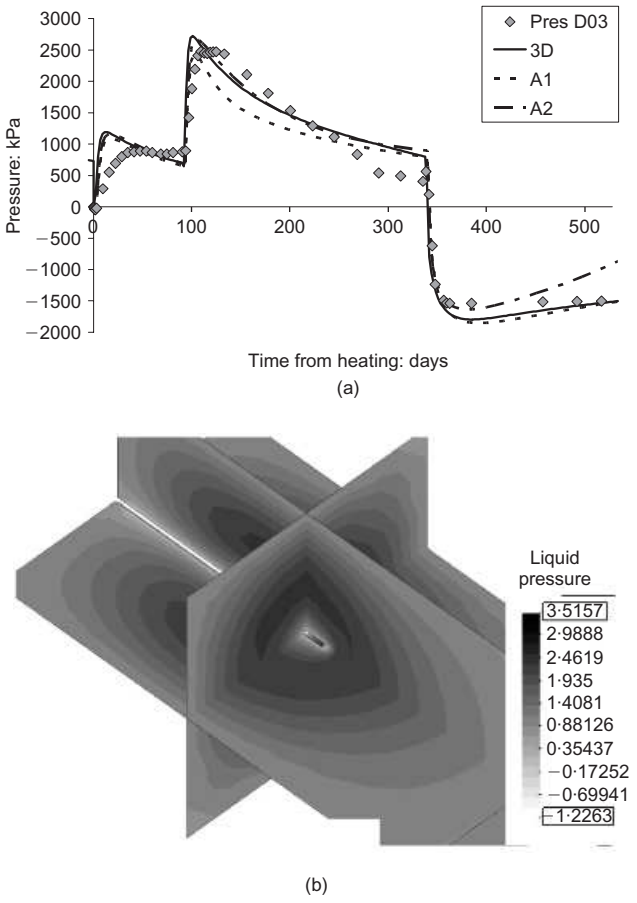

Fig. 76. Test HE-D: (a) observed and computed pore pressures in borehole D03; (b) three-dimensional pore pressure contours at day 338, the end of the second heating stage

ments (Pineda, personal communication, 2007). The measured moduli have been added to the plot of Fig. 77(a). The results obtained appear to confirm the existence of a damaged zone close to the heaters but, perhaps, not extending back into the clay as much as predicted by the computations at later times. The amount of independent experimental data, however, is not sufficient for drawing firm conclusions in this regard. Fig. 77(b) shows the distributions of permeability on the same section, derived from the amount of damage computed in the analysis. In the laboratory tests on damaged Opalinus clay samples reported by Coll (2005) the values of measured intrinsic permeability were in the range 10^{-17} to 10^{-19} m^2, similar to those predicted by the analysis. Unfortunately, no in situ permeability measurements were performed to allow an independent check of the predictions.

The availability of a conceptual and numerical model that is capable of simulating the main features of the test permits, by means of suitable sensitivity analysis, a deeper examination of the structure of the problem. For instance, it is possible to classify the degree of coupling between the various THM phenomena involved (Gens *et al.*, 2007), as follows.

(*a*) The strongest coupling is found from thermal to hydraulic and mechanical behaviour. Pore pressure generation is controlled primarily by temperature increase, and the largest contributor to deformation and displacements is thermal expansion.
(*b*) Significant but more moderate effects are identified from the coupling of hydraulic to mechanical behaviour. The dissipation of pore pressures induces additional displacements and strains, but, because of the large clay stiffness, they are smaller than thermally induced deformations.
(*c*) In principle, mechanical damage could impact on the hydraulic results because of the development of higher permeability due to material damage. The damaged zone, however, appears to be limited in this case, given the modest power of the heating elements.
(*d*) There is no noticeable coupling from hydraulic to thermal behaviour. Practically all heat transport is by conduction, and the thermal conductivity of the material does not change, as the material remains saturated throughout.
(*e*) Coupling from mechanical to thermal behaviour is negligible. The changes of clay porosity are so slight that they do not affect thermal conductivity. In addition, mechanical energy dissipation is insignificant in this non-isothermal case.

Thermal effects (high temperatures): summary

The consideration of thermal effects has required the incorporation of a new environmental variable, temperature, and the inclusion of a new balance equation expressing the conservation of energy. It is noteworthy that temperature has a pervasive effect on practically all phenomena considered: consequently most constitutive laws have to incorporate some degree of temperature dependence. In the case of the mechanical constitutive law, significant developments are required to capture the sometimes highly complex thermal effects on mechanical behaviour.

The formulation described has proved capable of capturing the main features of THM behaviour as observed in

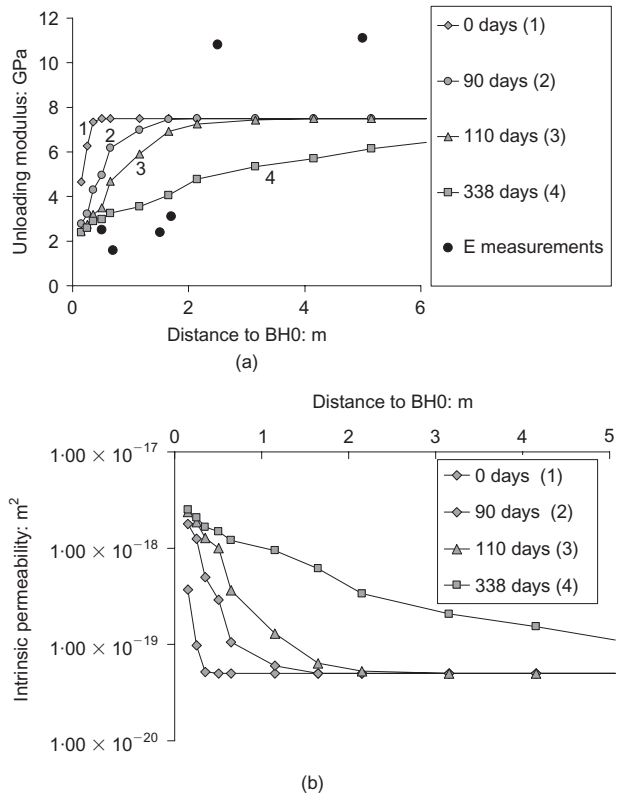

Fig. 77. Test HE-D: (a) distribution of computed unloading elastic modulus at various times on a section perpendicular to the heater (values of elastic modulus obtained from samples taken at the end of the test are plotted); (b) distribution of computed permeability values at various times on a section perpendicular to the heater

large-scale heating tests related to nuclear waste disposal. Satisfactory reproduction of behaviour has been achieved for both unsaturated and saturated problems addressing quite different phenomena. In the unsaturated case, evaporation, condensation, vapour migration and hydration are dominant. In the saturated case, the key issues are thermally induced pore pressure generation, pore pressure dissipation, and clay damage. An enhanced understanding of the overall repository system is undoubtedly one of the main benefits of the availability of a proper formulation, and of modelling tools capable of incorporating the main physical phenomena as well as their interactions.

THERMAL EFFECTS: LOW TEMPERATURES

General

This section deals with non-isothermal problems at low temperature, focusing on the study of frozen ground and freezing–thawing phenomena. Freezing and frozen ground has been a subject of permanent interest, especially but not exclusively for geotechnical engineers working in cold climates (e.g. Andersland & Ladanyi, 2004). For instance, foundation of freezing facilities and the use of ground freezing as a construction technique are problems that occur independently of climate conditions, and still require a good understanding of the physical processes involved. The same understanding can be used to achieve a better comprehension of glacial and periglacial processes, and their impact on present geomorphological features. Although the formulation to be described is general, the main application area is related to permafrost and freezing ground in cold regions. Permafrost underlies about 24% of the Northern hemisphere landmass, although of course most of those areas are thinly inhabited. However, resource and transport development in remote areas requires the performance of major engineering works in permafrost areas. As an example, in the recently constructed Qinhai-Tibet railway, of the total 1142 km length, 550 km are constructed on continuous permafrost and about 82 km more on discontinuous permafrost (Wu *et al.*, 2006). There is also concern about potential permafrost degradation due to possible climate changes (IPCC, 2007). Indeed, much of the material presented here is one result from a multidisciplinary project funded by BP to address the issue of climate change risk assessment in cold regions (Clarke *et al.*, 2008).

The process of soil freezing exhibits a certain degree of complexity. Assuming that the soil is saturated, when the temperature drops to 0°C, the water least bound to the solid surface starts to freeze. As the temperature drops further, more liquid water becomes frozen in a progressive manner. Liquid water/ice interfaces appear, which play a role similar to that of the liquid/gas interfaces in unsaturated soils (Fig. 78). A consequence of this ongoing process is that liquid water develops increasing values of suction as temperature reduces: this suction is responsible for attracting water from the unfrozen soil areas, in response to the difference in potential. Clearly, many of these concepts and phenomena recall analogous concepts and phenomena discussed earlier in the context of unsaturated soils.

An early paper by Williams (1964) examined, using calorimetric techniques, the evolution of the unfrozen water content with temperature for a range of soils (Fig. 79). The relationship between suction and water content for the unfrozen soils in an unsaturated condition was also established using a pressure plate apparatus. Thereby, the correlation between temperature and suction could be plotted for the various soils. As Fig. 80 shows, a practically unique relationship is obtained.

This direct relationship between suction and temperature can in fact be expected from thermodynamic equilibrium considerations. If it is assumed that the two phases are in equilibrium, ice and liquid water have the same chemical potential, although they may have different pressures (e.g. Kirillin *et al.*, 1976). Thus

$$-(s_{\mathrm{l}} - s_{\mathrm{i}})\mathrm{d}T + v_{\mathrm{l}}\mathrm{d}p_{\mathrm{l}} - v_{\mathrm{i}}\mathrm{d}p_{\mathrm{i}} = 0 \tag{61}$$

where s_{l}, v_{l} and p_{l} are the specific entropy, the specific volume and the pressure of liquid water respectively, and s_{i}, v_{i} and p_{i} are the same properties referred to ice. Rearran-

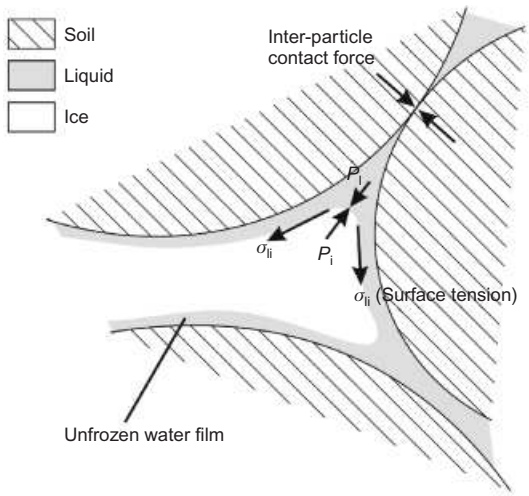

Fig. 78. Schematic arrangement of solid phase, unfrozen water, ice and interfaces in a frozen soil

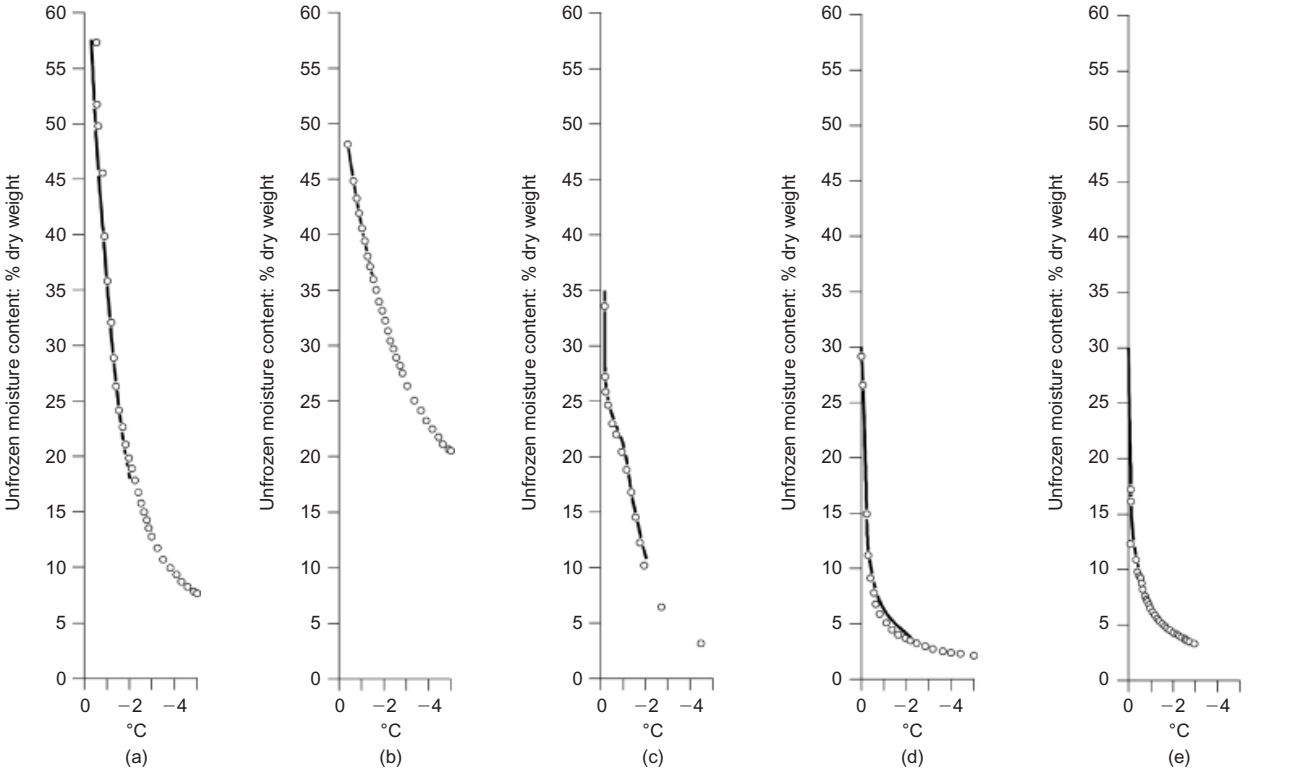

Fig. 79. Unfrozen water content as a function of temperature for various soils (Williams, 1964): (a) Leda clay GC-8; (b) Winnipeg clay B; (c) Leda clay KNB; (d) iron ore; (e) Niagara silt

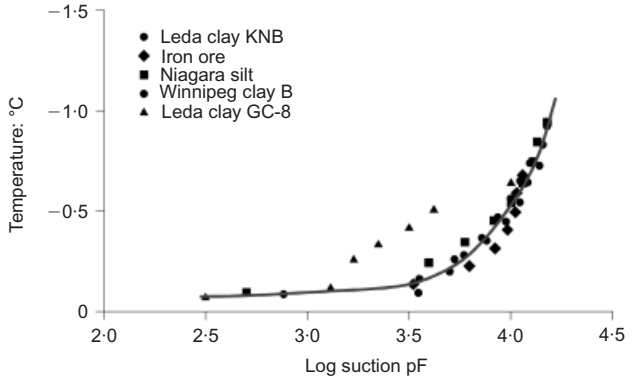

Fig. 80. Relationship between temperature and suction for various soils (Williams, 1964). Suction is given in pF units; pF is the logarithm of pore water potential in centimetres of water (head units). pF 4·0 = 1 MPa

ging, and knowing that specific volumes are in inverse relationship with mass density,

$$\mathrm{d}p_\mathrm{i} = \frac{\rho_\mathrm{i}}{\rho_\mathrm{l}}\mathrm{d}p_\mathrm{l} - \frac{\rho_\mathrm{i} l}{T}\mathrm{d}T \tag{62}$$

where ρ_l and ρ_i are the densities of liquid water and ice respectively, and l is the specific latent heat of fusion: $l = (s_\mathrm{l} - s_\mathrm{i})\ T$. This is a form of the well-known Clausius–Clapeyron–Poynting equation. The latent heat of melting is 333·7 kJ/kg. Equation (62) can be integrated, taking atmospheric pressure and $T = 273{\cdot}15$ K as references, to give

$$p_\mathrm{i} = \frac{\rho_\mathrm{i}}{\rho_\mathrm{l}}p_\mathrm{l} - \rho_\mathrm{i} l \ln\left(\frac{T}{273{\cdot}15}\right) \tag{63}$$

Therefore, in thermodynamic equilibrium, p_i, p_l and T must satisfy equation (63). This relationship must be incorporated into the formulation.

Coupled formulation for freezing and frozen soils

Much attention has been paid to the problem of frost heave involving freezing and thawing soils, leading to the development of numerous coupled thermo-hydraulic (TH) models using a variety of approaches: rigid-ice models (e.g. O'Neill & Miller, 1985), hydrodynamic models (e.g. Newman & Wilson, 1997), or the segregation potential model (Konrad & Morgenstern, 1980, 1981). Semi-coupled models (Selvadurai *et al.*, 1999a, 1999b), and fully coupled THM models (Blanchard & Fremond, 1985; Li *et al.*, 2000, 2002) are less common, and the architecture of such models does not appear to be well established yet (Nishimura *et al.*, 2009). Herein, the same pattern of formulation development used before is applied to the present low-temperature case.

Balance equations. Naturally, the relevant environmental variable is again the temperature. In this case, the required energy balance equation is developed for saturated soils: the only species are now solid mineral and water. Three phases are considered, however: solid (s), liquid (l) and ice (i). As before, mineral species and solid phase coincide.

The derivation of the energy balance equation follows the same procedure as for the high-temperature case. For an REV, it establishes that the change of internal energy must be equal to the net inflow/outflow of heat (plus any sink/source term that may exist). The following equation results:

$$\begin{aligned}&\frac{\partial}{\partial t}\left[E_\mathrm{s}\rho_\mathrm{s}(1-n) + E_\mathrm{l}\rho_\mathrm{l}S_\mathrm{l}n + E_\mathrm{i}\rho_\mathrm{i}S_\mathrm{i}n\right]\\ &\quad + \nabla(\boldsymbol{i}_\mathrm{c} + \boldsymbol{j}_\mathrm{Es} + \boldsymbol{j}_\mathrm{El} + \boldsymbol{j}_\mathrm{Ei}) = f^\mathrm{Q}\end{aligned} \tag{64}$$

where E_s, E_l and E_i are the specific internal energies of solid mineral, liquid water and ice respectively; $\boldsymbol{i}_\mathrm{c}$ is the heat flow by conduction, and $\boldsymbol{j}_\mathrm{Es}$, $\boldsymbol{j}_\mathrm{El}$ and $\boldsymbol{j}_\mathrm{Ei}$ are the total advective energy flows carried by the movement of the solid mineral, liquid water and ice respectively; f^Q is the sink/source term;

and S_l and S_i are the liquid and ice degrees of saturation, $S_l + S_i = 1$.

The specific internal energies are defined as

$$E_s = c_s T; \quad E_l = c_l T; \quad E_i = -l + c_i T \tag{65}$$

where c_s, c_l and c_i are the specific heats for solid mineral, liquid water and ice respectively. The specific heat of ice (2·05 kJ/(kg K) at 0°C) is significantly lower than that of liquid water (4·18 kJ/(kg K) at 25°C).

To complete the formulation, the energy balance equation must be solved together with the rest of the balance equations: solid mass balance (equation (17)), water mass balance,

$$\frac{\partial}{\partial t}\left(\theta_l^w S_l n + \theta_i^w S_i n\right) + \nabla\left(\boldsymbol{j}_l^w + \boldsymbol{j}_i^w\right) = f^w \tag{66}$$

and equilibrium (equation (18)). In equation (66) the reduction of density when liquid water turns into ice must be considered. After phase change, the density of ice is 916·2 kg/m^3, and it increases only slowly as the temperature reduces (e.g. 918·9 kg/m^3 at −10°C and 925·7 kg/m^3 at −100°C). In the formulation it is assumed that there is no flow of ice relative to the solid phase ($\boldsymbol{j}_i^w = \boldsymbol{j}_s$), a realistic hypothesis.

Constitutive equations. Only the most characteristic constitutive equations are briefly reviewed here. Again, the most important mechanism for energy transport is heat conduction, governed by Fourier's law (equation (52)). In this case the geometric mean of the thermal conductivities of the phases, weighted by volumetric fractions, appears also to provide an adequate estimate of the overall thermal conductivity (Côté & Konrad, 2005):

$$\lambda = \lambda_s^{1-n} \lambda_l^{S_l n} \lambda_i^{(1-S_l)n} \tag{67}$$

The thermal conductivity of liquid water (0·6 W/(m K) at 25°C) is significantly lower than that of ice (2·22 W/(m K) at 0°C).

As before, the advective flow of liquid, $\mathbf{q}_l$, is governed by Darcy's law (equations (19) and (20)). As for unsaturated soils, relative permeability varies by several orders of magnitude, depending on the degree of saturation of unfrozen water content (Fig. 81). As soon as the ice content in the soil grows, the flow of liquid water reduces drastically.

There is a clear parallel between the retention curve of unsaturated soils and the freezing characteristic function that relates the degree of liquid (unfrozen water) saturation S_l to soil suction (e.g. Black & Tice, 1989). Both of them are determined by the soil pore size characteristics and the interface surface tension (Fredlund & Xing, 1994; Coussy, 2005). Because of the requirement that the Clausius–Clapeyron–Poynting equation (63) be satisfied, a well-established effect of temperature on the freezing characteristic curve results.

The mechanical behaviour of frozen soils is undoubtedly complex. It has frequently been modelled using approaches based on total stresses (e.g. Ladanyi, 1972; Nixon, 1978; Jessberger, 1981; He *et al.*, 2000; Arenson & Springman, 2005). Effective stress approaches using a single stress variable have been less common. Li *et al.* (2000) adopted Bishop's expression for effective stress, replacing gas pressure by ice pressure. This approach has the drawback that, in ice-rich soils in which ice pressure is dominant, it leads to very low values of shear strength at low stresses, against observations.

Nishimura *et al.* (2009) have proposed a different mechanical constitutive law based on the BBM, and using two independent stress variables: net stress, $\boldsymbol{\sigma} = \boldsymbol{\sigma}_t - p_i \boldsymbol{I}$; and suction, $s = p_i - p_l$ (Fig. 82). Here ice pressure p_i plays the role of reference pressure. As shown in Fig. 82, the expansion of the yield surface when temperature reduces (associated with an increase of suction) involves both enhanced particle interlocking (expansion towards the right) and ice strengthening (expansion towards the left). In this simple way, the combined effects of porosity and ice strengthening are accounted for. Fig. 83 compares qualitatively the strength prediction of the model with experimental results obtained in tests on frozen Ottawa sand (Goughnour & Andersland, 1968). The model appears to accommodate the various factors contributing to the frozen soil strength. More information on the mechanical constitutive model is provided in Nishimura *et al.* (2009).

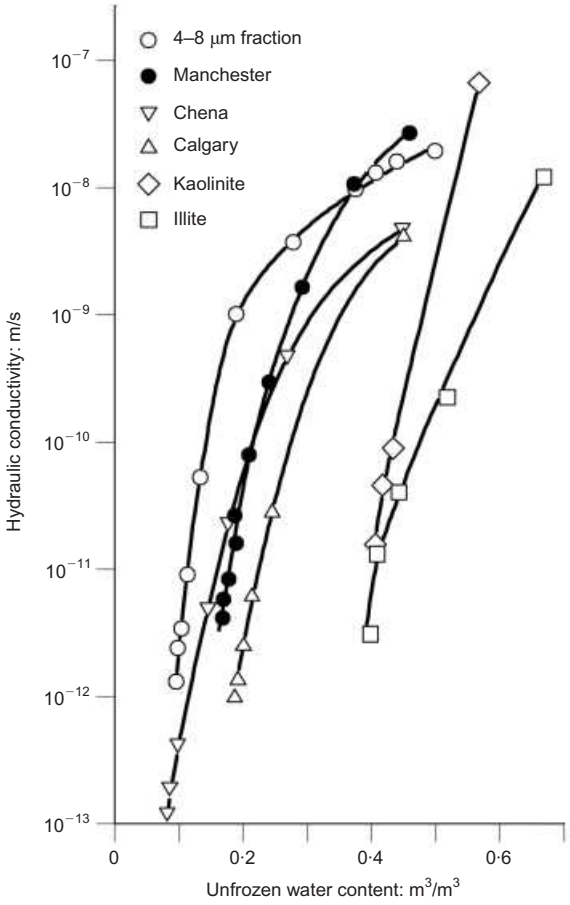

Fig. 81. Variation of hydraulic conductivity with unfrozen water content for various soils (Horiguchi & Miller, 1983)

Naturally, this very simple model fails to incorporate some important features of behaviour: the most obvious one is the characteristic time-dependent behaviour of frozen ground. Also, the model does not account for the phenomenon of cumulative thaw consolidation (Nixon & Morgenstern, 1973). To reproduce these behaviour features it is necessary to enhance the model to include a viscous formulation and cyclic behaviour inside the main yield locus, in a way similar to the generalisation of classical critical state models.

Development of ground freezing

It is interesting to test the formulation against current understanding of the development of ground freezing. If the temperature in the atmosphere drops below 0°C for an extended period of time, ground freezing will develop from the surface downwards (Fig. 84). The boundary between frozen and unfrozen soil will be in the region of the ground

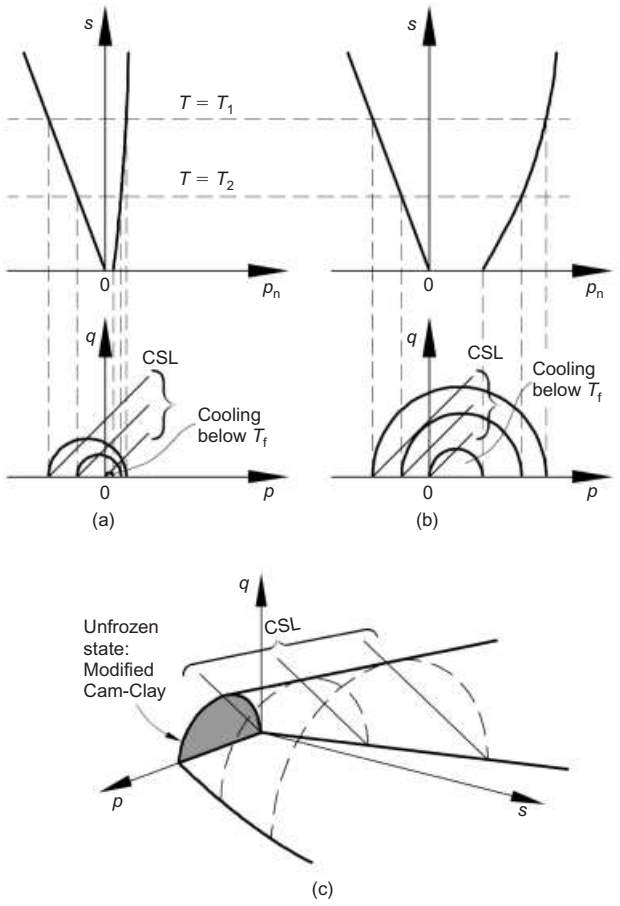

Fig. 82. Mechanical constitutive model for frozen soils (Nishimura *et al.*, 2009): (a) projections of the yield surface, ice-rich soil; (b) projections of the yield surface, ice-poor soil; (c) three-dimensional view of the yield surface for frozen soils

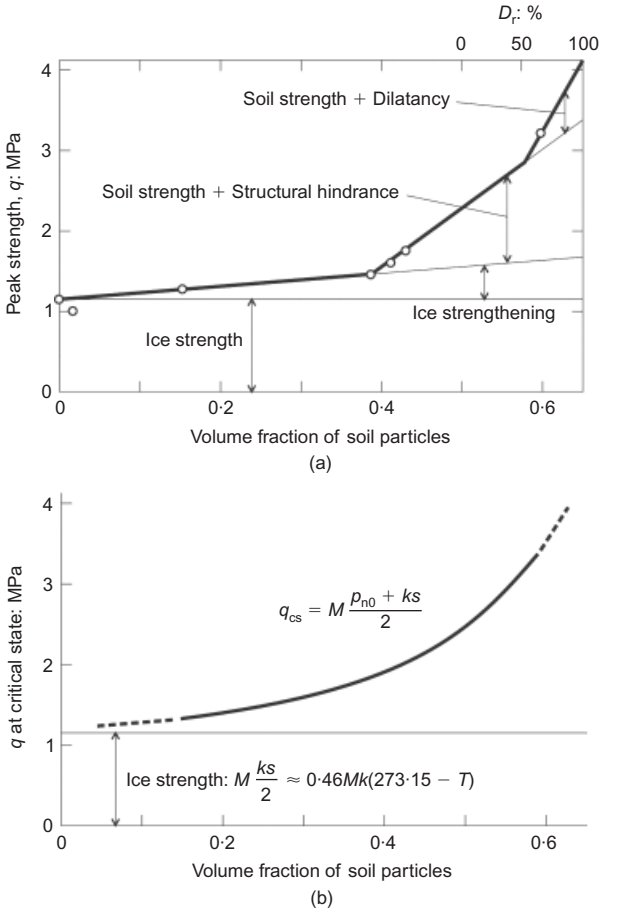

Fig. 83. Shear strength against porosity relationships: (a) experimental results from unconfined compression tests on Ottawa sand at −7°C and strain rate of $4{\cdot}4 \times 10^{-4}$ s^{-1} (after Goughnour & Andersland, 1968); (b) prediction of the constitutive model of Nishimura *et al.* (2009)

where the temperature hovers around 0°C, where a frozen fringe may develop. Liquid water is attracted to this region because of the suction developing in the soil due to freezing. When liquid water reaches the frozen fringe it freezes, leading to an accumulation of ice in the area. High suctions also exist in the frozen ground above, but there is practically no flow of liquid water because of the extreme reduction of permeability with increasing ice content. Fig. 85 shows the results of a one-dimensional analysis performed with the formulation outlined above. It has been assumed that the temperature at the surface drops to −8°C. The long-term distributions of liquid saturation, porosity, ice and liquid pressures and temperature are presented. A frozen fringe has developed at a depth between 2 m and 3 m, characterised by a rapid drop in liquid saturation and a large increase of porosity caused by ice accumulation. The development of a sizeable frozen fringe requires that the boundary between frozen and unfrozen ground remain approximately stationary for a significant period of time.

The evolution of porosity predicted by the model during freezing and subsequent thawing can be followed in Fig. 86. As freezing starts, net pressure reduces (because of increased ice pressure), and it may reach very low values (A–B). Accordingly, stiffness is very low, and the soil allows a large increase in porosity to accommodate ice accumulation (B–C). If at some point temperature rises again, net stress will increase again, owing to the reduction of ice pressure. The state of the soil will eventually travel down the virgin consolidation line until the initial stress condition is reached (C–D–F). A possible outcome is that, after the freezing–thawing cycle, the final soil porosity will be higher than the initial one. If thawing is fast, pore water pressures may develop, Δp_l, that will finally dissipate to reach the same final equilibrium condition (C–D–E–F).

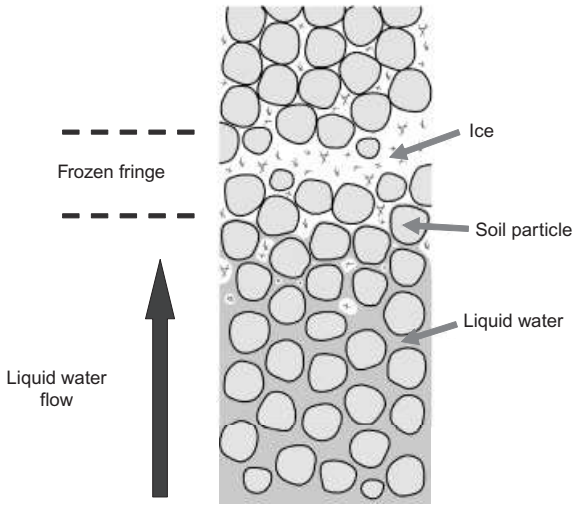

Fig. 84. Ground freezing phenomena with the development of an ice-rich frozen fringe

The study of both active and relic periglacial solifluction has been intense, because of the implications for slope stability in the areas where they are present (e.g. Hutchinson, 1970; Chandler, 1976; Chandler *et al.*, 1976; Skempton &

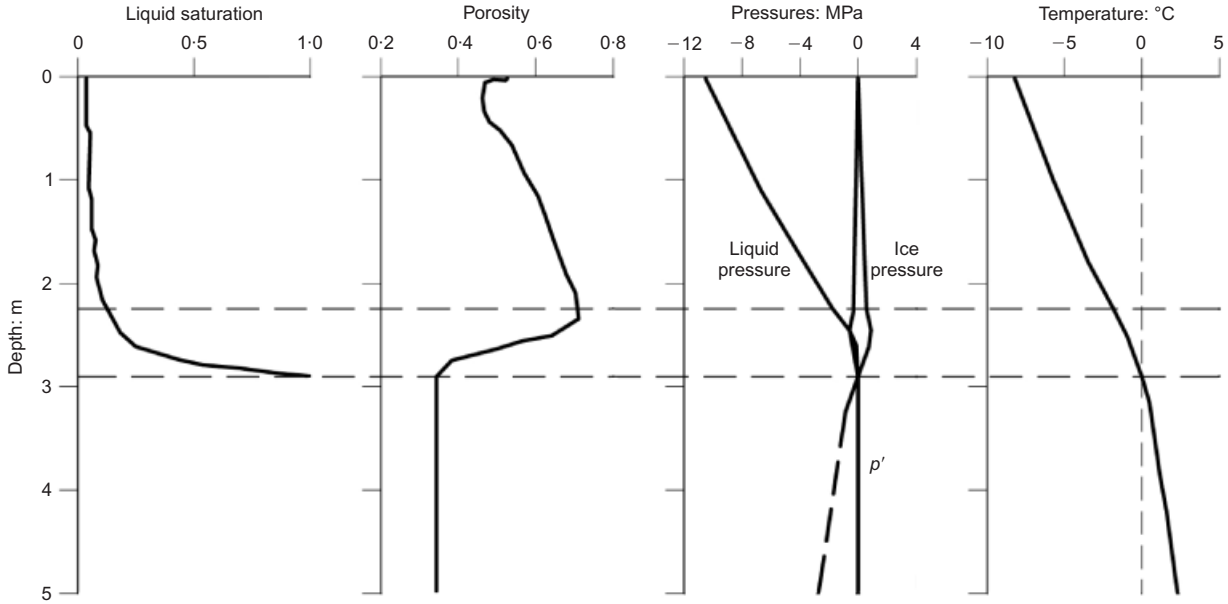

Fig. 85. Results from the numerical modelling of the development of ground freezing from the surface: a frozen fringe has developed

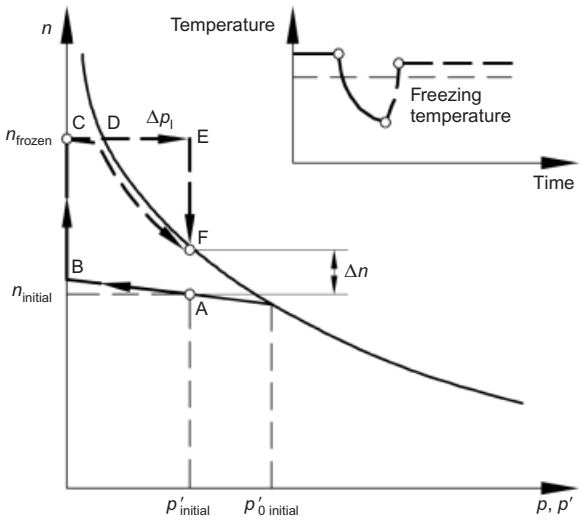

Fig. 86. Evolution of porosity during a cycle of freezing and thawing, according to the formulation

Weeks, 1976; Skempton *et al.*, 1990). Hutchinson (1991) proposed a three-stage mechanism for the formation of solifluction features in a London clay slope, as illustrated in Fig. 87. The mechanism can be related to the model results shown in Fig. 86. The first stage relates to the periglacial winter (Fig. 87(a)), where ground freezing occurs and produces a loose structure of the soil (A–B–C). During the second stage (periglacial summer; Fig. 87(b)), the ground melts, and if thawing is fast, positive pore pressures develop (C–D–E). Finally, in the third stage (Fig. 87(c)), pore pressures dissipate, leading to present-day conditions (E–F). Therefore it appears that a quite good correspondence exists between the porosity–stress paths derived from the model and the development of solifluction features inferred from geological evidence.

Case history: chilled pipeline buried in unfrozen ground

In permafrost regions, pipeline gas is transported chilled, in order to avoid melting the underlying ground. However, there are areas (for instance near water streams) in which the ground is not frozen, but it may become so owing to the passage of chilled gas. Frost heave phenomena affecting the pipeline may then occur. To examine this problem, a series of full-scale in situ tests were performed by Slusarchuk *et al.* (1978) in Calgary, Canada. They involved excavating trenches in permafrost-free silty soil and placing in them full-scale 1·22 m diameter steel pipelines that were chilled to a temperature of −8·5°C. The frost-susceptible soil was about 13% sand, 64% silt and 23% clay; water content was in the 18–22% region; and the Atterberg limits were $w_P = 14–18\%$ and $w_L = 24–31\%$. The excavated ground was used as backfill. Subsequent ground heave was monitored for periods from 3 to 10 years. The analyses of two sections are presented here: a control section, in which the pipeline invert was located 2 m below the surface; and a deep burial section, in which the invert depth was 2·9 m (Fig. 88). The pipeline temperature was reduced linearly from 6·5°C to −8·5°C over 50 days, and was then kept constant. In one series of analyses presented here, air temperature was kept constant and equal to 6·5°C. In another series, air temperature was varied on a monthly basis, between −8°C in January and +16·5°C in July. Computed pipeline heaves were very similar for the two hypotheses. The complete series of computations and the full details of the analyses are described in Nishimura *et al.* (2009).

In Fig. 89 the computed pipeline heave is compared with observations for the control case and the deep burial case. The heave in the latter case is well reproduced over the three years of comparison. In the control section comparison is also adequate up to about 600 days; some departures from observation are observed afterwards. Given the uncertainties in some of the test features, the results obtained provide a satisfactory partial validation of the formulation described. In Fig. 90 contours of porosities and distributions of liquid water flux vectors are shown at two different times for the control section. A fringe of much higher porosity develops around the pipeline (Figs 90(a) and 90(b)). It is clear that the ice accumulation in this area drives pipeline heave. The flow of water into the freezing region is plainly visible in Figs 90(c) and 90(d); in contrast, liquid water flow in the frozen ground area is completely negligible.

Carlson & Nixon (1988) reported a vertical distribution of final water content from an ‘insulated silt’ section in which an additional insulation layer was placed around the pipe (Fig. 91). No. equivalent data are available for the analysed control

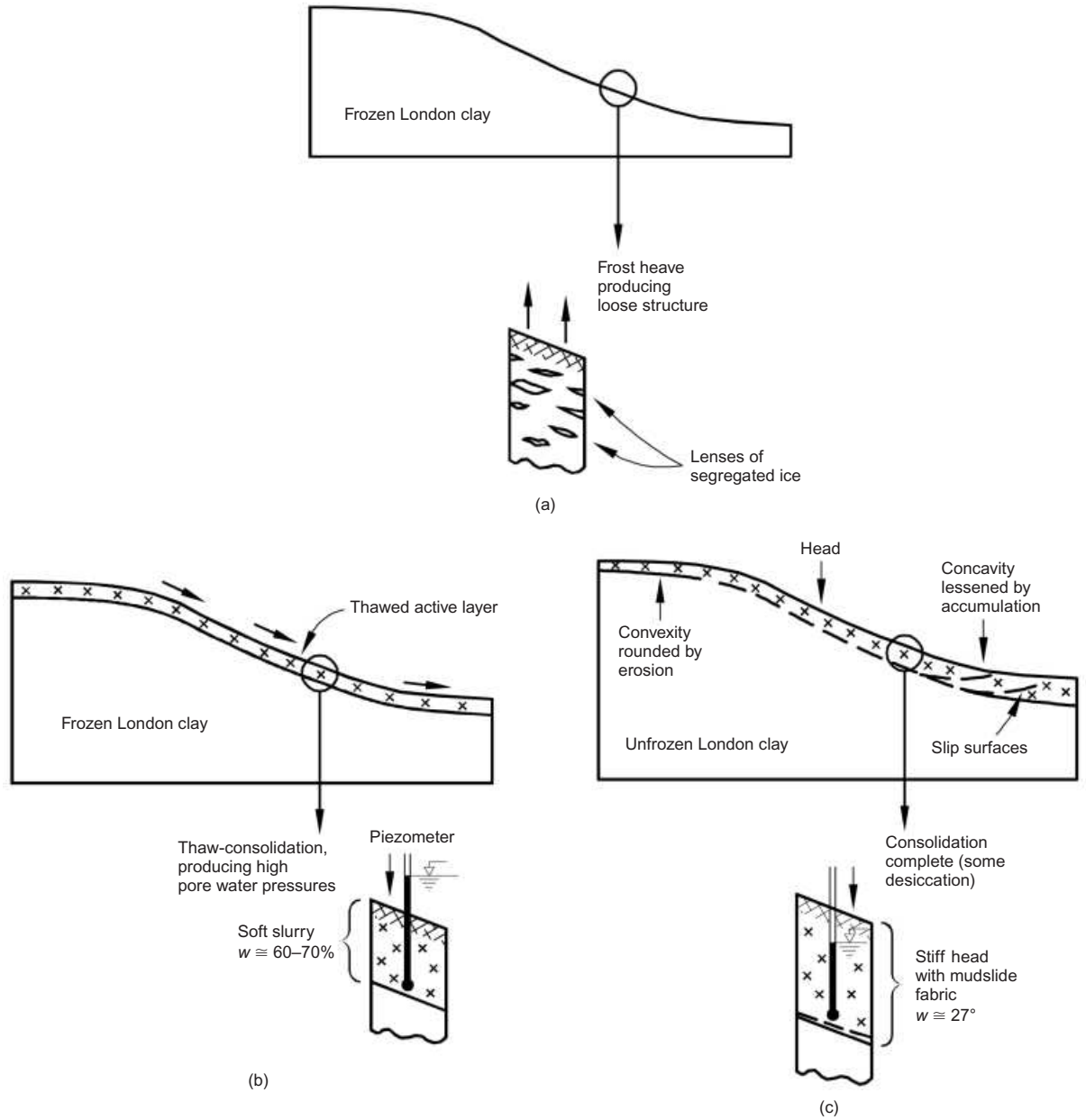

Fig. 87. Diagrammatic illustration of the active and relic stages of periglacial solifluction on a slope of stiff clay (Hutchinson, 1991): (a) periglacial winter (stable); (b) periglacial summer (slow, shallow mudsliding begins); (c) present day (stable convexo-concave slope)

and deep burial sections. The measured distribution of water content is similar to that obtained from the deep burial section calculation; perhaps the isolation layer has reduced frost heave in a way similar to that of deep burial. The frost penetration depth was similar in the two analyses, and is very close to the observed depth. The simulation also reproduces very well the observed trend for water content to increase gradually from the pipeline invert to the frozen ground base.

Thermal effects (low temperatures): summary

The consideration of thermal effects at low temperatures has again required the incorporation of an environmental variable, temperature, and a balance equation establishing the conservation of energy. The formulation has been restricted to the freezing of initially saturated soils. Constitutive laws have also been used incorporating thermal effects at low temperatures. In addition, the Clausius–Clapeyron–Poynting equation provides a direct relationship between temperature and the freezing characteristic curve.

It is highly significant that several concepts from unsaturated soil mechanics have analogous counterparts in the case of freezing soil, attesting to a conceptual continuity between the two areas of work. From this perspective, the successful transfer of BBM concepts to the modelling of the mechanical behaviour of frozen ground is another indication of this conceptual connection. The coupled formulation developed appears to provide realistic qualitative results concerning the development of freezing ground and the effects of a freeze–thaw cycle in periglacial conditions. The formulation has also provided a satisfactory account of the development of heave caused by a chilled pipeline buried in initially unfrozen ground.

CHEMICAL EFFECTS

Coupled THMC formulation: balance equations

Although chemical considerations sometimes appear distant from the conventional practice of geotechnical engineering, on many occasions they are unquestionably relevant to

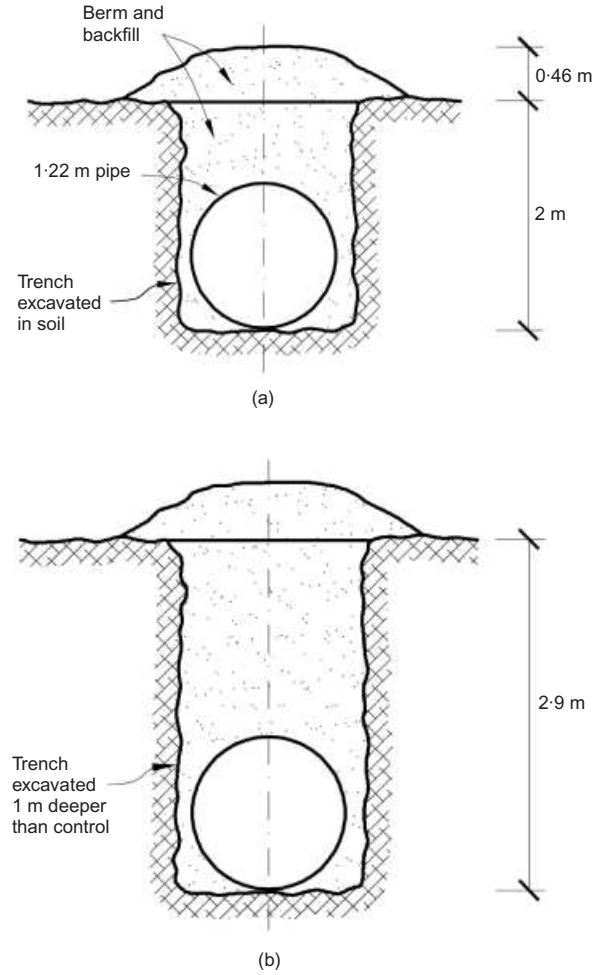

Fig. 88. Sections of a full-scale in situ pipeline frost heave test (after Slusarchuk *et al.*, 1978): (a) control section; (b) deep burial section

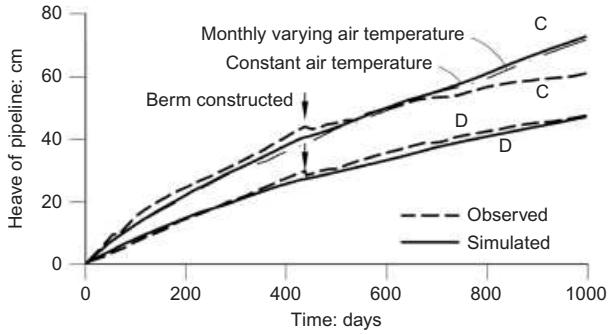

Fig. 89. Computed and observed pipeline heave: C, control section; D, deep burial section (Nishimura *et al.*, 2009)

engineering problems. Without being comprehensive, the following chemical processes can be mentioned as potentially relevant: precipitation/dissolution phenomena (e.g. concerning carbonates or sulphates), cation exchange, oxidation/reduction processes (e.g. involving pyrites or iron compounds), breaking down of silicate minerals, and sulphate reduction (Mitchell & Soga, 2005). These processes have a significant influence on the hydraulic and mechanical properties of soils and other geotechnical materials by way of cementation, degradation, volume change, porosity variations, modification of pore structure, change in swelling properties of clays and others. Chemical interactions also underlie important phenomena such as weathering, sulphate-induced swelling in tunnels, methane hydrate dissociation or biodegradation (Kimoto *et al.*, 2007; McDougall, 2007). Moreover, they are directly related to processes such as osmotic flow, which may be significant in some clay-rich materials (Barbour & Fredlund, 1989; Manassero & Dominijiani, 2003; Peters & Smith, 2004), and they are critical in areas such as contaminant transport and soil decontamination.

It seems appropriate, therefore, to generalise further the formulation developed hitherto in order to incorporate a range of relevant chemical phenomena (Gens *et al.*, 2002b, 2005). Additional chemical species, which may react with each other, must now be incorporated. Consequently, the solid phase now includes not only the main mineral but also precipitated minerals and absorbed cations, and the coincidence of solid phase and mineral species no longer applies. The liquid phase contains water, dissolved air and, in addition, dissolved chemical species. At present, no chemical species are considered in the gas phase, but they could be easily included if required. Chemical reactions considered in the formulation include

(*a*) homogeneous reactions involving only the liquid phase: aqueous complex formation, acid–base reactions, oxidation/reduction reactions
(*b*) heterogeneous reactions involving the liquid and solid phases: dissolution/precipitation of minerals and cation exchange.

Local equilibrium is assumed for all the chemical reactions except for some dissolution/precipitation of minerals, where kinetics may also be assumed. The use of one or other of these two hypotheses depends on the comparison between rates (or characteristic times) of concentration changes due either to chemical reactions or to transport (Steefel & Lasaga, 1994). Local equilibrium is the limiting case for kinetics when transport characteristic times are much higher than those of the chemical reactions as it is generally the case in porous materials, especially if they are fine-grained.

As before, new variables and new balance equations must be added to the formulation. The new variables are the concentrations c_i of each one of the additional chemical species, and the new balance equations are the reactive transport equations that express the conservation of mass of those chemical species. Assuming N chemical species, the balance equations are expressed as

$$\frac{\partial}{\partial t}(nS_l\rho_l c_i) + \nabla \boldsymbol{j}_i = R_i \quad (i = 1, \ldots, N) \tag{68}$$

where c_i is the concentration of species i, in mol/kg of solution, and R_i is the total production rate of species i due to chemical reactions, in mol/(m^3/s). In this case the right-hand side term is very important, because it expresses the effect of the chemical reactions that occur throughout the porous medium. $\boldsymbol{j}_i$ is the total flux of species i, expressed in mol/(m^2/s). It is convenient to express the total flux $\boldsymbol{j}_i$ as

$$\boldsymbol{j}_i = \boldsymbol{j}_i' + nS_l\rho_l c_i \dot{\boldsymbol{u}} \tag{69}$$

where $\dot{\boldsymbol{u}}$ is the solid phase velocity and $\boldsymbol{j}_i'$ is the flux of species i with respect to the solid phase. $\boldsymbol{j}_i'$ is given by the sum of the liquid advective flux and the non-advective flux,

$$\boldsymbol{j}_i = \rho_l c_i \boldsymbol{q}_l - \boldsymbol{D}_l \nabla c_i \tag{70}$$

where $\boldsymbol{q}_l$ is the Darcy's liquid flux and $\boldsymbol{D}_l$ is the hydrodynamic dispersion tensor. The non-advective flux is the consequence of both molecular diffusion and mechanical dispersion.

It is now necessary to introduce the reactions in local equilibrium to obtain the set of independent concentrations in the system. If N_x is the number of reversible independent

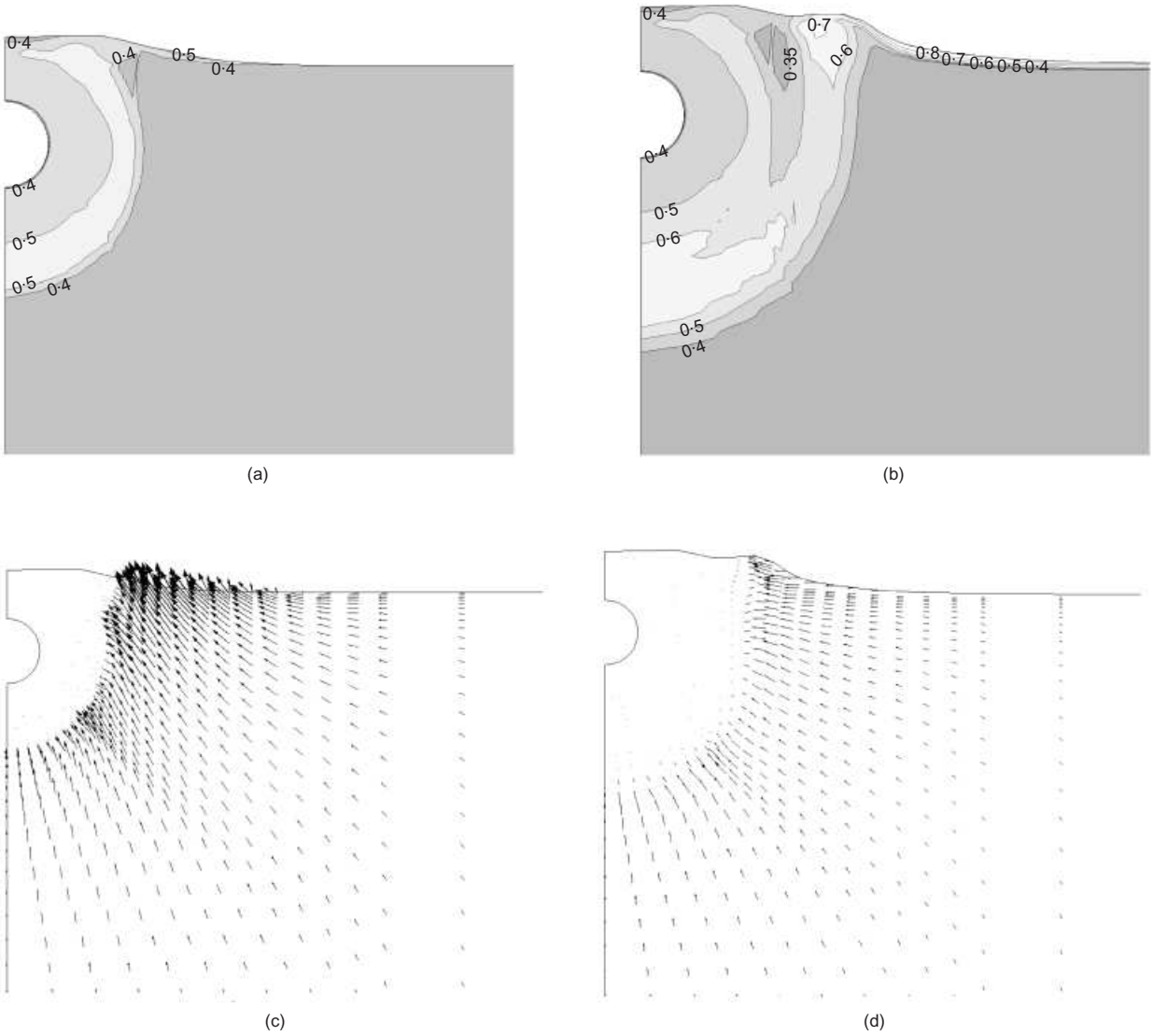

Fig. 90. Analysis of control section with monthly varying temperature (Nishimura *et al.*, 2009). Deformed geometry and porosity contours: (a) at day 300; (b) at day 1000. Liquid water flux vectors: (c) at day 300; d) at day 1000

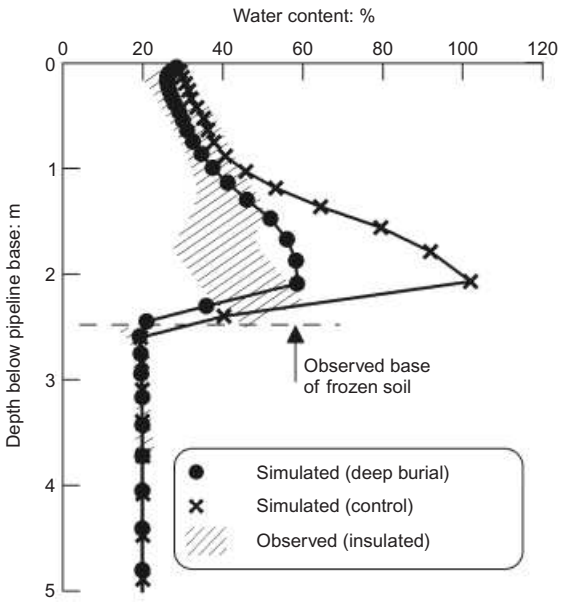

Fig. 91. Computed and observed water content distributions beneath the pipeline. Observations provided by Carlson and Nixon (1988) for the 'insulated silt' section

reactions in a system containing N species, then the number of independent chemical components is $N_c = N - N_x$. Reactions between the two types of species are expressed as

$$A_i = \sum_{j=1}^{N_c} \nu_{ij} A_j \qquad (i = 1, \ldots, N_x) \tag{71}$$

where A_j and A_i are the chemical formulae of the primary and secondary species respectively, and ν_{ij} is the number of moles of the primary species j in a mole of the secondary species i. The classification of the species into primary and secondary ones is not unique, but it is decided on the basis of the characteristics of the problem being analysed.

Only the equations of the primary variables enter the set of balance equations to be solved; the concentrations of the secondary variables are derived from the chemical equilibrium model outlined below. This allows the total number of degrees of freedom of the analyses to be reduced. Even with this reduction, the number of primary chemical species can be quite large in some cases. For instance, in the analysis of the coupled thermo-hydromechanical and chemical (THMC) behaviour of a bentonite sample subjected to heating and hydration, a total of 28 chemical species were considered, 10 of which were primary species (Gens *et al.*, 2008a). In many applications, however, less comprehensive chemical

models and fewer primary variables are required. A more detailed description of the THMC formulation has been presented in Guimarães (2002) and Guimarães *et al.* (1999, 2007). The formulation has been incorporated into a computer code, CODE_BRIGHT, capable of performing fully coupled THMC analyses (Guimarães *et al.*, 2006). Other general THMC schemes have been presented by Thomas *et al.* (2001), Seetharam *et al.* (2007) and Zheng & Samper (2008).

Coupled THMC formulation: constitutive equations

Chemical equilibrium and kinetics. Most reactive transport formulations use the mass action law to solve the chemical equilibrium equations (e. g. Steefel & Lasaga, 1994; Saaltink *et al.*, 1998). In the formulation presented here, an alternative (but thermodynamically equivalent) approach is used, based on the minimisation of Gibbs free energy. This approach has a wider application range, extending to non-ideal very concentrated systems. To compute the concentrations of the species in equilibrium, a Newton–Raphson algorithm is applied to the direct minimisation of Gibbs free energy. Lagrange multipliers are used to incorporate the restrictions of the problem (Harvie *et al.*, 1987).

The minimisation problem can thus be written as

$$\underset{n_j^c, n_i^x}{\text{minimize}}\ G = \sum_{j=1}^{N_c} \mu_j^c n_j^c + \sum_{i=1}^{N_x} \mu_i^x n_i^x \tag{72}$$

subject to:

$$\begin{aligned} n_j^U &= n_j^c + \sum_{i=1}^{N_x} \nu_{ij} n_i^x \quad (j = 1, \ldots, N_c) \\ n_j^c &\geqslant 0 \qquad\qquad\quad (j = 1, \ldots, N_c) \\ n_i^x &\geqslant 0 \qquad\qquad\quad (i = 1, \ldots, N_x) \end{aligned} \tag{73}$$

where G is the Gibbs free energy, and μ_j^c and μ_i^x are the chemical potentials of the primary and secondary species. n_j^c and n_i^x, the variables to be optimised, are the number of moles of the primary and secondary species in an REV. The number of moles n_j^c and n_i^x are directly related to concentrations. For the few chemical reactions that can be considered kinetics-controlled, the rate of species production is computed using a standard formulation (e.g. Fletcher, 1993).

Chemo-mechanical models. There are many chemical processes that affect the mechanical behaviour of soils. Because of this wide spectrum of phenomena, the tendency has been towards the development of chemo-mechanical models addressing the effects of an individual process or a limited set of phenomena, such as organic contaminant effects on clays (Hueckel, 1997), water-ion interaction in expansive clays (Gajo *et al.*, 2002; Loret *et al.*, 2002), pressure solution/precipitation in salt (Olivella & Gens, 2002) and in chalk (Pietruszczak *et al.*, 2006), ion exchange in swelling clays (Gens *et al.*, 2002b), chemical degradation of bonded geomaterials (Nova *et al.*, 2003), and degradation of soft clayey rocks (Pinyol *et al.*, 2007). Zhang & Zhou (2008) have presented a chemo-plastic model for unsaturated soils that combines the chemo-mechanical model of Hueckel (1997) with the unsaturated model of Gallipoli *et al.* (2003). In principle, the structure of a chemo-mechanical model would be

$$\begin{aligned} \mathrm{d}\boldsymbol{\sigma}^* = {} & \boldsymbol{D}(\varepsilon, s, T, \mathbf{c})(\mathrm{d}\boldsymbol{\varepsilon}) + \boldsymbol{h}(\boldsymbol{\varepsilon}, s, T, \boldsymbol{c})\mathrm{d}s \\ & + \boldsymbol{\beta}(\boldsymbol{\varepsilon}, s, T, \boldsymbol{c})\mathrm{d}T + \boldsymbol{\Gamma}(\boldsymbol{\varepsilon}, s, T, \boldsymbol{c})\mathrm{d}\boldsymbol{c} \end{aligned} \tag{74}$$

where a new term has been added that represents the mechanical contribution of the set of chemical species concentrations, c_i, grouped in the vector $\boldsymbol{c}$. Frequently, concentrations are not incorporated directly in the constitutive laws, but other chemically derived parameters are used instead. For instance, Nova *et al.* (2003) assumed that the various chemical state variables can be condensed into a single scalar function incorporating the effects of processes such as time of exposure to weathering or chemical attack intensity. Hueckel (1992) used the accumulated mass transfer of adsorbed water as constitutive parameter.

An example of a chemo-mechanical model is briefly sketched here. It deals with the effect of cation exchange in expansive clays such as bentonite, a phenomenon that is relevant to engineered barriers for nuclear waste disposal. Changes in cation content in these materials bring about significant mechanical effects, which may affect volume change characteristics and swelling pressure potential (Di Maio, 1996). An instance of bentonite behaviour that requires modelling is illustrated in Fig. 92, which shows the compression experienced by a sample of saturated bentonite when exposed to saturated solutions of different electrolytes. This behaviour is often attributed to changes in osmotic suction: in this case the osmotic suction applied is 185 MPa for the $CaCl_2$ solution, 39 MPa for the NaCl solution, and 24 MPa for the KCl solution. It is apparent that the relationship between osmotic suction and volumetric strain is not straightforward: the effect of the $CaCl_2$ solution is not much higher than those of the other electrolytes, and the volumetric strains for NaCl and KCl solutions are in fact reversed with respect to their values of osmotic suction. It is clear that the nature of the particular cation also plays a role in the observed mechanical behaviour of the bentonite.

The chemo-mechanical model is built upon the generalised-plasticity double-structure model used in the THM modelling of the mock-up test presented above (Sánchez *et al.*, 2005). It will be recalled that the model distinguishes between a macrostructural level and a microstructural level. As the microstructure is the seat of the physico-chemical interactions occurring in the vicinity of clay particles, the microstructural level provides a very convenient platform for introducing chemical effects. The relationship with the overall mechanical behaviour of the soil is then handled by the general configuration of the model. The chemical constitutive parameters selected for formulating the model are the

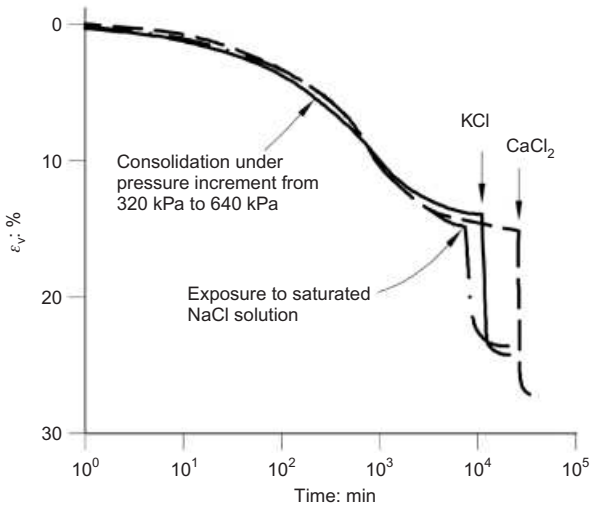

Fig. 92. Volume changes of Ponza bentonite subjected to the action of different solutions in an oedometer (after Di Maio, 1996)

osmotic suction and the equivalent fractions of exchangeable cations.

An essential component of the model is the interaction between the two structural levels. A basic assumption is that the microstructural behaviour is not influenced by the macrostructure. This is reasonable, as it is unlikely that the basic physico-chemical phenomena are affected by non-local variables. In contrast, microstructural deformations may modify or disrupt the macrostructural fabric, causing irreversible deformations. Suitable interaction functions provide the required link between the two levels.

It is assumed that the microstructure always remains saturated, owing to its very small pore size, and that microstructural behaviour is volumetric and reversible. The assumption of volumetric behaviour under isotropic conditions is reasonable, if the microfabric has no preferred orientation; otherwise deviatoric strains may appear. Reversibility stems from the fact that basic chemomechanical phenomena at the microstructural level are bound to be largely reversible. For simplicity, an exponential law is adopted to define the elastic volumetric microstructural strain, for a fixed cation content:

$$\mathrm{d}\varepsilon_{\mathrm{m}}^{\mathrm{e}} = \beta_{\mathrm{m}} \mathrm{e}^{-\alpha_{\mathrm{m}}\hat{p}} \mathrm{d}\hat{p} \tag{75}$$

where $\hat{p} = p + s_{\mathrm{m}}$; p is the net mean stress; and s_{m} is the microstructural suction, which in general has two components, matric suction and osmotic suction: that is, $s_{\mathrm{m}} = s + s_{\mathrm{o}}$. α_{m} and β_{m} are material parameters.

Osmotic suction can be computed as

$$s_{\mathrm{o}} = -10^{-6} \frac{RT}{v_{\mathrm{w}}} \ln (a_{\mathrm{w}}) \quad \text{(MPa)} \tag{76}$$

where v_{w} is the molar volume of water (in m^3/mol), and a_{w} is the activity of liquid water. a_{w} can be computed from the geochemical equilibrium model outlined above. In electrolyte solutions (both dilute and concentrated), a_{w} depends mainly on the concentration of dissolved salts.

To incorporate the influence of geochemical variables on the behaviour of the microstructure, it is postulated that the material parameter α_{m} is constant, and that β_{m} depends on the exchangeable cation concentrations according to

$$\beta_{\mathrm{m}} = \sum_i \beta_{\mathrm{m}}^i x_i \tag{77}$$

where x_i is the equivalent fraction of the exchangeable cation i, defined as

$$x_i = \frac{\text{concentration of exchangeable cation (meq/100 g of solid)}}{\text{CEC (meq/100 g of solid)}}; \qquad \sum_i x_i = 1 \quad 0 \leqslant x_i \leqslant 1 \tag{78}$$

and CEC is the cation exchange capacity.

The β_{m}^i values are parameters that control microstructure stiffness, and are defined for each of the exchangeable cations. If a rough analogy is established with the diffuse double layer theory, the values of β_{m}^i are related to the hydrated radii of the cations and to their valences. Finally, the microstructural volumetric strain is given by

$$\mathrm{d}\varepsilon_{\mathrm{m}}^{\mathrm{e}} = \beta_{\mathrm{m}} \mathrm{e}^{-\alpha_{\mathrm{m}}\hat{p}} \mathrm{d}\hat{p} - \frac{1}{\alpha_{\mathrm{m}}} \mathrm{e}^{-\alpha_{\mathrm{m}}\hat{p}} \mathrm{d}\beta_{\mathrm{m}} \tag{79}$$

Microstructural strains are therefore obtained from the contributions of two terms: the first expresses the influence of changes in effective stress (includes total stress, matric suction and osmotic suction), and the second represents the independent effect of changes in individual cations.

To illustrate the performance of the model, Figs 93(a) and 93(b) show the observed response of Ponza bentonite when subjected to different paths of loading and replacement of pore fluid in oedometer tests reported by Di Maio (1996). Figs 93(c) and 93(d) show that the model reproduces well the observed behaviour, including the volume changes due to the modifications of the cation content of the pore fluid applied at different stresses. Observed bentonite behaviour is not fully reversible (Figs 93(a) and 93(b)): this irreversibility is reproduced by the model, thanks to the interaction between microstructure and macrostructure.

To check the performance of the entire coupled formulation in a boundary vale problem, a chemical consolidation test performed by Santamarina & Fam (1995) in the oedometer depicted in Fig. 94 has been modelled. The material tested is a sodium bentonite with a liquid limit of 250%, a plastic limit of 50%, and a cation exchange capacity (CEC) between 80 and 85 meq/100 g of solid. The samples were prepared from slurry with an initial void ratio of 4·6. In the test, the sample can drain only from the top, whereas pore pressure is measured at the bottom. Shear wave velocity and dielectric permittivity are also measured, but those observations are not considered here. The sample is subjected to a load of 100 kPa first. Once mechanical consolidation is finished, the specimen is placed in contact with a KCl saline solution of 4·0M concentration through the upper surface of the sample.

In the numerical simulation the soil was subjected to the same sequence of mechanical and chemical actions. Advection flow driven by osmotic gradients has not been considered in this particular analysis. Fig. 95(a) shows that the effect of the electrolyte solution is to cause a significant reduction in the volume of the specimen. From the point of view of the proposed constitutive model, this compressive behaviour is explained by the combined effects of osmotic suction and cation exchange on the microstructure. When the specimen is exposed to a 4·0M KCl solution, the osmotic suction increases from 1·5 MPa to 19 MPa. In addition, the K^+ cation replaces the other cations in the bentonite. Both phenomena lead to a compression of the soil, which takes place over time because of the need for the K^+ cation to diffuse through the specimen. This process receives different names in the literature: it is called chemical consolidation by Kaczmarek & Hueckel (1998) and osmotic consolidation by Barbour & Fredlund (1989).

Of special interest is the observation of positive pore pressures measured at the bottom of the sample (Fig. 95(b)). A quite similar response is obtained in the computations, except at very early times. The pore pressure generation corresponds to the undrained response of the soil due to the tendency towards compression induced by the saline solution; pore pressures are generated because the diffusion of salts inside the sample is faster than the ability of the pore pressures to dissipate. Naturally, the magnitude of this phenomenon depends on the relative values of intrinsic permeability and the coefficient of molecular diffusion. This a clear example of interaction between geochemical variables and hydromechanical behaviour, satisfactorily reproduced by the formulation and constitutive model.

Case history: tunnel in sulphate-bearing ground

To widen the range of applications of the formulation, the case history selected to complete this section on chemical effects does not deal with the chemomechanical behaviour of expansive clays; it concerns a problem involving the construction of a tunnel in sulphate-bearing ground. Large

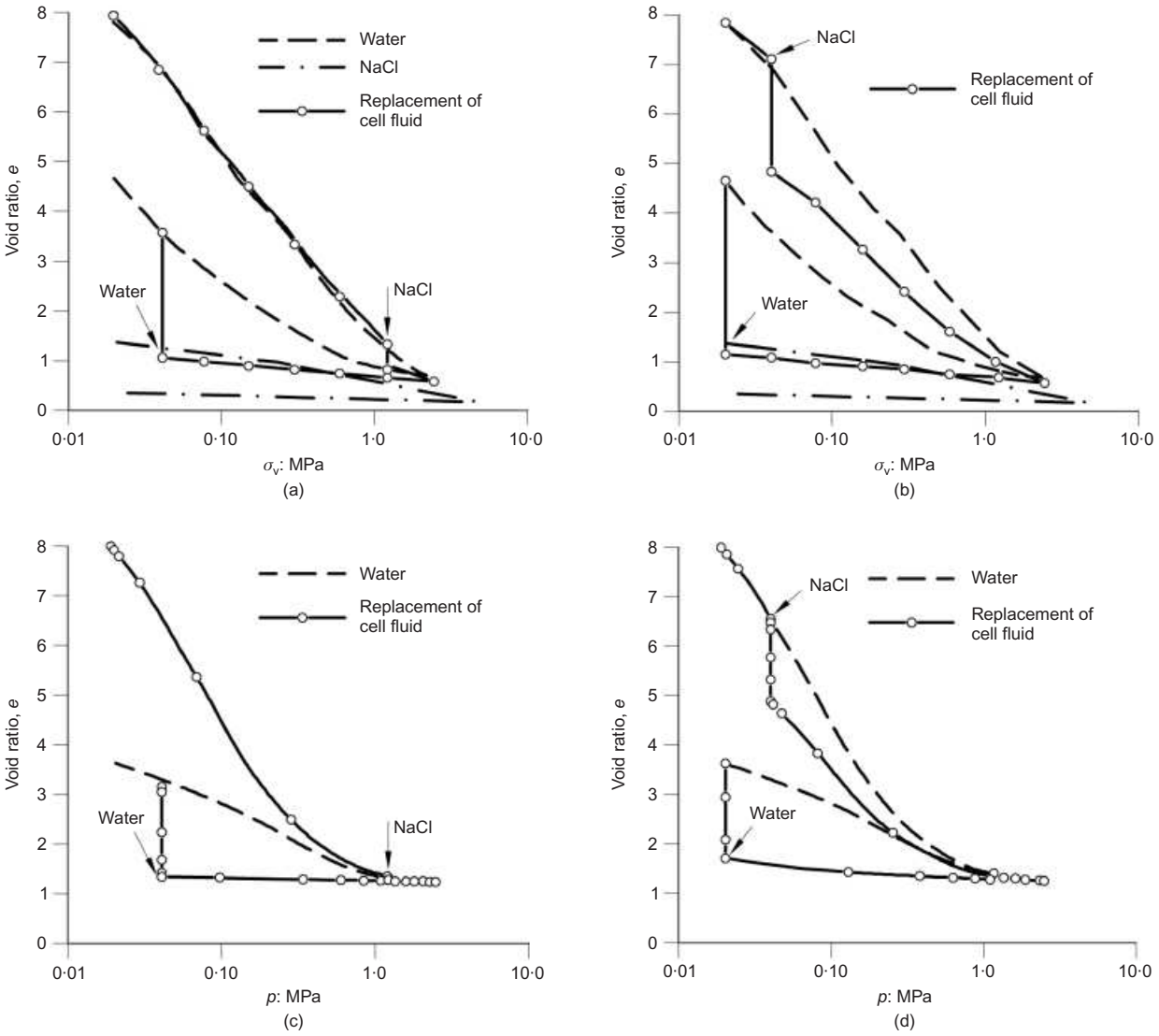

Fig. 93. (a, b) Volume changes of Ponza bentonite subjected to combined chemo-mechanical actions in an oedometer (after Di Maio, 1996); (c, d) computed volume changes using the chemo-mechanical model for Ponza bentonite subjected to combined chemo-mechanical actions

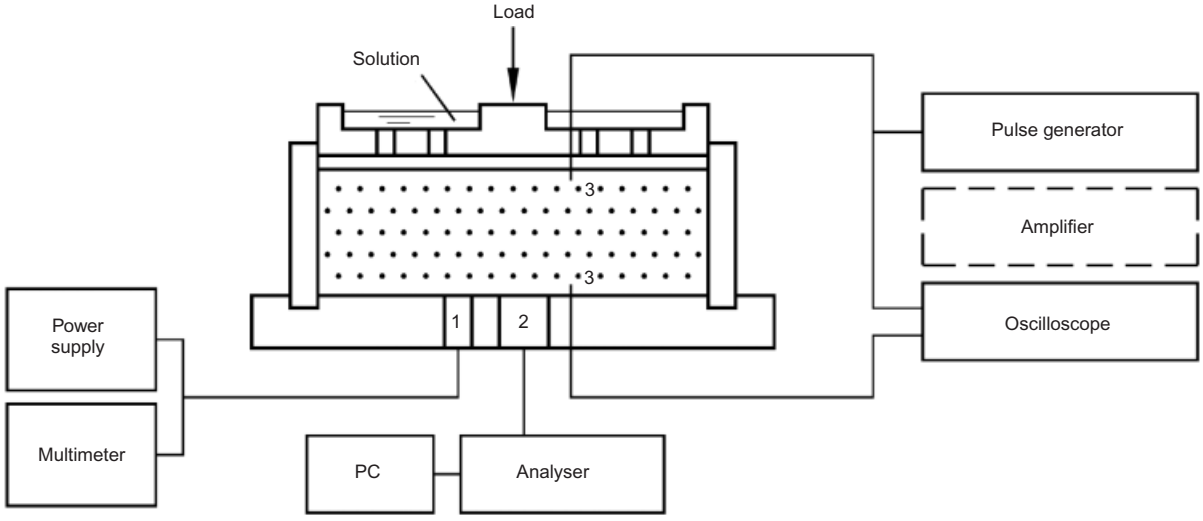

Fig. 94. Schematic layout of the oedometer test (Santamarina & Fam, 1995)

floor heave displacements and large swelling pressures have been observed in numerous tunnelling works performed in rocks containing anhydrites, and quite often have required major repairs. North-west Switzerland and South Germany are areas especially affected; tunnelling in this type of material is considered a major engineering problem (Kovári *et al.*, 1988; Wittke & Wittke, 2005; Berdugo *et al.*, 2009a, 2009b). Despite over 100 years of tunnelling in such ground,

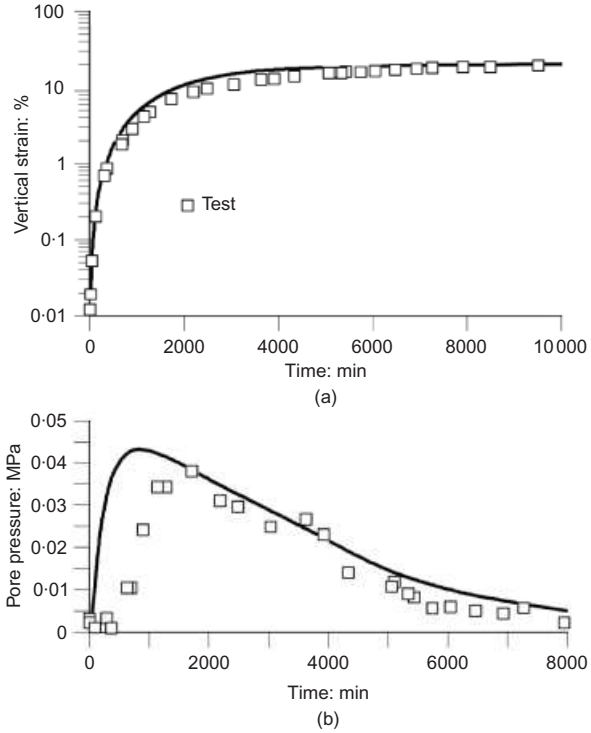

Fig. 95. Observed and computed results from a sodium bentonite oedometer sample exposed to a 4·0M solution of KCl: (a) vertical deformation; (b) pore pressure measured at the bottom of the specimen. Experimental results from Santamarina & Fam (1995)

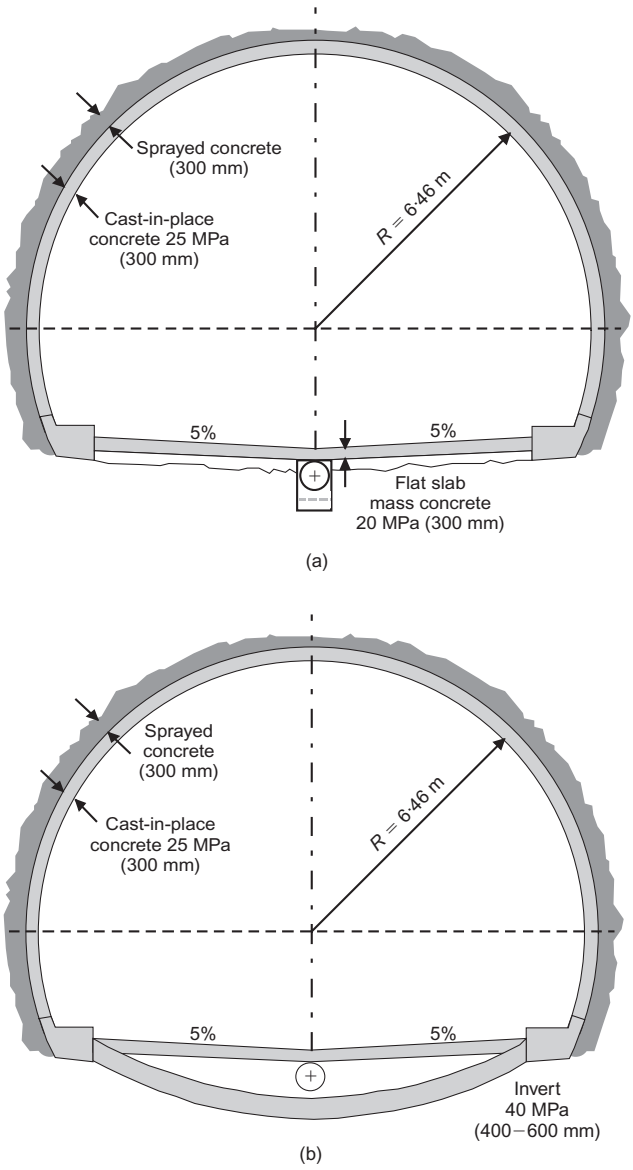

Fig. 96. Lilla tunnel: (a) generic cross-section; (b) cross-section with inverted arch

the basic phenomena involved are still not well understood (Anagnostou, 2007). The long duration of the swelling phenomena and the great variability of field conditions are serious obstacles to a systematic study of the problem. However, some advances in the understanding of the phenomena have been made recently, in connection with the case described below (Alonso *et al.*, 2005, 2007; Berdugo, 2007; Berdugo *et al.*, 2007a).

The case concerns the construction of three tunnels, part of a section of the new high-speed train line from Madrid to Barcelona, in the lower Tertiary Ebro Basin (northeast Spain), an area where other heave phenomena have already been reported (Gens *et al.*, 1993). All three tunnels had similar problems; only the case history of the longest one, the 2034 m-long Lilla tunnel, is discussed here. A full description of the case history, including the information given below, is presented in Berdugo (2007). The 117·3 m^2 horseshoe section was excavated by drill and blast from the two portals, dividing the section into advance and bench (Fig. 96(a)). Overburden along the tunnel varies between 10 m and 110 m. Temporal supports consisted of sprayed concrete and rock bolts; steel arch ribs (HEB 160) were installed only in zones of low-quality rock. Lining consisted of 300 mm-thick mass concrete (25 MPa). A 300 mm-thick flat slab constructed in mass concrete was placed on the tunnel floor, but it was concreted only after the total excavation of the bench. Therefore the floor of the tunnel was exposed to the action of environmental agents during most of the construction period. Because of the low permeability of the massif, waterproofing of the excavated section was restricted to portals.

The tunnel runs mainly through Early Eocenic argillaceous deposits containing anhydrite and a very complex system of cross-shaped, moderately dipping, fibrous gypsum veins (Fig. 97). The veins are from millimetric to centimetric in thickness; gypsum is also present as small nodules and flakes. The host argillaceous matrix is constituted of illite and paligorskite, of minerals rich in magnesium and calcium (dolomite) and, to a lesser extent, of quartz. Expansive clay minerals were detected only in small quantities, in isolated points of the matrix. An important aspect is the existence of a persistent system of open, low-friction-angle, slickensided surfaces related to local tectonics.

First heave manifestations were detected in the flat slab just after the full tunnel excavation was completed. Substantial expansive phenomena occurred in a generalised way at floor level, but movements were only slight in the unlined vault. Heave was followed by damage to the longitudinal drainage system and, finally, by local failures of flat slabs. As usual in this type of problem, the magnitude of heave was extremely variable, resulting in a very irregular tunnel floor surface. It is thought likely that the variability of heave is related to local permeability variations, connected perhaps to the presence of fissures or fractures. Fig. 98 shows the distribution of heave displacements along the tunnel during the first six months of observations, as well as the depth of the active zone in the areas where it was measured.

Figure 99(a) illustrates the evolution of heave in a number of sections. The movements are quite large, and do not show any indication of a decreasing rate of growth with time.

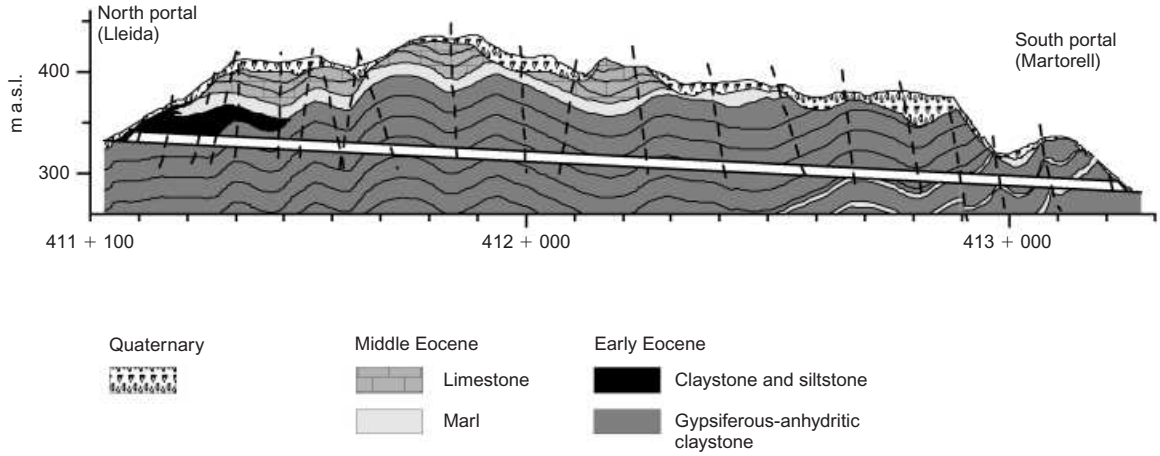

Fig. 97. Geological longitudinal section of the Lilla tunnel (Berdugo, 2007)

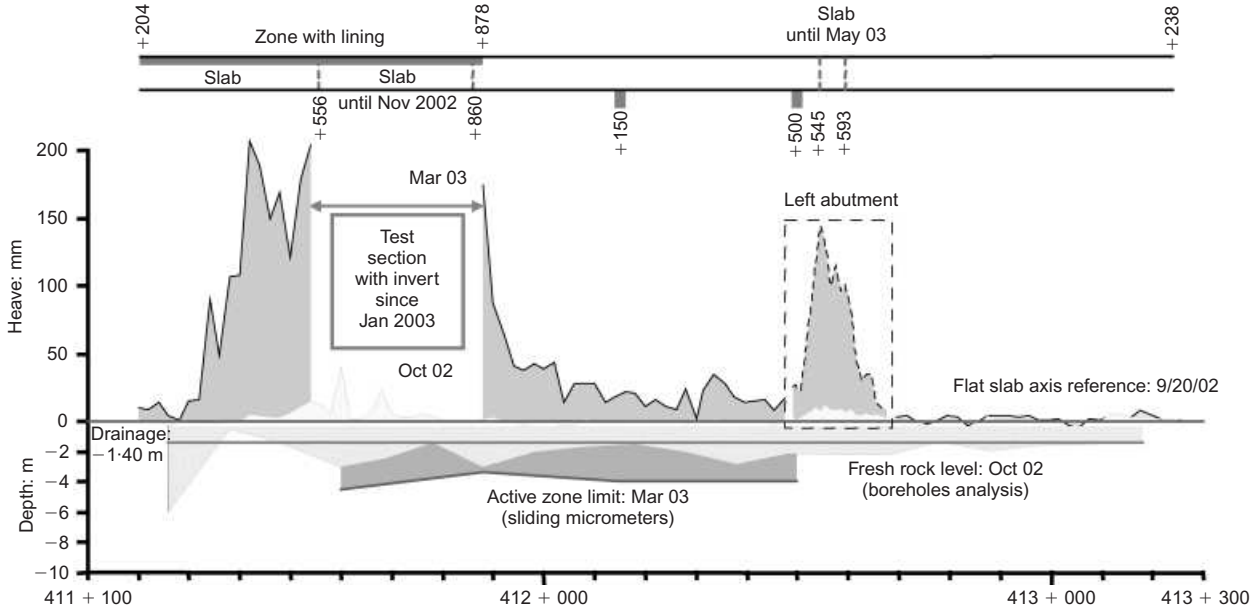

Fig. 98. Distribution of heave displacements and depth of active zone along the Lilla tunnel (Berdugo, 2007)

Sliding micrometers placed in some sections showed that movements were concentrated in the first 3–4 m under the tunnel slab (Fig. 100).

After the ground heave was observed, the section of the tunnel between chainages 411 + 556 and 411 + 860 was provided with an invert arch, of which 184 m had a thickness of 400 mm and 110 m had a thickness of 600 mm. Instrumentation was also installed, including total pressure cells on the underside of the invert and sliding micrometers to measure displacements under the floor. Fig. 99(b) shows the swelling stresses that were measured on the invert arch: very large stresses, of the order of several MPa, typical of this type of phenomenon, were recorded. In spite of the restraint provided by the invert arch, heave displacements of up to 27 mm were still measured, concentrated in the first 4–5 m below the new floor.

Remedial measures for this type of problem veer between the provision of a rigid support capable of resisting the very large swelling pressures, and the installation of a yielding support that allows rock deformation without causing undue damage to the floor. In this context, three test sections were built in a zone where the tunnel had been excavated to a full circular shape (Berdugo *et al.*, 2007b). The first section (20 m long) was designed according to the principle of resisting support. The other two (both 10 m long) were designed according to the principle of yielding support: one included sliding slots in the contact between the vault and the invert; in the second one, a polyurethane foam (approximately 150 mm thick) was placed in the interface between rock and invert. An excavated circular section was adopted to try to minimise overstressing of the rock and thereby limit damage and fracturing. The circular test sections were initially flooded under controlled conditions, using water from the rock massif. The direct access of water from the tunnel floor to the rock was possible owing to a series of boreholes drilled after building the circular sections. The flooding period was 30 days only.

Figure 101 shows clearly the dependence of swelling pressure on the stiffness of the support. Fig. 102 shows the distributions of heave displacements with depth for the resisting support section and for the yielding support section with slots. It is apparent that heave phenomena continue to take place below the newly excavated circular section. The measurements also suggest that the magnitude of the active zone is larger for the yielding support case; it appears that allowing the development of displacements to minimise

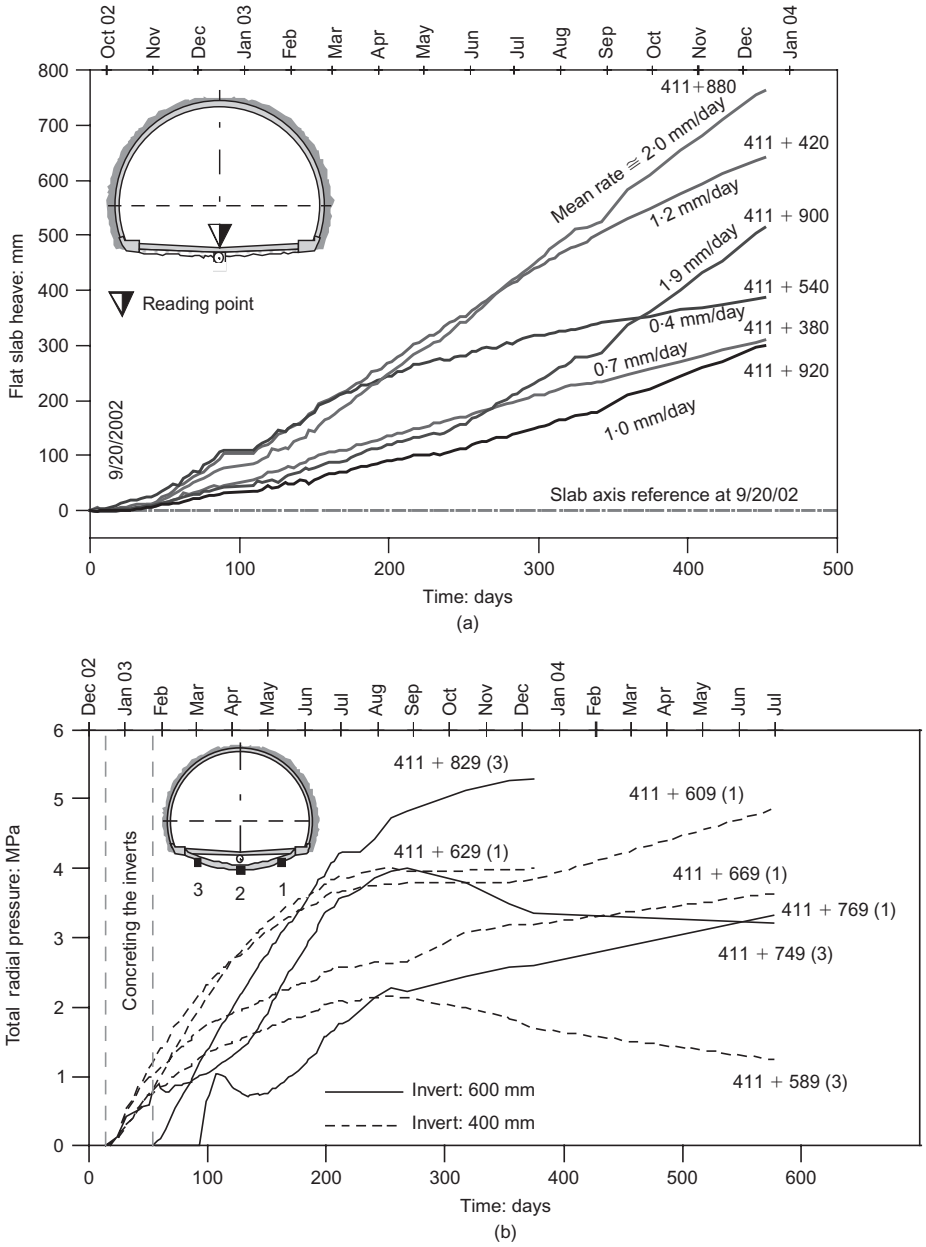

Fig. 99. (a) Evolution of heave displacements with time at various sections in the Lilla tunnel; (b) evolution of total swelling pressures on tunnel invert (Berdugo, 2007)

swelling pressures exposes the foundation material to a continuous degradation.

At the same time, a numerical analysis including the chemical component was undertaken to provide a better understanding of the phenomena occurring (Berdugo *et al.*, 2009c). It has often been assumed that the chemical swelling mechanism is due to the transformation of anhydrite into gypsum, which in an open system results in a volumetric increase of approximately 60%. However, this transformation is highly unlikely in field conditions, and all the evidence gathered at the Lilla tunnel points towards an isovolumetric replacement of one mineral by the other. The change from anhydrite to gypsum is likely to be by way of dissolution and precipitation, often in the form of new gypsum crystals, which have frequently been observed in the samples extracted from the active zone below the tunnel. Therefore the chemical model is focused on the phenomenon of dissolution/precipitation of sulphate minerals. Although in this type of mudstones there is sometimes a contribution of heave from the expansion of clay minerals, in this particular case it is unlikely to be relevant, owing to the absence of significant amounts of active clay minerals.

Consequently, a chemical system containing anhydrite and gypsum is considered, with their corresponding solubility constants,

$$K_{\mathrm{An}} = [\mathrm{Ca}] \cdot [\mathrm{SO_4}]$$
$$K_{\mathrm{Gy}} = [\mathrm{Ca}] \cdot [\mathrm{SO_4}] \cdot a_{\mathrm{w}}^2 \tag{80}$$

where a_{w} is the activity of water, defined as

$$a_{\mathrm{w}} = \exp\left[\frac{-s_{\mathrm{o}} M_{\mathrm{w}}}{RT\rho_{\mathrm{l}}}\right] \cdot \exp\left[\frac{-sM_{\mathrm{w}}}{RT\rho_{\mathrm{l}}}\right] \tag{81}$$

where the first term depends on the osmotic suction s_{o}, and the second one is related to the matric suction s. It is interesting to note the role played by osmotic and matric suctions in a context that appears to be far removed from conventional unsaturated soils. It is a powerful indication of

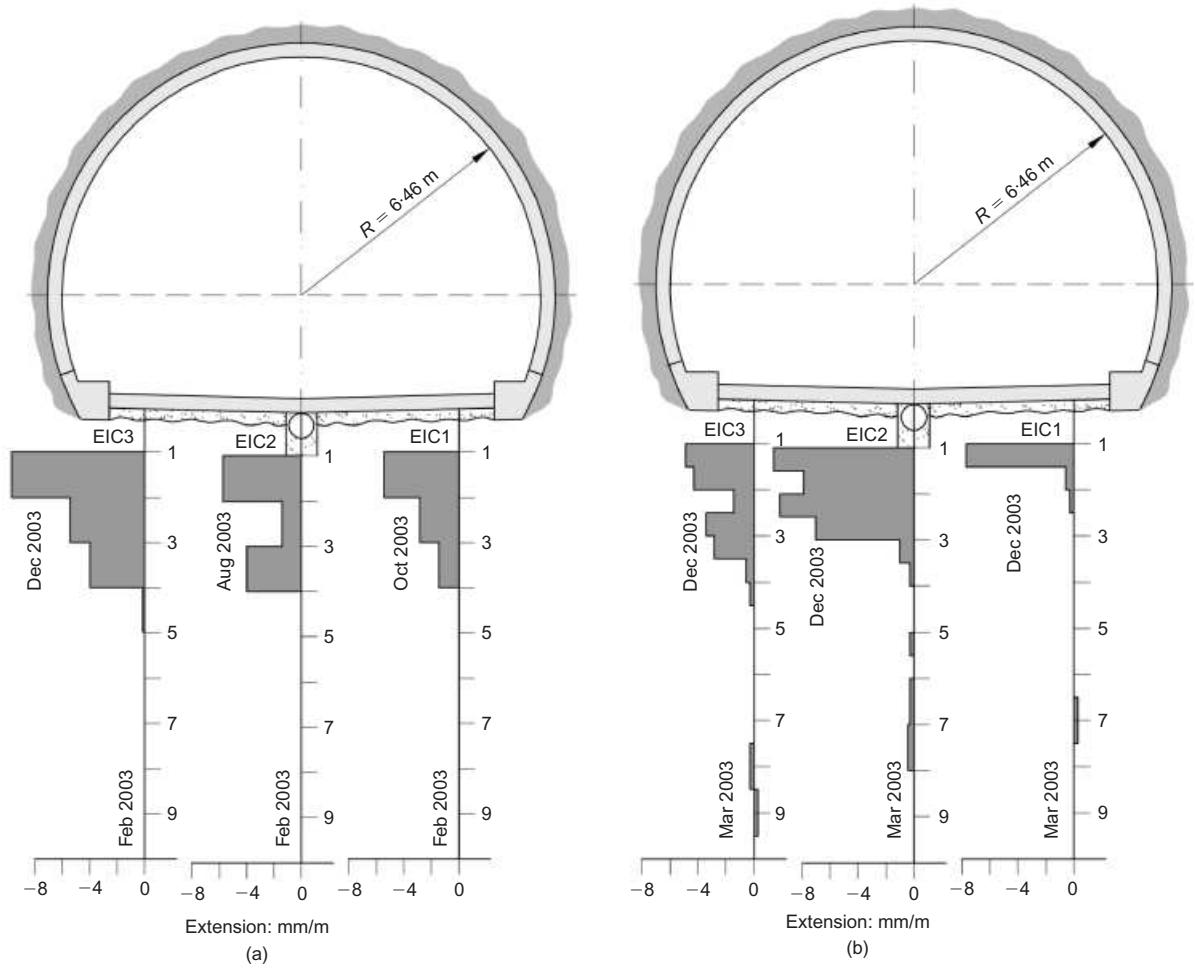

Fig. 100. Distributions of heave displacements with depth in two sections with flat slab (Berdugo, 2007): (a) chainage 412 + 150; (b) chainage 412 + 500

the basic consistency of the physical principles that underlie the progressive series of generalisations performed.

According to the chemical model, if the following inequality holds, $K_{An} < K_{Gy}/a_w^2$, anhydrite precipitates; if, on the other hand, $K_{Gy}/a_w^2 < K_{An}$, then gypsum precipitates. The variation of porosity of the medium, n, is derived from the mass conservation of the inert mineral species, and it is affected by chemical and mechanical phenomena according to

$$\frac{Dn}{Dt} = \frac{-n}{1+M_r}\frac{DM_r}{Dt} + \frac{1-n(1+M_r)}{1+M_r}\nabla \dot{\boldsymbol{u}} \tag{82}$$

where the first term expresses the chemically induced porosity changes, and the second term contains the variation of porosity due to volume change. M_r is the sum of reactive minerals obtained from the geochemical model. Finally, in this qualitative analysis, the volumetric deformation associated with precipitation/dissolution is simply assumed to be linearly related to the change of reactive mineral, according to

$$\dot{\varepsilon}_v^{ch} = \frac{D\varepsilon_v^{ch}}{Dt} = \eta \frac{n}{1-n(1+M_r)}\frac{DM_r}{Dt} \tag{83}$$

where ε_v^{ch} is the chemically induced volumetric strain and η is a multiplier parameter. A rigorous approach to this issue is presented in Coussy (2006).

The analyses have considered two different cases: infiltration of water into the rock (Fig. 103(a)) and evaporation of water into the tunnel (Fig. 103(b)). One-dimensional analyses have been performed, resulting in the evolutions of heave plotted in Fig. 104 for the two mechanisms examined. The magnitude of heave computed in the analyses is not significant, since parameters have been adjusted to obtain realistic values. However, it is interesting to observe the calculated evolution of the heave over time. The analyses predict a slowing-down of heave for the case of water entry into the rock, but a practically indefinite increase of heave for the evaporation case, at least for the simulation time used in the analysis. Performance of two-dimensional analyses has yielded similar results. It should be pointed out that, in the analysis, a homogenised medium has been assumed. In reality, flow (and probably most crystallisation) takes place in fractures and discontinuities: here the effects of those discontinuities are subsumed in the parameters of the overall medium. Also, no degradation of the clay matrix has been considered. Some details of the results of the analyses are shown in Fig. 105. The computations predict that heave will be concentrated into the 3–4 m adjacent to the tunnel, values similar to the observed ones (Figs 105(a) and 105(c)). The process driving the development of heave is mineral precipitation, the distributions of which are plotted in Figs 105(b) and 105(d) for different times.

To take a decision on the engineering solution of the problem and, in particular, whether to choose a resisting or a yielding support, a number of factors were taken into account: (a) the fact that it was a single tunnel with no alternative (major repairs would probably close down the high-speed line); (b) the idea that preventing movements

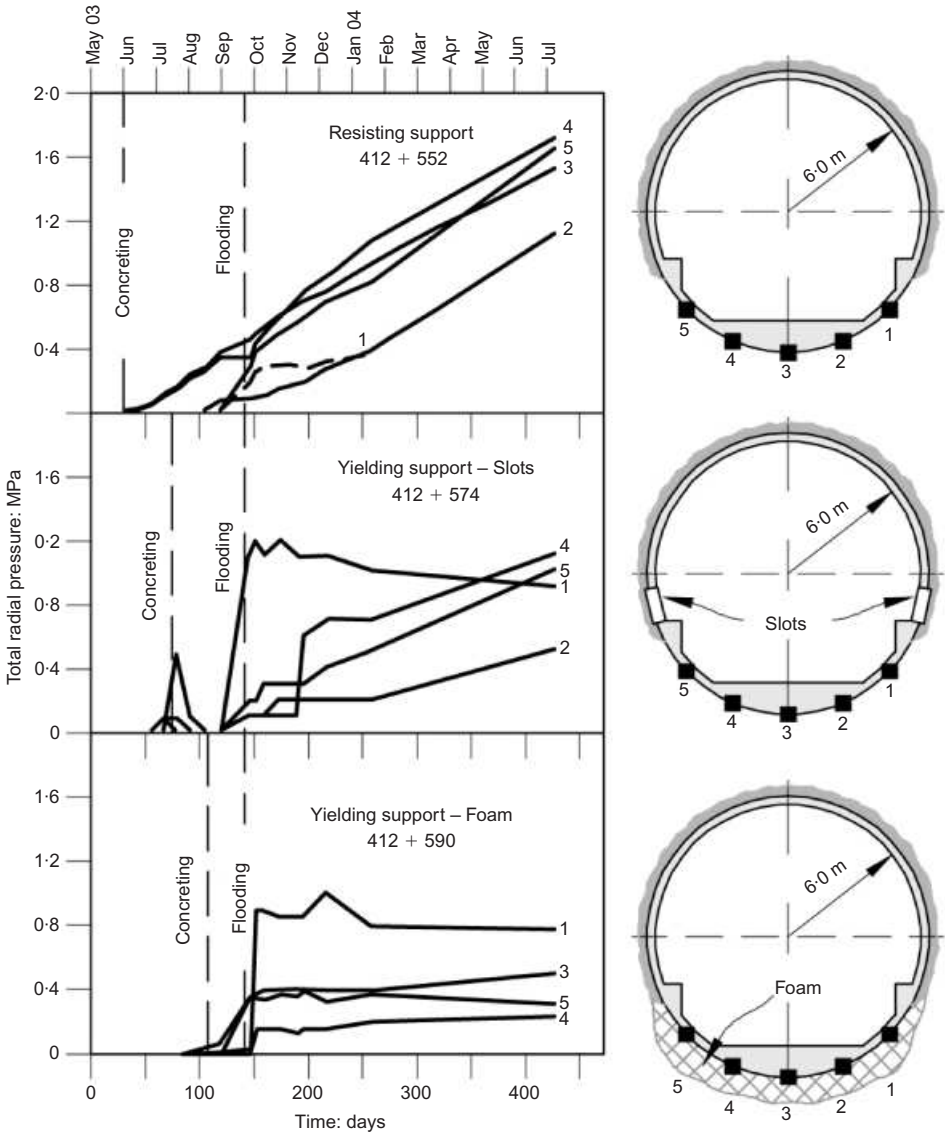

Fig. 101. Evolution of swelling pressures measured in three circular test sections (Berdugo *et al.*, 2007b)

might minimise damage of the rock, limiting the increase in permeability; and (c) previous experience seems to suggest phenomena stabilisation when using resisting support and continuing deformation when using yielding or no support. However, an additional key consideration was the potential existence, suggested by analysis, of a mechanism providing an apparently indefinite continuing heave. Eventually, a resisting support solution was adopted. The tunnel was excavated to a circular shape, and a very robust lining was provided all along the tunnel (Fig. 106). The lining was designed for a swelling pressure of 4·5 MPa (based on past observations) applied in a non-uniform distribution. High-strength concrete and heavy reinforcement were used to adjust the thickness of the additional lining to the available space.

Chemical effects: summary

The final stage in the progressive generalisation of the formulation has incorporated chemical effects. It has required the consideration of a number of chemical species, the incorporation of new environmental variables, concentrations of chemical species, and the introduction of new balance relationships, the reactive transport equations. In addition, geochemical models accounting for thermodynamically consistent chemical equilibrium and reaction kinetics are also necessary components of the formulation. Chemo-mechanical interactions encompass a large variety of different processes. In recent years there has been a very active development of chemo-mechanical models addressing generally the effects of individual phenomena.

Coupled HMC and THMC formulations are available to be applied to engineering problems. The description of a case history has provided an example where the results of analyses incorporating chemical effects have provided useful information for enhancing understanding of the problem and for taking engineering decisions.

CONCLUDING REMARKS

Table 4 contains an overall summary of the lecture. Four main areas have been covered, concerning various aspects of the interaction between soils and the environment: unsaturated soils; thermal effects at high temperatures; thermal effects at low temperatures; and chemical effects. In each of them the classical soil mechanics formulation has been progressively generalised to account for a broader range of phenomena and soil behaviour. This has been done by

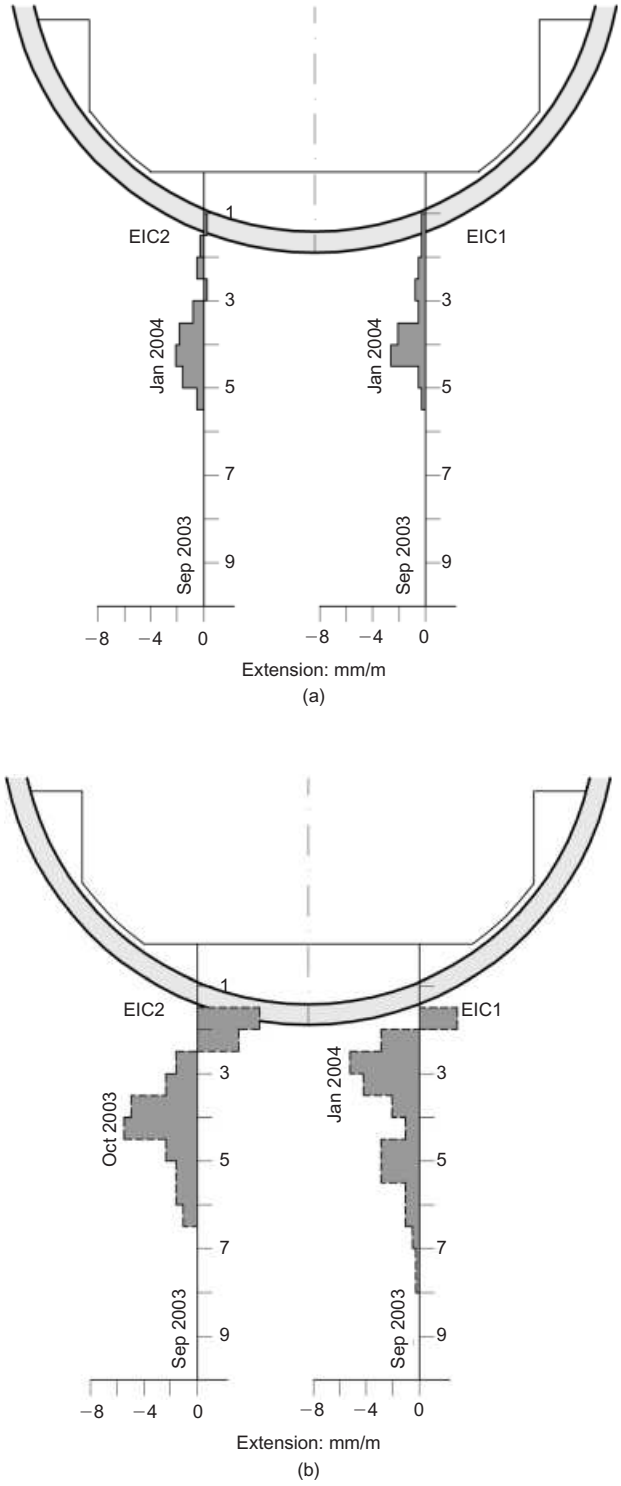

Fig. 102. Distribution of relative displacements in circular test sections: (a) resisting support; (b) yielding support (slots) (Berdugo *et al.*, 2007b)

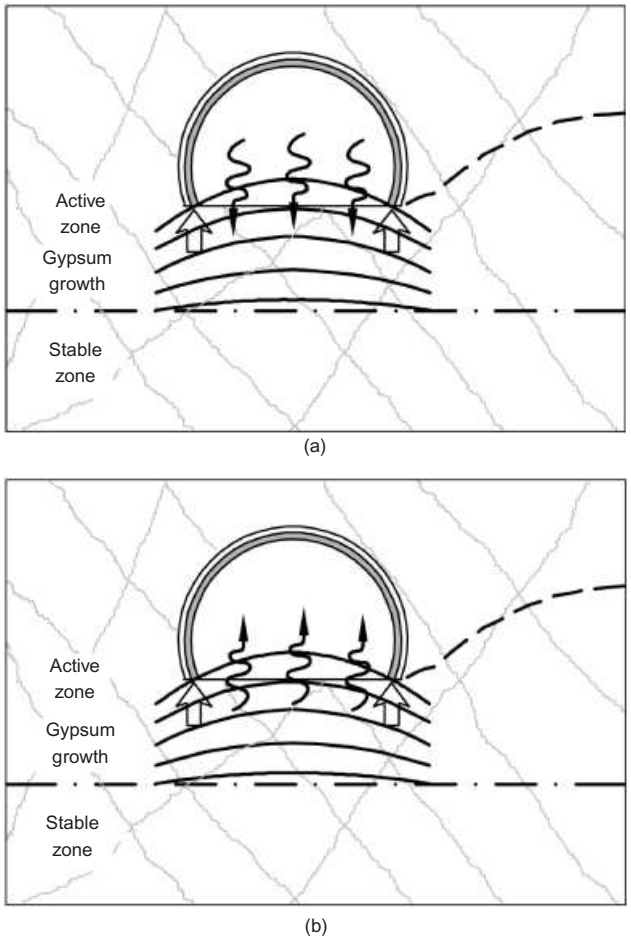

Fig. 103. Mechanisms considered in the analyses: (a) water infiltration into the rock; (b) water evaporation into the tunnel

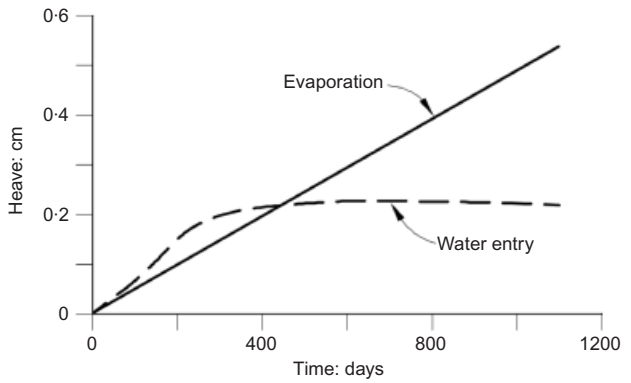

Fig. 104. Computed heave evolution for the two mechanisms examined

(*a*) introducing new basic variables: suction, temperature, concentration of chemical species
(*b*) adding or enhancing the balance equations as required by the formulation: water mass balance, air mass balance, energy balance, reactive transport equations (mass balance of the chemical species) and equilibrium (momentum balance). This has allowed the performance of coupled analysis of increasing degree of complexity: TH, THM, THMC.
(*c*) extending constitutive laws to account for generalised soil behaviour. New developments have especially been needed to describe the mechanical behaviour of soils, a key component of geotechnical engineering, and the focus of intense research activity. Of necessity, only a small number of mechanical constitutive laws have been briefly discussed in the lecture.
(*d*) demonstrating the application of the theoretical formulations to case histories in order to illustrate the relevance and usefulness of the developments described.

The full set of balance equations is collected in Table 5, and the evolving form of the constitutive laws as they progressively include additional phenomena is shown in Table 6.

It must be emphasised, however, that these developments have been made using the spirit and methods of classical

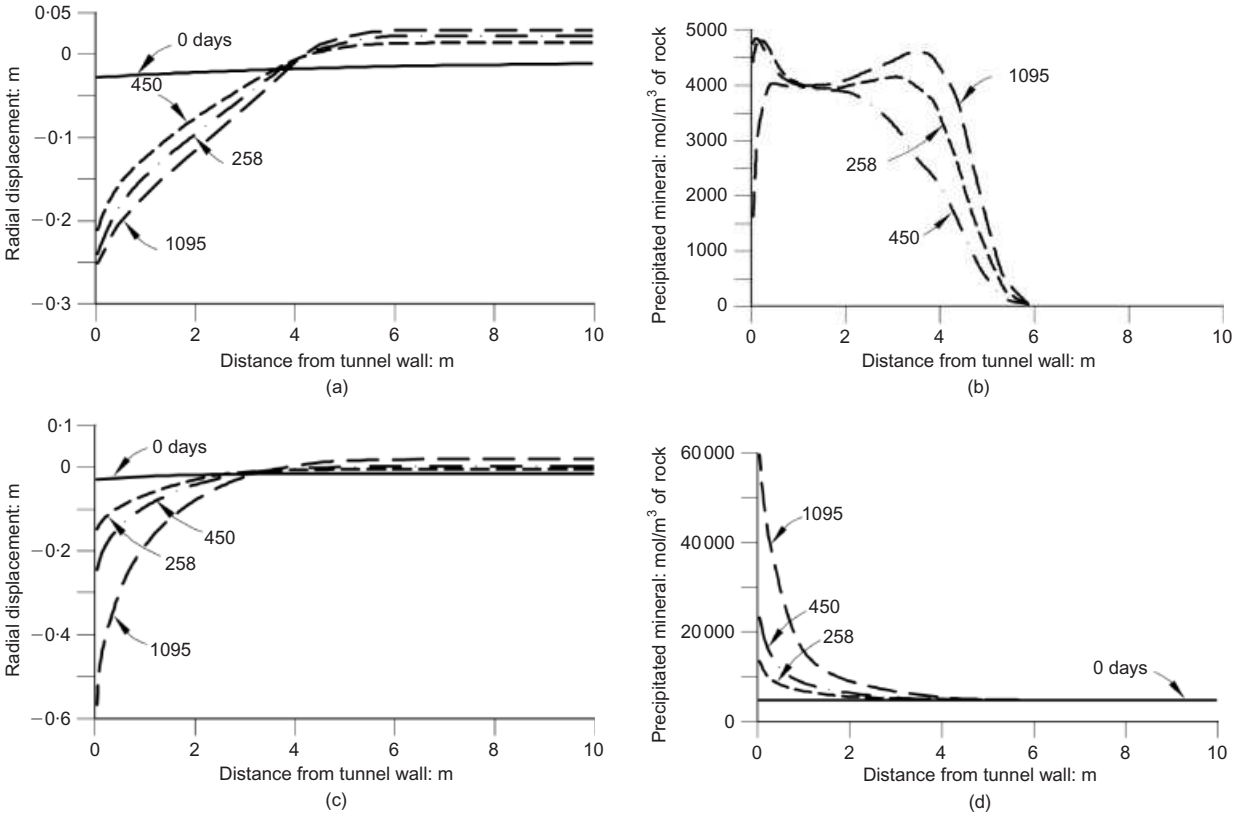

Fig. 105. Results of the analysis assuming water entry into the rock: (a) distributions of radial displacements at different times; (b) distribution of precipitated mineral at different times. Results of the analysis assuming water evaporation into the tunnel: (c) distributions of radial displacements at different times; (d) distribution of precipitated mineral at different times

soil mechanics. Indeed, it is possible to perceive several common themes, already present in classical soil mechanics, inspiring the advances presented.

(*a*) Materials are porous and multiphase.
(*b*) The relevant phenomena are generally coupled phenomena.
(*c*) Soil behaviour features are often closely linked, and may be understood in an integrated manner.
(*d*) Microstructure plays a significant role in soil behaviour.

There is no denying, in this context, that the issue of complexity is an important one. Problems facing geotechnical engineers are complex, and this often leads to complex formulations. It is possible, however, to reduce the risk of drowning in complexity (Biot, 1963). Although it will never be possible (or even sensible) to avoid the use of empirical rules based on experience, it is advisable, when dealing with new and complex problems, to base the formulations and theoretical approaches on sound physical principles as much as is practicable. Indeed, a good part of the basic unity that can be detected throughout the developments of this lecture derives from the common physical laws of solid–liquid–gas interactions. The fact that the concept of suction has appeared in various forms at all stages of the lecture is a strong indication of the deeper connections that underlie the various topics reviewed here.

In addition, in this type of problem, it is necessary to exercise sound engineering judgement in order to select only the relevant phenomena to be considered in each particular case, thereby making the problem amenable to solution. Moreover, when using simplifications, there is a crucial difference if it is done starting from a sound general framework and being conscious of the neglected phenomena, as compared with using a simplified approach from a condition of unawareness. Finally, the use of complex and general frameworks also requires the engineer to be especially alert to detect discrepancies from reality (Vaughan, 1994), so that they can be subject to modifications and further developments, as needed.

To conclude, it can be stated that the extension of classical soil mechanics, conducted with the same underlying spirit and approach, can provide the understanding and the tools that are required to tackle new, and not so new, coupled problems in geotechnical engineering. The possibilities exist, and they will come into increasing use in the future. In this context, it is appropriate to recall some words that I heard attending another Rankine lecture as a PhD student:

> The range of natural materials is so great and the contribution of geotechnical engineering to many technological undertakings is so central, that the limits of our profession expand continually. (Morgenstern, 1981)

Those are fitting, and still true, words to conclude the lecture.

ACKNOWLEDGEMENTS

The financial and technical support of several organisations, as well as their permission to publish research results, are gratefully acknowledged: ADIF (Spain), ANDRA (France), British Petroleum (UK), CESP (Brazil), CIEMAT (Spain), ENRESA (Spain), European Commission, Generalitat de Catalunya, Ministerio de Educación (Spain), Mont Terri Project, MUSE Network, SKB (Sweden), and SCK-CEN (Belgium). Many people generously gave valuable information and advice. Particular thanks are due to Z. Cabarkapa, V. De Gennaro, D. W. Hight, R. J. Jardine, S. Leroueil, R. J. Mair, D. Muir Wood, S. Nishimura, D. M. Potts, J. C. Santamarina, B. A. Schrefler, D. Sheng, C.

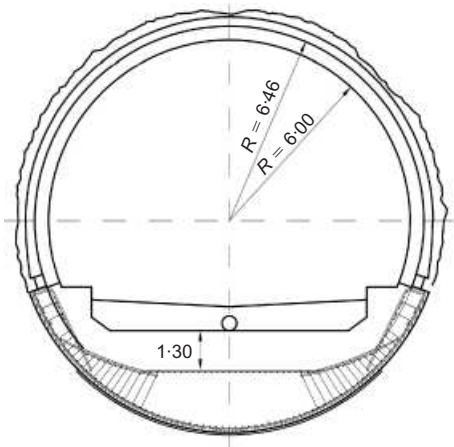

(a)

(b)

Fig. 106. (a) Resisting support solution with a lining designed to withstand heave pressures; (b) construction of the new lining

Viggiani, O. Vilar, M. V. Villar, H.-S. Yu and L. Zdravkovic. David Hight, Dave Potts and Lidija Zdravkovic also provided invaluable assistance in the final preparation of the lecture.

Most of the work presented has been done in collaboration with past and present members of the geotechnical group at the Technical University of Catalonia (UPC): J. Alcoverro, M. Arroyo, I. Berdugo, A. Di Mariano, D. Gallipoli, L. do N. Guimarães, B. Garitte, J. M. Gesto, N. González, A. Josa, A. Ledesma, A. Lloret, S. Olivella, R. A. Rodrigues, E. Romero, M. Sánchez, J. Suriol, B. Valleján, J. Vaunat and, of course, E. E. Alonso, who has been there from the beginning. I am very indebted to them for their numerous and important contributions.

Finally, special thanks go to my wife Dolors and my daughters, Clara, Júlia and Núria, who have patiently endured the long preparation and writing of this lecture, providing support and encouragement at all times.

NOTATION

A_i, A_j chemical formulae of primary and secondary species
a_w chemical activity of water
$\boldsymbol{b}$ vector of body forces
b Biot's coefficient
b_s linear thermal expansion coefficient of the solid phase
b_w volumetric thermal expansion coefficient of water
c_i concentration of chemical species i

Table 4. Summary of the lecture

	Variable	Balance equations					Coupled analysis	Constitutive equations	Case histories
		Water	Air	Energy	Reactive transport	Equilib.			
Saturated soils	Liquid pressure, p_l	Yes				Yes	HM	Barcelona Basic Model (Alonso *et al.*, 1990)	Foundation collapse in Pereira Barreto (Brazil)
Unsaturated soils	Suction, s	Yes	Yes			Yes	HM	Microstructure-based model (Gallipoli *et al.*, 2003)	Subsidence in Ravenna (Italy)
								Coupled hydro-mechanical model (Sheng *et al.*, 2004)	
Thermal, high temperatures	Temperature, T	Yes		Yes		Yes	THM	Double structure model (Sánchez *et al.*, 2005)	Febex mock-up test of an engineered barrier, Madrid (Spain)
								Bond-matrix elasto-plastic model (Vaunat & Gens, 2003a)	In situ heating test in Opalinus clay, Mont Terri (Switzerland)
Thermal, low temperatures	Temperature, T	Yes	Yes	Yes		Yes	THM	Enhanced BBM model (Nishimura *et al.*, 2009).	Chilled pipeline buried in unfrozen ground, Calgary (Canada)
Chemical	Concentration, c	Yes	Yes	Yes	Yes	Yes	THMC	Chemo-plastic model for cation exchange	Tunnel in sulphate-bearing rock, Lilla (Spain)

HM, hydro-mechanical; THM, thermo-hydro-mechanical; THMC, thermo-hydro-mechanical-chemical.

Table 5. Balance equations

Mass balance of solid	$\frac{\partial}{\partial t}[\theta_s(1-n)] + \nabla \cdot \boldsymbol{j}_s = 0$
Mass balance of water	$\frac{\partial}{\partial t}(\theta_l^w S_l n + \theta_g^w S_g n) + \nabla \cdot (\boldsymbol{j}_l^w + \boldsymbol{j}_g^w) = f^w$
Mass balance of air	$\frac{\partial}{\partial t}(\theta_l^a S_l n + \theta_g^a S_g n) + \nabla \cdot (\boldsymbol{j}_l^a + \boldsymbol{j}_g^a) = f^a$
Energy balance	$\frac{\partial}{\partial t}[E_s\rho_s(1-n) + E_l\rho_l S_l n + E_g\rho_g S_g n] + \nabla \cdot (\boldsymbol{i}_c + \boldsymbol{j}_{Es} + \boldsymbol{j}_{El} + \boldsymbol{j}_{Eg}) = f^Q$
Reactive transport equation (mass balance of chemical species)	$\frac{\partial}{\partial t}(nS_l\rho_l c_i) + \nabla \cdot \boldsymbol{j}_i = R_i \quad (i = 1, \ldots, N)$
Momentum balance (equilibrium)	$\nabla \cdot \boldsymbol{\sigma}_t + \boldsymbol{b} = 0$

Table 6. Structure of constitutive laws

Hydro-mechanical (HM) law: saturated soils	$\mathrm{d}\boldsymbol{\sigma}' = \boldsymbol{D}'(\boldsymbol{\varepsilon})(\mathrm{d}\boldsymbol{\varepsilon})$
Hydro-mechanical (HM) law: unsaturated soils	$\mathrm{d}\boldsymbol{\sigma}^* = \boldsymbol{D}(\boldsymbol{\varepsilon}, s)(\mathrm{d}\boldsymbol{\varepsilon}) + \boldsymbol{h}(\boldsymbol{\varepsilon}, s)\mathrm{d}s$
Thermo-hydro-mechanical law (THM)	$\mathrm{d}\boldsymbol{\sigma}^* = \boldsymbol{D}(\boldsymbol{\varepsilon}, s, T)(\mathrm{d}\boldsymbol{\varepsilon}) + \boldsymbol{h}(\boldsymbol{\varepsilon}, s, T)\mathrm{d}s + \boldsymbol{\beta}(\boldsymbol{\varepsilon}, s, T)\mathrm{d}T$
Thermo-hydro-mechanical-chemical law (THMC)	$\mathrm{d}\boldsymbol{\sigma}^* = \boldsymbol{D}(\boldsymbol{\varepsilon}, s, T, \boldsymbol{c})(\mathrm{d}\boldsymbol{\varepsilon}) + \boldsymbol{h}(\boldsymbol{\varepsilon}, s, T, \boldsymbol{c})\mathrm{d}s + \boldsymbol{\beta}(\boldsymbol{\varepsilon}, s, T, \boldsymbol{c})\mathrm{d}T + \boldsymbol{\Gamma}(\boldsymbol{\varepsilon}, s, T, \boldsymbol{c})\mathrm{d}\boldsymbol{c}$

$c_{p,m}$, $c_{v,m}$ specific heat capacity at constant pressure and at constant volume, in molar terms
c_α^i specific heat capacity of species i in phase α phase (i = w, a; α = l, g)
$\boldsymbol{D}$ matrix describing the relationship between increments of strains and constitutive stresses
$\boldsymbol{D}'$ matrix describing the relationship between increments of strains and effective stresses
$\boldsymbol{D}'_g$ mechanical dispersion tensor
$\boldsymbol{D}_g^w$ vapour diffusion coefficient in Fick's law
D_m^w molecular diffusion coefficient of vapour in open air
$D_s(\cdot)/Dt$ material derivative with respect to the solid
E_i specific internal energy of ice
E_α specific internal energy of phase α (α = s, l, g)
e void ratio
e_s void ratio in saturated virgin consolidation line
f^i external supply of species i (i = w, a)
f^Q external supply of energy
$f(s)$ mean interparticle force
G Gibbs free energy
$\boldsymbol{g}$ gravity vector
g gravitational acceleration
$\boldsymbol{h}$ vector that relates changes of constitutive stresses to changes in suction
h thickness of film of adsorbed water
$\boldsymbol{I}$ identity matrix
I_P plasticity index
$\mathbf{i}_c$ conductive heat flux
$\boldsymbol{i}_\alpha^i$ non-advective mass flux (i = w, a; α = l, g)
$\mathbf{j}_{E\alpha}$ advective energy flux in phase α with respect to a fixed reference system (α = s, l, g)
$\mathbf{j}_w$ total mass flux of water with respect to a fixed reference system
$\boldsymbol{j}_w^i$ total mass flux of ice with respect to a fixed reference system
$\boldsymbol{j}_\alpha^i$ total mass flux of species i in phase α with respect to a fixed reference system (i = w, a; α = l, g)
$\boldsymbol{j}_\alpha'^i$ total mass flux of species i in phase α with respect to the solid phase (i = w, a; α = l, g)
$\boldsymbol{K}_\alpha$ permeability tensor (α = l, g)
K bulk modulus of soil
K_l bulk modulus of liquid phase
K_m equilibrium constant for mineral–water reaction (m = An, Gy)
K_s bulk modulus of solid phase
$\boldsymbol{k}$ intrinsic permeability tensor
k permeability
l latent heat
M slope of critical state line
M_r total reactive minerals
M_w molecular mass of water
m inverse of bulk modulus
N_c number of independent chemical components
N_x number of reversible independent chemical reactions
n porosity
n_m number of moles
n^c, n^x number of moles of primary and secondary species
p mean net stress
p' mean effective stress in saturated soils; mean Bishop's stress in unsaturated soils
$\hat{p}$ microstructural effective stress ($= p + s_m$)
p_a air pressure
p^c reference stress in the BBM
p_i ice pressure
p_s left intercept of yield surface in the BBM
p_t mean total stress
p_v vapour pressure
p_v^0 vapour pressure at zero suction
p_w water pressure; pore water pressure
p_0 net mean yield stress at current suction
p_0^* net mean yield stress for saturated conditions
p_0^∞ limit value of p_0 for infinite suction
p_α pressure of phase α (α = l, g)
$\mathbf{q}_w$ volumetric flux of water with respect to the solid
$\boldsymbol{q}_\alpha$ volumetric flux of phase α with respect to the solid (α = l, g)
q triaxial deviatoric stress
R universal gas constant
R_c uniaxial compression strength
R_i rate of production of chemical species i
RH relative humidity
r parameter in the BBM
S_g gas degree of saturation
S_i ice degree of saturation
S_l (liquid) degree of saturation
s matric suction
s_i, s_l specific entropy of ice (i) and liquid water (l)
s_m microstructural suction
s_o osmotic suction
s_t total suction
T absolute temperature
t time
$\boldsymbol{u}$ solid displacement vector
u_a air pressure
u_w water pressure
V volume

v_i, v_l specific volume of ice (i) and liquid water (l)
v_w molar volume of water
W^p plastic work
w water content
w_L, w_P liquid limit, plastic limit
X_i concentration of secondary chemical species i
x_i equivalent fraction of exchangeable cation i
x, y space coordinates
z vertical space coordinate
α_m material parameter in chemo-mechanical model
α_T coefficient of linear thermal expansion of the medium
$\boldsymbol{\beta}$ vector that relates stresses and temperature changes
β parameter in the BBM
β_m material parameter in the chemo-mechanical model
β_w, β_s water and solid compressibilities
$\boldsymbol{\Gamma}$ matrix describing the relationship between increments of chemical concentrations and constitutive stresses
γ_w unit weight of water
$\boldsymbol{\varepsilon}$ strain tensor
ε_m microstructural strain
ε_v volumetric strain
ε_v^{ch} chemically induced volumetric strain
ε_v^p plastic volumetric strain
ε_w volumetric water content ($= nS_l$)
ε_γ triaxial deviatoric strain
ζ parameter defining the flow rule in the model by Sheng *et al.* (2004)
η parameter in chemo-mechanical model
θ_s density of solid phase
θ_t^w density of ice
θ_α^i ($= \rho_\alpha \omega_\alpha^i$) mass of species i in phase α per unit volume of phase α (i = w, a; α = l, g)
κ slope of unloading–reloading consolidation line
κ_c mean curvature of interface
κ_c^{-1} capillary length of water
λ thermal conductivity
λ_i thermal conductivity of ice
λ_{sat}, λ_{dry} thermal conductivity for saturated and dry states
λ_α thermal conductivity of phase α (α = s, l, g)
$\lambda(0)$ slope of saturated virgin consolidation line
$\lambda(s)$ slope of virgin consolidation line at suction s
μ^c, μ^x chemical potentials of primary and secondary species
μ_1 component of first constitutive variable
μ_2 second constitutive variable
μ_α dynamic fluid viscosity of phase α (α = l, g)
ν_{ij} number of moles of primary species j in a mole of secondary species i
ξ bonding variable in model by Gallipoli *et al.* (2003)
ρ_i density of ice
ρ_w density of water
ρ_α density of phase α (α = s, l, g)
$\boldsymbol{\sigma}$ net stress ($= \boldsymbol{\sigma}_t - \boldsymbol{I}\, p_g$)
$\boldsymbol{\sigma}'$ effective stress in saturated soils; Bishop's stress in unsaturated soils
$\boldsymbol{\sigma}^*$ constitutive stress variable
σ_a axial net stress
$\boldsymbol{\sigma}_t$ total stress
σ_s surface tension
σ_v vertical net stress
τ tortuosity
ϕ dissipation function
χ parameter in Bishop's expression for effective stress
ψ total potential
ψ_i components of total potential (i = g, gravitational; p, gas pressure; m, matric; o. osmotic)
ψ_2 part of Helmholtz free energy that depends on plastic strains
ω_α^i mass fraction of species i in phase α (i = w, a; α = l, g)
∇ gradient vector

ABBREVIATIONS

BBM Barcelona Basic Model
CSSM critical state soil mechanics
EDZ excavation-damaged zone
FCV first constitutive variable
HLW high-level waste
HM hydro-mechanical
LC loading–collapse
MCC Modified Cam-clay
MUSE Mechanics of Unsaturated Soils for Engineering
OBC operational base case
REV representative elementary volume
SCV second constitutive variable
SI suction increase
SD suction decrease
THM thermo-hydro-mechanical
THMC thermo-hydro-mechanical-chemical

REFERENCES

Abuel-Naga, H. M., Bergado, D. T., Bouazza, A. & Pender, M. (2009). Thermomechanical model for saturated clays. *Géotechnique* **59**, No. 3, 273–278.

Abuel-Naga, H. M., Bergado, D. T., Bouazza, A. & Ramana, G. V. (2007). Volume change behaviour of saturated clays under drained heating conditions: experimental results and constitutive modelling. *Can. Geotech. J.*, **44**, No. 8, 942–956.

Aitchison, G. D. (1965). Soil properties, shear strength and consolidation. *Proc. 6th Int. Conf. Soil Mechanics Found. Engng, Montreal* **3**, 318–321.

Aitchison, G. D. & Martin, R. (1973). A membrane oedometer for complex stress–strain studies in expansive clays. *Proc. 3rd Int. Conf. Expansive Soils, Haifa* **2**, 83–88.

Aitchison, G. D., Russam, K. & Richards, B. G. (1965). Engineering concepts of moisture equilibria and moisture changes in soils. In *Moisture equilibria and moisture changes in soils beneath covered areas* (ed. G. D. Aitchison), pp. 7–21. Sidney: Butterworth.

Alcoverro, J. (2003). The effective stress principle. *Math. Comput. Modelling* **37**, No. 5, 457–467.

Alonso, E. E., Batlle, F., Gens, A. & Lloret, A. (1988). Consolidation analysis of partially saturated soils: application to earthdam construction. In *Numerical models in geomechanics* (ed. G. Swoboda), pp. 1303–1308. Rotterdam: Balkema.

Alonso, E. E., Berdugo, I. R., Tarragó, D. & Ramon, A. (2007). Tunnelling in sulphate claystones. *Proc. 14th Eur. Conf. Soil Mech. Geotech. Engng, Madrid* **1**, 103–122.

Alonso, E. E. & Gens, A. (1994). On the mechanical behaviour of arid soils. In *Engineering characteristics of arid soils* (eds P. G. Fookes and R. H. G. Parry), pp. 173–205. Rotterdam: Balkema.

Alonso, E. E., Gens, A., Berdugo, I. R. & Romero, E. (2005). Expansive behaviour of a sulphated clay in a railway tunnel. *Proc. 16th Int. Conf. Soil Mech. Geotech. Engng, Osaka* **3**, 1583–1586.

Alonso, E. E., Gens, A. & Hight, D. W. (1987). Special problem soils: general report, *Proc. 9th Eur. Conf. Soil Mech. Found. Engng, Dublin* **3**, 1087–1146.

Alonso, E. E., Gens, A. & Josa, A. (1990). A constitutive model for partially saturated soils. *Géotechnique* **40**, No. 3, 405–430.

Alonso, E. E. & Lloret, E. E. (1982). Behaviour of partially saturated soil in undrained loading and step by step embankment construction. *Proceedings of the IUTAM symposium on deformation and failure of granular materials*, Delft, pp. 173–180.

Alonso, E. E., Vaunat, J. & Gens, A. (1999). Modelling the mechanical behaviour of expansive clays. *Engng Geol*. **54**, No. 1, 173–183.

Anagnostou, G. (2007). Design uncertainties in tunnelling through anhydritic swelling rocks. *Felsbau* **24**, No. 4, 48–54.

Andersland, O. B. & Ladanyi, B. (2004). *Frozen ground engineering*, 2nd edn. Hoboken, NJ: Wiley.

Arenson, L. U. & Springman, S. M. (2005). Mathematical descriptions for the behaviour of ice-rich frozen soils at temperature close to 0°C. *Can. Geotech. J.* **42**, No. 2, 431–442.

Baker, R. & Frydman, S. (2009). Unsaturated soil mechanics: critical review of physical foundations. *Engng Geol*. **106**, Nos 1–2, 26–39.

Baldi, G., Hueckel, T., Peano, A. & Pellegrini, R. (1991). *Developments in modelling of thermo-hydro-geomechanical behaviour of Boom clay and clay-based buffer materials*, Report 13365/2 EN. Luxembourg: Publications of the European Communities.

Barbour, S. & Fredlund, D. G. (1989). Mechanism of osmotic flow and volume change in clay soils. *Can. Geotech. J.* **26**, No. 4, 551–562.

Barden, L., Madedor, A. O. & Sides, G. R. (1969). Volume change characteristics of unsaturated clays. *J. Soil Mech. Found. Engng ASCE* **95**, No. SM1, 33–51.

Barrera, M. (2002). *Estudio experimental del comportamiento hidro-mecánico de suelos colapsables*. PhD thesis, Universitat Politecnica de Catalunya, Spain.

Berdugo, I. R. (2007). *Tunnelling in sulphate-bearing rocks: expansive phenomena*. PhD thesis, Universitat Politènica de Catalunya, Spain.

Berdugo, I. R., Alonso, E. E., Gens, A. & Romero, E. (2007a). Extreme expansive phenomena in a high-speed railway tunnel. *Proceedings of the international tunnelling congress*, Madrid, pp. 479–490.

Berdugo, I. R., Alonso, E. E., Gens, A. & Romero, E. (2007b). Alternative support designs for tunneling in gypsiferous-anhydritic claystones. *Proc. 11th Cong. Int. Soc. for Rock Mechanics, Lisbon* **2**, 775–778.

Berdugo, I. R., Alonso, E. E., Romero, E. & Gens, A. (2009a). Tunnelling and swelling in Triassic sulphate-bearing rocks. Part I: Case studies from Baden-Württemberg. *Épsilon*, No. 12, 13–37.

Berdugo, I. R., Alonso, E. E., Romero, E. & Gens, A. (2009b). Tunnelling and swelling in Triassic sulphate-bearing rocks. Part II: Case studies from Jura Mountains. *Épsilon*, No. 12, 39–53.

Berdugo, I. R., Guimarães, L. do N., Gens, A. & Alonso, E. E. (2009c). HMC analysis of a tunnel in swelling rock. *Proc. 2nd Int. Conf. on Computational Methods in Tunnelling, Bochum* **1**, 477–483.

Bertoni, W., Elmi, C. & Marabini, F. (2005). The subsidence of Ravenna. *Giornale di Geologia Applicata* **1**, 23–32.

Biot, M. A. (1941). General theory of three-dimensional consolidation. *J. Appl. Phys*. **12**, 155–164.

Biot, M. A. (1963). Are we drowning in complexity? *Mech. Engng* **85**, No. 2, 26–27.

Bishop, A. W. (1959). The principle of effective stress. *Teknisk Ukeblad* **106**, No. 39, 859–863.

Bishop, A. W., Alpan, I., Blight, G. E. & Donald, I. B. (1960). Factors controlling the strength of partly saturated cohesive soils. *Proceedings of the ASCE research conference on shear strength of cohesive soils*, Boulder, CO, pp. 503–532.

Bishop, A. W. & Blight, G. E. (1963). Some aspects of effective stress in saturated and partly saturated soils. *Géotechnique* **13**, No. 3, 177–197.

Black, P. B. & Tice, A. R. (1989). Comparison of soil freezing curve and soil water curve data for Windsor Sandy Loam. *Water Resour. Res*. **25**, No. 10, 2205–2210.

Blanchard, D. & Fremond, M. (1985). Soils frost heaving and thaw settlement. *Proc. 4th Int. Symp. on Ground Freezing, Sapporo* **1**, 209–216.

Blight, G. E. (1997). Interaction between the atmosphere and the Earth. *Géotechnique* **47**, No. 4, 715–767.

Bolzon, G., Schrefler, B. A. & Zienkiewicz, O. C. (1996). Elastoplastic soil constitutive laws generalized to semisaturated states. *Géotechnique* **46**, No. 2, 279–289.

Bolzon, G. & Schrefler, B. A. (2005). Thermal effects in partially saturated soil: a constitutive model. *Int. J. Numer. Anal. Meth. Geomech*. **29**, No. 9, 861–877.

Borja, R. I. (2006). On the mechanical energy and effective stress in saturated and unsaturated porous continua. *Int. J. Solids Struct*. **43**, No. 6, 1764–1786.

Brighenti, G., Gambolati, G., Gatto, P., Ricceri, G., Vuillermin, F. & Bertoni, W. (1994). *Commissione per lo studio della subsidenza di Ravenna*, Technical Report, Italian Law 854 /80.

Buisson, M. S. R. & Wheeler, S. J. (2000). Inclusion of hydraulic hysteresis in a new elastoplastic framework for unsaturated soils. In *Experimental evidence and theoretical approaches in unsaturated soils* (eds A. Tarantino and C. Mancuso), pp. 109–119. Rotterdam: Balkema.

Burghignoli, A., Desideri, A. & Miliziano, S. (2000). A laboratory study on the thermomechanical behaviour of clayey soils. *Can. Geotech. J.* **37**, No. 4, 764–780.

Burland, J. B. & Ridley, A. M. (1996). The importance of suction in soil mechanics. *Proc. 12th South-East Asian Conf. Soil Mech. Found. Engng, Kuala Lumpur* **2**, 27–49.

Buscarnera, G. & Nova, R. (2009). An elastoplastic strainhardening model for soil allowing for hydraulic bonding-debonding effects. *Int. J. Numer. Anal. Meth. Geomech*. **33**, No. 8, 1055–1086.

Campanella, R. G. & Mitchell, J. R. (1968). Influence of temperature variations on soil behaviour. *J. Soil Mech. Found. Div. ASCE* **94**, No. 3, 709–734.

Carlson, L. E. & Nixon, J. F. (1988). Subsoil investigation of ice lensing at the Calgary, Canada, frost heave test facility. *Can. Geotech. J.* **25**, No. 2, 307–319.

Casini, F., Munoz, J., Lorenco, S., Thorel, L., Vaunat, J., Delage, P. & Gallipoli, D. (2009). Centrifuge modelling of an unsaturated collapsible soil. In *Between theory and practice in unsaturated soil mechanics* (eds A. Tarantino and C. Mancuso). Rotterdam: Millpress.

Cekerevac, C. & Laloui, L. (2004). Experimental study of thermal effects on the mechanical behaviour of clays. *Int. J. Numer. Anal. Methods Geomech*. **28**, No. 3, 209–228.

Chandler, R. J. (1976). The history and stability of two Lias clay slopes in the upper Gwash valley, Rutland. *Phil. Trans. R. Soc. London A* **283**, 463–491.

Chandler, R. J., Kellaway, G. A., Skempton, A. W. & Wyatt, R. J. (1976). Valley slope sections in Jurassic strata near Bath, Somerset. *Phil. Trans. R. Soc. London A* **283**, 527–556.

Chapman, N. A. & McKinley, I. G. (1987). *The geological disposal of nuclear waste*. Chichester: Wiley.

Charles, J. A. (2008). The engineering behaviour of fills: the use, misuse and disuse of case histories. *Géotechnique* **58**, No. 7, 541–570.

Chiu, C. F. & Ng, C. W. W. (2003). A state-dependent elasto-plastic model for saturated and unsaturated soils. *Géotechnique* **53**, No. 9, 809–829.

Cho, W. J., Lee, J. O. & Chun, K. S. (1999). The temperature effects on hydraulic conductivity of compacted bentonite. *Appl. Clay Sci*. **14**, Nos 1–3, 47–58.

Clarke, B. G. (2009). Thermal behaviour of the ground. Editorial. *Géotechnique* **59**, No. 3, 157–158.

Clarke, J., Fenton, C., Gens, A., Jardine, R., Martin, C., Nethercot, D., Nishimura, S., Olivella, S., Reifen, C., Rutter, P., Strasser, F. & Toumi, R. (2008). A multi-disciplinary approach to assess the impact of global climate change on infrastructure in cold regions. *Proc. 9th Int. Conf. on Permafrost, Fairbanks, Alaska*, 279–284.

Coleman, J. D. (1962). Stress strain relations for partly saturated soil. Correspondence. *Géotechnique* **12**, No. 4, 348–350.

Coll, C. (2005). *Endommagement des roches argileuses et perméabilité induite au voisinage d'ouvrages souterrains*. Doctoral thesis, Université Joseph Fourier, Grenoble, France.

Collins, I. F. & Hilder, T. (2002). A theoretical framework for constructing elastic/plastic constitutive models of triaxial tests. *Int. J. Numer. Anal. Methods Geomech*. **26**, No. 13, 1313–1347.

Collins, J. F. & Houlsby, G. T. (1997). Application of thermomechanical principles to modelling of geotechnical materials. *Proc. R. Soc. London Ser. A* **453**, 1975–2001.

Côté, J. & Konrad, J.-M. (2005). A generalized thermal conductivity model for soils and construction materials. *Can. Geotech. J.* **42**, No. 2, 443–458.

Coussy, O. (2005). Poromechanics of freezing materials. *J. Mech. Phys. Solids* **53**, No. 8, 1689–1718.

Coussy, O. (2006). Deformation and stress from in-pore drying-induced crystallization of salt. *J. Mech. Phys. Solids* **54**, No. 8, 1517–1547.

Coussy, O. (2007). Revisiting the constitutive equations of unsaturated porous solids using a Lagrangian saturation concept. *Int. J. Numer. Anal. Methods Geomech*. **31**, No. 15, 1675–1694.

Coussy, O. & Dangla, P. (2002). Approche énergétique du comportement des sols non saturés. In *Mécanique des sols non saturés* (eds O. Coussy and J. M. Fleureau), pp. 137–174. Paris: Hermes.

Coussy, O., Pereira, J. M. & Vaunat, J. (2009). Revisiting the thermodynamics of plasticity for unsaturated soils. *Comput. Geotech*., doi: 10·1016/j.compgeo.2009·09·003.

Croney, D. (1952). The movement and distribution of water in soils. *Géotechnique* **3**, No. 1, 1–16.

Cui, Y. J. (1993). *Etude du comportement d'un limon compacté non saturé et da sa modelisation dans un cadre elasto-plastique*. Thèse de doctorat, Ecole Nationale des Ponts et Chaussées, France.

Cui, Y. J. & Delage, P. (1996). Yielding and plastic behaviour of an unsaturated compacted silt. *Géotechnique* **46**, No. 2, 291–311.
Cui, Y. J., Delage, P. & Sultan, N. (1995). An elasto-plastic model for compacted soils. In *Unsaturated soils* (eds E. E. Alonso and P. Delage), Vol. 2, pp. 703–709. Rotterdam: Balkema.
Cui, Y. J., Sultan, N. & Delage, P. (2000). A thermomechanical model for saturated clays. *Can. Geotech. J.* **37**, No. 3, 607–620.
Dakshanamurthy, V., Fredlund, D. G. & Rahardjo, H. (1984). Coupled three-dimensional consolidation theory of unsaturated porous media. *Proc. 5th Int. Conf. Expansive Soils, Adelaide*, 99–103.
Dangla, O. L., Malinsky, L. & Coussy, O. (1997). Plasticity and imbibition-drainage curves for unsaturated soils: a unified approach. *Proc. 6th Int. Conf. on Numerical Models in Geomechanics, Montreal*, 141–146.
De Gennaro, V., Delage, P., Collin, F. & Cui, Y.-J. (2004). On the collapse behaviour of oil reservoir chalk. *Géotechnique* **54**, No. 6, 415–420.
De Gennes, P.-G., Brochard-Wyart, F. & Quéré, D. (2004). *Capillary and wetting phenomena: Drops, bubbles, pearls, waves*. New York: Springer.
Delage, P., Schroeder, Ch. & Cui, Y.-J. (1996). Subsidence and capillary effects in chalk. *Proc. Eurock '96* (ed. G. Barla), pp. 1291–1298. Rotterdam: Balkema.
Delage, P., Sultan, N. & Cui, Y. J. (2000). On the thermal consolidation of Boom clay. *Can. Geotech. J.* **37**, No. 2, 343–354.
Delage, P., Suraj de Silva, G. P. R. & de Laure, E. (1987). Un novel appareil triaxial pour les sols non saturés. *Proc. 9th Eur. Conf. Soil Mech. Found. Engng, Dublin* **1**, 25–28.
Derjaguin, B. V., Churaev, N. V. & Muller, V. M. (1987). *Surface forces*. New York: Plenum.
Di Maio, C. (1996). Exposure of bentonite to salt solution: osmotic and mechanical effects. *Géotechnique* **46**, No. 4, 695–707.
Ehlers, W., Graf, T. & Ammann, M. (2004). Deformation and localization analysis of partially saturated soil. *Comput. Methods Appl. Mech. Engng* **193**, Nos 27–29, 2885–2910.
Ehlers, W., Graf, T. & Ammann, M. (2005). Non-linear behaviour in the deformation and localization analysis of unsaturated soil. In *Unsaturated soils: Numerical and theoretical approaches* (ed. T. Schanz), Vol. 2, pp. 41–52. Berlin: Springer.
Escario, V. & Jucá, J. F. T. (1989). Strength and deformation of partly saturated soils. *Proc. 12th. Int. Conf. Soil Mech. Found. Engng, Rio de Janeiro* **1**, 43–46.
Escario, V. & Sáez, J. (1973). Measurement of the properties of swelling and collapsing soils under controlled suction. *Proc. 3rd Int. Conf. Expansive Soils, Haifa*, 196–200.
Escario, V. & Sáez, J. (1986). The shear strength of partly saturated soils. *Géotechnique* **36**, No. 3, 453–456.
Feola, A., Lombardi, G., Pellegrino, A. & Viggiani, C. (2004). I dissesti de via Settembrini a Napoli a seguito dell'evento piovoso del 15 settembre 2001. *Proc. 22nd Italian Geotech. Conf., Palermo*, 107–118.
Fisher, R. A. (1926). On the capillary forces in an ideal soil: correction of formulae given by W. B. Haines. *J. Agric. Sci*. **16**, No. 3, 492–505.
Fletcher, P. (1993). *Chemical thermodynamics for earth scientists*. Harlow: Longman.
François, B. & Laloui, L. (2008). ACMEG-TS: A constitutive model for unsaturated soils under non-isothermal conditions. *Int. J. Numer. Anal. Methods Geomech*. **32**, No. 16, 1955–1988.
Fredlund, D. G. (2006). Unsaturated soil mechanics in engineering practice. *J. Geotech. Geoenviron. Engng ASCE* **132**, No. 3, 286–321.
Fredlund, D. G. & Morgenstern, N. R. (1976). Constitutive relations for volume change in unsaturated soils. *Can. Geotech. J.* **13**, No. 3, 261–276.
Fredlund, D. G. & Morgenstern, N. R. (1977). Stress state variables and unsaturated soils. *J. Geotech. Engng Div. ASCE* **103**, No. GT5, 447–466.
Fredlund, D. G. & Rahardjo, H. (1993). *Soil mechanics for unsaturated soils*. New York: Wiley.
Fredlund, D. G. & Xing, A. (1994). Equations for the soil-water characteristic curve. *Can. Geotech. J.* **31**, No. 3, 521–532.
Fredlund, D. G., Morgenstern, N. R. & Widger, R. A. (1978). The shear strength of unsaturated soils. *Can. Geotech. J.* **15**, No. 3, 313–321.
Fredlund, D. G., Rahardjo, H. & Gan, J. K. M. (1987). Non-linearity of strength envelope for unsaturated soils. *Proc. 6th Int. Conf. on Expansive Soils, New Delhi*, 49–54.
Gajo, A., Loret, B. & Hueckel, T. (2002). Electro-chemo-mechanical coupling in saturated porous media: elastic-plastic behaviour of heteroionic expansive clays. *Int. J. Solids Struct*. **39**, No. 16, 4327–4362.
Gallipoli, D., Gens, A., Sharma, R. S. & Vaunat, J. (2003). An elasto-plastic model for unsaturated soil including the effect of saturation degree on mechanical behaviour. *Géotechnique* **53**, No. 1, 123–35.
Gallipoli, D., Gens, A., Chen, G. & D'Onza, F. (2008). Modelling unsaturated soil behaviour during normal consolidation and at critical state. *Comput. Geotech*. **35**, No. 6, 825–834.
Gan, J. K. M. & Fredlund, D. G. (1988). Multistage direct shear testing of unsaturated soils. *ASTM Geotech. Test. J.* **11**, No. 2, 132–138.
Garitte, B., Vaunat, J. & Gens, A. (2006). A constitutive model that incorporates the effect of suction in cemented geological materials. *Proc. 4th Int. Conf. on Unsaturated Soils, Carefree, AZ* **2**, 1944–1955.
Garrels, R. M. & Christ, C. L. (1965). *Solutions, minerals and equilibria*. San Francisco: Freeman Cooper.
Gatmiri, B. & Arson, C. (2008). θ-STOCK, a powerful tool of thermohydromechanical behaviour and damage modelling of unsaturated porous media. *Comput. Geotech*. **35**, No. 6, 890–915.
Gawin, D., Baggio, P. & Schrefler, B. A. (1995). Coupled heat, water and gas flow in deformable porous media. *Int. J. Numer. Methods in Fluids* **20**, Nos 8–9, 969–987.
Geiser, F., Laloui, L. & Vulliet, L. (2000). Modelling the behaviour of unsaturated soils. In *Experimental evidence and theoretical approaches in unsaturated soils* (eds A. Tarantino and C. Mancuso), pp. 155–175. Rotterdam: Balkema.
Gens, A. (1995). Constitutive laws. In *Modern issues in non-saturated soils* (eds A. Gens, P. Jouanna and B. A. Schrefler), pp. 129–158. Wien: Springer-Verlag.
Gens, A. (1996). Constitutive modelling: application to compacted soils. In *Unsaturated soils* (eds Alonso and Delage), Vol. 3, pp. 1179–1200. Rotterdam: Balkema.
Gens, A. (1997). Suction and temperature, critical factors affecting soil behaviour. *Proc. 14th Int. Conf. Soil Mech. Found. Engng, Hamburg* **4**, 2169–2171.
Gens, A. (2003). The role of geotechnical engineering for nuclear energy utilisation. *Proc. 13th. Eur. Conf. Soil Mech. Geotech. Engng, Prague* **3**, 25–67.
Gens, A. & Alonso, E. E. (1992). A framework for the behaviour of unsaturated expansive clays. *Can. Geotech. J.* **29**, No. 6, 1013–1032.
Gens, A. & Nova, R. (1993). Conceptual bases for a constitutive model for bonded soils and weak rocks. In *Geotechnical engineering of hard soils–soft rocks* (eds A. Anagnostopoulos *et al.*), Vol. 1, pp. 485–494. Rotterdam: Balkema.
Gens, A. & Olivella, S. (2000). Non-isothermal multiphase flow in deformable porous media: coupled formulation and application to nuclear waste disposal. In *Developments in theoretical geomechanics: The John Booker Memorial Symposium* (eds D. W. Smith and I. P. Carter), pp. 619–640. Rotterdam: A. A. Balkema.
Gens, A. & Olivella, S. (2001a). THM phenomena in saturated and unsaturated porous media. *Rev. fr. génie civ.* **5**, No. 6, 693–717.
Gens, A. & Olivella, S. (2001b). Numerical analysis of radioactive waste disposal. In *Environmental geomechanics* (ed. B. A. Schrefler), pp. 203–234. Wien: Springer.
Gens, A. & Olivella, S. (2005). Numerical modelling in nuclear waste storage engineering. *Proc. 11th IACMAG Int. Conf., Turin* **4**, 555–570.
Gens, A., Alonso, E. E. & Delage, P. (1997). Computer modeling and applications to unsaturated soils. In *Unsaturated soil engineering practice* (eds S. L. Houston and D. G. Fredlund). ASCE Geotechnical Special Publication 68, pp. 299–330. Reston, VA: ASCE.
Gens, A., Alonso, E. E. & Josa, A. (1989). Elastoplastic modelling of partially saturated soils, *Proc. 3rd Int. Symp. on Numerical Models in Geomechanics (NUMOG III), Niagara Falls*, 163–170.

Gens, A., Alonso, E. E., Lloret, A. & Batlle, F. (1993). Prediction of long term swelling of expansive soft rock: a double-structure approach. *Geotechnical Engineering of Hard Soils–Soft Rocks* (eds A. Anagnostopoulos *et al.*), Vol. 1, pp. 495–500. Rotterdam: Balkema.

Gens, A., García-Molina, A. J., Olivella, S., Alonso, E. E. & Huertas, F. (1998). Analysis of a full scale in situ test simulating repository conditions. *Int. J. Numer. Anal. Methods Geomech.* **22**, No. 7, 515–548.

Gens, A., Guimarães, L. do N., Garcia-Molina, A. & Alonso, E. E. (2002a). Factors controlling rock–clay buffer interaction in a radioactive waste repository. *Engng Geol*. **64**, Nos 2–3, 297–308.

Gens, A., Guimarães, L. do N. & Olivella, S. (2002b). Coupled chemomechanical analysis for saturated and unsaturated soils. In *Environmental geomechanics* (eds L. Vulliet, L. Laloui and B. Schrefler), pp. 109–123. Lausanne: EPFL Press.

Gens, A., Guimarães, L. do N. & Olivella, S. (2005). THMC coupling in partially saturated geomaterials. *Rev. eur. génie civ.* **9**, Nos 5–6, 747–765.

Gens, A., Sánchez, M. & Sheng, D. (2006). On constitutive modelling of unsaturated soils. *Acta Geotech.* **1**, No. 3, 137–147.

Gens, A., Vaunat, J., Garitte, B. & Wileveau, Y (2007). In situ behaviour of a stiff layered clay subject to thermal loading: observations and interpretation. *Géotechnique* **57**, No. 2, 207–228.

Gens, A., Guimarães, L. do N., Fernández, A. M., Olivella, S. & Sánchez, M. (2008a). Coupled analysis of chemo-mechanical processes. In *Thermal-hydromechanical and chemical coupling in geomaterials and applications, Geoproc' 2008* (Shao, J.-F. & Burlion, N. eds.), pp. 41–57. London/Hobohen: Wiley-ISTE.

Gens, A., Guimarães, L. do N., Sánchez, M. & Sheng, D. (2008b). Developments in modelling the generalised behaviour of unsaturated soils. In *Unsaturated soils: Advances in geo-engineering* (eds D. G. Toll *et al.*), pp. 53–61. London: Taylor & Francis.

Gens, A., Garitte, B., Olivella, S. & Vaunat, J. (2009a). Applications of multiphysical geomechanics in underground nuclear waste storage. *Eur. J. Env. Civil Engng* **13**, No. 7–8, 937–962.

Gens, A., Sánchez, M., Guimarães, L. do N., Alonso, E. E., Lloret, A., Olivella, S., Villar, M. V. & Huertas, F. (2009b). A full-scale in situ heating test for high-level nuclear waste disposal: observations, analysis and interpretation. *Géotechnique* **59**, No. 4, 377–399.

Georgiadis, K., Potts, D. M. & Zdravkovic, L. (2003). The influence of partial soil saturation on pile behaviour. *Géotechnique* **53**, No. 1, 11–25.

Gili, J. A. (1988). *Modelo microestructural para medios granulares no saturados*. PhD thesis, Universitat Politècnica de Catalunya, Spain.

Gili, J. A. & Alonso, E. E. (2002). Microstructural deformation mechanisms of unsaturated granular soils. *Int. J. Numer. Anal. Methods Geomech*. **26**, No. 5, 433–468.

Goughnour, R. R. & Andersland, O. B. (1968). Mechanical properties of a sand-ice system. *J. Soil Mech. Found. Div.* ASCE **94**, No. SM4, 923–950.

Graham, J., Tanaka, N., Crilly, T. & Alfaro, M. (2001). Modified Cam-Clay modelling of temperature effects in clays. *Can. Geotech. J.* **38**, No. 3, 608–621.

Gray, W. G. & Schrefler, B. A. (2001). Thermodynamic approach to effective stress in partially saturated porous media. *Eur. J. Mech. A/Solids* **20**, No. 4, 521–538.

Gray, W. G. & Schrefler, B. A. (2007). Analysis of the solid stress tensor in multiphase porous media. *Int. J. Numer. Anal. Methods Geomech*. **31**, No. 4, 541–581.

Guimarães, L. do N. (2002). *Análisis multi-componente no isotermo en medio poroso deformable no saturado*. PhD thesis, Universitat Politècnica de Catalunya, Spain.

Guimarães, L. do N., Gens, A. & Olivella, S. (1999). THM and reactive transport coupling in unsaturated porous media. *Proc. 7th Int. Symp. on Numerical Models in Geomechanics, Graz*, 303–308.

Guimarães, L. do N., Gens, A., Sánchez, S. & Olivella, S. (2006). THM and reactive transport analysis of expansive clay barrier in radioactive waste isolation. *Commun. Numer. Methods Engng* **22**, No. 8, 849–859.

Guimarães, L. do N., Gens, A. & Olivella, S. (2007). Coupled thermo-hydro-mechanical and chemical analysis of expansive clay subjected to heating and hydration. *Transp. Porous Media* **66**, No. 3, 341–372.

Gulhati, S. K. & Satija, B. S. (1981). Shear strength of partially saturated soils. *Proc. 10th. Int. Conf. Soil Mech. Found. Engng, Stockholm* **1**, 609–612.

Harvie, C., Greenberg, J. & Weare, J. (1987). A chemical equilibrium algorithm for highly non-ideal multiphase systems: free energy minimization. *Geochim. Cosmochim. Acta* **51**, No. 5, 1045–1057.

Hassanizadeh, S. M. & Gray, W. G. (1980). General conservation equations for multiphase systems. 3: Constitutive theory for porous media. *Adv. Water Resour.* **3**, No. 1, 25–40.

He, P., Zhu, Y. & Cheng, G. (2000). Constitutive models of frozen soil. *Can. Geotech. J.* **37**, No. 4, 811–816.

Ho, D. Y. F. & Fredlund, D. G. (1982). Increase in strength due to suction for two Hong Kong soils. *Proceedings of the ASCE specialty conference on engineering and construction in tropical and residual soils*, Hawaii, pp. 263–295.

Horiguchi, K. & Miller, R. D. (1983). Hydraulic conductivity functions of frozen materials. *Proc. 4th Int. Conf. on Permafrost, Fairbanks*, 504–508.

Houlsby, G. T. (1997). The work input to an unsaturated granular material. *Géotechnique* **47**, No. 1, 193–196.

Houlsby, G. T. & Puzrin, A. M. (2006). *Principles of hyperplasticity: An approach to plasticity theory based on thermodynamic principles*. London: Springer-Verlag.

Hueckel, T. (1992). Water mineral interaction in hydromechanics theory approach. *Can. Geotech. J.*, **29**, No. 6, 1071–1086.

Hueckel, T. (1997). Chemo-plasticity of clays subjected to stress and flow of a single contaminant. *Int. J. Numer. Anal. Methods Geomech*. **21**, No. 1, 43–72.

Hueckel, T. & Baldi, G. (1990). Thermoplasticity of saturated clays: experimental constitutive study. *J. Geotech. Engng ASCE* **116**, No. 12, 1768–1796.

Hueckel, T. & Borsetto, M. (1990). Thermoplasticity of saturated soils and shales: constitutive equations. *J. Geotech. Engng ASCE* **116**, No. 12, 1765–1777.

Huertas, F., Fariña, P., Farias, J., García-Siñériz, J. L., Villar, M. V., Fernández, A. M., Martín, P. L., Elorza, F. J., Gens, A., Sánchez, M., Lloret, A., Samper, J. & Martínez, M. A. (2006). *Full-scale engineered barrier experiment*, Updated Final Report, Technical Publication 05-0/2006. Madrid: Enresa.

Hutchinson, J. N. (1970). A coastal mudflow on the London Clay cliffs at Beltinge, North Kent. *Géotechnique* **20**, No. 4, 412–438.

Hutchinson, J. N. (1991). Theme lecture: Periglacial and slope processes. In *Quaternary engineering geology* (eds A. Forster, M. G. Culshaw, J. C. Cripps, J. A. Little and C. F. Moon), Geological Society Engineering Geology Special Publication No. 7, pp. 283–331. London: Geological Society.

Hutter, K., Laloui, L. & Vulliet, L. (1999). Thermodynamically based mixture models for saturated and unsaturated soils. *Mech.-Cohesive Frictional Mater.* **4**, No. 4, 295–338.

IPCC (2007). *Climate change 2007: The physical science basis*, Contribution of Working Group I to the Fourth Assessment Report of the Intergovernmental Panel on Climate Change. Cambridge: Cambridge University Press.

Jardine, R. J., Gens, A., Hight, D. W. & Coop, M. R. (2004). Developments in understanding soil behaviour. In *Advances in geotechnical engineering: The Skempton conference*, pp. 103–206. London: Thomas Telford.

Jennings, J. E. B. & Burland, J. B. (1962). Limitations to the use of effective stresses in partly saturated soils. *Géotechnique* **12**, No. 2, 125–144.

Jessberger, H. L. (1981). A state-of-the-art report. Ground freezing: mechanical properties, processes and design. *Engng Geol*. **18**, Nos 1–4, 5–30.

Jommi, C. (2000). Remarks on constitutive modelling of unsaturated soils. In *Experimental evidence and theoretical approaches in unsaturated soils* (eds A. Tarantino and C. Mancuso.), pp. 139–153. Rotterdam: Balkema.

Jommi, C. & di Prisco, C. (1994). Un semplice approccio teorico per la modellazione del comportamento meccanico dei terreni granulari parzialmente saturi. *Proc. Conf. il ruolo dei fluidi nei problemi di ingegneria geotecnica*, Mondovı, pp. 167–188.

Josa, A., Balmaceda, A., Gens, A. & Alonso, E. E. (1992). An

elastoplastic model for partially saturated soil exhibiting a maximum of collapse. In *Computational plasticity III* (eds D. R. J. Owen, E. Onate and E. Hinton), Vol. 1, pp. 815–826. Swansea: Pineridge Press.

Justo, J. L., Saura, J., Jaramillo, A., Manzanares, J. L., Rodríguez, J. E. & González, A. (1985). A FEM for lineal canals on expansive-collapsing soils. *Proc. 11th Int. Conf. Soil Mech. Found. Engng, San Francisco* **2**, 769–772.

Kaczmarek, M. & Hueckel, T. (1998). Chemo-mechanical consolidation of clays: analytical solutions for a linearized one-dimensional problem. *Transp. Porous Media* **32**, No. 1, 49–74.

Karube, D. (1983). Effect of suction on soil behavior. *Proc. 7th. Asian Conf. on Soil Mechanics Found. Eng*. Haifa, **1**, 30–35.

Karube, D. & Kato, S. (1994). An ideal unsaturated soil and the Bishop's soil. *Proc. 13th Int. Conf. Soil Mech. Found. Engng, New Delhi* **1**, 43–46.

Kavvadas, M. J. (2000). General report: Modelling the soil behaviour – Selection of soil parameters. In *The Geotechnics of hard soils – soft rocks* (eds A. Evangelista and L. Picarelli), Vol. 3, pp. 1441–1481. Rotterdam: Balkema.

Kerisel, J. (1987). *Down to earth. Foundations past and present: the invisible art of the builder*. Rotterdam: Balkema.

Khalili, N. & Khabbaz, M. H. (1998). A unique relationship for chi for the determination of the shear strength of unsaturated soils. *Géotechnique* **48**, No. 5, 681–687.

Khalili, N., Geiser, F. & Blight, G. E. (2004). Effective stress in unsaturated soils: review with new evidence. *Int. J. Geomech*. **4**, No. 2, 115–126.

Khalili, N., Habte, M. A. & Zargarbashi, S. (2008). A fully coupled flow deformation model for cyclic analysis of unsaturated soils including hydraulic and mechanical hysteresis. *Comput. Geotech*. **35**, No. 6, 872–889.

Khalili, N. & Loret, B. (2001). An elasto-plastic model for non-isothermal analysis of flow and deformation in unsaturated porous media: formulation. *Int. J. Solids Struct*. **38**, No. 46–47, 8305–8330.

Khemissa, M. (1998). Mesure de la perméabilité des argiles sous contrainte et température. *Rev. Fr. Géotech*. **82**, 11–22.

Kimoto, S., Oka, F., Fushita, F. & Fujiwaki, M. (2007). A chemo-thermo-mechanically coupled numerical simulation of the subsurface ground deformations due to methane hydrate dissociation. *Comput. Geotech*. **34**, No. 4, 216–228.

Kirillin, V. A., Sychev, V. V. & Sheindlin, A. E. (1976). *Engineering thermodynamics*. Moscow: Mir Publishers.

Kohgo, Y., Nakano, M. & Miyazaki, T. (1993). Theoretical aspects of constitutive modelling for unsaturated soils. *Soils Found*., **33**, No. 4, 49–63.

Kohler, R. & Hofstetter, G. (2008). A cap model for partially saturated soils. *Int. J. Numer. Anal. Methods Geomech*. **32**, No. 8, 981–1004.

Konrad, J.-M. & Morgenstern, J. R. (1980). A mechanistic theory of ice lens formation in fine-grained soils. *Can. Geotech. J.* **17**, No. 4, 473–486.

Konrad, J.-M. & Morgenstern, J. R. (1981). The segregation potential of a freezing soil. *Can. Geotech. J.* **18**, No. 4, 482–491.

Kovári, K., Amstad, Ch. & Anagnostou, G. (1988). Design/construction methods: tunneling in swelling rocks. *Proc. 28th US Symp. on Key Questions in Rock Mechanics, Minessota*, 17–32.

Ladanyi, B. (1972). An engineering theory of creep of frozen soils. *Can. Geotech. J.* **9**, No. 1, 63–80.

Laloui, L. & Cekerevac, C. (2003). Thermo-plasticity of clays: an isotropic yield mechanism. *Comput. Geotech*. **30**, No. 8, 649–660.

Laloui, L. & Cekerevac, C. (2008). Non-isothermal plasticity model for cyclic behaviour of soils. *Int. J. Numer. Anal. Methods Geomech*. **32**, No. 5, 437–460.

Laloui, L. & Nuth, M. (2005). An introduction to the constitutive modelling of unsaturated soils. *Rev. eur. génie civ.* **9**, Nos 5–6, 651–670.

Laloui, L. & Nuth, M. (2009). On the use of the generalised effective stress in the constitutive modelling of unsaturated soils. *Comput. Geotech*. **36**, Nos 1–2, 20–23.

Laloui, L., Geiser, F. & Vulliet, L. (2001). Constitutive modelling of unsaturated soils. *Rev. fr. génie civ.*, **5**, No. 6, 797–807.

Laloui, L., Klubertanz, G. & Vulliet, L. (2003). Solid-liquid-air coupling in multiphase porous media. *Int. J. Numer. Anal. Methods Geomech*. **27**, No. 3, 183–206.

Lambe, T. W. & Whitman, R. V. (1979). *Soil mechanics*. New York: Wiley.

Leroueil, S. & Barbosa, P. S. de A. (2000). Combined effects of fabric, bonding and partial saturation on yielding of soils. In *Unsaturated soils for Asia* (eds H. Rahardjo, D. G. Toll and E. C. Leong), pp. 527–532. Rotterdam: Balkema.

Leroueil, S. & Vaughan, P. R. (1990). The general and congruent effects of structure in natural soils and weak rocks. *Géotechnique* **40**, No. 3, 467–488.

Lewis, R. W. & Schrefler, B. A. (1987). *The finite element method in the deformation and consolidation of porous media*. Chichester: Wiley.

Li, N., Chen, B., Chen, F. & Xu, X. (2000). The coupled heat-moisture-mechanic model of the frozen soil. *Cold Regions Sci. Technol*. **31**, No. 3, 199–205.

Li, N., Chen, F., Su, B. & Cheng, G. (2002). Theoretical frame of the saturated freezing soil. *Cold Regions Sci. Technol*. **35**, No. 2, 73–80.

Li, X. S. (2003). Effective stress in unsaturated soil: a microstructural analysis. *Géotechnique* **53**, No. 2, 273–277.

Lima, A. (2009). *Thermo-hydro-mechanical behaviour of natural Boom clay: an experimental study.* PhD thesis, Universitat Politècnica de Catalunya, Spain (in preparation).

Lloret, A. & Alonso, E. E. (1980). Consolidation of unsaturated soils including swelling and collapse behaviour. *Géotechnique* **30**, No. 4, 449–477.

Lloret, A. & Alonso, E. E. (1985). State surfaces for partially saturated soils, *Proc. 11th Int. Conf. Soil Mech. Found. Engng, San Francisco* **2**, 557–562.

Lloret, A. & Villar, M. V. (2007). Advances on the knowledge of the thermo-hydro-mechanical behaviour of heavily compacted FEBEX bentonite. *Phys. Chem. of the Earth, Parts A/B/C* **32**, Nos 8–14, 701–715.

Loret, B. & Khalili, N. (2000). A three-phase model for unsaturated soils. *Int. J. Numer. Anal. Methods Geomech*. **24**, No. 11, 893–927.

Loret, B. & Khalili, N. (2002). An effective stress elastic-plastic model for unsaturated porous media. *Mech. Mater.* **34**, No. 2, 97–116.

Loret, B., Hueckel, T. & Gajo, A. (2002). Chemo-mechanical coupling in saturated porous media: elastic–plastic behaviour of homoionic expansive clays. *Int. J. Solids Struct*. **39**, No. 10, 2773–2806.

Lu, N. (2008). Is matric suction a stress variable? *J. Geotech. Geoenviron. Engng, ASCE* **134**, No. 7, 899–905.

McDougall, J. (2007). A hydro-bio-mechanical model for settlement and other behaviour in landfill waste. *Comput. Geotech*. **34**, No. 4, 229–246.

Manassero, M. & Domijiani, A. (2003). Modelling the osmosis effect on solute migration through porous media. *Géotechnique* **53**, No. 5, 481–492.

Marques, M. E. S., Leroueil, S. & Almeida, M. S. S. (2004). Viscous behaviour of St-Roch-de-l'Achigan clay, Quebec. *Can. Geotech. J.* **41**, No. 1, 25–38.

Masin, D. & Khalili, N. (2008). A hypoplastic model for mechanical response of unsaturated soils. *Int. J. Numer. Anal. Methods Geomech*. **32**, No. 15, 1903–1926.

Maswoswe, J. (1985). *Stress path for a compacted soil during collapse due to wetting*. PhD thesis, Imperial College, London.

Matyas, E. L. & Radhakrishna, H. S. (1968). Volume change characteristics of partially saturated soils. *Géotechnique* **18**, No. 4, 432–448.

Menin, A., Salomoni, V. A., Saltgiuliana, R., Simoni, L., Gens, A. & Schrefler, B. A. (2008). A mechanism contributing to subsidence above gas reservoirs and its application to a case study. *Int. J. Comput. Methods Engng Sci. Mech*. **9**, No. 5, 270–287.

Mitchell, J. K. (1991). Conduction phenomena: from theory to geotechnical practice. *Géotechnique* **41**, No. 3, 299–340.

Mitchell, J. K. & Soga, K. (2005). *Fundamentals of soil behaviour*, 3rd edn. Hoboken, NJ: Wiley.

Modaressi, A. & Abou-Bekr, N. (1994). A unified approach to model the behaviour of saturated and unsaturated soils. *Proc. 8th Int. Conf. on Computer Methods and Advances in Geomechanics (IACMAG), Morgantown, VA*, 1507–1513

Modaressi, A., Abou-Bekr, N. & Fry, J. J. (1996). Unified approach to model partially saturated and saturated soil. *Proc 1st Int. Conf. on Unsaturated Soils* **3**, 1495–1502.

Morgenstern, N. R. (1981). Geotechnical engineering and frontier resource development. *Géotechnique* **31**, No. 3, 305–365.
Muir Wood, D. (2004). *Geotechnical modelling*. London: Spon Press.
Newman, G. P. & Wilson, G. W. (1997). Heat and mass transfer in unsaturated soils during freezing. *Can. Geotech. J.* **34**, No. 1, 63–70.
Nishimura, S., Gens, A., Olivella, S. & Jardine, R. J. (2009). THM-coupled finite element analysis of frozen soil: formulation and application. *Géotechnique* **59**, No. 3, 159–171.
Nitao, J. J. & Bear, J. (1996). Potentials and their role in transport in porous media. *Water Resour. Res*. **32**, No. 2, 225–250.
Nixon, J. F. (1978). Foundation design approaches in permafrost areas. *Can. Geotech. J.* **15**, No. 1, 96–112.
Nixon, J. F. & Morgenstern, N. R. (1973). The residual stress in thawing soils. *Can. Geotech. J.* **10**, No. 4, 571–580.
Nova, R., Castellanza, R. & Tamagnini, C. (2003). A constitutive model for bonded geomaterials subject to mechanical and/or chemical degradation. *Int. J. Numer. Anal. Methods Geomech*. **27**, No. 9, 705–732.
Nur, A. & Byerlee, J. D. (1971). An exact effective stress law for elastic deformation of rock with fluids. *J. Geophys. Res*. **76**, No. 6, 6414–6419.
Nuth, M. & Laloui, L. (2008). Effective stress concept in unsaturated soils: clarification and validation of a unified framework. *Int. J. Numer. Anal. Methods Geomech*. **32**, No. 7, 771–801.
Oka, F., Kodaka, T., Kimoto, S., Kim, Y.-S. & Yamasaki, N. (2006). An elastoviscoplastic model and multiphase coupled FE analysis for unsaturated soil. *Proc. 4th Int. Conf. on Unsaturated Soils, Phoenix, AZ* **2**, 2039–2050.
Olivella, S. & Gens, A. (2000). Vapour transport in low permeability unsaturated soils with capillary effects. *Transp. Porous Media* **40**, No. 2, 219–241.
Olivella, S. & Gens, A. (2002). A constitutive model for crushed salt. *Int. J. Numer. Anal. Methods Geomech*. **26**, No. 7, 719–746.
Olivella, S., Carrera, J., Gens, A. & Alonso, E. E. (1994). Non-isothermal multiphase flow of brine and gas through saline media. *Transp. Porous Media* **15**, No. 3, 271–293.
Olivella, S., Carrera, J., Gens, A. & Alonso, E. E. (1996a). Porosity variations in saline media caused by temperature gradients coupled to multiphase flow and dissolution/precipitation. *Transp. Porous Media* **25**, No. 1, 1–25.
Olivella, S., Gens, A., Carrera, J. & Alonso, E. E. (1996b). Numerical formulation for a simulator (CODE_BRIGHT) for the coupled analysis of saline media. *Engng Comput*. **13**, No. 7, 87–112.
O'Neill, K. & Miller, R. D. (1985). Exploration of a rigid ice model of frost heave. *Water Resour. Res*. **21**, No. 3, 281–296.
Pakzad, M. (1995). *Modelisation du comportement hydro-mecanique des argiles gonflantes a faible porosité*. PhD thesis, Université d'Orleans.
Pellegrino, A. (2005). Dissesti idrogeologici nel sottosuolo della città di Napoli: Analisi ed interventi. In *Questioni di ingegneria geotecnica: Scritti de Arturo Pelegrino* (ed. G. Urciuoli), pp. 241–267. Benevento: Hevelius Edizioni.
Pereira, J. M., Wong, H., Dubujet, P. & Dangla, P. (2005). Adaptation of existing behaviour models to unsaturated states: application to CJS model. *Int. J. Numer. Anal. Methods Geomech*. **29**, No. 11, 1127–1155.
Peters, G. P. & Smith, D. W. (2004). The influence of advective transport on coupled chemical and mechanical consolidation of clays. *Mech. Mater*. **36**, Nos 5–6, 467–486.
Philip, J. R. (1977). Unitary approach to capillary condensation and adsorption. *J. Chem. Phys*. **66**, No. 11, 5069–5075.
Pietruszczak, S., Lydzba, D. & Shao, J. F. (2006). Modelling of deformation response and chemo-mechanical coupling in chalk. *Int. J. Numer. Anal. Methods Geomech*. **30**, No. 10, 997–1018.
Pinyol, N., Vaunat, J. & Alonso, E. E. (2007). A constitutive model for soft clayey rocks that includes weathering effects. *Géotechnique* **57**, No. 2, 137–151.
Pollock, D. W. (1986). Simulation of fluid flow and energy transport processes associated with high-level radioactive waste disposal in unsaturated alluvium. *Water Resour. Res*. **22**, No. 5, 765–775.
Priol, G., De Gennaro, V., Delage, P. & Cui, Y. J. (2005). On suction and time dependent behaviour of reservoir chalks. In *Unsaturated soils: Advances in testing, modelling and engineering applications* (eds C. Mancuso and A. Tarantino), pp. 43–54. London: Taylor & Francis.
Priol, G., De Gennaro, V., Delage, P., Collin, F. & Charlier, R. (2006). Suction and time effects on the behaviour of a reservoir chalk. *Proc. 2006 Eur. Rock Mechanics Symp. EUROCK 2006, Liège*, 519–526.
Rampino, C., Mancuso, C. & Vinale, F. (2000). Experimental behaviour and modelling of an unsaturated compacted soil. *Can. Geotech. J.* **37**, No. 3, 747–763.
Richards, B. G. (1984). Finite element analysis of volume change in expansive clays. *Proc. 5th Int. Conf. on Expansive Soils, Adelaide*, 141–148.
Romero, E. (1999). *Characterisation and thermo-hydro-mechanical behaviour of unsaturated Boom clay: an experimental study*. PhD thesis, Universitat Politènica de Catalunya, Spain.
Romero, E., Gens, A. & Lloret, A. (1999). Water permeability, water retention and microstructure of unsaturated compacted Boom clay. *Engng Geol*. **54**, Nos 1–2, 117–127.
Romero, E., Gens, A. & Lloret, A. (2001). Temperature effects on the hydraulic behaviour of an unsaturated clay. *Geotech. Geol. Engng* **19**, Nos 3–4, 311–332.
Romero, E., Gens, A. & Lloret, A. (2003). Suction effects on a compacted clay under non-isothermal conditions. *Géotechnique* **53**, No. 1, 65–81.
Roscoe, K. H. & Burland, J. B. (1968). On the generalised stress–strain behaviour of 'wet' clay. In *Engineering plasticity* (eds J. Heyman and F. A. Leckie), pp. 535–609. Cambridge: Cambridge University Press.
Roscoe, K. H., Schofield, A. N. & Worth, C. P. (1958). On the yielding of soils. *Géotechnique* **8**, No. 1, 22–52.
Russell, A. R. & Khalili, N. (2006). A unified bounding surface plasticity model for unsaturated soils. *Int. J. Numer. Anal. Methods Geomech*. **30**, No. 3, 181–212.
Saaltink, M., Ayora, C. & Carrera, J. (1998). A mathematical formulation for reactive transport that eliminates mineral concentrations. *Water Resour. Res*. **34**, No. 7, 1649–1656.
Sánchez, M. & Gens, A. (2006). *Final report on thermo-hydro-mechanical modelling. Febex Project*, Publicación Técnica 05-2/2006. Madrid: Enresa.
Sánchez, M., Gens, A., Guimarães, L. do N. & Olivella, S. (2005). A double structure generalized plasticity model for expansive materials. *Int. J. Numer. Anal. Methods Geomech*. **29**, No. 8, 751–787.
Sánchez, M., Gens, A., Guimarães, L. do N. & Olivella, S. (2008). Implementation algorithm of a generalised plasticity model for swelling clays. *Comput. Geotech*. **35**, No. 6, 860–871.
Santagiuliana, R. & Schrefler, B. A. (2006). Enhancing the Bolzon—Schrefler–Zienkiewicz constitutive model for partially saturated soil. *Transp. Porous Media* **65**, No. 1, 1–30.
Santamarina, J. C. & Fam, M. (1995). Changes in dielectric permittivity and shear wave velocity during concentration diffusion. *Can. Geotech. J.* **32**, No. 4, 647–659.
Schofield, A. N. & Wroth, C. P. (1968). *Critical state soil mechanics*. London: McGraw-Hill.
Scholtès, L., Hicher, P.-Y., Nicot, F., Chareye, B. & Darve, F. (2009). On the capillary stress tensor in wet granular materials. *Int. J. Numer. Anal. Methods Geomech*. **33**, No. 10, 1289–1313.
Schrefler, B. A. (1984). *The finite element method in soil consolidation (with applications to surface subsidence)*. PhD thesis, University College of Swansea, Wales.
Seetharam, S. C., Thomas, H. R. & Cleall, P. J. (2007). Coupled thermo/hydro-chemical/mechanical model for unsaturated soils: numerical algorithm. *Int. J. Numer. Methods Engng* **70**, No. 12, 1480–1511.
Selvadurai, A. P. S., Hu, J. & Konuk, I. (1999a). Computational modelling of frost heave induced soil-pipeline interaction. I: Modelling of frost heave. *Cold Regions Sci. Technol*. **29**, No. 3, 215–228.
Selvadurai, A. P. S., Hu, J. & Konuk, I. (1999b). Computational modelling of frost heave induced soil-pipeline interaction. II: Modelling of experiments at the Caen test facility. *Cold Regions Sci. Technol*. **29**, No. 3, 229–257.
Sharma, R. S. (1998). *Mechanical behaviour of unsaturated highly expansive clays*. PhD thesis, University of Oxford, UK.
Sheng, D. & Fredlund, D. G. (2008). Elastoplastic modelling of

unsaturated soils: an overview. *Proc. 12th Int. Conf. of International Association for Computer Methods and Advances in Geomechanics (IACMAG), Goa*, 2084–2105 (CD-ROM).
Sheng, D., Fredlund, D. G. & Gens, A. (2008a). A new modelling approach for unsaturated soils using independent stress variables. *Can. Geotech. J.* **45**, No. 4, 511–534.
Sheng, D., Smith, D. W., Sloan, S. W. & Gens, A. (2003a). Finite element formulation and algorithms for unsaturated soils. Part II: Verification and application. *Int. J. Numer. Anal. Methods Geomech*. **27**, No. 9, 767–790.
Sheng, D., Sloan, S. W., Gens, A. & Smith, D. W. (2003b). Finite element formulation and algorithms for unsaturated soils. Part I: Theory. *Int. J. Numer. Anal. Methods Geomech*., **27**, No. 9, 745–765.
Sheng, D., Sloan, S. W. & Gens, A. (2004). A constitutive model for unsaturated soils: thermomechanical and computational aspects. *Comput. Mech*. **33**, No. 6, 453–465.
Sheng, D., Gens, A., Fredlund, D. G. & Sloan, S. W. (2008b). Unsaturated soils: from constitutive modelling to numerical algorithms. *Comput. Geotech*. **35**, No. 6, 810–824.
Sivakumar, V. (1993). *A critical state framework for unsaturated soil*. PhD thesis, University of Sheffield, UK.
Skempton, A. W. (1961). Effective stress in soils, concrete and rocks. In *Pore pressure and suction in soils*, pp. 4–16. London: Butterworth.
Skempton, A. W., Norbury, D. & Petley, D. J. (1990). Solifluction shears at Carsington, Derbyshire. *Preprints of the 25th Ann. Conf. of the Engineering Group of the Geological Society, Edinburgh*, 277–285.
Skempton, A. W. & Weeks, A. G. (1976). The Quaternary history of the Lower Greensand escarpment and Weald clay vale near Sevenoaks, Kent. *Phil. Trans. R. Soc. London A* **283**, 493–526.
Slusarchuk, W. A., Clark, J. I., Nixon, J. F., Morgenstern, N. R. & Gaskin, P. N. (1978). Field test results of a chilled pipeline buried in unfrozen ground. *Proc. of 3rd Int. Conf. on Permafrost, Edmonton* **1**, 878–883.
Steefel, C. & Lasaga, A. (1994). A coupled model for transport of multiple chemical species and kinetic precipitation/dissolution reactions with application to reactive flow in single phase hydrothermal systems. *Am. J. Sci*. **294**, 529–592.
Sultan, N., Delage, P. & Cui, Y.-J. (2002). Temperature effects on the volume change behaviour of Boom clay. *Engng Geol*. **64**, Nos 2–3, 135–145.
Sun, D. A., Matsuoka, H., Cui, H. B. & Xu, Y. F. (2003). Three-dimensional elasto-plastic model for unsaturated compacted soils with different initial densities. *Int. J. Numer. Anal. Methods Geomech*. **27**, No. 12, 1079–1098.
Sun, D. A., Matsuoka, H. & Xu, Y. F. (2004). Collapse behavior of compacted clays in suction-controlled triaxial tests. *Geotech. Test. J. ASTM* **27**, No. 4, 362–370.
Sun, D. A., Sheng, D., Cui, H. B. & Sloan, S. W. (2007a). A density-dependent elastoplastic hydro-mechanical model for unsaturated compacted soils. *Int. J. Numer. Anal. Methods Geomech*. **31**, No. 11, 1257–1279.
Sun, D. A., Sheng, D. & Sloan, S. W. (2007b). Elastoplastic modelling of hydraulic and stress–strain behaviour of unsaturated soil. *Mech. Mater*. **39**, No. 3, 212–221.
Sun, D. A., Sheng, D. & Xu, Y. (2007c). Collapse behaviour of unsaturated compacted soil with different initial densities. *Can. Geotech. J.* **44**, No. 6, 673–686.
Tamagnini, R. (2004). An extended cam-clay model for unsaturated soils with hydraulic hysteresis. *Géotechnique* **54**, No. 3, 223–228.
Tamagnini, R. & Pastor, M. (2005). A thermodynamically based model for unsaturated soil: a new framework for generalized plasticity. In *Unsaturated soils: Advances in testing, modelling and engineering applications* (eds C. Mancuso and A. Tarantino), pp. 121–134. London: Taylor & Francis.
Tang, A.-M., Cui, Y.-J. & Barnel, N. (2008). Thermo-mechanical behaviour of a compacted swelling clay. *Géotechnique* **58**, No. 1, 45–54.
Tarantino, A., Mongiovi, L. & Bosco, G. (2000). An experimental investigation on the isotropic stress variables for unsaturated soils. *Géotechnique* **50**, No. 3, 275–282.
Teatini, P., Ferronato, M., Gambolati, G., Bertoni, W. & Gonella (2005). A century of land subsidence in Ravenna, Italy. *Environ. Geol*. **47**, No. 6, 831–846.
Terzaghi, K. (1925a). *Erdbaumechanik auf bodenphisikalischer Grundlage*. Leipzig/Vienna: Deuticke.
Terzaghi, K. (1925b). Principles of soil mechanics. *Engng News Record* **95**, No. 19, 742–746; No. 20, 796–800; No. 21, 832–836; No. 22, 874–878; No. 23, 912–915; No. 25, 987–999; No. 26, 1026–1029; No. 27, 1064–1058. New York: Mc-Graw Hill (1926 edition).
Terzaghi, K. (1936). The shearing resistance of saturated soils and the angle between the planes of shear. *Proc. 1st Int. Conf. on Soil Mechanics, Cambridge, MA* **1**, 54–56.
Terzaghi, K. & Frölich, O. K. (1936). *Theorie der Setzung von Tonschichten*. Leipzig/Vienna: Deuticke.
Thomas, H. R. & He, Y. (1995). Analysis of coupled heat, moisture and air transfer in a deformable unsaturated soil. *Géotechnique* **45**, No. 4, 677–689.
Thomas, H. R. & He, Y. (1997). A coupled heat-moisture transfer theory for deformable unsaturated soil and its algorithmic implementation. *Int. J. Numer. Methods Engng* **40**, No. 18, 3421–3441.
Thomas, H. R., Cleall, P. J. & Hashm, A. A. (2001). Thermal/hydraulic/chemical/mechanical (THCM) behaviour of partly saturated soil. *Proc. 10th Int. Conf. on Computer Methods and Advances in Geomechanics, Tucson, AZ* **1**, 743–748.
Thu, T. M., Rahardjo, H. & Leong, E. C. (2007). Elastoplastic model for unsaturated soil with incorporation of the soil-water characteristic curve. *Can. Geotech. J.* **44**, No. 1, 67–77.
Thury, M. & Bossart, P. (1999). The Mont Terri rock laboratory, a new international research project in a Mesozoic shale formation, in Switzerland. *Engng Geol*. **52**, Nos 3–4, 347–359.
Toll, D. G. (1990). A framework for unsaturated soil behaviour. *Géotechnique* **40**, No. 1, 31–44.
Toll, D. G. & Ong, B. H. (2003). Critical state parameters for an unsaturated residual sandy clay. *Géotechnique* **53**, No. 1, 93–103.
Towhata, I., Kuntiwattanakul, P., Seko, I. & Ohishi, K. (1993). Volume change of clays induced by heating as observed in consolidation tests. *Soils Found*. **33**, No. 4, 170–183.
Tuller, M., Or, D. & Dudley, L. M. (1999). Adsorption and capillary condensation in porous media: liquid retention and interfacial configurations in angular pores. *Water Resour. Res*. **35**, No. 7, 1949–1964.
Uchaipichat, A. & Khalili, N. (2009). Experimental investigation of thermo-hydro-mechanical behaviour of an unsaturated silt. *Géotechnique* **59**, No. 4, 339–353.
Vanapalli, S. K., Fredlund, D. G., Pufahl, D. E. & Clifton, A. W. (1996). Model for the prediction of shear strength with respect to soil suction. *Can. Geotech. J.* **33**, No. 3, 379–392.
Vaughan, P. R. (1994). Assumption, prediction and reality in geotechnical engineering. *Géotechnique* **44**, No. 4, 573–609.
Vaughan, P. R. (1999). Special lecture: Problematic soil or problematic soil mechanics? *Proceedings of the international symposium on problematic soils*, Sendai, Vol. 2, pp. 803–814.
Vaunat, J., Jommi, C. & Gens, A. (1997). A strategy for numerical analysis of the transition between saturated and unsaturated flow conditions. *Proc. 6th Int. Symp. on Numerical Models in Geomechanics, Graz*, 297–302.
Vaunat, J., Cante, J. C., Ledesma, A. & Gens, A. (2000a). A stress point algorithm for an elastoplastic model in unsaturated soils. *Int. J. Plasticity* **16**, No. 2, 121–141.
Vaunat, J., Romero, E. & Jommi, C. (2000b). An elastoplastic hydromechanical model for unsaturated soils. In *Experimental evidence and theoretical approaches in unsaturated soils* (eds A. Tarantino and C. Mancuso), pp. 121–138. Rotterdam: Balkema.
Vaunat, J. & Gens, A. (2003a). Bond degradation and irreversible strains in soft argillaceous rock. *Proc. 12th Panamerican Conf. Soil Mech. Geotech. Engng, Boston* **1**, 479–484.
Vaunat, J. & Gens, A. (2003b). Numerical modelling of an excavation in a hard soil/soft rock formation using a coupled damage/plasticity model. *Proc. 7th Int. Conf. on Computational Plasticity, Barcelona* (CD-ROM).
Villar, M. V. (2002). *Thermo-hydro-mechanical characterisation of a bentonite from Cabo de Gata. A study applied to the use of bentonite as sealing material in high level radioactive waste repositories*, Technical Publication 01/2002. Madrid: Enresa.
Villar, M. V. & Lloret, A. (2004). Influence of temperature on the hydro-mechanical behaviour of a compacted bentonite. *Appl. Clay Sci*. **26**, Nos 1–4, 337–350.

Villar, M. V., Martin, P., Lloret, A. & Romero, E. (2004). *Final Report on Thermo-Hydro-Mechanical Laboratory Test*, Enresa Report 70-IMA-L-0-97. Madrid: FEBEX II.

Volckaert, G., Bernier, F., Alonso, E. E., Gens, A., Samper, J., Villar, M. V., Martin-Martin, P. L., Cuevas, J., Campos, R., Thomas, H., Imbert, C. & Zingarelli, V. (1996). *Thermal-hydraulic-mechanical and geochemical behaviour of the clay barrier in radioactive waste repositories (model development and validation)*, EUR 16744 EN. Luxembourg: Publications of the European Communities.

Wheeler, S. J. (1996). Inclusion of specific water volume within an elastoplastic model for unsaturated soils. *Can. Geotech. J.* **33**, No. 1, 42–57.

Wheeler, S. J. (2005). *The mechanics of unsaturated soils*. 2005 Géotechnique lecture (available on CD, British Geotechnical Association).

Wheeler, S. J. & Karube, D. (1996). State of the art report: constitutive modelling. *Proc. 1st Int. Conf. on Unsaturated Soils, Paris* **3**, 1323–1356.

Wheeler, S. J. & Sivakumar, V. (1993). Development and application of a critical state model for unsaturated soil. *Proceedings of the Wroth Memorial Symposium on Predictive Soil Mechanics* (eds G T. Houlsby and A. N. Schofield), pp. 709–728. London: Thomas Telford.

Wheeler, S. J. & Sivakumar, V. (1995). An elasto-plastic critical state framework for unsaturated soil. *Géotechnique* **45**, No. 1, 35–53.

Wheeler, S. J. & Sivakumar, V. (2000). Influence of compaction procedure on the mechanical behaviour of an unsaturated compacted clay. Part 2: shearing and constitutive modelling. *Géotechnique* **50**, No. 4, 369–376.

Wheeler, S. J., Gallipoli, D. & Karstunen, M. (2002). Comments on use of the Barcelona Basic Model for unsaturated soils. *Int. J. Numer. Anal. Methods Geomech*. **26**, No. 15, 1561–1571.

Wheeler, S. J., Sharma, R. S. & Buisson, M. S. R. (2003). Coupling of hydraulic hysteresis and stress–strain behaviour in unsaturated soils. *Géotechnique* **53**, No. 1, 41–54.

Wileveau, Y. (2005). *THM behaviour of host rock (HE-D) experiment: Progress Report. Part 1*. Technical Report TR 2005-03. Mont Terri Project.

Williams, P. J. (1964). Unfrozen water content of frozen soils and soil moisture suction. *Géotechnique* **14**, No. 3, 231–246.

Wittke, W. & Wittke, M. (2005). Design, construction and supervision tunnels in swelling rock. In *Underground space use: analysis of the past and lessons for the future* (eds Y. Erdem and T. Solak), pp. 1173–1178. London: Taylor & Francis.

Wong, H. N. & Ho, K. K. S. (1997). The 23 July 1994 landslide at Kwun Lung Lau, Hong Kong. *Can. Geotech. J.* **34**, No. 6, 825–840.

Wu, W., Li, X., Charlier, R. & Collin, E. (2004). A thermo-hydro-mechanical constitutive model and its numerical modelling for unsaturated soils. *Comput. Geotech*. **31**, No. 2, 155–167.

Wu, Q. B., Cheng, G. D., Ma, W., Niu, F. & Sun, Z. Z. (2006). Technical approaches on permafrost thermal stability for Qinghai–Tibet Railway. *Geomech. Geoeng.* **1**, No. 2, 119–127.

Yang, C., Cui, Y.-J., Pereira, J. M. & Huang, M. S. (2009). A constitutive model for unsaturated cemented soils under cyclic loading. *Comput. Geotech*. **35**, No. 6, 853–859.

Zhang, H. W. & Zhou, L. (2008). Implicit integration of a chemo-plastic constitutive model for partially saturated soils. *Int. J. Numer. Anal. Methods Geomech*. **32**, No. 14, 1715–1735.

Zheng, L. & Samper, J. (2008). Coupled THMC model of FEBEX mock-up test. *Phys. Chem. of the Earth* **33**, Suppl. 1, S486–S498.

VOTE OF THANKS

Professor D. M. POTTS, Imperial College of Science, Technology and Medicine, London.

Ladies and gentlemen, it is a great pleasure for me to give this vote of thanks. I have known Antonio since 1979 when I first joined the staff at Imperial. In those days Antonio was carrying out laboratory tests for his PhD, a seminal piece of work which is still widely referred to today. We worked on theoretical problems together and wrote several papers. While this in itself is not particularly unusual for a researcher, when taken in the context that he was also simultaneously performing five or six complex laboratory stress-path tests, all of which took several weeks to perform and involved manual control (PCs had not been invented yet), and was writing papers with both David Hight and Peter Vaughan, it is extremely impressive. In fact, it was my first encounter with parallel processing, something Antonio seems to have a natural gift for, but has only recently been cracked by the computer industry. It was clear that Antonio was a highly gifted and talented individual who had the potential to become one of the best geotechnical engineers of his generation. He was also a nice guy and an absolute pleasure to work with. I still refer to him as one of the most gifted people I have ever had the privilege to work with.

Well, 28 years on and Antonio is back at Imperial and has just presented the 47th Rankine Lecture, arguably the most prestigious international lecture in the field of geotechnical engineering. I think we can confidently conclude that Antonio has more than fulfilled his early potential.

For those privileged few that are invited to give a Rankine Lecture it often forms the pinnacle of their career. However, acceptance of the invitation presents the lecturer with an enormous challenge. On the one hand the lecture must be interesting, of wide appeal, understandable, stimulating and ground breaking. On the other hand the audience consists of a vast spectrum of people ranging from consultants and contractors to academics, from those just starting their careers to those coming to the ends of theirs, people of varied backgrounds and countries of origin. In many respects it is a daunting, almost impossible task to reconcile these conflicting criteria (boundary conditions) and much time and effort is spent in selecting a topic and the material to be included so that there is something for everyone. I know that Antonio spent much time and effort on this and I have no doubt that both he and his family have suffered in the process.

Was it worth the effort? I believe so. Did Antonio satisfy the conflicting criteria? I believe he did. The lecture started with two quotes, one from Karl Terzaghi (the master) and one from Professor Peter Vaughan. Although not explicitly stated, it was implied that Terzaghi got it wrong and Vaughan got it right. Such controversy was always going to grab the attention of the audience and focus their minds. The lecture then pursued Vaughan's suggestion of adapting the soil mechanics to fit the soil. The introduction summarised classical soil mechanics and very elegantly defined it using three ingredients; namely identifying the governing variables, establishing the necessary balance equations and developing appropriate constitutive models. It then went on to show how these ingredients could be simply extended to account for various effects not accounted for by classical soil mechanics. Although this approach may seem obvious in retrospect, like so many other scientific breakthroughs, it takes someone of a high intellect to think of them in the first place. Unsaturated soils, the effects of temperature, both heating and freezing, and chemical effects were considered. The necessary extensions to the basic theoretical ingredients were explained and their use demonstrated by considering case histories. These case histories were all relevant to modern engineering and are likely to become even more so in the future as we tackle the effects of climate change and global warming.

Antonio, you have delivered an excellent Rankine Lecture, one that will be remembered and referred to for a long time.

You have demonstrated that you are an expert in both experimental and theoretical soil mechanics and that you are able to apply this expertise to solve real-world geotechnical problems. It has been privilege and pleasure to listen to you tonight. On behalf of the British Geotechnical Association and this evening's audience, it is a great pleasure to thank you most sincerely for preparing and delivering the 47th Rankine Lecture.